Université de Montréal

Linear Block Copolymers of L–Lactide and 2–Dimethylaminoethyl Methacrylate: Synthesis and Properties

par

Maksym A. Kryuchkov

Département de chimie

Faculté des arts et des sciences

Thèse présentée à la Faculté des études supérieures et postdoctorales

en vue de l'obtention du grade de

Ph.D. en chimie

Fevrier 2012

Université de Montréal
Faculté des études supérieures et postdoctorales

Cette thèse intitulée:

Linear Block Copolymers of L–Lactide and 2–Dimethylaminoethyl Methacrylate: Synthesis and Properties

Présentée par :
Maksym A. Kryuchkov

a été évaluée par un jury composé des personnes suivantes :

Prof. Robert E. Prud'homme, président-rapporteur
Prof. C. Géraldine Bazuin, directrice de recherche
Prof. William Skene, membre du jury
Prof. Jung Kwon Oh, examinateur externe
Prof. Yves Lepine, représentant du Doyen de la Faculté

RÉSUMÉ

Les copolymères séquencés amphiphiles sont très prometteurs pour des applications de technologie de pointe en raison de leur capacité à s'auto-assembler dans des structures bien organisées à l'échelle du micro– et du nanométre, et de leur sensibilité à des stimulations de différentes natures. La formation des nanomotifs bien ordonnés dans les films et/ou en masse fournit un substitut à la nanolithographie et est utile pour le design et l'ingénierie de nanomembranes et de matériaux nanoporeux. L'auto–assemblage dans des solvants sélectifs, en incluant la sensibilité au pH et à la température, peut être ajusté pour correspondre aux besoins de différentes applications biomédicales, telles que l'encapsulation et/ou relargage de médicaments, l'ingénierie de tissus, etc. Dans ce contexte, des copolymères séquencés de type L–lactide (LLA) et méthacrylate 2–diméthylaminoéthyl (DMAEMA) sont d'un grand intérêt.

Comme le contrôle sur l'auto–assemblage des copolymères séquencés est permis au niveau moléculaire, il est très important de préparer des copolymères bien définis avec des longueurs de bloc prévisibles et de faible polydispersité. Ainsi, une partie de cette étude a été consacrée au développement de procédures synthétiques optimales et à la caractérisation détaillée de copolymères di– et triblocs de LLA et de PDMAEMA. Un outil simple pour déterminer la présence d'homo–PLLA résiduel a été développée; cela a permis de déterminer et d'expliquer plusieurs voies de synthèse indésirables. La dernière inclut la participation possible de l'amorceur bifonctionnel utilisé, et nous avons alors proposé un système alternatif d'amorceur bifonctionnel/catalyseur. La racémisation du LLA par les unités amine de (P)DMAEMA a été observée pendant la polymérisation, limitant ainsi l'utilisation première du bloc PDMAEMA pour la préparation des copolymères PLLA–b–PDMAEMA. Les études thermiques et de cristallisation, en incluant les copolymères séquencés partiellement quaternisés, ont révélé un retard significatif de la vitesse de cristallisation, en présence du bloc de PDMAEMA. Nous avons constaté que les blocs sont miscibles pour de faibles masses molaires et que la miscibilité partielle est maintenue après quaternisation. Selon la longueur et le taux de quaternisation du bloc PDMAEMA, la cristallisation du PLLA a été étudiée dans un environnement restreint et confiné, faiblement ou fortement. La torsion des lamelles cristallines observée pour certains copolymères biséquencés a été accentuée dans les copolymères triséquencés, où la formation de sphérolites annelés a été observée dans toutes les conditions thermiques utilisées.

Mots-clés : copolymères séquencés, L–lactide, méthacrylate, octoate d′étain, cristallisation, Avrami, sphérolite, amorceur bifonctionnel, synthèse en une étape.

ABSTRACT

Multi–functional amphiphilic block copolymers have much promise for various high technology applications thanks to the controlled stimuli–responsive self–assembly into well–organized structures on the micro– and nanometer scales. The formation of well–ordered nanopatterns in films and/or in bulk provides a competitive substitute to nanolithography and is useful in the design and engineering of nanomembranes and nanoporous materials. Solution self–assembly in selective solvents, including pH and temperature sensitivity, can be tuned to match the needs of different biomedical applications, such as drug encapsulation/delivery, tissue engineering, etc. In this context, block copolymers of L–lactide (LLA) and 2–dimethylaminoethyl methacrylate (DMAEMA) are of great interest.

Since the control over self–assembly of block copolymer systems is enabled on a molecular level, it is of great importance to prepare well–defined block copolymers with predictable block lengths and low polydispersity. Thus, a major part of the research in this study was devoted to developing optimal synthetic procedures with detailed characterization of linear di– and triblock copolymers of LLA and PDMAEMA. A simple tool to determine homo–PLLA impurity was developed, which helped to determine and explain several undesired routes. The latter includes possible involvement of the bifunctional initiator used, and an alternative bifunctional initiator/catalyst system was proposed. Racemization of LLA by (P)DMAEMA moieties was observed during LLA polymerization thus limiting the utilization of PDMAEMA–first approach for the preparation of PLLA–b–PDMAEMA. Thermal and crystallization studies, including on quaternized block copolymers, revealed a significant retardation effect of the PDMAEMA block on the crystallization kinetics. The blocks were found to be miscible in the melt at low molecular weights, and maintained partial miscibility after quaternization. Depending on the length and the quaternization degree of PDMAEMA, PLLA crystallization was studied in a templated, soft or hard confinement environment. Crystalline lamellae twisting observed in certain diblock copolymers was facilitated in triblock copolymers, where the formation of banded spherulites was observed in all thermal conditions used.

Keywords : block copolymer, L–lactide, methacrylate, tin octoate, crystallization, Avrami, spherulite, bifunctional initiator, one–pot synthesis.

TABLE OF CONTENTS

CHAPTER 4

Crystallization, morphology and kinetics in linear diblock copolymers of L–lactide and 2–dimethylaminoethyl methacrylate, and effect of partial quaternization

CHAPTER 5

Synthesis and Crystallization Studies of Linear ABA–type Triblock Copolymers of L–Lactide and 2–Dimethylaminoethyl Methacrylate with poly(L–Lactide) as a central block

CHAPTER 6

General conclusions and future work

List of Figures

List of Schemes

List of Charts

List of Tables

List of acronyms, abbreviations and symbols used

ABC	amphiphilic block copolymer
AIBN	2,2'–azo–diisobutyronitrile
ATRP	atom–transfer radical polymerization
BDM	1,4–benzenedimethanol
BIB	2–bromo–isobutyryl bromide
CL	ε–caprolactone
conv.	conversion
DCM	dichloromethane
DHN	1,5–dihydroxynaphtalene
DLA	D–lactide
DMAEMA	2–dimethylaminoethyl methacrylate
DMF	dimethyl formamide
DMSO	dimethyl sulfoxide
dn/dc	refractive index increment
DSC	differential scanning calorimetry
f	weight fraction
FDA	Food and Drugs Administration
G	spherulite growth rate
GTP	group–transfer polymerization
HBBIB	2–hydroxybutyl–2–bromo–isobutyryl bromide
HEBIB	2–hydroxyethyl–2–bromo–isobutyryl bromide
HMTETA	1,1,4,7,10,10–hexamethyltriethylenetetramine
homo–	homopolymer
iPBA	4–isopropylbenzyl alcohol
K	overall crystallization rate constant
LA–LA	lactoyl lactate

LLA	L–lactide
LS	light–scattering
M	molar concentration
MMA	methyl methacrylate
M_n	number–average molecular weight
MPS	mononuclear phagocytosis system
n	Avrami nucleation constant
N	number of units in polymer chain
NMP	nitroxide–mediated radical polymerization
NPs	nanoparticles
ODT	order–disorded transition
P(L)LA	refers to both highly isotactic and atactic polylactides
P3HT	poly(3–hexylthiophene)
P4VP	poly(4–vinylpyridine)
PCL	poly(ε–caprolactone)
PDI	polydispersity index
PDLA	poly(D–lactide)
PDLLA	atactic polylactide
PDMAEMA	poly(2–dimethylaminoethyl methacrylate)
PDMS	polydimethylsiloxane
PDP	3–pentadecylphenol
PEO	poly(ethylene oxide)
PGA	poly(glycolic acid)
PHBV	poly(hydroxybutyrate–co–hydroxyvalerate)
PI	polyisoprene
PLA	poly(lactic acid)
PLLA	poly(L–lactide)
PMDETA	1,1,4,7,7–pentamethyldiethylenetriamine
PMMA	poly(methyl methacrylate)

polym.	polymerization
POM	polarized optical microscopy
PPDX	poly(p–dioxanone)
PS	polystyrene
PVA	poly(vinyl alcohol)
qPDMAEMA	quaternized PDMAEMA
quat.	quaternization
RAFT	reversible addition–fragmentation chain–transfer polymerization
RI	refractive index
ROP	ring–opening polymerization
SAXS	small–angle X–ray scattering
tBC	triblock copolymer
tBMA	t–butyl methacrylate
$\mathbf{T_c}$	crystallization temperature
TEA	triethylamine
TEM	transmission electron microscopy
temp.	temperature
TFMSA	trifluoromethanesulfonic acid
$\mathbf{T_g}$	glass–transition temperature
TGA	thermogravimetric analysis
THF	tetrahydrofurane
$\mathbf{T_m}$	melting temperature
TMS	tetramethylsilane
v/v	by volume
W	weight fraction
w/w	by weight
WAXD	wide–angle X–ray diffraction
$\boldsymbol{\chi}$	Flory–Huggins segment–segment interaction parameter

Acknowledgements

Fisrt of all, I would like to thank my supervisor, Prof. C. Geraldine Bazuin, for giving me an opportunity to join her group and continue to pursue my career at Université de Monréal. I'm very grateful for her trust in me as a synthetic chemist when giving me this project, for financial support, including coverage of trips and participation at different conferences. A very special thanks for her enormous efforts in correcting/reviewing all my paperwork, for valuable discussions and particular attention to the details, allowing me to more critically revise the results of my work, and for the endless optimism and support of my ideas. In addition, I would like to say thank you from my family for care, support and understanding, and very special thanks from little Diana, whose happy childhood in Canada is also closely related to "*Mme Géraldine*"

I thank Prof. Robert E. Prud'homme for valuable discussions, ideas and critical analysis of my results to help me conquer the unknown (for me), yet fascinating field of crystallization phenomena in polymers.

Many thanks to Dr. Xavier Sallenave, a former postdoctoral fellow in the Bazuin group, for his instant readiness for assistance in any part of everyday lab life, from helping me to get acquainted with the lab facilities to introduction to the major instrumentation (POM, FTIR, TGA, NMR and WAXD).

I am grateful to Prof. Robert Jérôme for giving me the opportunity to join his group (CERM, Université de Liége, Belgium) for two months, where I mastered controlled polymer synthesis. The skills gained there were used to complete my PhD research.

Thanks a lot to Dr. Christophe Detrembleur and Christophe Hubens (CERM, Université de Liége, Belgium), who introduced me to the world of controlled polymer synthesis, for assistance in the lab and fruitful discussions. I appreciate the kind assistance from other CERM members, with very special thanks to Rosica Mincheva (and Alex Stoynov), Ani Nedelcheva, Reni Bryaskova and Dimitriya Bozukova (and Metodi Bozukov and little Yoana), who accepted me as a friend and made my stay in Belgium unforgettable.

I acknowledge Julie Boivin and Dr. Alexandra Furtos for MALDI–TOF analysis and discussion of results that allowed me to better understand this magic technique.

I greatly appreciate the endless assistance of Pierre Ménard–Tremblay with the SEC–LS system, the second major technique (after NMR) ensuring successful polymer synthesis.

Special thanks to Sylvain Essiembre, for not only providing invaluable support in DSC, WAXD and TGA instrumentation, and not only for the fruitful discussions and some great ideas that improved the interpretation of results, but also for being a good friend and a person able to discuss virtually any subject from our everyday life, with a great sense of humour.

Lots of thanks to Huguette Dinel and Hélène Laliberté, whose help, everyday joy and sense of humour made my NMR teaching assistance for undergraduate labs a real pleasure, despite the number of samples to do.

I thank Elena Nadezhina for dedicated elemental analyses, and for finally putting "misbehaving" sulfur in its place, and for a good sense of humour.

I acknowledge help and support of Prof. Christian Pellerin, and his group members Damien Mauran and Xiaoxiao Wang, provided in infrared spectroscopy instrumentation, analyses and discussion of results.

I appreciate the kind assistance of Dr. Alexis Laforgue (former postdoctoral fellow in the Bazuin group) and Sébastien Roland in AFM analysis. Thanks also to Sébastien for assistance and discussion on the dip–coating technique, and to Gwen Bazin for helping me to get acquainted with DLS instrument. I am also grateful to Xin Wang (and Qian Zhang, former PhD student of Bazuin group) for EDAX analyses.

I would like to acknowledge Prof. Richard Register and Bryan Beckingham (Princeton University, USA) for SAXS analysis. I really appreciate collaboration with you and very grateful for valuable discussions and ideas regarding the obtained results.

For permission to use different instrumentation to fulfill my experimental needs, I would like to thank Profs. Robert Prud'homme, Julian Zhu, William Skene, Christian Pellerin and André Charette.

I would like to thank all the former and present members of the groups of Profs Géraldine Bazuin (especially Stéphanie Boissé for readily assistance in French), Robert Prud'homme, Julian Zhu, William Skene, Suzanne Giasson, Christian Pellerin, Françoise Winnik, James Wuest, Antonella Badia and Michel Lafleur for the great fun within and outside science that we had during the years at different student meetings, workshops, conferences and, of course, "wine–posiums". My very special thanks to Marc–André Gagnon (and Luce and little Édouard) for their friendship.

I acknowledge Lyne Laurin (and Céline Millette) and, especially, Prof. André Beauchamp for smooth guidance through the bureaucratic labyrinths of graduate school.

The financial support provided by Faculté des études supérieures et postdoctorales (FESP, Université de Montréal), le fonds québécois de la recherche sur la nature et les technologies (FQRNT, Québec, Canada), Natural Sciences and Engineering Research Council of Canada (NSERC, Canada), Ministère des relations internationales (MRI) and Ministère des développement économique, innovation and exportation (MDEIE) (Québec, Canada), and Commissariat général aux relations internationales de la Communauté française (CGRI, Belgium) is greatly acknowledged. I appreciate my membership in the interuniversity Centre for Self-Assembled Chemical Structures (CSACS/CRMAA) and Advanced Food and Materials Network (AFMNet).

I am infinitely grateful to my English Teacher, Iryna Popova, who brought my English to the level of free communication, and to Marina Shvets, my first Chemistry Teacher, who introduced me to this fascinating world of Chemistry, which finally became indispensable part of my life. I am especially grateful to Iryna Sokolets for her endless support and assistance in pursuing my Chemistry career. My greatest thanks to Profs Georgiy Rozantsev, Elena Shved, Nelli Maleeva and Margarita Zayats (Chemical Faculty, Donetsk National University, Ukraine), who gave me a solid Chemistry knowledge background to successfully continue my research career.

I am very thankful to Prof. Sergey Tolkunov (InPOC, Donetsk, Ukraine), my first supervisor, for teaching me A–to–Z synthetic lab skills, thus making me a real synthetic chemist, for his respect and understanding during scientific arguments, for support, both scientific and financial, and his sparkling enthusiasm during departmental parties.

Endless care and support, in both Chemistry and regular life, from Igor, Dmitrii and Inna Perepichka is invaluable, I couldn’t have done without you.

I am deeply grateful to my parents, Anatolii and Larysa, for their patience, love and support of all my career developments throughout my life.

Iryna Perepichka is acknowledged for not only doing LB and AFM experiments for me, but also for being a loving (and loved) wife and a good "mother–in–science", who gave me a perfect gift of Diana, *la plus parfaite petite fille dans le monde entier*.

To Yevghenii (Jack), Iryna and Diana

GENERAL INTRODUCTION AND SCOPE OF THE THESIS 1

1.1 Block copolymers as a versatile tool for nanotechnology

Polymeric materials, since their discovery, play a significant role in our everyday life. Nature uses biopolymers as a building material, for energy storage and even as the memory device for the translation of the genetic information. An important difference between natural and synthetic polymers is in their polydispersity, which nature controls perfectly; that is, nature can achieve a polydispersity of one, where every macromolecular chain has exactly the same molecular weight. Approaching a polydispersity of one is the goal of controlled polymerization techniques for synthetic polymers. This is particularly important for block copolymers, which are macromolecules consisting of two chemically different homopolymers linked together via a covalent bond.

Normally, chemically different polymers macrophase separate when melted together due to the domination of energetic over entropic contributions. Even weak repulsive interactions between repeat units in different polymer chains are magnified due to

the high number of units in each polymer, as opposed to very little gain from entropic mixing:

$$\Delta G_{(\text{phase separation})} = \Delta H_{(\text{repulsive interactions})} - T\Delta S_{(\text{thermal motion})}$$

Thus, the repulsive interactions usually dominate the thermal motion of polymer chains causing macrophase separation. However, if two incompatible polymers are linked together through a covalent bond, they can phase–separate only on a local molecular scale. This leads to the formation of periodic structures, creating a basis for various nanotechnology applications. To obtain well–defined periodic structures, the polydispersity of the blocks must be low.[1]

When chemically different blocks separate on the nanometer scale, different types of ordered nanoscopic structures can be obtained, depending on the nature and relative sizes of the blocks. Classical examples are spherical, cylindrical and lamellar morphologies, but other ordered structures, like gyroid and hexagonally–perforated lamellar morphologies can also form (*Figure 1.1*). The type of the equilibrium morphology at given temperature is determined by the molar fraction of each block (f), the total length of the polymer (N) and the repulsive/attractive interactions that are represented by the Flory–Huggins segment–segment interaction parameter chi (χ).

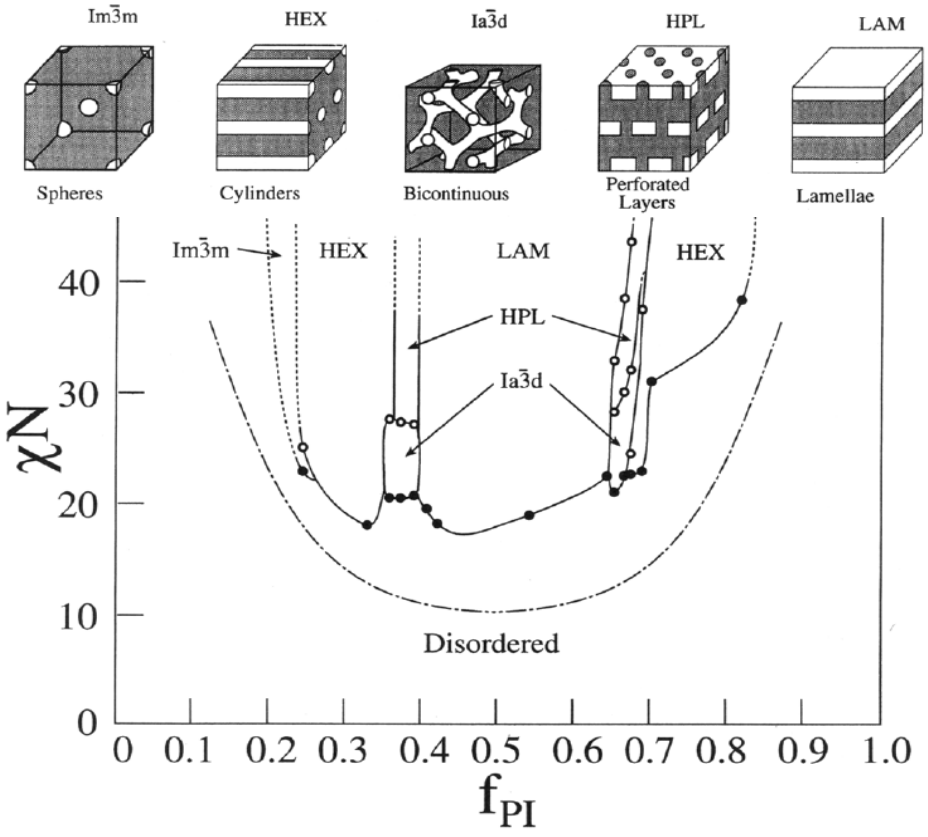

Figure 1.1. Phase diagram representing the compositional dependence of different morphologies in polystyrene–b–polyisoprene (PS–b–PI). The dash–dot curve is the mean field prediction for the order–disorder transition (reproduced from Ref. 2, © 1995 the American Chemical Society)

The composition independent χ parameter is inversely proportional to the temperature, so as the temperature increases, the value of the product χN decreases, meaning that repulsive interactions between different chains become compensated by thermal motion, leading to phase transitions. At a particular temperature, the thermal motion dominates and the system becomes disordered. This temperature is defined as the temperature of the order–disorder transition (T_{ODT}).

When a semi–crystalline polymer and an amorphous polymer are incorporated into one block copolymer, the morphology of the resulting microstructure will be determined by a competition between microphase separation and crystallization. The microstructure formed in the melt (see *Figure 1.1*) can be either preserved or destroyed by crystallization, depending on the crystallization temperature (T_c^c), the glass transition of the amorphous block (T_g^a) and the T_{ODT} (*Figure 1.2*).

Specifically, when $T_c^c > T_{ODT} > T_g^a$, then the final morphology is driven by the crystallization without regards to microphase separation.[3,4] When $T_{ODT} > T_g^a > T_c^c$ (which is termed "hard confinement" for crystallization), the ordered structure resulting from microphase separation is preserved after crystallization due to the glassy domains formed by the amorphous block.[5] Finally, if $T_{ODT} > T_c^c \geq T_g^a$ (termed "soft confinement"), then both the crystallization and the repulsive interactions between different monomer links ("strength of segregation") determine the final morphology.[6] In strongly segregated systems the ordered structure will be maintained despite crystallization,[7] whereas for intermediate segregation, depending on the type of phase–separated morphology, the structure can be templated in unconnected domains (spheres, cylinders) or broken out by crystallization (termed "break–out crystallization"), most often observed for lamellar morphology.[8]

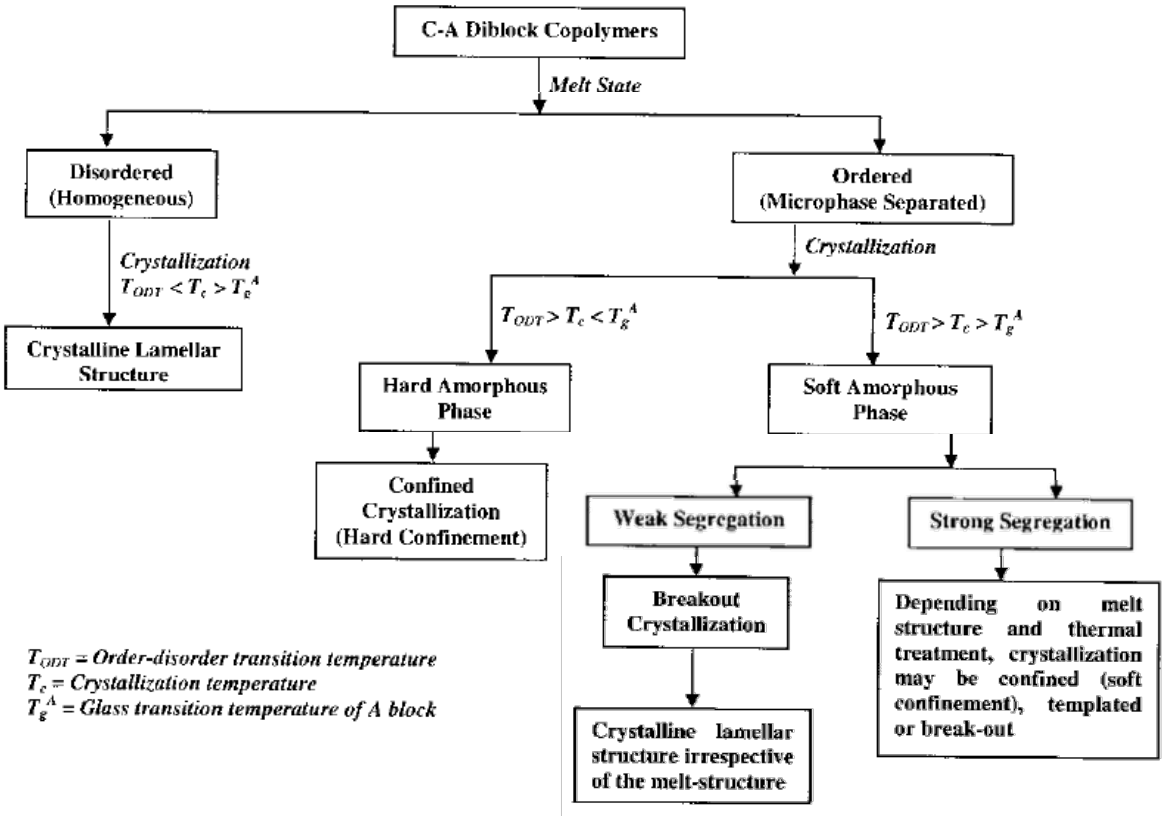

Figure 1.2. Schematic illustration of various scenarios of structure development after crystallization in semi-crystalline–amorphous block copolymers (reproduced from Ref. 4, © 2006 Taylor & Francis)

When one of the blocks is capable of forming hydrogen, ionic or covalent bonds, there is another possibility of controlling block copolymer self–assembly on the nanoscopic level. Complexation with surfactants or appropriately functionalized liquid crystals leads to supramolecular self–assembly and thus hierarchically self–assembled structures or, in other words, structures within structures (*Figure 1.3*). Interactions of this type are important because they allow more precise tuning of the microstructure by varying the geometry of small molecules and/or the way of their interaction with the functional block, thus serving as a background for further nanotechnology applications.

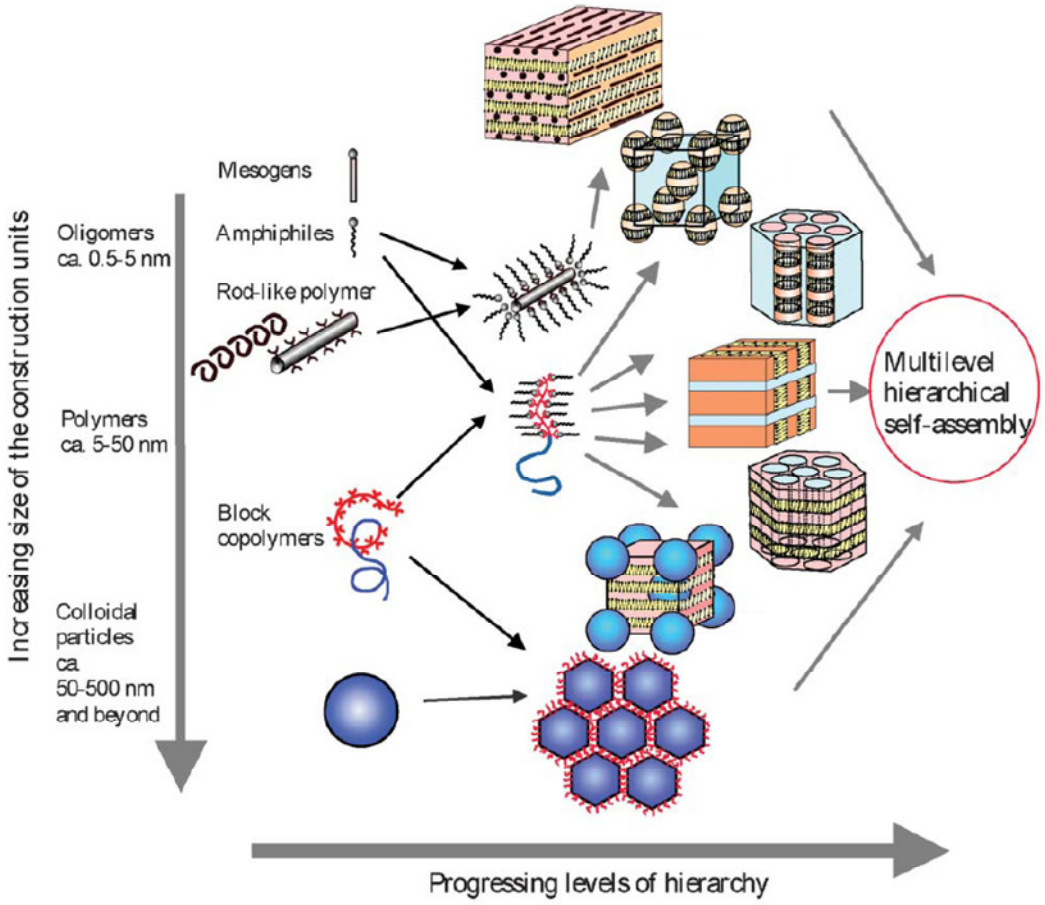

Figure 1.3. Potential scenarios for constructing hierarchically self–assembled block copolymer structures (reproduced from Ref. 9, © 2004 the Royal Society of Chemistry)

In addition, temperature and solvent can be used as tools to control ordered nanoscale structures in interesting ways in supramolecular block copolymer systems. It was observed, for example, that a functional molecule supramolecularly bonded to one of the blocks partially dissolves into the second block at higher temperatures, thus causing a morphology change.[10]

Furthermore, if the bulk nanostructure of a supramolecular block copolymer is rinsed by a solvent in which only the small molecule is soluble, then the core structure

remains intact and nanocavities appear.[9,11] This is one of the ways to obtain well–organized nanoporous materials for potential use as a sorptive material with extremely high surface area or for use in nanomembrane manufacturing.

Using dip– or spin–coating methods, hierarchically self–assembled block copolymer structures of different morphologies can be obtained as thin or thick films on solid surfaces, shown in Figure 4 for polystyrene– poly(4–vinylpyridine) (PS–P4VP) block copolymers where the P4VP is hydrogen–bonded with 1,5–dihydroxynaphtalene[12] and 3–pentadecyl phenol (PDP),[13] respectively, showing nodules and upright cylinders, respectively, of P4VP+(small molecule) in a PS matrix. The film thickness can be controlled by solution concentration, substrate withdrawal rate (dip–coated films), and spinning time/velocity (spin–coated films). After rinsing out the small molecule, the film becomes nanoporous. Depending on the thickness of the initial film, the porous microdomains range from nano–holes (~10 nm depth)[12] to nano–channels (up to 100 nm depth)[13] (*Figure 1.4*). These well–ordered patterns can serve as nanotemplates for particular nanotechnology applications.

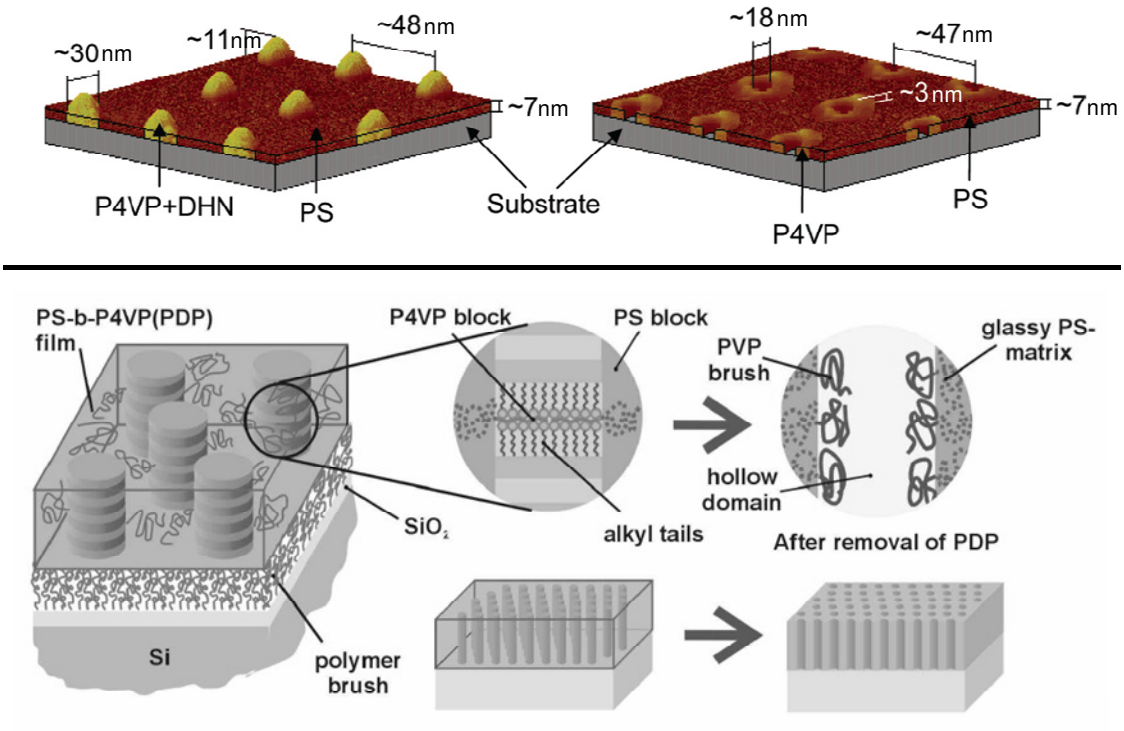

Figure 1.4. The formation of nanopores of different sizes after selective rinsing of 1,5–dihydroxynaphtalene (DHN) (upper image) and of 3–pentadecyl phenol (PDP) (lower image) from dip–coated and spin–coated block copolymer films, respectively {reproduced from Ref. 12 (upper image, © 2006 the American Chemical Society), and from Ref. 13 (lower image, © 2002 the Materials Research Society}

Selective affinity of the small molecules to one of the blocks, either hydrophobic or hydrophilic, is widely used in the preparation of drug–loaded micelles. In general, polymeric micelles have several advantages as drug carriers compared to conventional vaccines that use attenuated or disabled pathogens, proteins or protein subunits. First, polymer–based carriers are applicable to a wide variety of therapeutic agents ranging from hydrophobic substances to metal complexes to charged macromolecules such as polypeptides and polynucleotides.[14] Second, the physical loading of drugs is easy and does not require any chemical modification of the polymeric drug carrier. Third, the preparation

of micelles, simply by varying the solvent system and temperature conditions, requires no special tools and is not time consuming. Finally, high drug loading capacity and controlled drug release can be optimized by modulating the micelle core–forming blocks depending on the chemical properties of the drugs[15] (*Figure 1.5*).

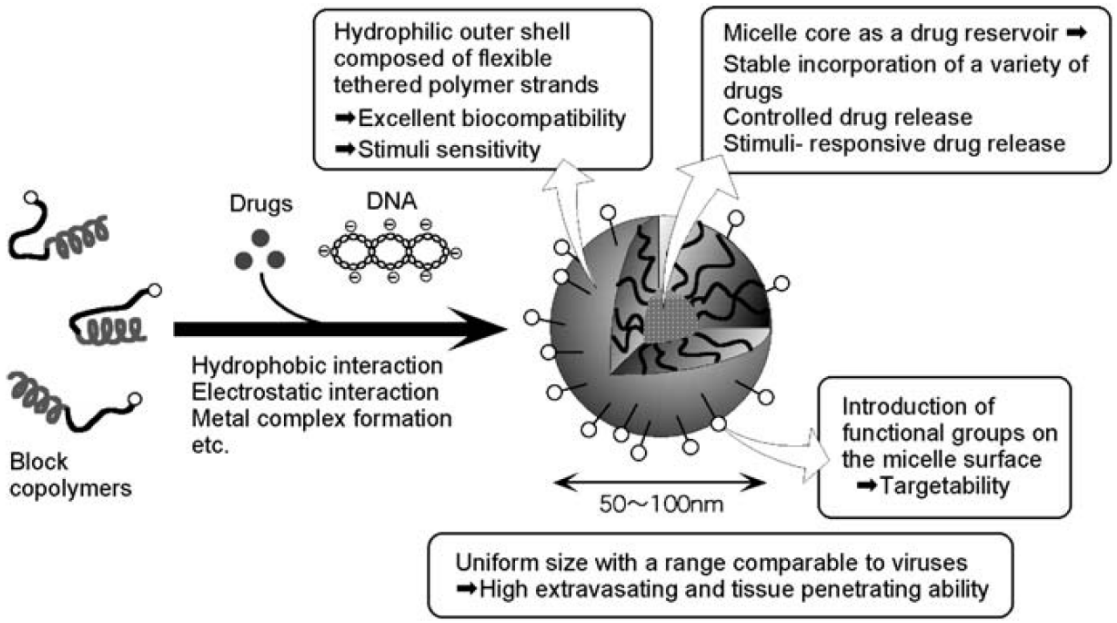

Figure 1.5. Schematic representation of the smart block copolymer micelle concept (reproduced from Ref. 16 with license from Springer)

1.2 Block copolymers in the present work

In our choice of block copolymers, we wanted to combine several characteristics to obtain multi–purpose block copolymers. First, in a view of potential biomedical or biotechnology applications, we wanted the potential polymer blocks to be biocompatible and non–toxic. Second and third, we aimed for the resulting block copolymer to be amphiphilic and include one functional block allowing further modification and/or complexation with functional small molecules like surfactants or functional liquid crystals (of interest to the Bazuin group, who has previously investigated liquid crystalline supramolecular systems involving functional homopolymers).[17,18] A very good candidate as a post–modifiable/ complexable block is poly(2–dimethylaminoethyl methacrylate) (PDMAEMA) which is hydrophilic, biocompatible and provides the needed functionality. Finally, we were interested in a second block that is crystallizable, in view of the Prud'homme group's recent research efforts on confined polymer crystallization in (ultra)thin films, especially involving poly(L–lactide) (PLLA).[19,20] This polymer is of particular interest due to its availability from renewable resources and its relatively high degree of crystallinity. When PLLA and PDMAEMA are covalently linked together, the resulting block copolymer is expected to have excellent biocompatibility, amphiphilic properties, the ability to crystallize, and amine functionality providing an opportunity for chemical modification and supramolecular complexation.

1.3 Polylactic acid and its block copolymers in (bio)technology

Poly(lactic acid) or polylactide (PLA) is an optically active macromolecule that may consist of a single optical isomer, either L– or D–lactic acid (isotactic PLLA or PDLA), or contain both of them in alternating order (syndiotactic PLA) or in random order (racemic PLA, PDLLA), as depicted in *Chart 1.1*.

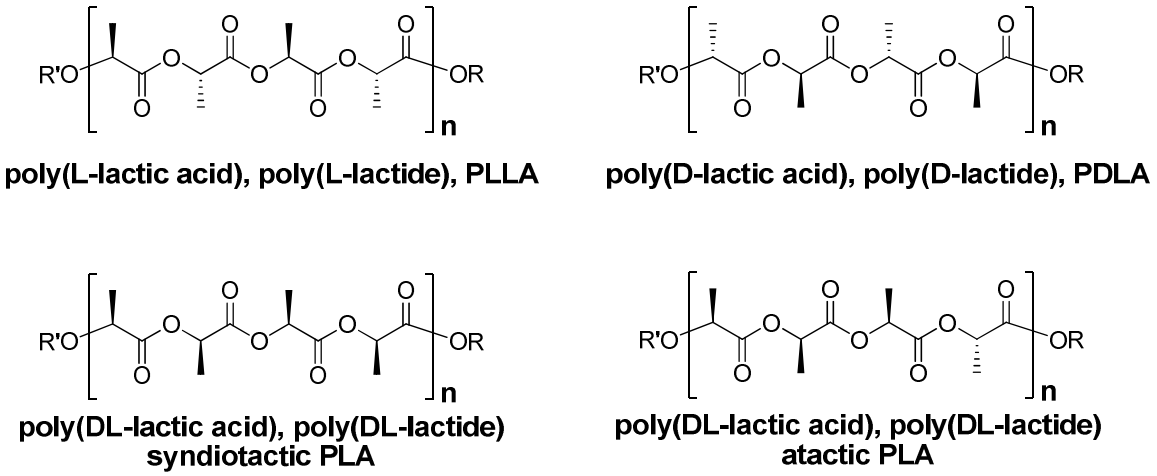

Chart 1.1. Different poly(lactic acid) structures

The natural occurrence of L–lactic acid as the main metabolite in anaerobic fermentation/oxidation of carbohydrates[21] allows industrial scale production of L–lactide (LLA) from renewable resources, pioneered by Cargill Inc.[22] In contrast, D–lactic acid is not available from natural resources and thus D–lactide (DLA) is relatively difficult to obtain. One of the indirect methods towards DLA consists of the separation of crude lactide, obtained by the above method, into LLA and meso–lactide, followed by alcoholysis of the latter catalyzed by enantioselective lipase (Novozym 435) to obtain a mixture of

alkyl D–lactate (further used to obtain DLA) and alkyl L,L–lactoyl lactate.[23] Given that the properties of PLLA are the same as those of PDLA, the utilization of DLA and PDLA is mainly limited to stereocomplex studies.[24,25]

Ring–opening polymerization (ROP) of LLA by Food and Drugs Administration (FDA)–approved Sn(II)–based catalysts facilitates the use of PLLA for environmental applications where recovery of the product is not practical, like agricultural mulch films and bags, as neither the production nor use nor degradation of poly(lactic acid) has a negative environmental impact due to its biodegradability under physiological conditions to carbon dioxide and water.[26] Excellent grease and oil resistance, low temperature sealability and good barrier capabilities for flavours and aromas make PLLA an excellent packaging material, although it is still surpassed by polyethylene and polystyrene in terms of physical properties and cost.[27]

The mechanical strength of semi–crystalline PLLA makes it suitable for suture design,[28] and rheological characteristics of the PLLA melt that can be easily modified by PDLA addition without affecting its biomedical properties[29] create an excellent background for tissue engineering.[30] Non–enzyme hydrolysis and subsequent enzyme biodegradation *in vivo* is also a key property for targeted drug–release applications,[31] and since biodegradation is also a function of crystallinity, utilization of racemic PLA instead of PLLA is one of the ways to control the degradation rate.[32] To additionally increase the rate of degradation, random copolymers of PLA with glycolide (GA) or ε–caprolactone (CL) are often used, as the presence of GA and CL units within the main PLA backbone accelerates and slows down, respectively, the degradation rate of PLA.[16]

One of the main challenges for successful biomedical application of PLA, as well as of other polyesters like polyglycolide (PGA), poly(ε–caprolactone) (PCL) and their copolymers is their hydrophobicity. For drug delivery applications, for example, the hydrophobicity is necessary for encapsulating hydrophobic drugs; however, it also enhances the uptake of drug–loaded nanoparticles (NPs) through the mononuclear phagocyte system (MPS). This results in a short residence time in circulation, and therefore in a decrease in drug efficiency *in vivo*.[33]

To extend the circulation time of hydrophobic NPs *in vivo*, their surface must be hydrophilic. One approach to obtaining a hydrophilic surface is by physisorption of biocompatible cationic polymers onto preformed PLA–based NPs.[34] Furthermore, chitosan, polyethyleneimine (PEI) and PDMAEMA have been adsorbed onto the surface of NPs and studied as DNA carriers. It is worth noting that PDMAEMA–coated NPs showed the highest efficiency of the investigated polymers towards DNA transfection.[35]

Another approach to increase the hydrophilicity of PLA–containing NPs is to combine PLA with a hydrophilic polymer in the form of an amphiphilic block copolymer (ABC) system. These block copolymers spontaneously self–assemble in water to form spherical core–shell micelles with a hydrophobic PLA core and a hydrophilic corona, where the PLA core is capable of carrying hydrophobic therapeutic agents and the hydrophilic corona ensures water–solubility and biocompatibility of the resulting NPs.[16] In addition, PLA–based ABCs were explored for the development of other biomaterials, including in the form of crosslinked hydrogels for use as tissue engineering scaffolds[36] and in the form of self–assembled metal hybrid nanomaterials for use as imaging platforms.[37]

A further challenge is to engineer PLA–based ABCs capable of bioconjugation with ligand biomolecules for targeting specific cells as well as promoting biocompatibility with living cells. This has been approached by designing PLA–based ABCs with functional polymers. The functional groups that have been incorporated with the second block include carboxylic acid [–COOH; poly(acrylic acid)[38] or poly(methacrylic acid)[39]], hydroxyl [–OH; poly(2–hydroxyethyl methacrylate)[40]], amide [–$CONR_2$; poly(N–isopropyl acrylamide)[41], polyacrylamide[42]], and amine [–NR_2; polyethyleneimine[43], PDMAEMA[44]].

1.4 Poly(2–dimethylaminoethyl methacrylate) and its block copolymers in (bio)technology

Water soluble polymers have gained much attention and are undergoing rapid development due to growing concerns with environmental protection. Nonionic [poly(alkylene oxide)] and anionic (polysulfonate, polycarboxylate) polymers were extensively studied over the past three decades. Studies on cationic polyelectrolytes, though not as numerous, are presently a subject of growing interest, with applications in environmental fields like wastewater treatment as well as in biomedical research due to their biocompatibility. Among the known cationic polyelectrolytes, special interest is paid to PDMAEMA due to its DNA–binding ability, and thus great potential in gene transfection applications (Figure 1.6). PDMAEMA properties of interest include hydrophilicity, pH and temperature sensitivity, ease of quaternization, availability of the functional amine/ammonium moiety for complexation with acidic/anionic substances that make it attractive for wide–ranging applications, including as flocculation agents,[45] as biocides,[46] and in gene delivery.[47]

An even wider range of potential applications of PDMAEMA is opened up by its incorporation into block copolymers with either hydrophilic or hydrophobic polymers. The latter leads to amphiphilic block copolymer systems characterized by unique self–assembling properties that can be controlled by external stimuli like temperature, solvent variation and pH. Thus, PDMAEMA diblock copolymers with, for example, various other polymethacrylates,[48 – 53] poly(caprolactone),[54,55] poly(ethylene oxide) or poly(ethylene oxide)–poly(propylene oxide),[56] polystyrene,[57,58] poly(2–vinyl pyridine),[59] and poly(ethylene–co–butylene)[46] were synthesized and studied in the past two decades.

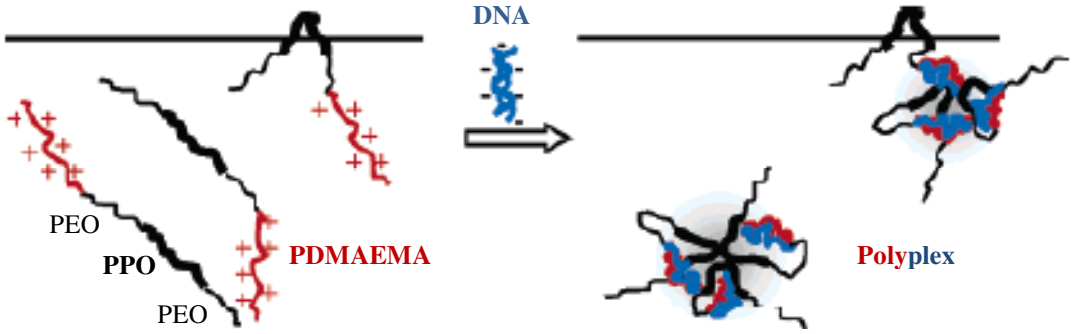

Figure 1.6. Schematic representation of cationic block copolymer–DNA association (reproduced from Ref. 56, © 2005 the American Chemical Society)

Recently, synthesis and studies on block copolymers composed of PLA and PDMAEMA in different architectures have been reported. Possessing an amphiphilic nature, such block copolymers can serve as a host for both hydrophilic and hydrophobic guest molecules. For example, polysaccharides grafted with PLLA–b–PDMAEMA were tested for perfume or flavour ingredient encapsulation.[44] Drug–encapsulating[60] and pH–responsive behaviour[61] of star–block copolymers, as well as of linear block copolymers[62,63]

were also studied. Results of these studies indicate that this relatively new block copolymer system has much potential. From a synthetic point of view, the relatively low molecular weight of the incorporated PLA block (<10,000 g/mol) to date makes further development of this system attractive.

1.5 Methods of controlled (L)LA polymerization

1.5.1 General overview

Monomeric lactic acid, as was mentioned in §1.3, can be converted into polymer by polycondensation, but due to the difficulties in removing traces of water produced by the polycondensation reaction, only low molecular weight prepolymer (~ 5000 g/mol) is achievable.[27] High molecular weight PLA is obtained instead by catalytic ROP of lactides, the latter produced by thermal cracking of the polycondensed PLA prepolymer. In the industrial process developed by Cargill Inc., high temperature tin catalysis is used to depolymerize low molecular weight prepolymer into a stereomixture of lactides. This is then vacuum distilled to isolate the lactide, followed by ROP in a continuous process with only H_2O as a side–product.

ROP of lactide can take place by anionic,[64] cationic[65] or coordination–insertion[66] mechanisms, depending on the catalytic system used. In anionic polymerization, to avoid racemization of LLA, lower temperatures are desirable, and since this polymerization is done in solution, the maximum molecular weight of the resulting PLA is limited due to solubility issues. Furthermore, methoxide–mediated anionic polymerization of lactide

(*Scheme 1.1*) is highly sensitive to any protic molecule, including water and open lactide that can lead to chain termination and/or catalyst deactivation.

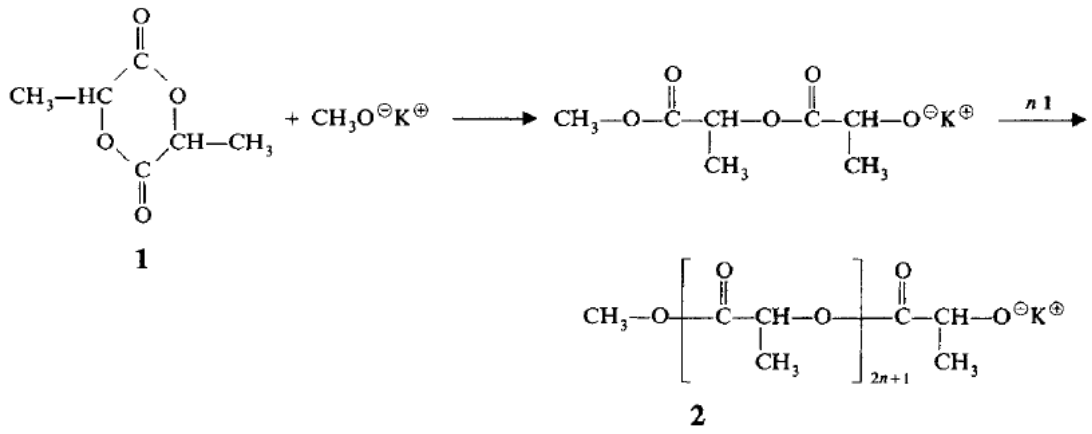

Scheme 1.1. Mechanism of anionic polymerization of LLA (reproduced from Ref. 64 with license from John Wiley & Sons)

To date, the only catalyst that has proven to be successful in cationic ROP of LLA is trifluoromethanesulfonic acid (TFMSA).[67] As shown in *Scheme 1.2*, it proceeds through an activated monomer mechanism that involves protonation of the oxygen atom in the cycle.[68] It may also involve protonation of the carbonyl oxygen, but this does not affect the reaction course.[69] As deduced from the low extent of transesterification, trifluoromethanesulfonic acid selectively activates the monomer, and not the polymeric chain. No racemization has been observed using this polymerization. PLLA obtained by cationic polymerization showed higher thermal and hydrolytic stability compared to linear PLLA of similar molecular weight obtained with the ROH/Sn(Oct)$_2$ initiating system discussed below.[70,71] This is explained by the cyclic nature of the resulting polymer (that is more stable than linear), as the two terminal HO– and CF_3SO_2COO– groups allow efficient

end–to–end cyclization.[68] This can be avoided by conducting cationic polymerization of LLA by TFMSA in the presence of a protic agent, such as 2–propanol. The maximum molecular weight reported using cationic polymerization was 18,000 g/mol (PS standards, no correction factor applied).[69]

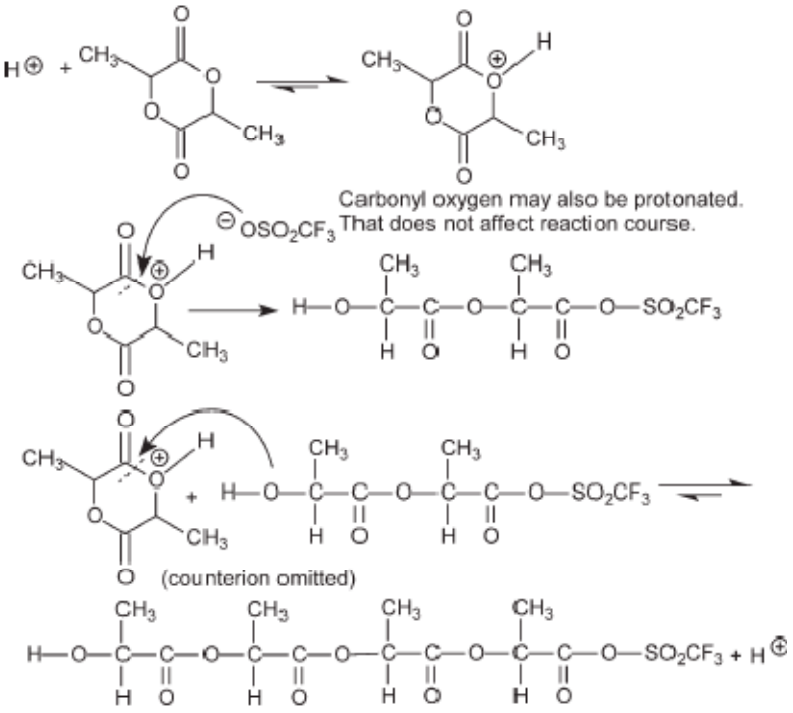

Scheme 1.2. Mechanism of cationic polymerization of LLA (reproduced from Ref. 68 with license from John Wiley & Sons)

Unlike ionic polymerization, coordination–insertion polymerization of lactide by metal compounds, including metal complexes, can be conducted in the bulk at higher temperatures (up to the melting temperature of the resulting PLLA), giving high molecular weight polylactides in high yields and, for some catalytic systems, with minimal racemization or transesterification. The greatest concern is related to the presence of metal

ion residue in the final product when used for biomedical applications. Residues of Ca, Mg, Fe and Zn ions are not a problem, since they are involved in human metabolism. Unfortunately, catalysts based on these metals tend to produce low molecular weight polymers and significant racemization, limiting their usefulness.[72] However, the catalysis of LLA (co)polymerization by calcium complexes with Schiff–base tridentate ligands[73] was considered to be successful with good control over stereochemistry and molecular weight distribution, despite some yield issues. The most promising results in cyclic lactide/lactone polymerization have been achieved using two catalytic systems, aluminium alkoxide(s) and tin 2–ethylhexanoate, described in detail in the next two sections.

1.5.2 Aluminium alkoxide–mediated ROP

Aluminium alkoxide–mediated polymerization of cyclic esters was first filed by Cox and Hostettler in 1959.[74] The high potential of the newly described catalytic system was based on the wide range of suitable catalyst concentrations (relative to the monomer) and the wide temperature range of polymerization, preferably conducted in solution.

Aluminium butoxide R–Al$(OBu)_2$, as part of the bimetallic (Al, Zn) μ–oxoalkoxide system, was first tested by the group of Teyssié.[75] Living character, along with the relatively good control over polydispersity (1.3–1.5) was shown for CL. It was also noted that only one of four alkoxide groups in the catalyst of formula $(C_4H_9O)_2Al–O–Zn–O–Al(OC_4H_9)_2$ takes part in PCL chain formation, presumably due to the known coordination association behaviour of alkoxide units[76] that was successfully overcome by addition of C_4H_9OH.

Mechanistic studies on the aggregation of aluminium alkoxide and its influence on the polymerization process was carried out on aluminium isopropoxide $Al(OiPr)_3$ by Duda and Penczek, and involved polymerization of CL[77]] and LLA.[78] Trimer and tetramer aggregates (*Chart 1.2*) were found to be the most stable forms that usually appear during vacuum distillation (common way of purification) of $Al(OiPr)_3$.

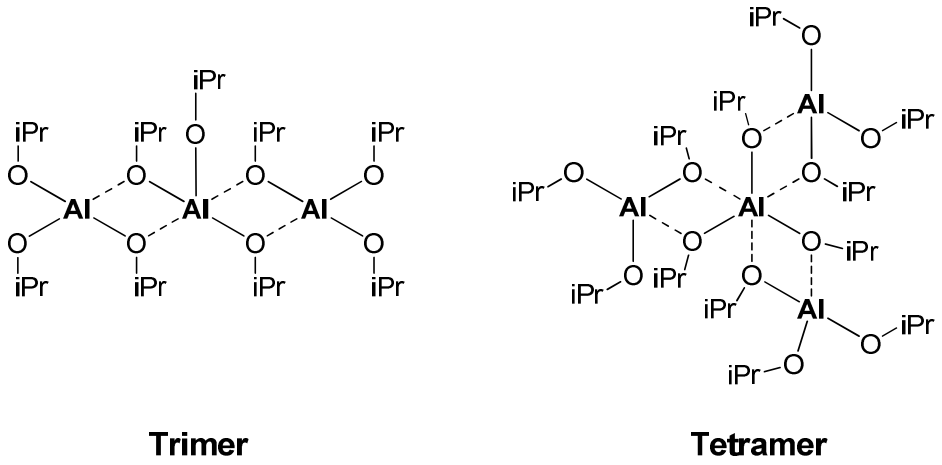

Chart 1.2. Chemical structures of the trimer and tetramer of aluminium isopropoxide

Trimer aggregates, which predominate, are much more reactive than tetramer aggregates. Thus, in the case of CL, tetramer aggregates remain in the post–polymerization mixture, and the molecular weight of the PCL obtained does not correspond well to the initial monomer/Al ratio. It was observed that the rate of interchange between the trimer and tetramer aggregates is slow compared to the propagation rate of CL. Therefore, it was concluded that during CL polymerization only the trimer aggregates were consumed completely, whereas the tetramer aggregates remained unreacted, at least within the time required for complete CL polymerization. In the case of LLA (*Scheme 1.3*), the

polymerization process did not depend on $Al(OiPr)_3$ aggregation and the molecular weight of the final PLLA was in good agreement with that expected from the initial monomer/Al ratio. This was explained by the lower reactivity of LLA compared to that of CL, giving more time for the tetramer aggregates to be transformed into more reactive trimer. Only 2% tetramer was found in the post–polymerization mixture after complete consumption of LLA.

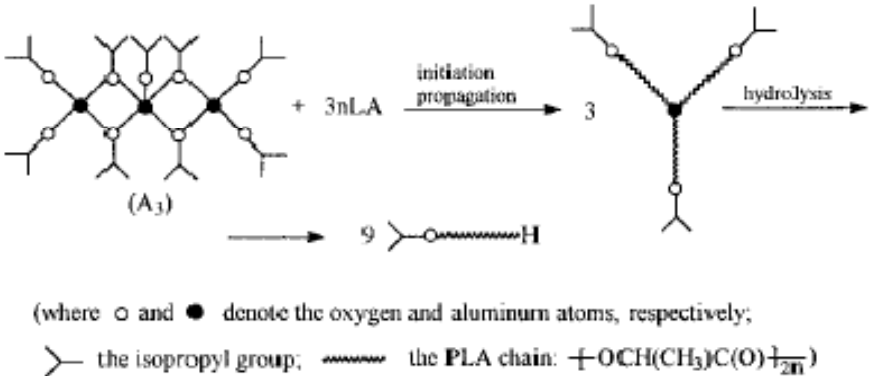

Scheme 1.3. Simplified mechanism of LLA polymerization by aluminium isopropoxide (reproduced from Ref. 78, © 1998 the American Chemical Society)

Detailed kinetic studies of LLA polymerization catalyzed/initiated by $Al(OiPr)_3$ was undertaken by Dubois et al.[79] It proceeds well at 70 °C in toluene, and is accompanied by very low or no racemization of the monomer, and is thus suitable for stereocontrolled LLA or DLA polymerization. Narrow polydispersity (1.1–1.4) and the ability to predict the molecular weight from the monomer/Al molar ratio is indicative of the living character of the polymerization. It was also shown, from the slope of the linear dependence of the degree of polymerization on the monomer/Al ratio, that for LLA each of the three alkoxide

units participates in the LLA polymerization. However, at higher temperature (>90 °C), or when the molecular weight exceeds 77,000 g/mol ([LLA]/[Al] > 1600), secondary intra– and intermolecular transesterification reactions of the growing chains are responsible for limiting the molecular weight of PLLA and account for a non–living process.

1.5.3 Tin (II) octoate mediated ROP

Tin (II) 2–ethylhexanoate [tin octoate, $Sn(Oct)_2$] is the most commonly used catalyst for bulk and solution preparation of poly(lactic acid) for several reasons. First, $Sn(Oct)_2$ is a highly efficient catalyst and allows high conversions even at monomer/catalyst ratios as high as 80000:1.[80] Second, tin octoate does not induce racemization of LLA, and optically pure PLLA can be prepared even at 150 °C during several hours.[81] Third, it is soluble in molten LLA, thus allowing controlled polymerization in the melt (bulk). Finally, $Sn(Oct)_2$ is an approved food additive in numerous countries, meaning that its toxicity is much lower compared to other heavy metal salts. What greatly favours tin octoate over aluminium–based catalysts is that aluminium derivatives were found to have neurotoxic effects and may be a factor in the development of Alzheimer′s disease.[82]

The mechanism of $Sn(Oct)_2$–mediated ROP of LLA (*Scheme 1.4*), though initially controversial,[71] has been resolved and involves the interaction of tin octoate with alcohol (co–initiator) to form tin alkoxide, which is the true initiator. This was shown by the observation (through NMR spectroscopy) that the molecular weight of the PLLA obtained depends on the LLA/alcohol ratio and not on the LLA/Sn ratio. Coordination–insertion

polymerization proceeds as a living process allowing good control over polydispersity and molecular weights up to 500,000 g/mol .[83]

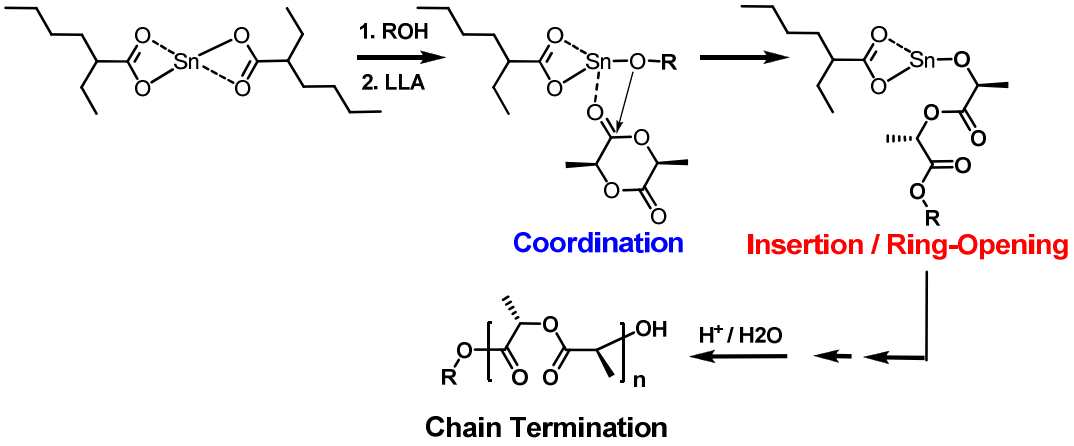

Scheme 1.4. Simplified coordination–insertion mechanism of the ROP of LLA by $Sn(Oct)_2$

1.6 Methods of controlled DMAEMA polymerization

For studies of PDMAEMA as a homopolymer where narrow polydispersity and precise molecular weight are not required, such as investigations of acid–base properties and hydrolytic stability[84] or the preparation of cross–linked composite membranes for gas separation,[85] the least expensive and fastest method is free–radical polymerization of DMAEMA initiated by 2,2′–azo–bis–isobutyronitrile (AIBN).

However, for applications requiring narrow polydispersity, such as block copolymerization, only controlled polymerization techniques are suitable. The controlled polymerization methods that have been applied towards PDMAEMA preparation are anionic polymerization,[50] group–transfer polymerization (GTP),[86] reversible addition–fragmentation chain transfer polymerization (RAFT),[87] and atom–transfer radical

polymerization (ATRP).[88] Despite the advantages of the first two methods, some complications like side reactions on the ester function during anionic polymerization,[89] and the limited applicability of GTP to monomers without conjugated carbonyl groups hinder the versatility of these techniques in block copolymer synthesis.[90]

In RAFT polymerization (*Scheme 1.5*), a thiocarbonyl compound (RAFT agent) plays the role of the dormant species and the propagating radicals add to the sulfur of the thiocarbonylthio center producing a carbon–centered radical. This radical can then undergo β–scission to either form a new radical capable of initiating polymerization or re–form the propagating radical. As a result, the RAFT agent is converted into a poly–RAFT agent in symmetrical equilibrium with the propagating radical. Though proven successful for the polymerization of various functional monomers, including DMAEMA,[87] RAFT polymerization is not very popular because RAFT agents are not commercially available (except dithiocarbamate) and have to be prepared prior to polymerization. Moreover, to achieve good control of the polymerization, the reactivity of the RAFT agent must match the reactivity and stability of the propagating polymer radical.[91]

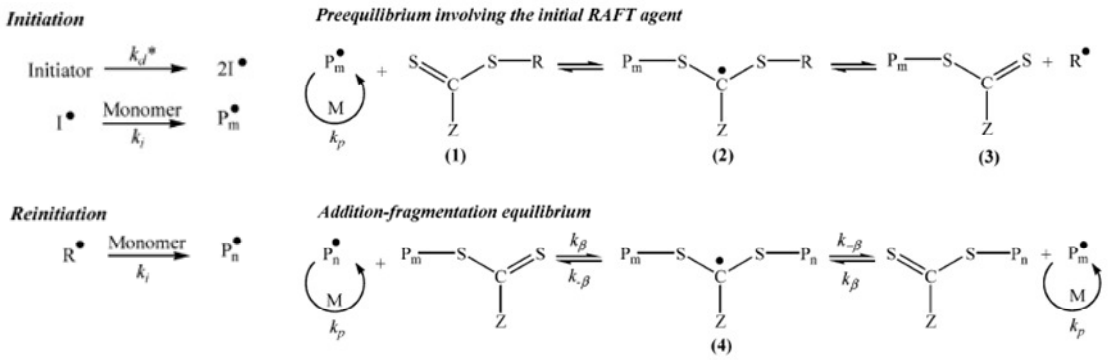

Scheme 1.5. Mechanism of RAFT polymerization (reproduced from Ref. 92, © 2002 the American Chemical Society)

As for ATRP, the most important component is the catalyst. The main prerequisites for an efficient transition metal catalyst are two readily accessible one–electron oxidation states and reasonable affinity towards a halogen. Transition metals from groups VI–X of the Periodic Table, while they fulfill the basic requirements, cannot compete with copper (group XI) in terms of versatility and cost.[93]

The key equilibrium in copper–mediated ATRP is shown in *Scheme 1.6* and consists of the following steps. Oxidative addition of copper (I) chloride or copper (I) bromide (activator) to secondary or tertiary alkylbromide (dormant species) leads to the formation of a copper (II) compound and a free radical capable of initiating the polymerization of the monomer. Radicals react with the oxidized copper complex to reform the dormant species and the activator. This equilibrium, which is strongly shifted towards dormant species, is responsible for the uniform growth of polymer chains. According to the reaction scheme, copper (II) acts as a deactivator, and at the early stages of polymerization its concentration might not be sufficient for a rapid rate of deactivation, so that radical

coupling may occur leading to chain termination and the accumulation of Cu(II) in the system. Initial addition of Cu(II) (ca. 10 mol % relative to the activator), although it slows down the overall rate of ATRP, greatly reduces the amount of terminated chains, reducing the polydispersity, especially for polymerization in the bulk.[93] The possibility of conducting ATRP in a variety of solvents, including water[94] and supercritical carbon dioxide,[95] easily accessible initiators, and superior versatility and catalytic activity of copper catalysts in the polymerization of virtually any vinyl monomer have made ATRP a major tool in controlled preparation of polystyrenes, poly(meth)acrylamides, poly(meth)acrylates, etc.

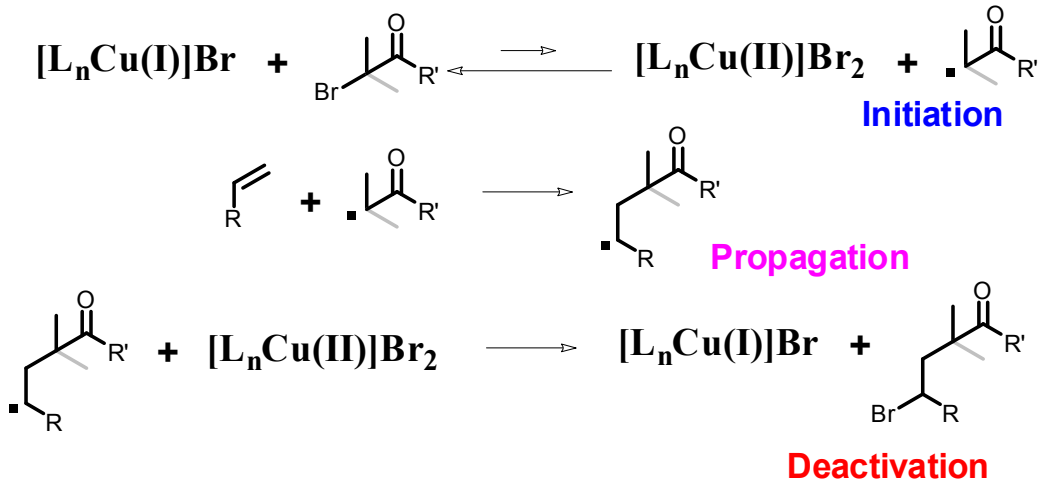

Scheme 1.6. Simplified mechanism of ATRP of vinyl monomers by Cu(I) complex

Typically, the polymerization of DMAEMA by ATRP is initiated by bromo–(iso)butyryl esters and catalyzed by CuBr or CuCl ligated by 1,1,4,7,7–pentamethyldiethyl-enetriamine (PMDETA), 1,1,4,7,10,10–hexamethylenetriethylenetriamine (HMTETA), or aromatic amines like 2,2′–bipyridyl and its derivatives.[88] The choice of ligand is dictated

mainly by the solvent used for polymerization. For some polymerizations, Cu(II) is added to control possible chain termination and to decrease the polydispersity,[46] as explained above.

1.7 Block copolymer synthesis

1.7.1 General approaches

Aside from the synthesis of block copolymers by coupling two properly functionalized homopolymers (known as "click" chemistry)[96–98] to obtain diblock or multiblock copolymers, there are three basic approaches towards block copolymer polymerization, as summarized in *Figure 1.7*.

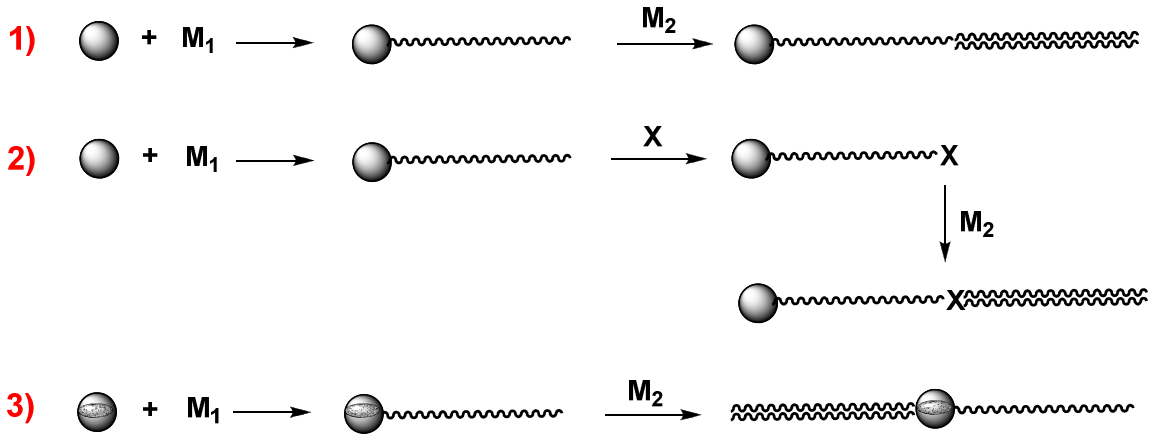

Figure 1.7. Generalized approach towards block copolymer synthesis

Path 1, or sequential monomer addition, is used to prepare block copolymers when both monomers are polymerized using the same polymerization method. The first block may or may not be isolated before addition of the monomer for the second block.

Path 2, a three–step process, is used to combine blocks requiring different polymerization methods, and where terminal group modification of the first block polymerized is needed to provide the initiating site ("macroinitiator") for the next polymerization. Generally speaking, this approach is much more versatile than **Path 1**, since it allows combining substantially different polymers in one block copolymer. The main limitation is the necessity to modify appropriately the terminal group by a clean reaction giving easily removable small molecule side–products (if any) and 100% yield to ensure completeness of the terminal group modification. If unmodified polymer remains, it will be present in the final product as a homopolymer impurity.

Path 3, or the bifunctional initiator approach, implies the use of a dual–function molecule that can initiate both polymerizations of choice. One advantage is that this avoids the terminal group modification step in **Path 2**, which must be neat and quantitative, as opposed to small molecule synthesis for the preparation of a bifunctional initiator. Moreover, the introduction of the two different initiating sites in one molecule allows the preparation of block copolymers that are inaccessible through **Path 2** if appropriate terminal group modification is not possible or that are more challenging if synthesis of a modifying agent is required. In choosing the polymerization types, one must ensure that each polymerization takes place independently, and that no interaction between terminal functional units of growing chains occurs in either polymerization condition. In cases

where both monomers polymerize at similar temperatures and there is no interaction between the catalysts, there is the possibility of conducting both polymerizations simultaneously. In this case, the desired block ratio can be tuned by the monomer feed.

1.7.2 PLA–based block copolymers: sequential monomer addition

Sequential monomer addition allows for the preparation of block copolymers of PLA with other polyesters, such as PGA or PCL.[99] Interestingly, the sequence of monomer addition plays a critical role in the case of LLA and CL block copolymerization. Block copolymers are obtained if CL is polymerized first and then LLA. If LLA is polymerized first, then, depending on the catalyst used, polymerization of CL either does not take place at all (aluminium isopropoxide catalyst),[100] or random copolymers are formed due to transesterification reactions (tin octoate catalyst).[101] Presumably, it is because the reactivity of the PLA–derived secondary hydroxyl end groups is much lower compared to the PCL–derived primary hydroxyl end groups.

1.7.3 PDMAEMA–based block copolymers: sequential monomer addition

The preparation of PDMAEMA–based block copolymers with other vinyl monomers using sequential monomer addition has been reported for the major controlled polymerization techniques. RAFT sequential block copolymerization of DMAEMA and potassium acrylate,[87] with the PDMAEMA block prepared first, indicated a low initiating efficiency of the PDMAEMA macroinitiator, and after completion of the potassium acrylate polymerization, the final product had to be purified from unreacted PDMAEMA

homopolymer by selective precipitation into chloroform. Sequential anionic block copolymerization of DMAEMA and methyl methacrylate (MMA)[50] or tert–butyl methacrylate (tBMA)[51] required the presence of LiCl as a scavenger of associated polymeric ion pairs, since associated ion pairs react more slowly than non–associated ion pairs, resulting in increased polydispersity. In block copolymerization of DMAEMA with other methacrylates by GTP,[102] it was found that the nature of the alkyl groups in the second methacrylate block plays a crucial role, and low reactivity (ex. tBMA) limits the molecular weight of the second block.

Utilization of ATRP in the synthesis of DMAEMA–based block copolymers has been reported to be free from complications like incomplete initiation or dramatically different polymerization kinetics of different monomers [ex. Refs 52 and 58]. Mild conditions of polymerization, moderate reaction times and controlled living character has made ATRP the major technique used to prepare block copolymers of DMAEMA in a controlled manner with low to moderate polydispersity.

1.7.4 PLA– and PDMAEMA–based block copolymers: three–step synthesis

The three–step method or, in other words, the mechanism transformation, although allowing the preparation of block copolymers by a combination of different polymerization techniques, is nevertheless limited in the choice of polymerization mechanisms that can be combined. Esterification of the terminal hydroxyl group of ROP–prepared polyesters with bromoalkyloyl bromide provides an initiating site for subsequent ATRP.[103] The most commonly used reagent for this modification is 2–bromoisobutyryl bromide (BIB), and

recently this approach was used to combine PLA with PDMAEMA in the form of graft diblock,[44] star diblock,[60] and linear diblock[62,63] copolymers. Furthermore, using a customized modifying agent, ROP of LLA and CL initiated by a pentaarm alcohol initiator can be followed by RAFT polymerization of DMAEMA to produce star multiblock copolymers.[61]

PLA–based and PDMAEMA–based block copolymers with a poly(3–hexylthiophene) (P3HT) block have been prepared by combining Grignard metathesis polymerization with ROP[104] and ATRP,[105] respectively. The P3HT block was prepared first and then functionalized by a hydroxyl end–group. The P3HT–OH obtained was either used directly for subsequent ROP of lactide (*Scheme 1.7*) or further treated by BIB to transform P3HT–OH into P3HT–Br and used as a macroinitiator for subsequent ATRP of DMAEMA (*Scheme 1.8*).

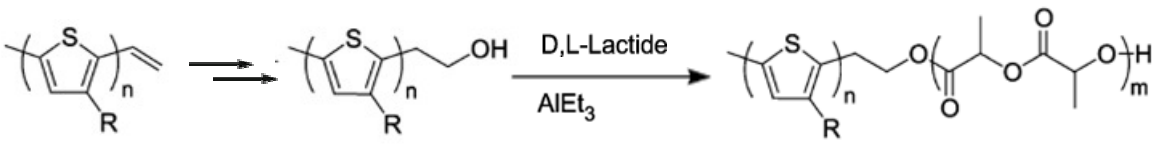

Scheme 1.7. Introduction of a terminal –OH group into P3HT followed by lactide polymerization (adapted from Ref. 104, © 2008 the American Chemical Society)

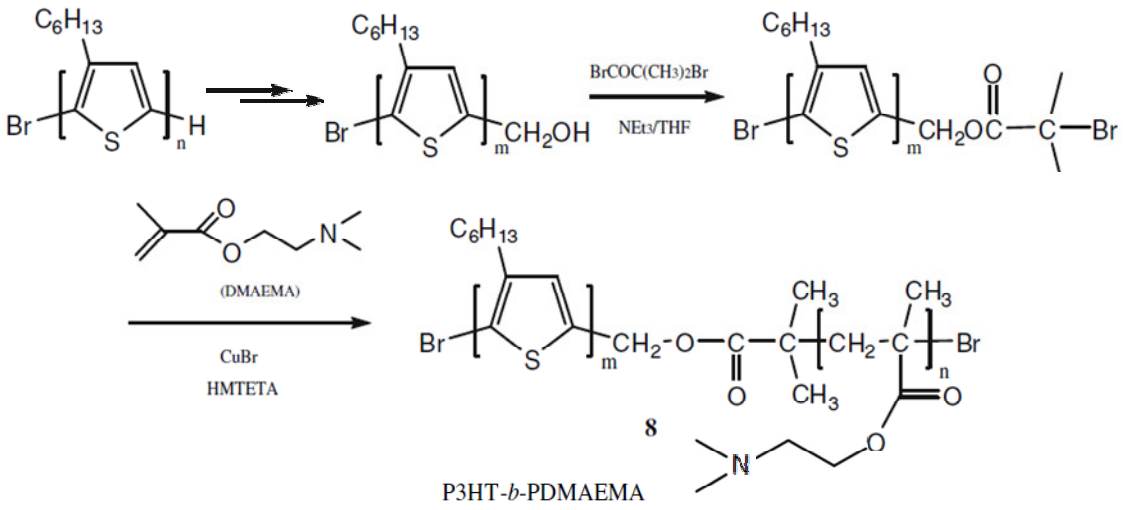

Scheme 1.8. Introduction of terminal –Br group into P3HT followed by the DMAEMA polymerization (adapted from Ref. 105 with license from Springer)

1.7.5 PLA– and PDMAEMA–based block copolymers: double–initiator approach

Instead of modifying the terminal group of one polymer to make it suitable to initiate the polymerization of the next block, both initiating moieties for the different polymerizations can be combined in one small molecule. Some examples are given in *Chart 1.3*. A simple bifunctional initiator that is available commercially is thioethylene glycol, $HSCH_2CH_2OH$, used for successive RAFT of N–isopropylacrylamide (NIPAAM) and ROP of DL–lactide.[41] More advanced custom bifunctional initiators for ROP and RAFT were used for synthesizing PS–b–PLA, PMMA–b–PLA, PDMAEMA–b–PLA diblock copolymers[106] and PLA–b–PNIPAAM–b–PLA triblock copolymers.[107]

Initiating sites for ROP and nitroxide–mediated polymerization (NMP) were also combined, and, depending on the catalyst used for ROP, the polymerizations were

conducted successively[106] or simultaneously[108] to yield diblock copolymers. However, the most straightforward and most commonly used combination of polymerizations is ROP and ATRP. The ease of the bifunctional initiator preparation for this combination,[54] the versatility of ATRP, and the choice between aluminium– or tin–mediated ROP allows obtaining diblock copolymers by both successive,[40,109] and simultaneous[110,111] ROP and ATRP.

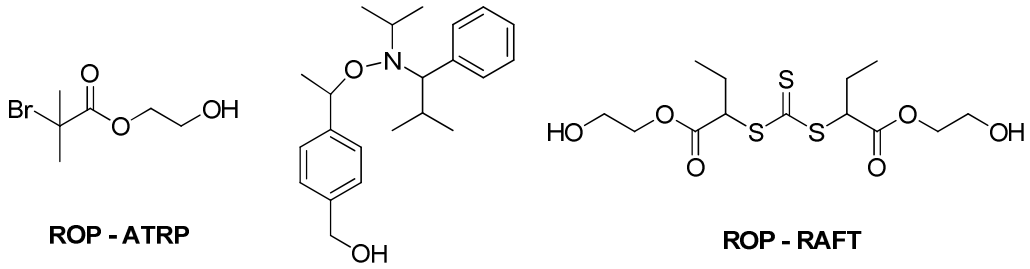

Chart 1.3. Representative examples of bifunctional initiators for selected block copolymerizations

1.8 Crystallization behaviour of PLLA or PDLA

1.8.1 General

Polylactide in its isotactic form (PLLA or PDLA) is a semi–crystalline material that crystallizes in a temperature region between its glass transition (T_g) and melting (T_m) temperatures. The molecular weight dependence of T_g and T_m levels off at ca. 15,000 g/mol, where T_g = 60 °C, and the maximum reported T_m for a 1,000,000 g/mol molecular weight PLLA, crystallized for 384 h at 100 °C, is 188 °C.[70] The reported enthalpy of melting for maximally crystallized PLLA is 65 J/g, which corresponds to 71% crystallinity

(assuming that the melting enthalpy of the infinite PLLA crystal is 91 J/g).[112] Random incorporation of DLA units into the PLLA backbone dramatically decreases its ability to crystallize. Specifically, the incorporation of more than 15% DLA completely prevents PLLA crystallization.[27] The specific optical rotatory power for optically pure PLLA was reported to be –157°.[113]

Crystal growth kinetics of the PLLA homopolymer can be determined by application of Avrami equation

$$1 - V_c = \exp(-Kt^n) \quad (1)$$

to the experimental data obtained from isothermal crystallization, where V_c is the volume crystallinity that represents the crystallized fraction of PLLA, K is the overall crystallization rate constant and n is the Avrami index. The latter is composed of two terms:

$$n = n_d + n_n, \quad (2)$$

where n_d is the dimensionality of the growing crystals, and can only have the integer values 1, 2 and 3, corresponding to one–, two– and three–dimensional crystallization, respectively. The term n_n represents the time dependence of nucleation and, ideally, can only have the values of 0 and 1, corresponding to instantaneous (e.g. at large supercooling) and sporadic (at small supercooling) nucleation, respectively.[114] The constants in the Avrami equation can be obtained by taking the double logarithm of *Eq. (1)*:

$$\log[-\ln(1-V_c)] = n \log t + \log K. \quad (3)$$

For PLLA, the usual values of the Avrami index n are 3 and 4, corresponding to spherulites (three–dimensional aggregates of radial lamellas), obtained at small (sporadic nucleation) and large (instantaneous nucleation) supercoolings, respectively.[115] However, in

many cases, the Avrami index has a noninteger value, and one of the explanations is that the nucleation is intermediate to being completely instantaneous and completely sporadic.[116]

1.8.2 Crystallization behavior of PLLA (PDLA) in blends with other polymers

Polymer blends are a class of multicomponent systems that gained much attention due to the cost–effective modification of physical properties of polymers not requiring chemical modification. Impact strength, rigidity, processability and other macroscopic properties can be modified through an appropriate choice of the second polymer. Depending on the compatibility of the blended polymers, important physical characteristics like density, glass transition temperature and crystallinity can be tailored according to needs relatively easy.

Blending of PLLA with other polymers usually aims at improving its hardness, reducing its brittleness, and controlling biodegradability.[117] Miscibility is not always required for eventual biomedical applications, as the degradation rate depends on the surface interaction between the material and its environment, and the accessibility of the inner surfaces can be controlled by the blend composition, as simulated by percolation theory.[118]

To improve the processing characteristics of PLLA, solution blending of PLLA with flexible microbially fermented poly(hydroxybutyrate–co–hydroxyvalerate) (PHBV) was used to obtain films that appeared homogeneous, but, as these polymers are immiscible, actually were pseudohomogeneous.[119] Although the dried blend was characterized by two distinct T_gs and a PLLA melting temperature that did not depend on the blend composition,

as is typical of immiscible systems, a gradual decrease in the total melting enthalpy with a decrease in PLLA content, as well as some broadening of the T_g region of PHBV, indicated that part of the PLLA, attributed to a low molecular weight fraction, is dispersed and/or miscible within the PHBV matrix.[120] This allows the formation of a larger interfacial area between the two polymers that enhances the stability of the blend relative to simple physical dispersion.

Blending of PLLA with natural polymers will maintain the overall biodegradability of the system, and also add hydrophilic properties. The blends of PLLA with the most abundant natural polymers, chitosan,[121] starch and talc,[122] also reduce the cost of PLLA–based materials. Although such blends compromise the mechanical properties of PLLA, studies of crystallization kinetics showed that starch and talc increase the rate of PLLA crystallization. In these essentially immiscible blends, starch and talc nanoparticles serve as effective nucleating agents. Thus, a significant increase in the crystallization constant (by several orders of magnitude) was observed at 1 wt % of talc, although accompanied by a decrease in overall degree of crystallinity. For starch, the largest increase in crystallization rate was observed at 40 wt % and the degree of crystallinity was hardly affected. Little influence of these PLLA additives on the maximum melting temperature was observed.[122]

Blending of polylactides of different tacticity has also found an application in modifying the physical properties of PLLA. Thus, optically pure PLLA and PDLA, when mixed together, form a new crystalline phase with a melting temperature of ca. 50 °C higher than the T_m of each initial enantiomer.[24] The term “stereocomplexation” was introduced[25] for this phenomenon, and the thermal and crystalline properties of

PLLA/PDLA stereocomplexes were studied in detail.[19,20,123] Interestingly, the incorporation of a small amount of PDLA enhances the crystallization behaviour of PLLA due to the formation of stereocomplex nanocrystals that serve as nucleating agents.[124]

The crystallization behaviour of PLLA–based miscible blends strongly depends on the state (soft or hard) of the second component at the temperature of PLLA crystallization. PLLA crystallization in a soft environment can be exemplified by the PLLA/PEO blend.[125] The melting temperature of PEO lies in the glass transition region of PLLA, and it was found that the presence of the molten PEO enhances crystallization of the PLLA, increasing both the crystallization rate and the degree of crystallinity. Crystallization in a hard environment can be exemplified by the PLLA/poly(vinyl alcohol) (PVA) blend.[126] The melting temperature of PVA is ca. 230 °C, and crystallization of PLLA is enhanced in the presence of the crystallized PVA; i.e., the degree of crystallinity and the melting temperature of PLLA both increase in blends containing up to 20 wt % PVA, followed by a decrease at higher PVA content.

1.8.3 Crystallization behavior of PLLA in block copolymers

Block copolymerization of PLLA with other polymers is another way (although much more costly than blending) to modify its physical properties, and, in particular, crystallization behaviour, without the problems of macrophase separation that become apparent at elevated molecular weights for otherwise miscible systems. Depending on the properties of the second block, different morphology development scenarios can be involved in the formation of the final crystallized structure.

Figure 1.8 shows an example of PLLA crystallization in a lamellar–forming PS–b–PLLA system, where PS is amorphous. The T_{ODT} of this block copolymer is ca. 400 °C, as predicted using small–angle X–ray scattering (SAXS), and is much higher than the melting point of the PLLA block, which is ~150 °C (determined by SAXS). The block copolymer is also characterized by strong segregation, so that the lamellar morphology is conserved in the melt. The T_g of PS block is ca. 85 °C.[127] These characteristics allow studying the effect of crystallization on the melt morphology in conditions of either hard or soft confinement, by crystallizing below and above the T_g of PS.[128]

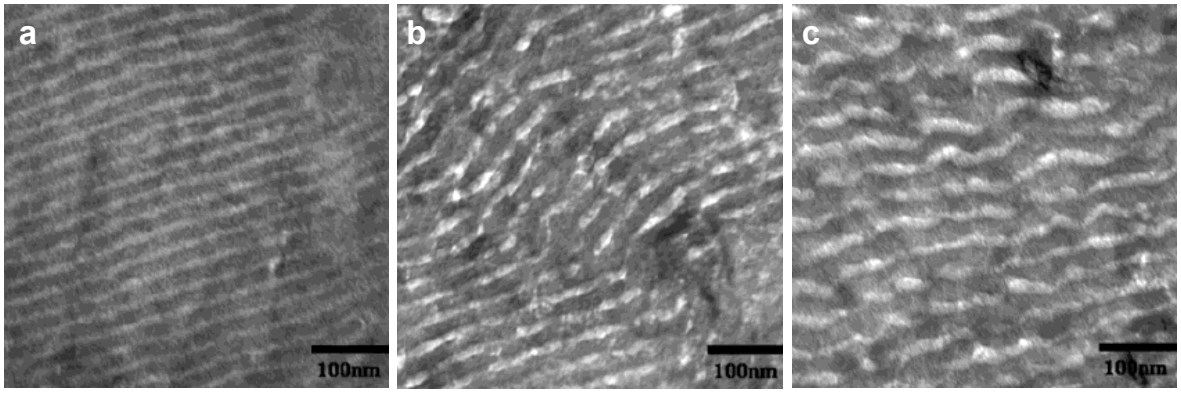

Figure 1.8. Transmission electron microscopy (TEM) micrographs of unoriented PS(30,000)–b–PLLA(19,000) samples crystallized at a) 70 °C ($T_{c(PLLA)} < T_{g(PS)}$), b) 85 °C ($T_{c(PLLA)} \approx T_{g(PS)}$) and c) 100 °C ($T_{c(PLLA)} > T_{g(PS)}$) (adapted from Ref. 128, © 2004 the American Chemical Society)

When the sample is crystallized at 70 °C (below the PS T_g), the lamellar morphology is preserved (*Figure 1.8a*), which is typical of hard confinement crystallization ($T_{c(PLLA)} < T_{g(PS)}$). Crystallization at 85 °C (soft confinement, $T_{c(PLLA)} \approx T_{g(PS)}$) leads to partial distortion of the repetitive structure, although the overall lamellar morphology was

preserved (*Figure 1.8b*). Surprisingly, when the crystallization temperature is raised to 100 °C (soft confinement, $T_{c(PLLA)} > T_{g(PS)}$), a unique "undulated" morphology is obtained (*Figure 1.8c*). Crystallization kinetics studies showed some retardation of the crystallization process under confinement, and the value of the Avrami exponent rises from 1 at lower temperatures to above 2 at 100 °C, indicating a gradual change from a homogeneous nucleating process under hard confinement conditions to heterogeneous nucleation under soft confinement conditions (typical values of the Avrami exponent for PLLA homopolymers are around 3 and indicate domination of a heterogeneous nucleating process).

Most of the studies on block copolymers where PLLA can crystallize freely without any confinement effects involve double–crystalline biodegradable block copolymers where the second block is either PEO or PCL. In these cases, the crystallization temperature of the PLLA lies much higher than the melting points of PEO and PCL, and its crystallization occurs in the amorphous melt.

The miscibility of PCL and PLLA varies from a homogeneous melt at low molecular weights to strongly segregated melts with T_{ODT} close to the PLLA T_m at high molecular weights. Since the T_g of PLLA overlaps the melting region of PCL, alternative methods like rheological measurements or small–angle X–ray scattering (SAXS), including the determination of the χN parameter, were used to study the melting phase behaviour of PLLA–b–PCL.[129] The crystallization behaviour of a high molecular weight immiscible system (M_n = 77,000 g/mol, w_{PCL} = 0.32) and miscible low molecular weight system (M_n = 19,000 g/mol, w_{PCL} = 0.374) was investigated at 110 and 140 °C. Although similar degrees

of PLLA crystallinity were measured for both block copolymers, the PLLA crystallization rate is much faster for lower molecular weight at both crystallization temperatures (based on the crystallization half–time, $t_{1/2}$, derived from DSC data).[130] More recent crystallization studies of PLLA–b–PCL block copolymers of varying composition revealed that an increase in PCL content leads to a decrease in crystallization rate of PLLA.[131] The PLLA melting enthalpy gradually increases with a decrease in PLLA content as well as its molecular weight.[132] Overall, the PCL melt can be considered as a diluent that retards the rate of crystallization, but also facilitates reorganizational processes within the PLLA phase that result in double melting peaks of the latter and might contribute to an increase in degree of crystallinity of the PLLA.[131]

Block copolymers of PEO and PLLA are essentially miscible in the entire molecular weight range studied and their miscibility is composition independent, with phase separation occurring only during crystallization.[129] As in the case of PLLA–b–PCL, the PLLA T_g and the PEO T_m are very close, which complicates the evaluation of block miscibility. Interestingly, the PEO block (molecular weight 5000 g/mol) was found to increase the crystallization rate of PLLA (molecular weights 15,000, 5000, and 2500 g/mol), as followed from $t_{1/2}$ measurements, and the rate increase observed was up to 10 times compared with a PLLA homopolymer of similar molecular weight (9,000 g/mol). Moreover, the presence of the molten PEO "solvent" causes crystalline lamellae twisting that leads to the formation of banded spherulites. The periodic distance of the extinction rings was observed to increase with crystallization temperature (*Figure 1.9*).[115]

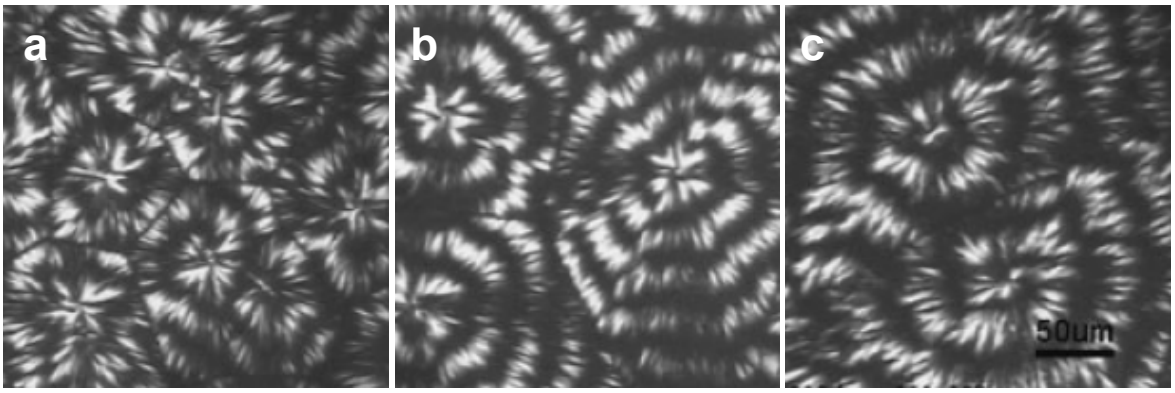

Figure 1.9. Banded spherulites of PLLA(5000)–b–PEO(5000) after isothermal crystallization at a) 90 °C; b) 95 °C; c) 100 °C (adapted from Ref. 115, © 2006 the Society of Polymer Science, Japan)

Consistent with other reports on PLLA–b–PEO block copolymers,[133,134] it can be concluded that the molten PEO block promotes the ability of the PLLA chains to diffuse more easily to the crystallization sites and/or to generate new crystallization nuclei. Furthermore block miscibility causes a decrease in the T_g with increase in PEO content, resulting in an increase of the effective PLLA crystallization window, and therefore, the mobility of the PLLA chains at larger supercoolings is higher compared to the homopolymer.

Very recently, the crystallization behaviour of PLLA–b–PDMAEMA block copolymers of relatively low molecular weight PLLA≤(10, 000 g/mol) was described.[135] Specifically, the crystallization behaviour of the two block copolymers, PLLA(4000)–b–PDMAEMA(5000) and PLLA(10,000)–b–PDMAEMA(6000), was studied by DSC and SAXS. The block copolymers studied are miscible in the melt, as shown by a single T_g and the absence of any maximum in the SAXS profile of the melt at 175 °C, indicating structural homogeneity. The disappearance of the cold–crystallization peak of the PLLA block during cooling indicates the retardation of the crystallization rate by the presence of

the PDMAEMA block. The Avrami parameters, *n*, were determined using the kinetic data for homo– and block copolymers. The values of *n* that were determined are higher for the block copolymers (~4) than for homopolymers (~3), indicating the formation of sporadically nucleated three–dimensional crystalline structures.[116]

1.9 Scope and the structure of the present work

One of the main goals of this thesis was to develop optimal synthetic procedures towards a well–defined series of amphiphilic diblock (and, to a lesser extent, triblock) copolymers possessing hydrophobic semi–crystalline PLLA and hydrophilic amorphous PDMAEMA, using a combination of the controlled polymerization techniques, ROP and ATRP, respectively. Secondly, the well–defined series obtained were characterized for their thermal and crystallization properties. The investigation of the thermal properties aimed to determine transition temperatures and the state of phase separation between the two blocks as a function of the block molecular weight. Kinetic studies of PLLA block crystallization and subsequent calculation of the Avrami coefficient, *n*, and the crystallization constant, *K*, was to determine any peculiarities of crystallization behaviour in the presence of the PDMAEMA block, such as any evidence of confinement effects. There were no publications describing P(L)LA–PDMAEMA block copolymers when the present research began, but several appeared during the course of the research (as specified above), which is indicative of the current interest of this particular combination of blocks.

Technical details on the common instrumentation, experimental and synthetic setup are given in the experimental sections of *Chapter 2* and *Chapter 4*, and complimentary

details (if any) are described in the experimental sections of *Chapter 3* and *Chapter 5*. Thus, the experimental **Chapter** is split and present as a corresponding section in *Chapters 2–5*.

Chapter 2 (a verbatim copy of the full paper, published in Macromolecules 2011, 44, 5209–5217) deals with the preparation of a well–defined series of PLLA–PDMAEMA block copolymers using a sequential three–step procedure, starting with the PLLA block. The targeted molecular weights of the PLLA cover a range of 5000–20,000 g/mol, and those of the PDMAEMA blocks are half of, equal to and twice that of each PLLA macroinitiator. The controlled polymerization techniques, i.e. ROP and ATRP, allow the preparation of block copolymers with controlled molecular weights and low PDI. Investigation of the thermal properties shows that the blocks are miscible when one of them is of low molecular weight (~5000 g/mol). Crystallization rates were found to be lowered by the PDMAEMA block, but the melting points and degrees of crystallinity were affected only a little.

Chapter 3 describes various synthetic approaches using a bifunctional initiator and a combination of ROP by $Sn(Oct)_2$ and ATRP by CuBr/HMTETA, with either block prepared first, or simultaneously. It is shown that substantial LLA racemization occurs at the polymerization temperature in the presence of PDMAEMA, when the latter is prepared first. Thus, if high stereoregularity is desired, it is necessary to start with the PLLA block. Furthermore, considerable undesired homopolymer formation takes place, as found by a quaternization/precipitation method that will be described. It is concluded that the

bifunctional initiator approach using tin octoate as a catalytic system for LLA polymerization inevitably leads to PLLA homopolymer formation regardless of the polymerization sequence.

Chapter 4 describes kinetic studies of PLLA block crystallization of the PLLA–PDMAEMA block copolymer in the bulk and in thin/thick films. To increase the PDMAEMA T_g and the segregation strength, block copolymers with partially quaternized PDMAEMA were also investigated. The parameters of the Avrami equation were determined using DSC data for bulk samples, and the crystallization rates as well as the spherulitic morphology were studied in thick films by polarizing optical microscopy. The crystallization rate was retarded most in miscible systems based on PLLA(5000). Overall, sigmoidal crystallization kinetics and instantaneous nucleation followed by two–dimensional crystallization (n = 2) were found in both non–quaternized and partially quaternized block copolymers. A SAXS experiment conducted on a block copolymer with similar molecular weights of PLLA and PDMAEMA blocks suggested that PLLA crystallizes in soft confinement within lamellar microdomains at relatively large supercooling. However, the change of the length scale of the microdomain peak after several melting (175 °C)/quenching cycles indicated that significant chain scission takes place during SAXS experiment (later shown by NMR), presumably caused by the presence of PDMAEMA, thus making the stability of the material a limiting factor in successful SAXS experiments.

Chapter 5 describes the synthesis of ABA triblock copolymers of PLLA and PDMAEMA, with the PLLA as the central block. They were prepared by a three–step procedure starting from a double–headed alcohol initiator. Thermal properties and crystallization behaviour were studied using DSC and POM. The crystallization rate was decreased more than in the diblock copolymers of similar block composition, indirectly indicating, along with a T_g analysis, the successful preparation of triblock copolymers. Crystallization kinetics and nucleation type were determined from DSC investigations and use of the Avrami equation.

Chapter 6 discusses and summarizes the main achievements of the present work and describes their contribution to original knowledge. Perspectives and ideas for continued research are proposed.

References to Chapter 1

1. Li, M.; Coenjarts, C. A.; Ober, C. K. *Adv. Polym. Sci*. **2005**, 190, 183–226.
2. Khandpur, A.; Förster, S.; Bates, F.; Hamley, I.; Ryan, A.; Bras, W.; Almdal, K.; Mortensen, K. *Macromolecules*, **1995,** 28, 8796–8806.
3. Zhu, L.; Chen, Y.; Zhang, A.; Calhoun, B. H.; Chun, M.; Quirk, R. P.; Cheng, S. Z. D.; Hsiao, B. S.; Yeh, F.; Hashimoto, T. *Phys. Rev. B* **1999**, 60, 10022–10031.
4. Nandan, B.; Hsu, J.–Y.; Chen, H.–L. *J. Macromol. Sci C: Polym. Rev.* **2006**, 46,143–172.
5. Loo, Y. L.; Register, R. A.; Ryan, A. J. *Phys. Rev. Lett.* **2000**, 84, 4120–4123.
6. Hillmyer, M. A.; Bates, F. S. *Macromol. Symp.* **1997**, 117, 121–130.
7. Loo, Y.–L.; Register, R. A.; Ryan, A. J. *Macromolecules* **2002**, 35, 2365–2374.
8. Loo, Y. L.; Register, R. A. *Crystallization within Block Copolymer Mesophases* in Developments in Block Copolymer Science and Technology (Ed. Hamley, I. W.), *John Wiley & Sons Ltd*, Chichester, **2004**, Ch. 6.
9. Ikkala, O.; ten Brinke, G. *Chem. Commun.*, **2004**, 2131–2137.
10. Valkama, S.; Ruotsalainen, T.; Nykanen, A.; Laiho, A.; Kosonen, H.; ten Brinke, G.; Ikkala, O.; Ruokolainen, J. *Macromolecules*, **2006**, 39, 9327–9336.
11. Mäki–Ontto, R.; de Moel, K.; de Odorico, W.; Ruokolainen, J.; Stamm, M.; ten Brinke, G.; Ikkala, O. *Adv. Mat.* **2001**, 13, 117–121.
12. Laforgue, A.; Bazuin, C. G.; Prud'homme, R. E. *Macromolecules*, **2006**, 39, 6473–6482.
13. Tokarev, I.; Minko, S.; Stamm, M. *Mat. Res. Soc. Symp. Proc.*, **2002**, 728, 11–16.
14. Ganta, S.; Devalapally, H.; Shahiwala, A.; Amiji, M. *J. Contr. Release* **2008**, 126, 187–204.
15. Wang, C.; Ge, Q.; Ting, D.; Nguyen, D.; Shen, H–R.; Chen, J.; Eisen, H. N.; Heller, J.; Langer, R.; Putnam, D. *Nat. Mat*. **2004**, 3, 190–196.
16. Nishiyama, N.; Kataoka, K. *Adv. Polym. Sci.* **2006**, 193, 67–101.
17. Sallenave, X.; Bazuin, C. G. *Macromolecules* **2007**, 40, 5326–5336.

18. Zhang, Q.; Wang, X.; Barrett, C. J.; Bazuin, C.G. *Chem. Mater.* **2009,** 21, 3216–3227.

19. Maillard,D.; Prud'homme, R. E. *Macromolecules* **2010**, 43, 4006–4010.

20. Wang, X.; Prud'homme, R. E. *Macromol. Chem. Phys*. **2011**, 212, 691–698.

21. Othmer, K. *Encyclopedia of Chemical Technology*, 2nd ed.; *Wiley–Interscience*, New York, **1963**, Vol. 12, 177.

22. Gruber, P. R.; Hall, E. S.; Kolstad, J. J.; Iwen, M. L.; Benson, R. D.; Borchardt, R. L. *European Patent Application* EP0623153A1; *International Patent* WO9315127, **1993**.

23. Jeon, N. Y.; Ko, S.–J.; Won, K.; Kang, H.–Y.; Kim, B. T.; Lee, Y. S.; Lee, H. *Tet. Lett.* **2006**, 47, 6517–6520.

24. Murdoch, J. R.; Loomis, G. L. *Patent No.* US4719246, **1988**.

25. Ikada, Y.; Jamshidi, K.; Tsuji, H.; Hyon, S. H. *Macromolecules*, **1987**, 20, 904–906.

26. Dechy–Cabaret, O.; Martin–Vaca, B.; Bourissou, D. *Chem. Rev.* **2004**, 104, 6147–6176.

27. Drumright, R. E.; Gruber, P. R.; Henton, D. E. *Adv. Mater.* **2000**, 12, 1841–1846.

28. Heino, A.; Naukkarinen, A.; Kulju, T.; Törmälä, P.; Pohjonen, T.; Mäkelä, E. A. *J. Biomed. Mater. Res.;* **1996**, 30, 187–192.

29. Yamane, H.; Sasai, K.; Takano, M.; Takahashi, T. *J. Rheol*. **2004**, 48, 599–609.

30. Wang, M. *Am. J. Biochem. Biotechnol.* **2006**, 2, 80–84.

31. Lassalle, V.; Ferreira, M. L. *Macromol. Biosci.* **2007**, 7, 767–783.

32. Uhrich, K. E.; Cannizzaro, S. M.; Langer, R. S.; Shakesheff, K. M. *Chem. Rev.* **1999**, 99, 3181–3198.

33. Oh, J. K. *Soft Matter*, **2011**, 7, 5096–5108.

34. Janes, K.A.; Calvo, P.; Alonso, M.J. *Adv. Drug Deliv. Rev.* **2001**, 47, 83–97.

35. Munier, S.; Messai, I.; Delair, T.; Verrier, B.; Ataman–Önal, Y. *Coll. and Surf. B: Biointerfaces*, **2005**, 43, 163–173.

36. Sanabria–DeLong, N.; Crosby, A. J.; Tew, G. N. *Biomacromolecules* **2008**, 9, 2784–2791.

37. Tam, J. M.; Tam, J. O.; Murthy, A.; Ingram, D. R.; Ma, L. L.; Travis, K.; Johnston, K. P.; Sokolov, K. V. *ACS Nano* **2010**, 4, 2178–2184.

38. Sun, H.; Meng, F.; Dias, A. A.; Hendriks, M.; Feijen, J.; Zhong, Z.; *Biomacromolecules* **2011**, 12, 1937–1955.

39. Xiao, Y.; Xu, Y.; Lu, J.; Zhu, X.; Fan, H.; Zhang, X. *Mater. Lett.* **2007**, 61, 2601–2605.

40. Wolf, F. F.; Friedemann, N.; Frey, H. *Macromolecules* **2009**, 42, 5622–5628.

41. Kohori, F.; Sakai, K.; Aoyagi, T.; Yokoyama, M.; Sakurai, Y.; Okano, T. *J. Control. Release* **1998**, 55, 87–98.

42. Calandrelli, L.; De Rosa, G.; Errico, M. E.; La Rotonda, M. I.; Laurienzo, P.; Malinconico, M.; Oliva, A.; Quaglia, F. *J. Biomed. Mat. Res.* **2002**, 62, 244.

43. Wang, C. H; Hsiue, G. H. *Bioconjugate Chem.* **2005,** 16, 391–396 .

44. Firmenich, S.; Berthier, D.; Ouali, L. *Patent No.* WO 2005/108471 A1.

45. Gu, L.; Zhu S.; Hrymak, A. N. *Coll. Polym. Sci.* **2002**, 280, 167–175.

46. Lenoir, S.; Pagnoulle, Ch.; Detrembleur, C.; Galleni, M.; Jérôme, R. *J. Polym. Sci.: Part A: Polym. Chem.* **2006**, 44, 1214–1224.

47. Fonseca, M. J.; Storm, G.; Hennink, W. E.; Gerritsen, W. R.; Haisma, H. J. *J. Gene Med.* **1999**, 1, 407–414.

48. Baines, F. L.; Billingham, N. C.; Armes, S. P. *Macromolecules* **1996**, 29, 3416–3420.

49. Baines, F. L.; Armes, S. P.; Billingham, N. C.; Tuzar, Z. *Macromolecules* **1996**, 29, 8151–8159.

50. Creutz, S.; Teyssié, Ph.; Jérôme, R. *Macromolecules*, **1997**, 30, 6–9.

51. Gohy, J.–F.; Antoun, S.; Sobry, R.; Van den Bossche, G.; Jérôme, R. *Macromol. Chem. Phys.* **2000**, 201**,** 31–41.

52. Narrainen, A. P.; Pascual, S.; Haddleton, D. M. *J. Polym. Sci.: Part A: Polym. Chem.;* **2002**, 40, 439–450.

53. Ravi, P.; Sin, S. L.; Gan, L. H.; Gan, Y. Y.; Tam, K. C.; Xia, X. L.; Hu, X. *Polymer*, **2005**, 46, 137–146.

54. Jakubowski, W.; Lutz, J.–F.; Slomkowski, S.; Matyjaszewski, K. *J. Polym. Sci.: Part A: Polym. Chem.;* **2005**, 43, 1498–1510.

55. Bougard, F.; Jeusette, M.; Mespouille, L.; Dubois, Ph.; Lazzaroni, R. *Langmuir*, **2007**, 23, 2339–2345.

56. Alvarez–Lorenzo, C.; Barreiro–Iglesias, R.; Concheiro, A.; *Langmuir*, **2005**, 21, 5142–5148.

57. Hu, D.; Cheng, Z.; Zhu, J.; Zhu, X. *Polymer*, **2005**, 46, 7563–7571.

58. Guice, K. B.; Loo, Y.–L. *Macromolecules* **2006**, 39, 2474–2480.

59. Gohy, J.–F.; Antoun, S.; Jérôme, R.; *Macromolecules* **2001**, 34, 7435–7440.

60. Yuan, W.; Yuan, J.; Zheng, S.; Hong, X. *Polymer* **2007**, 48, 2585–2594.

61. Li, J.; Ren, J.; Cao, Y.; Yuan, W. *Polymer* **2010**, 51, 1301–1310.

62. Spasova, M.; Mespouille, L.; Coulembier, O.; Paneva, D.; Manolova, N.; Rashkov, I.; Dubois, P. *Biomacromolecules* **2009**, 10, 1217–1223.

63. Karanikolopoulos, N.; Zamurovic, M.; Pitsikalis, M.; Hadjichristidis, N. *Biomacromolecules* **2010**, 11, 430–438.

64. Jedlinski, Z.; Walach, W.; Kurcok, P.; Adamus, G. *Makromol. Chem.* **1991**, 192, 2051–2057.

65. Penczek, S.; Kubisa, P.; Matyjaszewski, K. *Adv. Polym. Sci.* **1980**, 37, 8–38.

66. Kohn, F. E.; van Ommen, J. G.; Feuen, J. E*ur. Polym. J.* **1983**, 19, 1081–1088.

67. Kricheldorf, H.; Dunsing, R. *Makromol. Chem.* **1986**, 187, 1611–1625.

68. Baśko, M.; Kubisa, P. *J. Polym. Sci.: Part A: Polym. Chem*. **2010**, 48, 2650–2658.

69. Bourissou, D..; Martin–Vaca, B.; Dumitrescu, A.; Graullier, M.; Lacombe, F. *Macromolecules* **2005**, 38, 9993–9998.

70. Leenslag, J. W.; Pennings, A. J. *Makromol. Chem.* **1987**, 188, 1809–1814.

71. Kricheldorf, H. R.; Kreiser–Saunders, I.; Boettcher, C. *Polymer* **1995**, 36, 1253–1259.

72. Kricheldorf, H.; Damrau, D.–O. *Makromol. Chem. Phys.* **1997**, 198, 1767–1774.

73. Darensbourg, D. J.; Choi, W.; Richers, C. P. *Macromolecules* **2007**, 40, 3521–3523.

74. Cox, F. E.; Hostettler, F. *US Patent* 3 021 313, **1962**.

75. Hamitou, A.; Jérôme, R.; Hubert, A. J.; Teyssié, Ph. *Macromolecules* **1973**, 6, 651–652.

76. Osgan, M.; Pasero, J. J.; Teyssié, Ph. *J. Polym. Sci. B: Polym. Lett.;* **1970**, 8, 319–321.

77. Duda, A.; Penczek, S. *Macromolecules* **1995**, 28, 5981–5992.

78. Kowalski, A.; Duda, A.; Penczek, S. *Macromolecules* **1998**, 31, 2114–2122.

79. Dubois, P.; Jacobs, C.; Jérôme, R.; Teyssié, P. *Macromolecules* **1991**, 24, 2266–2270.

80. Witzke, D. R.; Narayan, R.; Kolstad, J. J. *Macromolecules* **1997**, 30, 7075–7085.

81. Nijenhuis, A. J.; Grijpma, D. W.; Pennings, A. J. *Macromolecules* **1992**, 25, 6414–6424.

82. Guptaa, V. B.; Anithaa, S.; Hegdea, M. L.; Zeccab, L.; Garrutoc, R. M.; Ravidd, R.; Shankare, S. K.; Steinf, R.; Shanmugavelu, P.; Jagannatha Rao, K. S. *Cell. Mol. Life Sci.* **2005**, 62, 143–158.

83. Kowalski, A.; Duda, A.; Penczek, S. *Macromolecules* **2000**, 33, 7359–7370.

84. van de Wetering, P.; Zuidam, N. J.; van Steenbergen, M. J.; van der Houwen, O. A. G. J.; Underberg, W. J. M.; Hennink, W. E. *Macromolecules* **1998**, 31, 8063–8068.

85. Du, R.; Chakma, A.; Feng, X. *J. of Membr. Sci.* **2007**, 290, 19–28.

86. Beadle, P. M.; Rowan, L.; Mykytiuk, J.; Billingham, N. C.; Armes, S. P. *Polymer* **1993**, 34, 1561–1563.

87. Liu, Y.; Jing, F.; Sun, Y.; Zhao, G.; Jiu, H.; Zhang, Q. *Polym. Sci.; Ser. B.* **2010**, 52, 492–497.

88. Zhang, X.; Xia, J.; Matyjaszewski, K. *Macromolecules* **1998**, 31, 5167-5169.

89. Nazarov, A.; Mukhitdinova, N. A.; Azimov, Z. A.; Askarov, M. A. *Vysokomol. Soedin.; Ser. B* **1974**, 16, 628–649.

90. Sandler, S. R.; Karo, W. Polymer Syntheses, Vol. I. *Academic Press*, San Diego, **1974**.

91. Barner–Kowollik, C. Handbook of RAFT Polymerization. *Wiley–VCH*, Weinheim, **2009**.

92. Lansalot, M.; Davis, T. P.; Heuts, J. P. A. *Macromolecules* **2002**, 35, 7582–7591.

93. Matyjaszewski, K.; Davis, T. P. Handbook of Radical Polymerization. *John Wiley & Sons Ltd*, Hoboken, **2003**.

94. Qiu, J.; Gaynor, S.; Matyjaszewski, K. *Macromolecules* **1999**, 32, 2872–2875.

95. Xia, J.; Johnson, T.; Gaynor, S.; Matyjaszewski, K.; DeSimone, J. *Macromolecules* 1999, 32, 4802–4805.

96. Golas, P. L.; Tsarevsky, N. V.; Sumerlin, B. S.; Walker, L. M.; Matyjaszewski, K. *Aust. J. Chem.* **2007**, 60, 400–404.

97. Wang, W. J.; Li, T.; Yu, T.; Zhu, F. M. *Macromolecules* **2008**, 41, 9750–9754.

98. Urien, M.; Erothu,H.; Cloutet, E.; Hiorns, R. C.; Vignau, L.; Cramail, H. *Macromolecules* **2008**, 41, 7033–7040.

99. Dubois, P.; Coulembier, O.; Raquez, J.–M. (Eds.) Handbook of Ring–Opening Polymerization. *Wiley–VCH*, **2009**.

100. Jacobs, C.; Dubois, P.; Jérôme, R.; Teyssié, P. *Macromolecules* **1991**, 24, 3027–3034.

101. In′t Veld, P. J. A.; Velner, E. M.; Van de Witte, P.; Hamhuis, J.; Dijkstra, P. J.; Feijen, J. *J. Polym. Sci.: Part A: Polym. Chem.* **1997**, 35, 219–226.

102. Lowe, A. B.; Billingham, N. C.; Armes, S. P. *Macromolecules* **1998**, *31,* 5991–5998

103. Dove, A. P. *Chem. Commun.* **2008**, 6446–6470.

104. Boudouris, B. W.; Frisbie, C. D.; Hillmyer, M. A. *Macromolecules* **2008**, 41, 67–75.

105. Nguyen, H. T.; Coulembier, O.; Winter, J. D.; Gerbaux, P.; Crispin, X.; Dubois, P. *Polym. Bull.* **2011**, 66, 51–64.

106. Coulembier, O.; Lohmeijer, B. G. G.; Dove, A. P.; Pratt, R. C.; Mespouille, L.; Culkin, D. A.; Benight, S. J.; Dubois, Ph. Waymouth, R. M.; Hedrick, J. L. *Macromolecules* **2006**, 39, 5617–5628.

107. You, Y.; Hong, C.; Wang, W.; Lu, W.; Pan, C. *Macromolecules* **2004**, 37, 9761–9767.

108. Chagneux, N.; Trimaille, T.; Rollet, M.; Beaudoin, E.; Gérard, P.; Bertin, D.; Gigmes, D. *Macromolecules* **2009**, 42, 9435–9442.

109. Mao, J.; Ji, X.; Bo, S. *Macromol. Chem. Phys.* **2011**, 212, 744–752.

110. Mecerreyes, D.; Moineau, G.; Dubois, P.; Jérôme, R.; Hedrick, J. L.; Hawker, C. J.; Malmström, E. E.; Trollsas, M. *Angew. Chem. Int. Ed.* **1998**, 37, 1274–1276.

111. Wilbon, P.A.; Zheng, Y.; Yao, K.; Tang, C. *Macromolecules* **2010**, 43, 8747–8754.

112. Pyda, M.; Bopp, R. C.; Wunderlich, B. *J. Chem. Thermodyn.* **2004**, 36, 731–742.

113. Tsuji, H.; Hyon, S. H.; Ikada, Y. *Macromolecules*, **1991**, 24, 5651–5656.

114. Lorenzo, A. T.; Arnal, M. L.; Albuerne, J.; Müller, A. J. *Polym. Test* **2007**, 9, 222–231.

115. Yang, J.; Zhao, T.; Liu, L.; Zhou, Y.; Li, G.; Zhou, E.; Chen, X. *Polymer J.* **2006**, 38, 1251–1257.

116. Gedde, U. W. Polymer Physics, *Chapman & Hall*, London, **1995**.

117. Yu, L.; Dean, K.; Li, L. *Prog. Polym. Sci.* **2006**, 31, 576–602.

118. Peneasky, J. S.; Long, J. M.; Wool, R. P. *J. Polym Sci. B: Polym. Phys.***1991**, 29, 565–579.

119. Dave, P. B.; Ashar, N. J.; Gross, R. A.; McCarthy, S. P. *Polym. Prepr*. **1990**, 31, 442–443.

120. Iannace, S.; Ambrosio, L.; Huang, S. G.; Nicolais, L. *J. Appl. Polym. Sci.* **1994**, 54, 1525–1536.

121. Suyatma, N. E.; Copinet, A.; Tighzert, L.; Coma V. *J. Polym. Environ.* **2004**, 12, 1–6.

122. Ke, T.; Sun, X. *J. Appl. Polym. Sci.* **2003**, 89, 1203–11.

123. Tsuji, H. *Macromol. Biosci*. **2005**, 5, 569–597.

124. Schmidt, S. C.; Hillmyer, M. A. *J. Polym. Sci. B: Polym. Phys*. **2001**, 39, 300–313.

125. Pluta, M. *Polymer* **2004**, 45, 8239–8251.

126. Yeh, J.–T.; Yang, M.–C.; Wu, C.–J.; Wu, X.; Wu, C.–S. *Polym.–Plast. Tech. Eng*. **2008**, 47, 1289–1296.

127. Zalusky, A. S.; Olayo–Valles, R.; Wolf, J. H.; Hillmyer, M. A. *J. Am. Chem. Soc.* **2002**, 124, 12761–12773.

128. Ho, R.–M.; Lin, F.–H.; Tsai, C.–C.; Lin, C.–C.; Ko, B.–T.; Hsiao, B. S.; Sics, I. *Macromolecules* **2004**, 37, 5985–5994.

129. Castillo, R. V.; Müller, A. J. *Prog. Polym. Sci*. **2009**, 34, 516–560.

130. Kim, J. K.; Park, D.–J.; Lee, M.–S.; Ihn, K. J. *Polymer* **2001**, 42, 7429–7441.

131. Castillo, R. V.; Müller, A. J.; Raquez, J.–M.; Dubois, P. *Macromolecules* **2010**, 43, 4149–4160.

132. Hamley, I. W.; Parras, P.; Castelletto, V.; Castillo, R. V.; Müller, A. J.; Pollet, E.; Dubois, P.; Martin, C. M. *Macromol. Chem. Phys*. **2006**, 207, 941–953.

133. Sun, J.; Hong, Z.;Yang, L.; Tang, Z.; Chen, X.; Jing, X. *Polymer* **2004,** 45, 5969–5977.

134. Shin, D.; Shin, K.; Aamer, K. A.; Tew, G. N.; Russell, T. P.; Lee, J. H.; *Macromolecules* **2005,** 38, 104–109.

135. Michell, R. M.; Müller, A. J.; Spasova, M.; Dubois, P.; Burattini, S.; Greenland, B. W.; Hamley, I. W.; Hermida–Merino, D.; Cheval, N.; Fahmi, A. J. Polym. Sci. B: Polym. Phys. **2011**, 49, 1397–1409.

SYNTHESIS AND THERMAL PROPERTIES OF LINEAR AMPHIPHILIC DIBLOCK COPOLYMERS OF L–LACTIDE AND 2–DIMETHYLAMINOETHYL METHACRYLATE

2

2.1 Introduction

Poly(lactic acid) or polylactide (PLA) combines many desirable characteristics, including availability from renewable resources, that make these materials useful for a variety of engineering and biomedical applications. In stereochemical form, the most common being poly(L–lactide) (PLLA), the material is semi–crystalline with a high melting point, conferring good mechanical properties over a wide range of use temperatures. The well–known degradability and biocompatibility of PLA[1] are attractive for applied areas such as tissue engineering[2] and suture design.[3] Moreover, PLA hydrophobicity and biodegradability enable drug–encapsulating and –release capabilities to materials containing this component.[4] As one of the blocks in block copolymer systems, PLA can serve as an easily removable moiety in the design of nanoporous materials and films.[5] The

possibility of stereocomplexing PLLA with its D–lactide form, PDLA, further expands the versatility of these materials.[6,7] On the other hand, poly(2–dimethylaminoethyl methacrylate) (PDMAEMA) has received considerable attention due to its hydrophilicity, pH and temperature sensitivity, ease of quaternization, and availability of the functional amine/ammonium moiety for complexation with acidic/anionic substances that make it attractive for wide–ranging applications including as flocculation agents,[8] as biocides,[9] and in gene delivery[10] systems.

In developing these materials and their applications, both PLA and PDMAEMA have been associated with a variety of other polymers in the form of block copolymers, a quintessential route for forming self–assembling meso– and nano–structured materials. PLA has been combined with, for example, poly(caprolactone),[11,12] poly(ethylene oxide),[13,14] polystyrene,[15–17] poly(isopropylacrylamide),[18,19] polyethylene,[20,21] poly(vinyl pyrrolidone)[22] and polythiophene,[5] and PDMAEMA with, for example, various other polymethacrylates,[23–28] poly(caprolactone),[29,30] poly(ethylene oxide),[31] polystyrene,[32,33] poly(2–vinyl pyridine),[34] and poly(ethylene–co–butylene).[9] Cationic PDMAEMA has also been adsorbed onto PLA nanoparticles to enhance DNA delivery.[35] The combination of PLA and PDMAEMA into block copolymers has appeared only recently.[36–41] Amphiphilic block copolymer systems such as these have particular interest, since they can form micelles (or gels at higher concentration) in both organic and aqueous media and interact with both polar and nonpolar solutes, providing, for example, an adaptable drug delivery matrix. Combining the amphiphilicity with the individual characteristics of PLA and PDMAEMA in block copolymers potentially make of them highly versatile materials for a large variety of applications, both in solution and in the solid state. For example,

stereocomplexes of PLLA–*b*–PDMAEMA with PDLA–*b*–PDMAEMA were prepared for the fabrication of antibacterial and hemostatic electrospun fibers[39,40] and dendritic star–block copolymers for controlled drug release applications.[38] As bulk and thin film materials, the microphase–separated structure of these block copolymers can be coupled with the ability to modulate the microstructure and functionality of the material by hydrogen–bonding, ionically complexing or quaternizing the PDMAEMA block with appropriate molecules or by selectively post–degrading or stereocomplexing the PLA (PLLA) block.

In this context, it is of interest to synthesize and characterize PLA–PDMAEMA block copolymers with a wide range of well–controlled block lengths and narrow polydispersity. Among the syntheses described in Ref. 37–41, one involves such a series, where the PLA block is in the PDLLA form and is restricted to low molecular weight (1.3–3.7 kg/mol).[41] In the present contribution, we describe the synthesis of similar block copolymers, but where the PLA block is in the stereochemical PLLA form and has a much wider molecular weight range (5–20 kg/mol). A three–step synthetic procedure similar to that in Refs. 39 and 41 was used, involving ring–opening polymerization (ROP) of LLA, followed by appropriate end group conversion to obtain PLLA macroinitiators, and finally by addition of the PDMAEMA block using atom transfer radical polymerization (ATRP). PDMAEMA blocks with molecular weights that are half of, equal to, and twice that of each of the three macroinitiators synthesized were targeted. In addition, we investigated the thermal properties of the well–defined series to observe transition temperatures, the effect of the PDMAEMA block on PLLA crystallization, and the state of phase separation of the blocks, all as a function of block molecular weight. Knowledge of these characteristics is

important to efficiently exploit these materials in various applications, particularly in the bulk and as films.

2.2 Experimental section

2.2.1 Techniques

^{1}H–NMR spectra were recorded at room temperature on a Bruker Avance 400 MHz spectrometer using $CDCl_3$ (Aldrich) solutions containing 0.03% of tetramethylsilane (TMS) as an internal standard. Sequential size exclusion chromatography (SEC) and light scattering (LS) data of the PLLA homopolymers and block copolymers were obtained using a Waters 510 HPLC pump, PLgel columns (Polymer Laboratories) with 5–μm pore sizes (50x7.5, 300x7.5 and 600x7.5 mm), a Wyatt EOS refractive index (RI) detector and a Wyatt QUELS LS detector. Tetrahydrofuran (THF) with 2–5% v/v of triethylamine (TEA) was used as the mobile phase, at a flow rate of 1 mL/min. The performance of the SEC–LS system was verified using polystyrene standards. The data were collected and processed using the ASTRA software package. Dn/dc measurements of the homopolymers and six representative copolymers (not necessarily those presented in this manuscript) were determined to a precision of ±0.001 mL/g for a series of five solutions per sample with precise concentrations ranging between 1 and 5 mg/mL, using the Wyatt EOS RI detector (operating at 691 nm) and a flow rate of 0.2 mL/min. The dn/dc values for PLLA and PDMAEMA in THF (with 2–3% TEA) were found to be 0.048 and 0.084 mL/g, respectively. The relationship between dn/dc and block composition including the homopolymers was found to be linear, as it should be,[42] and was used to interpolate the

dn/dc values for the subsequent copolymers synthesized. The specific optical rotatory powers, [α_L], of the PLLA macroinitiators and representative block copolymers were measured at room temperature in chloroform solution at a concentration of ca. 1 g/dL, using a PerkinElmer 341 polarimeter operating at 589 nm.

Thermogravimetric analysis (TGA) was performed with a TA Instruments Hi–Res TGA 2950 analyzer under nitrogen flow at a heating rate of 10 °C/min. Differential scanning calorimetry (DSC) measurements were acquired with a TA Instruments Q1000 DSC, using standard aluminium pans, an indium standard for calibration, and nitrogen as the purge gas. Scan details are given in the Supporting Information. Melting/crystallization temperatures were determined by their peak values. Glass transition temperatures of the homopolymer were identified by the inflection points in the heating thermograms. For the copolymers, where baselines, especially between two T_g's, were often difficult if not impossible to determine, T_g's were identified by the peak values in the first derivative curves.

2.2.2 Materials

L–Lactide (LLA), obtained from Aldrich, was recrystallized twice from anhydrous ethyl acetate (distilled over P_2O_5 prior to use) and stored under dry nitrogen prior to use. Stannous 2–ethylhexanoate [tin octoate, $Sn(Oct)_2$],[43–45] 4–isopropylbenzyl alcohol (iPBA), 1,1,4,7,10,10–hexamethyltriethylenetetramine (HMTETA), 2–bromoisobutyryl bromide (BIB), triethylamine, and 2–dimethylaminoethyl methacrylate (DMAEMA),[45] all supplied by Aldrich, were used as received. 2–Hydroxyethyl–2–bromoisobutyrate (HEBIB) was

prepared following a procedure described in Ref. 29 [^{1}H–NMR: δ_H, *ppm* 1.96 (s, $2CH_3$), 2.42 (br. s, OH), 3.81–3.93 (m, CH_2OH), 4.26–4.34 (m, OCH_2)]. Copper (I) bromide (Aldrich) was dispersed in boiling glacial acetic acid under vigorous stirring for a few hours, then filtered, washed successively with ethanol and ether, and dried under reduced pressure at 60 °C. The assembled reaction system (flask, magnetic stirrer, 3–way adapter) was thoroughly dried/ deoxygenated by repeated evacuate(10 mTorr)–heat(250 °C)–refill(dry N_2) cycles prior to synthesis.

2.2.2.1 Synthesis of bromine–terminated poly(L–lactic acid) (PLLA–Br) (*Scheme 2.1*)

PLLA–Br macroinitiators were synthesized as shown in Scheme 1, using a procedure similar to those described previously for ring–opening polymerization of LLA[46,47] to give PLLA–OH, followed by terminal group modification using BIB.[9,39] The polymerization took place in concentrated solution (ca. 3 M in toluene) at 120 °C using iPBA as initiator and tin octoate as catalyst [5:1 iPBA:$Sn(Oct)_2$]. Specifically, 2–3 g of LLA were charged into the prepared flask and three vacuum–nitrogen cycles were carried out. Calculated amounts of freshly prepared solutions of tin octoate (0.44 M in toluene) and iPBA (0.06 M in toluene), followed by 8 mL of dry toluene, were then added through a septum via a syringe under nitrogen flow. Finally, the system was closed under positive nitrogen pressure, and polymerization proceeded under stirring at 120 °C. The degree of conversion was monitored by NMR analysis of reaction mixture aliquots, and polymerization was stopped at ca. 95% conversion by cooling to room temperature. The solidified reaction

mixture was dispersed in 30 mL of methanol, then poured into 200 mL of methanol containing 1 mL of concentrated HCl to remove Sn residue. The white solid was collected by filtration, washed with methanol, dried, redissolved in 10 mL of dry dichloromethane or chloroform, and precipitated dropwise into 300 mL of methanol containing 1 mL of concentrated HCl. The fibrous precipitate was collected by filtration, washed with methanol and dried in vacuo at 30 °C for 72 h. ^{1}H–NMR (400 MHz, $CDCl_3$): δ_H, *ppm* 1.24 (d, J = 6.8 Hz, 2 CH_3, initiator fragment), 1.58 (d, J = 7.2 Hz, CH_3, PLLA), 5.16 (q, J = 7.2 Hz, CH, PLLA).

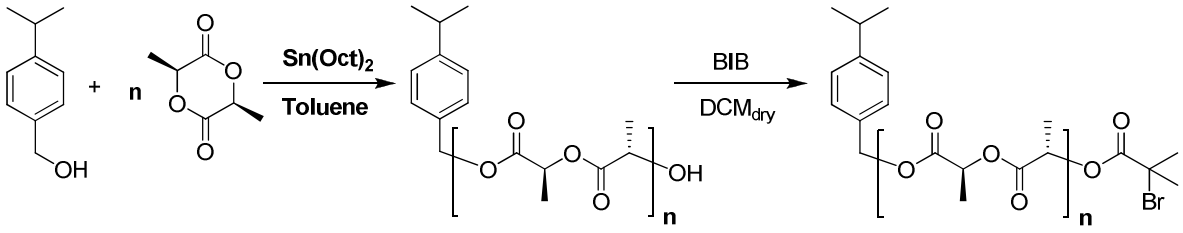

Scheme 2.1. Synthesis of the PLLA macroinitiator by ROP followed by terminal group modification

After end–capping the hydroxyl end groups of PLLA–OH by BIB following a literature procedure,[39] the resulting PLLA–Br were dried in vacuo at 30 °C for at least 72 h. ^{1}H–NMR (400 MHz, $CDCl_3$): δ_H, *ppm* 1.24 (d, J = 6.8 Hz, 2 CH_3, initiator fragment), 1.58 (d, J = 7.2 Hz, CH_3, PLLA), 1.95 (s, CH_3, BIB endgroup), 1.98 (s, CH_3, BIB endgroup), 5.16 (q, J = 7.2 Hz, CH, PLLA).

2.2.2.2 Synthesis of poly(L–lactic acid)–*b*–poly(2–dimethylaminoethyl methacrylate), PLLA–*b*–PDMAEMA (*Scheme 2.2*).

Macroinitiated atom–transfer radical polymerization (ATRP) of DMAEMA is well described in the literature,[9,29,37] with variations in the detailed procedures such as in the choice of ligand or in the structure of the terminal Br–containing moiety. The procedure we used has been optimized for obtaining copolymers with a low polydispersity as follows. PLLA–Br (0.5 g), 1 eq. of CuBr and 4 eqs. of HMTETA were charged into the reaction flask and deoxygenated by three vacuum–nitrogen cycles. After addition of 3.5–4.5 mL (more for the longer PLLA macroinitiators) of dry deoxygenated toluene, the mixture was stirred at 40°C and further heated if necessary to achieve dissolution (as was the case for the longer PLLAs), until a clear light–green solution was formed. Finally, the required amount of DMAEMA was introduced via a syringe, the system was closed under positive nitrogen pressure, and then polymerization proceeded under stirring at 70 °C for the required time (maximum of 81 h). For the longer PLLA macroinitiators, polymerization was carried out initially at higher temperature, notably at ca. 90 °C for ca. 2 h, to avoid solution cloudiness, and 70 °C for the remaining time.

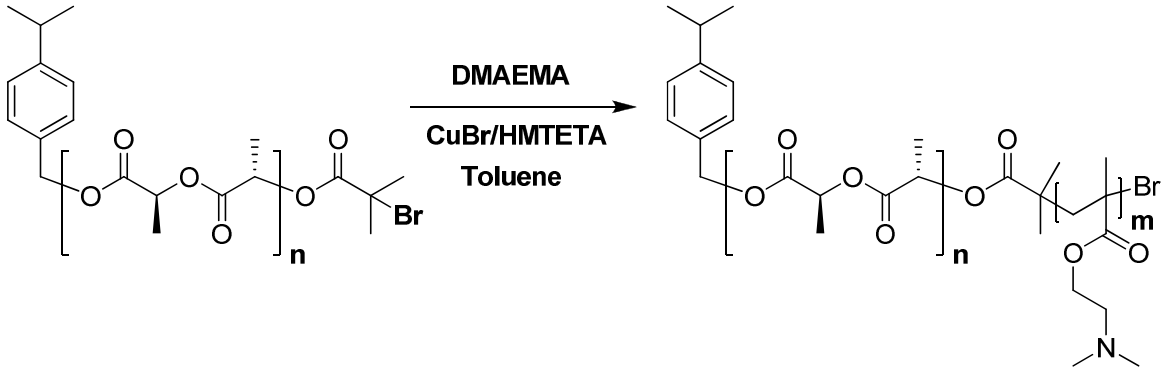

Scheme 2.2. Synthesis of PLLA–*b*–PDMAEMA block copolymers following standard ATRP procedures

Polymerization was stopped at an estimated DMAEMA conversion of 97–98%, monitored by NMR, by cooling to room temperature and diluting with ca. 40 mL of THF. The solution was then passed through a short silica column to remove the copper residue, followed by flushing of the column with 40 mL of THF. The resulting light–yellow solution was evaporated to dryness, and the product was redissolved in 10 mL of dichloromethane, and precipitated dropwise into hexane. Sticky flakes were isolated by filtration, washed with hexane and dried in vacuo at 30 °C for at least 72 h. ^{1}H–NMR (400 MHz, $CDCl_3$): δ_H, *ppm* 0.80–1.12 (m, CH_3, PDMAEMA), 1.58 (d, J = 7.2 Hz, CH_3, PLLA), 1.65–2.15 (m, CH_2, PDMAEMA), 2.20–2.35 (m, $N(CH_3)_2$, PDMAEMA), 2.50–2.65 (m, NCH_2, PDMAEMA), 3.95–4.20 (m, OCH_2, PDMAEMA), 5.16 (q, J = 7.2 Hz, CH, PLLA).

A PDMAEMA homopolymer was synthesized by ATRP following the procedure described in Ref. 9, but using HEBIB as the initiator. ^{1}H–NMR (400 MHz, $CDCl_3$): δ_H, *ppm* 0.81–1.11 (m, CH_3), 1.71–2.07 (m, CH_2), 2.23–2.33 (m, $N(CH_3)_2$), 2.50–2.63 (m, NCH_2), 3.96–4.15 (m, OCH_2). SEC–LS in THF (with added 2% v/v TEA): M_n = 15,800 g/mol, M_w/M_n = 1.21.

The nomenclature of the homopolymers and copolymers are given in terms of number–average molecular weights, as in $PLLA_{xk}$–$PDMAEMA_{yk}$, where x and y refer to the molecular weight rounded off to the nearest thousand (k). The copolymers will also be referred to frequently as xk–yk.

2.3 Results and discussion

2.3.1 Synthesis and characterization of the PLLA macroinitiators

The targeted range of the PLLA–Br macroinitiators synthesized was limited to about 20 kg/mol in the present series, in order to be able to proceed with ATRP under optimal conditions; i.e., in concentrated solution without unduly high viscosity. ROP was conducted in concentrated solution as a compromise between the best conditions for obtaining narrow PDI (in dilute solution) and reasonable reactions times (fastest for bulk ROP). Moreover, 4–isopropylbenzyl alcohol was chosen as the ROP initiator to optimize molecular weight determination by ^{1}H NMR, particularly for the longer PLLA chain lengths targeted. This initiator provides a PLLA terminal moiety giving a well–defined and isolated 6–proton signal at 1.24 ppm [–C_6H_4–CH($C\boldsymbol{H_3}$)$_2$; *c* in *Figure 2.1*] for comparison with the polymer chain methine signal at 5.16 ppm [–OC(=O)–C***H***(CH_3)–; *a* in *Figure 2.1*]. This affords up to a 6–fold improvement in NMR molecular weight determination, compared to using the very weak and concentration–dependent signal of the terminal methine protons of PLLA–OH (4.35 ppm, –O–C(=O)–C***H***(CH_3)–OH, *d* in *Figure 1*).[37,48] End–capping with BIB introduces another well–defined and isolated 6–proton signal at 1.96 ppm [O–C(=O)–C($C\boldsymbol{H_3}$)$_2$–Br; *e* in Figure 1]. This allows comparison of the integrals of the signals at 1.24

ppm from the initiator moiety and at 1.96 ppm from the BIB moiety to determine the completeness of terminal group modification, which is also more accurate than relying on the disappearance of the signal at 4.34 ppm.

The NMR–determined M_n's of the synthesized PLLAs are given in *Table 2.1*. They correspond well to the theoretical M_n's determined from the monomer/initiator feed ratios. The differences observed between the PLLA–OH and corresponding PLLA–Br are within experimental uncertainty. For further comparison and to determine polydispersity indices, SEC–LS experiments were performed in THF containing 2–3% v/v TEA (TEA added for consistency with the block copolymer conditions). The SEC–LS M_n values correspond well to the NMR–determined M_n values. The PDIs are relatively narrow, between 1.1 and 1.3. As also shown in Table 1, the specific optical rotatory powers, $[\alpha_L]$, of the different PLLA–OH and PLLA–Br were all in the range of −150±5º, compared to literature values for PLLA considered as optically pure that range from −145 to −160º.[6,39,46,49,50] This indicates that the optical purity of the macroinitiators is very high, certainly better than 90%. The high optical purity was supported by ^{13}C and ^{1}H homonuclear decoupling NMR experiments that show no evidence of racemization in either OH– or Br–terminated PLLA (see Appendix to Chapter 2).

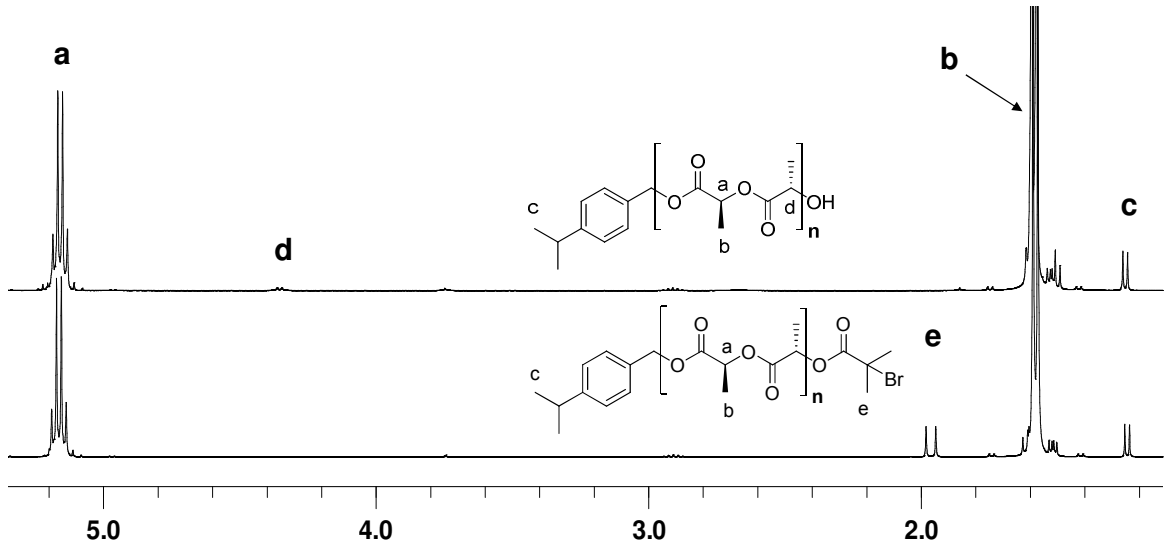

Figure 2.1. ^{1}H–NMR spectra of $PLLA_{5k}$–OH (upper) and $PLLA_{5k}$–Br (lower).

Table 2.1. Molecular weight characteristics and optical rotatory powers of the PLLA homopolymers and macroinitiators synthesized

Sample[a]	M_n (theor. [b]) g/mol	M_n (NMR [c]) g/mol	M_n (SEC–LS [d]) g/mol	PDI (SEC–LS [d])	$[\alpha_L]$ [e] °
$PLLA_{5k}$–OH	4900	4600	4600	1.11	–152
$PLLA_{13k}$–OH	11600	11600	13000	1.19	–155
$PLLA_{19k}$–OH	17300	19000	19800	1.14	–156
$PLLA_{5k}$–Br	5100	4900	5200	1.09	–147
$PLLA_{13k}$–Br	11700	13800	13200	1.32	–153
$PLLA_{19k}$–Br	17400	18900	19500	1.20	–145

[a] The subscript in the sample nomenclature indicates the average molecular weight (rounded off to the nearest 1k) of the four M_n values from the NMR and SEC–LS measurements considering both the OH and Br forms. [b] Theoretical assuming 95% conversion, $M_n = [([LLA]_0/[I]_0) \times 144) \times 0.95] + M_{initiator}$ (+ M_{BIB}). [c] Estimated by comparing the integrals of the PLLA methine protons (5.16 ppm) and the methyl protons of the initiator fragment (1.24 ppm), and adding $M_{initiator}$ and/or M_{BIB}. [d] Determined in THF with 2% (v/v) TEA, dn/dc = 0.048 mL/g. [e] Measured at room temperature.

2.3.2 Synthesis and molecular weight characterization of the PLLA–*b*–PDMAEMA copolymers

Because PLLA–Br is not soluble in DMAEMA, the synthesis of PLLA–*b*–PDMAEMA was carried out in toluene solution. DMAEMA polymerization was initiated from the PLLA–Br block using the CuBr/HMTETA ATRP catalyst, generally at 70 °C. However, since PLLA solubility in toluene decreases with increasing molecular weight, the solutions of PLLA–Br of molecular weights greater than 10,000 g/mol were diluted and polymerization took place initially at 90 °C. In the course of polymerization, the temperature was reduced to the usual polymerization temperature (70 °C), the good solubility of the PDMAEMA block in toluene maintaining the copolymer in solution.

Reaction feeds for each PLLA macroinitiator were calculated to target three block copolymers compositions, namely 0.5:1, 1:1 and 2:1 LLA:DMAEMA weight ratio, corresponding to approximately 1:1, 2:1 and 4:1 LLA:DMAEMA molar ratio. The experimental block molar ratios obtained were determined from ^{1}H NMR spectra (*Figure 2.2*) by comparison of the integrals of the PLLA methine signals at 5.16 ppm [–OC(=O)–C***H***(CH_3)–, *a* in *Figure 2.2*] with the integrals of the PDMAEMA signal at 4.06 ppm [–C(=O)–O–C***H*****$_2$**–CH_2–, *f* in *Figure 2.2*]. The molecular weights, based on the block molar ratios and on the average of the four NMR and SEC–LS molecular weight values for the PLLA–OH/Br in *Table 2.1*, are given in *Table 2.2*, and generally correspond well to the targeted values (only $PLLA_{19k}$–$PDMAEMA_{5k}$ has a PDMAEMA block that is about half of what was targeted). The SEC elugrams of the block copolymers are monomodal, with no shoulder on the low molecular weight side, thus showing no evidence of unreacted

macroinitiator. The molecular weights obtained by SEC–LS correspond well to the sum of the M_n for the individual blocks (*Table 2.2*). The low PDI's, between 1.1 and 1.2, are indicative of well–controlled polymerization. Specific optical rotatory power measurements of three copolymers, adjusted to the PLLA content, gave values of –145 °, –148 ° and –147 ° for 5k–4k, 13k–12k and 19k–17k, respectively, indicating essentially no change in the purity of the PLLA block compared to the parent homopolymer/macroinitiator.

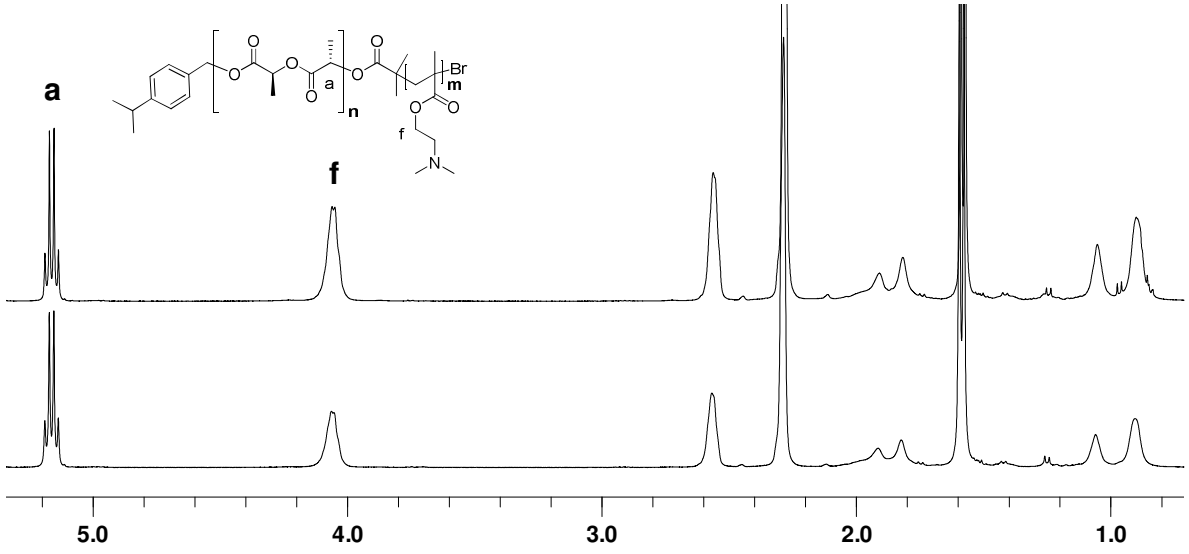

Figure 2.2. ^{1}H–NMR spectra of PLLA–*b*–PDMAEMA [13k–12k (lower) and 13k–23k (upper)].

Table 2.2. Molecular weight characterization of the PLLA–*b*–PDMAEMA copolymers synthesized

Sample	PLLA M_n (g/mol) / DP_n [a]	PDMAEMA M_n (g/mol) / DP_n [b]	Total (SEC–LS) M_n (g/mol) / PDI [c]
5k–2k	4800 / 63	2200 / 14	8100 / 1.10
5k–4k	4800 / 63	3800 / 24	9600 / 1.13
5k–10k	4800 / 63	9500 / 60	16900 / 1.15
13k–5k	12900 / 175	5000 / 32	18600 / 1.18
13k–12k	12900 / 175	12100 / 77	26000 / 1.16
13k–23k	12900 / 175	22900 / 146	38300 / 1.20
19k–5k	19300 / 264	5400 / 34	20500 / 1.20
19k–17k	19300 / 264	16600 / 106	37300 / 1.11
19k–35k	19300 / 264	35100 / 223	54200 / 1.19

[a] The M_n value given is the average of the four M_n values determined by NMR and SEC–LS for PLLA–OH and PLLA–Br (Table 1). DP_n: degree of polymerization. [b] Determined by NMR by comparison of the integrals for the PLLA *a* and PDMAEMA *f* signals (see Figure 2). [c] Determined by SEC–LS in THF with 3% (v/v) TEA; dn/dc values used are 0.055 (19k–5k), 0.058 (5k–2k, 13k–5k), 0.068 (5k–4k, 13k–12k, 19k–17k) and 0.073 (5k–10k, 13k–23k, 19k–35k).

To further confirm the absence of homopolymer impurity in the block copolymers, particularly of the initial (PLLA) block,[51,52] the PDMAEMA block of an aliquot of the block copolymer was quaternized by methyl iodide in dichloromethane (DCM). This procedure results in a gel (except for low PDMAEMA content, such as in samples 5k–2k, 13k–5k and 19k–5k), which can be broken up mechanically or by ultrasound to obtain insoluble and filterable block copolymer. The filtrate, which would contain any PLLA

homopolymer that might be present, is then evaporated, weighed, and analyzed by NMR using $CDCl_3$. Samples 5k–10k, 13k–23k and 19k–35k were tested in this way, and no trace of PLLA homopolymer was found in any of them, thus confirming successful chain extension. It may be added that elemental analysis of the quaternized block copolymers corresponded to the composition based on the molecular weight determination above.

TGA thermograms of several PLLA–*b*–PDMAEMA block copolymers compared with the two homopolymers are shown in the Supporting Information. PLLA degrades in a single step in the 280–360 °C region, whereas PDMAEMA degrades in two steps, the first in the 250–325 °C region, and the second in the 375–425 °C region. With the two blocks degrading in distinct temperature regions separated by a pseudo–plateau, TGA can be used to roughly estimate the relative block composition by determining the wt % sample remaining in the block copolymers at 375 °C, where the PLLA block is completely degraded, relative to the wt % sample remaining in the PDMAEMA homopolymer at 375 °C. The resulting estimations are given in *Table 2.3* and correspond satisfactorily to the ^1H NMR data.

Table 2.3. Composition of PLLA–*b*–PDMAEMA determined by TGA compared with NMR

Sample	wt % PDMAEMA, NMR [a]	wt % residue at 375 °C, TGA	wt % PDMAEMA, TGA [b]
$PDMAEMA_{16k}$		46	100
5k–2k	31	10	22
5k–4k	44	19	41
5k–10k	66	33	72
13k–5k	28	14	30
13k–12k	48	26	56
13k–23k	64	31	67
19k–5k	22	11	24
19k–17k	46	25	54
19k–35k	65	32	69

[a] Calculated from the NMR–determined block ratios; experimental uncertainty estimated as ±2 wt %. [b] wt % PDMAEMA = wt % residue ($PLLA_{xk}$–$PDMAEMA_{yk}$)×100% / wt % residue (PDMAEMA homopolymer); experimental uncertainty estimated as ±5 wt % at best.

2.3.3 DSC characterization of PLLA–OH/Br

DSC data for the PLLA homopolymers and macroinitiators are given in *Table 2.4*, and will serve as reference for the thermal analysis of the block copolymers. It may also be noted that, despite the growing importance of this polymer, there is limited thermal data as a function of PLLA molecular weight in the the available literature (although there is extensive data for certain molecular weights, particularly regarding crystallization

phenomena, as noted below), which is further reason to describe the tendencies observed. Since there are no significant differences in the data for the PLLA–OH/Br pairs, unless otherwise noted, what follows will refer to both as PLLA. The melting temperature of the highest molecular weight PLLA ($PLLA_{19k}$) is 172 °C, which is in the range expected for optically pure medium–to–high molecular weight PLLA [e.g. 167–169 °C for $PLLA_{10–20k}$;[6,46] 170–176 °C for $PLLA_{40–220k}$;[53] 175 °C for $PLLA_{200k}$ with 1.5% D–lactide content following 15 h of isothermal crystallization at 145 °C[54]]. It is slightly lower for $PLLA_{13k}$ (although higher than the 161 °C reported in Ref. 53 for a $PLLA_{15k}$) and is significantly lower for $PLLA_{5k}$, in accordance with the well–known dependence of T_m on molecular weight. It may also be mentioned that the melting peaks are dominated by a single sharp peak, often accompanied by a shoulder or smaller peak a few degrees lower (see *Figure 2.3*). The appearance of two (or more) melting peaks, depending on molecular weight and thermal history, has been reported frequently for PLLA, and its origin has been ascribed to melting–recrystallization and/or to two different crystalline forms, α (highly ordered and more stable) and α' (relatively disordered and less stable).[53,55–57] The heats of fusion obtained by integrating both peaks are ca. 60 J/g for all samples in all conditions measured (nascent, after controlled cooling at rates of 5 and 10 °C/min, and after cold crystallization of melt–quenched samples). This indicates a degree of crystallinity of ca. 65%, when referenced to 91 J/g for 100% crystalline PLLA.[54,58,59] On cooling from the melt (at rates of −5 and −10 °C/min), crystallization occurs at peak values between 110 and 90 °C (with a weak tendency to increase in temperature with increase in molecular weight) in all PLLA samples. Cold crystallization in quenched samples (as well as in $PLLA_{13k}$–Br under all

thermal histories tested, even if already partially crystallized, and in nascent $PLLA_{13k}$–OH and $PLLA_{19k}$) occurs in this same temperature range. Crystallization peaks are usually relatively sharp (both in cooling curves and in cold crystallization), with associated enthalpies (37–45 J/g) that are somewhat lower than for melting. Finally, the T_g's of quenched samples were determined to be 57 °C for $PLLA_{13k}$ and $PLLA_{19k}$ and 49 °C for $PLLA_{5k}$ (*Figure 2.3*). Given the T_g of 59 °C measured for amorphous $PLLA_{200k}$,[54] it can be concluded that only $PLLA_{5k}$ in the present series is in the sharply molecular weight dependent T_g range, similar to the T_m dependence. The ΔCp's are 0.58±0.01 $J \cdot g^{-1} \cdot K^{-1}$, very close to the value of 0.61 $J \cdot g^{-1} \cdot K^{-1}$ reported in Ref. 54 for a completely amorphous sample.

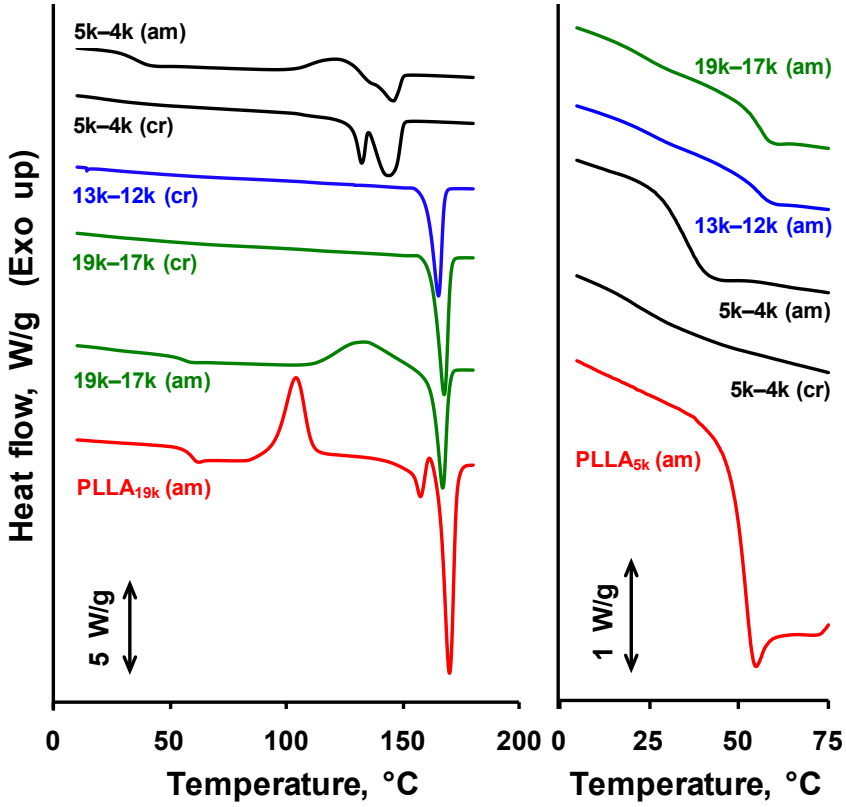

Figure 2.3. DSC thermograms of representative PLLA–*b*–PDMAEMA copolymers and PLLA homopolymers, scanned at 10°C/min (except PLLA, scanned at 20°C/min); "am" indicates samples that are initially amorphous (following a cooling scan of –10 °C/min for the xk–yk and following quenching for $PLLA_{xk}$) and "cr" indicates samples that are initially crystallized (following 1 h of annealing at 100 °C).

Table 2.4. DSC characterization of the PLLA homopolymers and PLLA–*b*–PDMAEMA copolymers synthesized

Sample [a]	W_{PLLA} [b] %	T_g (ΔCp) [c,d] °C ($J \cdot g^{-1} \cdot K^{-1}$)	T_g (ΔCp) [c,e] °C ($J \cdot g^{-1} \cdot K^{-1}$)	T_m °C	ΔH_m^{total} J/g (% cryst) [f]
$PLLA_{5k}$–OH	100		48 (0.58)	151 (155 [g])	60 (66)
$PLLA_{5k}$–Br	100		50 (0.56)	154	64 (70)
$PLLA_{13k}$–OH	100		57 (0.57)	164 (168 [g])	59 (65)
$PLLA_{13k}$–Br	100		57 (0.58)	168	57 (63)
$PLLA_{19k}$–OH	100		57 (0.57)	171	57 (63)
$PLLA_{19k}$–Br	100		58 (0.59)	172	58 (64)
5k–2k (cr)	69	27 (0.19)		144 (148 [h])	37 (59)
5k–2k (am)	69		40 (0.54)		
5k–4k (cr)	56	21 (0.20)		144 (149 [h])	30 (59)
5k–4k (am)	56		35 (0.48)		
5k–10k (cr)	34	20 (0.16)		140 (146 [h])	15 (49)
5k–10k (am)	34	26 (0.35)			
13k–5k (cr)	72		40 (0.19)	166 (168 [h])	37 (57)
13k–5k (am)	72		52 (0.47) [i]		
13k–12k (cr)	52	22 (0.1)		165 (167 [h])	24 (51)
13k–12k (am)	52	25 (0.1)	55 (0.20)		
13k–23k (cr)	36	20 (0.17)		163 (165 [h])	18 (55)
13k–23k (am)	36	22 (0.20)	54 (0.14)		
19k–5k (cr)	78		45 (0.22)	167 (169 [h])	43 (61)
19k–5k (am)	78		52 (0.50) [i]		
19k–17k (cr)	54	20 (0.10)		167 (169 [h])	26 (53)
19k–17k (am)	54	23 (0.09)	56 (0.23)		
19k–35k (cr)	35	20 (0.18)	58 (0.07)	167 (168 [h])	16 (50)
19k–35k (am)	35	21 (0.19)	56 (0.15)		

(Ended on the next page)

(Ending of **Table 2.4**)

[a] The notations "cr" and "am" refer to crystallized samples (annealed at 100 °C for 1 h) and amorphous samples (no crystallization observed in the preceding 10 °C/min cooling scan from the melt), respectively. [b] $W_{PLLA} = [M_{n(PLLA)} \times 100\%] / [M_{n(PLLA)} + M_{n(PDMAEMA)}]$, using the M_n values given in *Table 2.2*. [c] The T_g's were determined from inflection points for PLLA (20 °C/min curves, quenched samples) and from first derivative maxima for the copolymers (10 °C/min curves, average of two scans per point). ΔCp's were estimated from the heating curves. [d] PDMAEMA or PDMAEMA–rich phase. [e] PLLA or PLLA–rich phase. [f] For the copolymers, obtained from 10 °C/min heating curves of samples previously annealed at 100 °C for 1 h (two experiments). The ΔH_m^{total} values are relative to the total copolymer weight. The % cryst (= % crystallinity) is relative to the PLLA weight fraction: $[(\Delta H_m / W_{PLLA})/\Delta H_{m(ideal\ PLLA\ cryst)}] \times 100\%$, where $\Delta H_{m(ideal\ PLLA\ cryst)} = 91$ J/g.[54] [g] First heating scan only. [h] Maximum T_m observed (usually in the first heating scan, often also in the second heating scan). [i] The first derivative peak showed pronounced asymmetry on the low temperature side.

2.3.4 DSC characterization of PLLA–*b*–PDMAEMA

DSC thermograms of representative copolymers are illustrated in *Figure 2.3* and the results of the DSC analysis are compiled in *Table 2.4*. It was observed, first of all, that no crystallization was detected by DSC in any of the samples during cooling scans from the melt for scan speeds as low as 5 °C/min, in contrast to the PLLA homopolymers, which is ascribed to the PDMAEMA block significantly slowing down the rate of crystallization. Subsequent cold crystallization was similarly affected, with its occurrence and extent decreasing with increase in scan rate and in relative PDMAEMA block length (details given in the Supporting Information). Cold crystallization temperatures range from ca. 95 to 135 °C, tending to increase somewhat with increasing PLLA block molecular weight and scan rate (see Supporting Information for further details). The cold crystallization peaks are

usually fairly sharp, but sometimes broad, particularly in the presence of the longest PDMAEMA blocks and when occurring at higher temperatures.

The degree of crystallinity in the block copolymers (given in *Table 2.4* for samples annealed for 1 h at 100 °C) relative to that in PLLA tends to decrease mildly with increase in relative PDMAEMA block length. For example, after 1 h of annealing at 100 °C, the degree of crystallinity of the PLLA component ranges from 50 to 60% for the various block copolymers (compared to *ca.* 65% for PLLA), usually near the lower and upper end of the range for the longest and shortest relative PDMAEMA block lengths, respectively. The reduction in the degree of crystallinity of individual copolymers compared to the corresponding parent PLLA homopolymer ranges from 2–3% (19k–5k, the copolymer with the least PDMAEMA content) to *ca.* 20% (5k–10k). For longer annealing times (tested at 120 °C for 24 h on one representative block copolymer, 19k–17k, and parent homopolymer, $PLLA_{19k}$), the degree of crystallinity is increased but remains significantly lower in the copolymer compared to the homopolymer, 63 vs. 77 %.

For well–crystallized samples (*i.e.*, after annealing or after significant cold crystallization), it is observed that the DSC melting peaks of the 19k–yk and 13k–yk series are essentially monomodal and sharp, with peak values ranging from 163 to 169 °C (2–3 °C higher in the initial scan than in the two scans following annealing, as well as 1–4 °C higher for the 19k–yk series compared to the 13k–yk series scanned under the same conditions). In some cases (especially in the 13k–yk series), the sharp, intense peak is accompanied by a slight shoulder or weak, sharp peak located a few degrees lower. Only the 20 °C/min curves of 13k–5k and 19k–5k show two closely spaced, similar intensity peaks. Overall, both the form and the melting temperatures in these two copolymer series

are similar to what is observed in the corresponding parent homopolymers. In contrast, the 5k–yk series shows more complex melting, generally composed of at least two melting peaks, a sharp lower temperature one and a broader higher temperature one, their maxima typically separated by 10–15 °C. The melting endotherms in this series span the temperature range of ca. 110–150 °C, much lower than for the other two series due, first of all, to the low PLLA molecular weight. In addition, compared to the $PLLA_{5k}$ parent polymer, the melting region in the 5k–yk copolymers is both more complex and reduced in temperature by ca. 10 °C (comparing peak values). This, as will be shown below, can be related to the miscibility of the low molecular weight blocks. It may be added, for completeness, that a broad and very weak exotherm just before the melting peak was sometimes observed in the heating curves of the copolymers, particularly (but not always and not only) in the heating curves of the annealed samples, observed also by others in PLLA homopolymers and possibly related to additional crystallization or recrystallization.[53,54a,57]

Analysis of the T_g's of the block copolymers can provide information about block miscibility. For this purpose, we examined in detail the T_g region in the 10 °C/min heating thermograms, obtained both after 10 °C/min cooling (completely amorphous samples) and after 1 h annealing at 100 °C (semi–crystalline samples), with each of the two thermal histories repeated twice. The T_g data, given in Table 4, were determined from the maxima in the first derivative curves, which was found to provide the most reliable values. It may be mentioned that the T_g's determined from the 20 °C/min curves (first derivative maxima, one scan per sample) were usually 1–3 °C higher than in the corresponding PLLA homopolymers (which were scanned, in the completely amorphous state, at only this

heating rate), and also that the T_g of the minor phase in these curves was often less obvious than in the curves scanned at lower rates.

The four copolymers, 13k–yk (y=12k, 23k) and 19k–yk (y=17k, 35k), in their amorphous state, show two well–separated T_g's, the higher one associated with a PLLA or PLLA–rich phase and the lower one with a PDMAEMA or PDMAEMA–rich phase. The higher T_g is essentially identical to that of the PLLA parent homopolymers (taking into account the higher scan rate for the latter), indicative of complete immiscibility of the PDMAEMA block in the PLLA block. The lower T_g, at 23±2 °C, is somewhat higher than the T_g of 17 °C measured for the $PDMAEMA_{16k}$ homopolymer [18 °C reported in Ref. 60 for $PDMAEMA_{100k}$], suggesting slight miscibility of PLLA in PDMAEMA, particularly for 13k–12k, the lowest total molecular weight copolymer of the four, with its T_g of 25 °C. In the corresponding semi–crystalline samples, this T_g lies at 20 °C (22 °C for 13k–12k), which is still a little higher than that of the PDMAEMA homopolymer. Although T_g determinations by DSC are typically assumed to have a precision of ±2 °C, the observation that a 50/50 (w/w) blend of $PLLA_{13k}$–Br and PDMAEMA also displays a T_g of 20 °C compared to 17 °C for the PDMAEMA homopolymer (both tested in a sequence of seven DSC scans up to 180 °C) suggests that very slight miscibility of PLLA in PDMAEMA remains in the crystallized samples, possibly arising in particular from the lowest PLLA molecular weight fraction. The PLLA T_g is difficult to detect in the phase–separated block copolymers when the PLLA block is semi–crystalline (there is just a slight baseline deviation in the first derivative curves over a relatively wide temperature range, except for

19k–35k, where its value is the same as for $PLLA_{19k}$), due, of course, to the much lower fraction of amorphous PLLA (in the blend, its value is the same as for $PLLA_{13k}$ alone).

In contrast to the above four copolymers showing two distinct T_g's, only one T_g is detectable in the two copolymers of the same two series having the shortest PDMAEMA block length (13k–5k and 19k–5k). In the completely amorphous samples, the T_g value of these two copolymers is 5 °C lower than in the parent PLLA homopolymers. This suggests that the absence of a second (lower) T_g is not due to the low PDMAEMA content rendering the T_g difficult to detect, but rather to the miscibility of the short PDMAEMA block (5k) in the amorphous PLLA phase. This miscibility is confirmed by the observation of a much lower T_g in the semi–crystalline samples (40–45 °C), where the amorphous phase is now composed of a much greater PDMAEMA fraction compared to the non–crystallized samples.

Miscibility is also evident when both blocks are short (5k–yk series). The completely amorphous samples, in particular, show single well–defined T_g's at values that are intermediate to the corresponding homopolymer values, approximately weighted according to the block composition. The T_g's are much lower in the presence of PLLA crystallization, but it is clear that for the 5k–2k copolymer, with its T_g of 27 °C, the amorphous fraction of PLLA still forms a miscible phase with PDMAEMA. This is probably also true for the semi–crystalline 5k–4k copolymer (T_g = 21 °C), considering that the T_g of the corresponding low molecular weight PDMAEMA homopolymer may be expected to be significantly lower than 20 °C. For the 5k–10k copolymer, PLLA crystallization reduces the T_g to 20 °C, indicating minimal solubility of PLLA in PDMAEMA, as discussed above for the 12k to 35k PDMAEMA blocks.

For a more quantitative evaluation, predicted T_g's for miscible phases were calculated using the Fox equation, $1/T_g = w_A/T_{gA} + w_B/T_{gB}$, where w_A and w_B represent the weight fractions of A (PLLA) and B (PDMAEMA) and T_{gA} and T_{gB} their glass transition temperatures in K (assuming a molecular weight–independent T_g of 17 °C for PDMAEMA). It can be observed from *Table 2.5* that the measured T_g's compare satisfactorily with the predicted T_g's and are certainly consistent with the blocks being essentially completely miscible in the amorphous state when one or both of them are of low molecular weight (up to at least 5k).

Table 2.5. T_g values predicted by the Fox equation, compared with the measured T_g's, for the miscible PLLA–*b*–PDMAEMA block copolymers in their completely amorphous and semi–crystalline states

Copolymer	Sample state [a]	PLLA fraction (amorphous), % [b]	Predicted T_g °C	Measured T_g °C
5k–2k	am	69	38	40
5k–2k	cr	48	31	27
5k–4k	am	56	33	35
5k–4k	cr	34	27	21
5k–10k	am	34	27	26
5k–10k	cr	20	23	20
13k–5k	am	72	45	52
13k–5k	cr	52	36	40
19k–5k	am	78	47	52
19k–5k	cr	58	39	45

[a] The sample states are identified by "am" for completely amorphous samples and "cr" for semi–crystalline samples. The measured T_g's are taken from Table 4. The calculated T_g's were determined using 17 °C for PDMAEMA in all cases, 48 °C for $PLLA_{5k}$, and 57 °C for $PLLA_{13k}$ and $PLLA_{19k}$. [b] The PLLA fraction of the amorphous part in the semi–crystalline samples was determined using the degree of crystallinity reported in Table 2.4.

2.4 Conclusions

A series of well–defined linear poly(L–lactide)/poly(2–dimethylaminoethyl methacrylate) (PLLA–b–PDMAEMA) diblock copolymers with narrow polydispersity were successfully prepared by ring–opening polymerization of L–lactide, endgroup conversion of the PLLA homopolymers to suitable macroinitiators, followed by addition of the PDMAEMA block by atom transfer radical polymerization. This method allows the synthesis of low to high molecular weight PLLA–b–PDMAEMA. In this work, three PLLA block lengths, with molecular weights ranging from 5,000 and 20,000 g/mol (shown to span the range from molecular weight dependent to essentially independent T_g's and T_m's), were each coupled with three PDMAEMA block lengths corresponding to approximately equal to, half of, and one–quarter of PLLA in molar ratio. DSC analysis indicates that low molecular weight blocks of ca. 5,000 g/mol and less are miscible in the amorphous phase, including in the presence of PLLA crystallinity, as shown by T_g's that are intermediate to those of the corresponding homopolymers and by the significant decrease in the melting point of the PLLA crystalline phase. With increase in PDMAEMA block length, the degree of crystallinity of the PLLA block tends to decrease mildly, whereas the kinetics of crystallization are significantly reduced.

References and notes to Chapter 2

1. Dechy–Cabaret, O.; Martin–Vaca, B.; Bourissou, D. *Chem. Rev.* **2004**, *104*, 6147–6176.
2. Wang, M. *Am. J. Biochem. Biotechnol.* **2006**, *2*, 80–84.
3. Heino, A.; Naukkarinen, A.; Kulju, T.; Törmälä, P.; Pohjonen, T.; Mäkelä, E. A. *J. Biomed. Mater. Res.*, **1996**, *30*, 187–192.
4. Lassalle, V.; Ferreira, M. L. *Macromol. Biosci.* **2007**, *7*, 767–783.
5. Boudouris, B. W.; Frisbie, C. D.; Hillmyer, M. A. *Macromolecules* **2008**, *41,* 67–75.
6. Tsuji, H.; Horii, F.; Hyon, S.–H.; Ikada, Y. *Macromolecules* **1991**, *24*, 2719–2724.
7. Sarasua, J. R.; Prud'homme, R. E.; Wisniewski, M.; Le Borgne, A.; Spassky, N. *Macromolecules* **1998**, *31,* 3895–3905.
8. Gu, L.; Zhu S.; Hrymak, A. N. *Coll. Polym. Sci.* **2002**, *280*, 167–175.
9. Lenoir, S.; Pagnoulle, Ch.; Detrembleur, C.; Galleni, M.; Jérôme, R. *J. Polym. Sci.: Part A: Polym. Chem.* **2006**, *44*, 1214–1224.
10. Fonseca, M. J.; Storm, G.; Hennink, W. E.; Gerritsen, W. R.; Haisma, H. J. *J. Gene Med.* **1999**, *1*, 407–414.
11. Jacobs, C.; Dubois, P.; Jérôme, R.; Teyssié, P. *Macromolecules*, **1991***, 24,* 3027–3034.
12. Veld, P. J. A. I.; Velner, E. M.; Witte, P. V. D.; Hamhuis, J.; Dijkstra, P. J.; Feijen, J. *J. Polym. Sci.: Part A: Polym. Chem.* **1997**, *35*, 219–226.
13. (a) Rashkov, I.; Manolova, N.; Li, S. M.; Espartero, J. L.; Vert, M. *Macromolecules* **1996**, *29,* 50–56. (b) Li, S. M.; Rashkov, I.; Espartero, J. L.; Manolova, N.; Vert, M. *Macromolecules* **1996**, *29,* 57–62.
14. Otsuka, H.; Nagasaki, Y.; Kataoka, K. *Biomacromolecules* **2000**, *1*, 39–48.
15. Zalusky, A. S.; Olayo–Valles, R.; Wolf, J. H.; Hillmyer, M. A. *J. Am. Chem. Soc.* **2002**, *124*, 12761–12773.
16. Tao, L.; Luan, B.; Pan, C. Y. *Polymer* **2003**, *44*, 1013–1020.

17. Chen, D.; Gong, Y.; He, T. *Macromolecules* **2006**, *39,* 4101–4107.

18 Kohori, F.; Sakai, K.; Aoyagi, T.; Yokoyama, M.; Sakurai, Y.; Okano, T. *J. Controlled Release* **1998**, *55*, 87–98.

19. You, Y.; Hong, C.; Wang, W.; Lu, W.; Pan, C. *Macromolecules* **2004**, *37,* 9761–9767.

20. Ring, J. O.; Thomann, R.; Mülhaupt, R.; Raquez, J. M.; Degée, P.; Dubois, P. *Macromol. Chem. Phys*. **2007**, *208*, 896–902.

21. Castillo, R. V.; Müller, A. J.; Lin, M.–C.; Chen, H.–L.; Jeng, U–S.; Hillmyer, M. A. *Macromolecules* **2008**, *41*, 6154–6164.

22. Luo, L.; Ranger, M.; Lessard, D. G.; Le Garrec, D.; Gori, S.; Leroux, J.–C.; Rimmer, S.; Smith, D. *Macromolecules* **2004**, 37, 4008–4013.

23. Baines, F.L.; Billingham, N. C.; Armes, S. P. *Macromolecules* **1996**, *29,* 3416–3420.

24. Baines, F. L.; Armes, S. P.; Billingham, N. C.; Tuzar, Z. *Macromolecules* **1996**, 29, 8151–8159.

25. Creutz, S.; Teyssié, Ph.; Jérôme, R. *Macromolecules*, **1997**, 30, 6–9.

26. Gohy, J.–F.; Antoun, S.; Sobry, R.; Van den Bossche, G.; Jérôme, R. *Macromol. Chem. Phys.* **2000**, 201**,** 31–41.

27. Narrainen, A. P.; Pascual, S.; Haddleton, D. M. *J. Polym. Sci.: Part A: Polym. Chem.*, **2002**, 40, 439–450.

28. Ravi, P.; Sin, S. L.; Gan, L. H.; Gan, Y. Y.; Tam, K. C.; Xia, X. L.; Hu, X. *Polymer*, **2005**, 46, 137–146.

29. Jakubowski, W.; Lutz, J.–F.; Slomkowski, S.; Matyjaszewski, K. *J. Polym. Sci.: Part A: Polym. Chem.*, **2005**, 43, 1498–1510.

30. Bougard, F.; Jeusette, M.; Mespouille, L.; Dubois, Ph.; Lazzaroni, R. *Langmuir*, **2007**, 23, 2339–2345.

31. Alvarez–Lorenzo, C.; Barreiro–Iglesias, R.; Concheiro, A.; *Langmuir*, **2005**, 21, 5142–5148.

32. Hu, D.; Cheng, Z.; Zhu, J.; Zhu, X. *Polymer*, **2005**, 46, 7563–7571.

33. Guice, K. B.; Loo, Y.–L. *Macromolecules* **2006**, 39, 2474–2480.

34. Gohy, J.–F.; Antoun, S.; Jérôme, R.; *Macromolecules* **2001**, 34, 7435–7440.

35. Munier, S.; Messai, I.; Delair, T.; Verrier, B.; Ataman–Önal, Y. *Coll. Surf. B* **2005**, *43*, 163–173.

36. Firmenich, S.; Berthier, D.; Ouali, L. Patent No. WO 2005/108471 A1.

37. Coulembier, O.; Lohmeijer, B. G. G.; Dove, A. P., Pratt, R. C.; Mespouille, L.; Culkin, D. A.; Benight, S. J.; Dubois, Ph. Waymouth, R. M.; Hedrick, J. L. *Macromolecules* **2006**, *39*, 5617–5628.

38. Yuan, W.; Yuan, J.; Zheng, S.; Hong, X. *Polymer* **2007**, *48*, 2585–2594.

39. Spasova, M.; Mespouille, L.; Coulembier, O.; Paneva, D.; Manolova, N.; Rashkov, I.; Dubois, P. *Biomacromolecules* **2009**, *10*, 1217–1223.

40. Spasova, M.; Manolova, N.; Paneva, D.; Mincheva, R.; Dubois, P.; Rashkov, I.; Maximova, V.; Danchev, D. *Biomacromolecules* **2010**, *15*, 151–159.

41. Karanikolopoulos, N.; Zamurovic, M.; Pitsikalis, M.; Hadjichristidis, N. *Biomacromolecules* **2010**, *11*, 430–438.

42. Huglin, M. B. Light scattering from polymer solutions, ch. 7. Academic Press, London, **1972**.

43. Labouriau, A.; Taylor, D.; Stephens, T. S.; Pasternak, M. *Polym. Degrad. Stab.* **2006**, *91*, 1896–1902.

44. Kricheldorf, H. R.; Kreiser–Saunders, I.; Stricker, A. *Macromolecules* **2000**, *33*, 702–709.

45. It is common to distill tin octoate (to remove 2–ethylhexanoic acid) and to put DMAEMA through alumina column (to remove inhibitor) prior to use. In practice, even after distillation 2–ethylhexanoic acid appears again, and the inhibitor was not observed to affect the ATRP process significantly.

46. Jalabert, M.; Fraschini, C.; Prud'homme, R. E. *J. Polym. Sci., Part A: Polym. Chem.* **2007**, *45*, 1944–1955.

47. Dubois, P.; Jacobs, C.; Jérôme, R.; Teyssié, P. *Macromolecules* **1991**, *24*, 2266–2270.

48. Espartero, J. L.; Rashkov, I.; Li, S. M.; Manolova, N.; Vert, M. *Macromolecules* **1996**, *29,* 3535–3539.

49. Tsuji, H.; Hyon, S. H.; Ikada, Y. *Macromolecules* **1991**, *24*, 5651–5656.

50. Kricheldorf, H. R.; Dunsing, R. *Makromol. Chem.* **1986**, *187*, 1611–1625.

51. Park, S.; Park, I.; Chang, T.; Ryu, C. Y. *J. Am. Chem. Soc.* **2004**, *126*, 8906–8907.

52. Chung, B.; Park, S.; Chang, T. *Macromolecules* **2005**, *38*, 6122–6127.

53. Pan, P.; Kai, W.; Zhu, B.; Dong, T.; Inoue, Y. *Macromolecules* **2007**, *40*, 6898–6905.

54. (a) Pyda, M.; Bopp, R. C.; Wunderlich, B. *J. Chem. Thermodynamics* **2004**, *36*, 731–742. (b) Pyda, M.; Wunderlich, B. *Macromolecules* **2005**, *38,* 10472–10479.

55. Zhang, J.; Tashiro, K.; Domb, A. J.; Tsuji, H. *Macromol. Symp*. **2006**, *242*, 274–278.

56. Kawai, T.; Rahman, N.; Matsuba, G.; Nishida, K.; Kanaya, T.; Nakano, M.; Okamoto, H.; Kawada, J.; Usuki, A.; Honma, N.; Nakajima, K.; Matsuda, M. *Macromolecules* **2007**, *40,* 9463–9469.

57. Shieh, Y.–T.; Liu, G.–L. *J. Polym. Sci: Part B: Polym. Phys.* **2007**, *45*, 466–474.

58. Fischer, E. W.; Sterzel, H. J.; Wegner, G. *Kolloid–Z. u. Z. Polymere* **1973**, *251*, 980–990.

59. A number of different values for the heat of fusion of 100% crystalline PLLA have been used in the literature, ranging from 81 to 203 J/g, as also discussed in Ref. 7. However, most often, values in the low range are used, and the value of 91 J/g determined in Ref. 54 appears highly reliable and is very similar to the frequently cited value of 93 J/g determined in Ref. 58.

60. Arce, A.; Fornasiero, F.; Rodrıguez, O.; Radke, C. J.; Prausnitz, J. M. *Phys. Chem. Chem. Phys.* **2004**, *6*, 103–108.

Appendix to Chapter 2

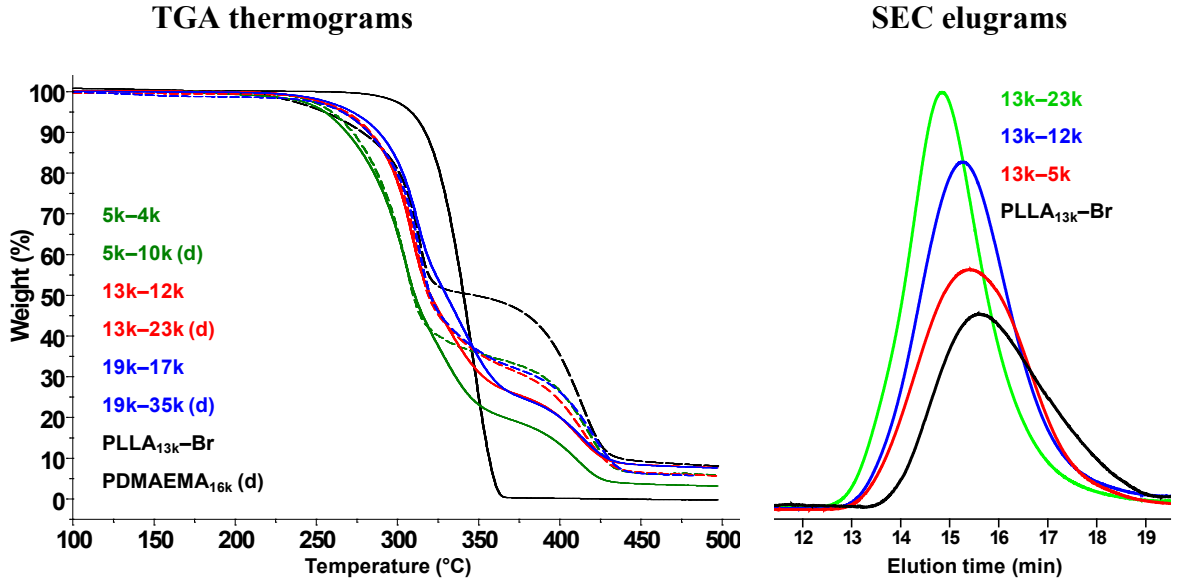

Figure A2.1. Left: TGA thermograms of selected PLLA–*b*–PDMAEMA block copolymers and PLLA and PDMAEMA homopolymers, (d) indicating dashed lines. Right: SEC elugrams of the $PLLA_{13k}$ block copolymer series in THF (with 5% TEA); where the block copolymer elugram intensities were normalized to a dichlorobenzene (DCB) peak at 22.7 min (1 mg/mL DCB added to verify the flow rate).

DSC experiments

Scan sequence. The following scan sequence, between the temperature limits of –20 and 185 °C, was applied to DSC analysis of the block copolymers: (a) initial heat of as–prepared samples at 10 °C/min, (b) first cool at 5 °C/min, (c) second heat at 5 °C/min, (d) second cool at 50 °C/min, (e) third heat at 20 °C/min, (f) third cool at 10 °C/min, (g) isothermal at 100 °C for 1 h, (h) fourth heat at 10 °C/min, (i) fourth cool at 10 °C/min, (j) fifth heat at 10 °C/min, (k) fifth cool at 10 °C/min, (l) isothermal at 100 °C for 1 h, (m) sixth heat at 10 °C/min, (n) sixth cool at 10 °C/min, (o) seventh heat at 10 °C/min, (p)

seventh cool at 10 °C/min. A reduced sequence was applied to the simpler PLLA homopolymers, but a quench (nominally 200 °C/min) was necessary to obtain completely amorphous samples, which was followed by a heating scan at 20 °C/min for the T_g determination.

Dependence of cold crystallization on DSC scan rate and relative PDMAEMA block length. When the PDMAEMA block is about half the weight of PLLA, cold crystallization was observed for all three scan rates tested (5, 10 and 20 °C/min), but to a much lesser degree for 20 °C/min. (The 19k–5k sample, where the PDMAEMA block is about a quarter of the weight of the PLLA block, shows a similar degree of crystallization for all three scan rates). For similar molecular weight blocks, scans at 20 °C/min showed a very small amount of cold crystallization in the shortest block copolymer (5k–4k), and none in the others. For the longest relative PDMAEMA block weights, cold crystallization in the 5 °C/min heating curves is sharply reduced (5k–10k), barely noticeable (13k–23k), and absent (19k–35k), in order of increasing total molecular weight.

Temperature of cold crystallization. Cold crystallization temperatures tend to be lower in the initial (10 °C/min) and second (5 °C/min) heating curves (approximately 95–100 °C for $PLLA_{5k}$, 105–110 °C for $PLLA_{13k}$, 110–120 °C for $PLLA_{19k}$) and higher in the later 10 °C/min heating curves (approximately 110–115 °C for $PLLA_{5k}$, 120 °C for $PLLA_{13k}$, 130–135 °C for $PLLA_{19k}$).

Copolymer versus blend. A comparison was also made between the 13k–12k copolymer and a 50/50 (w/w) blend of $PLLA_{13k}$–Br with $PDMAEMA_{16k}$ (the same blend as described in the main text in connection with the discussion concerning the T_g's). No crystallization was observed in the cooling scans of either the copolymer or the blend (–10

°C/min); however, whereas little cold crystallization was observed in the subsequent heating scans (10 °C/min) of the copolymer (as indicated by a shallow broad endotherm centered at ca. 140 °C followed by a weak melting peak, both giving a PLLA degree of crystallinity of ca. 7%), the blend showed significant cold crystallization giving a PLLA degree of crystallinity of 40 %, as shown by a sharp peak at 101–104 °C (three scans). Furthermore, the PLLA degree of crystallinity was greater for the blend after 30 min of annealing at 100 °C (59%, like in pure $PLLA_{13k}$) than for the copolymer after 60 min of annealing at 100 °C (51%, Table 4). This comparison illustrates the much more important effect on PLLA crystallization of the covalently linked second block compared to that of the blend (which is essentially immiscible according to the Tg analysis; see main text).

NMR experiments

Since the specific optical rotatory powers, $[\alpha_L]$, for two of the three PLLA homopolymers are a little lower for the macroiniator compared to the PLLA–OH parent, possibly suggesting slight racemization during the terminal group modification step (*Table 2.1*), these samples were verified by ^{13}C and homonuclear decoupling NMR experiments, which can both show evidence of PLLA racemization. The experiments were done with $CDCl_3$ solutions containing ~0.1% TMS, using the Bruker ARX 400 instrument. Here, we give the results for $PLLA_{19k}$, for which the greatest decrease in $[\alpha_L]$ (11 °) was observed. *Figure A2.2* shows the ^{13}C NMR spectra of hydroxy– and Br–terminated $PLLA_{19k}$. None of the three carbon signals (169.7, 69.2 and 16.8 ppm corresponding to the carbonyl, methine and methyl groups, respectively) show any evidence of additional peaks indicative of decreased isotacticity in PLLA–Br. Similarly, homonuclear decoupling to saturate the signal at 1.58

ppm (methyl hydrogens of the LLA repeat unit; decoupling frequency 632 Hz) results in a clear singlet for the signal at 5.16 ppm (methine hydrogen) for both samples (*Figure A2.3*), as expected for highly isotactic PLLA. The slight distortion on the low ppm side of the signal, stronger for PLLA–OH than for PLLA–Br, was also present in the TMS and CDCl3 signals, indicating that it is an artefact. The same observations hold for the other two PLLA pairs. The melting points determined by DSC, in comparison with literature values, described in the main text, are also indicative of very high optical purity, with no significant differences observed between the OH and Br pairs (*Table 2.4* in main text).

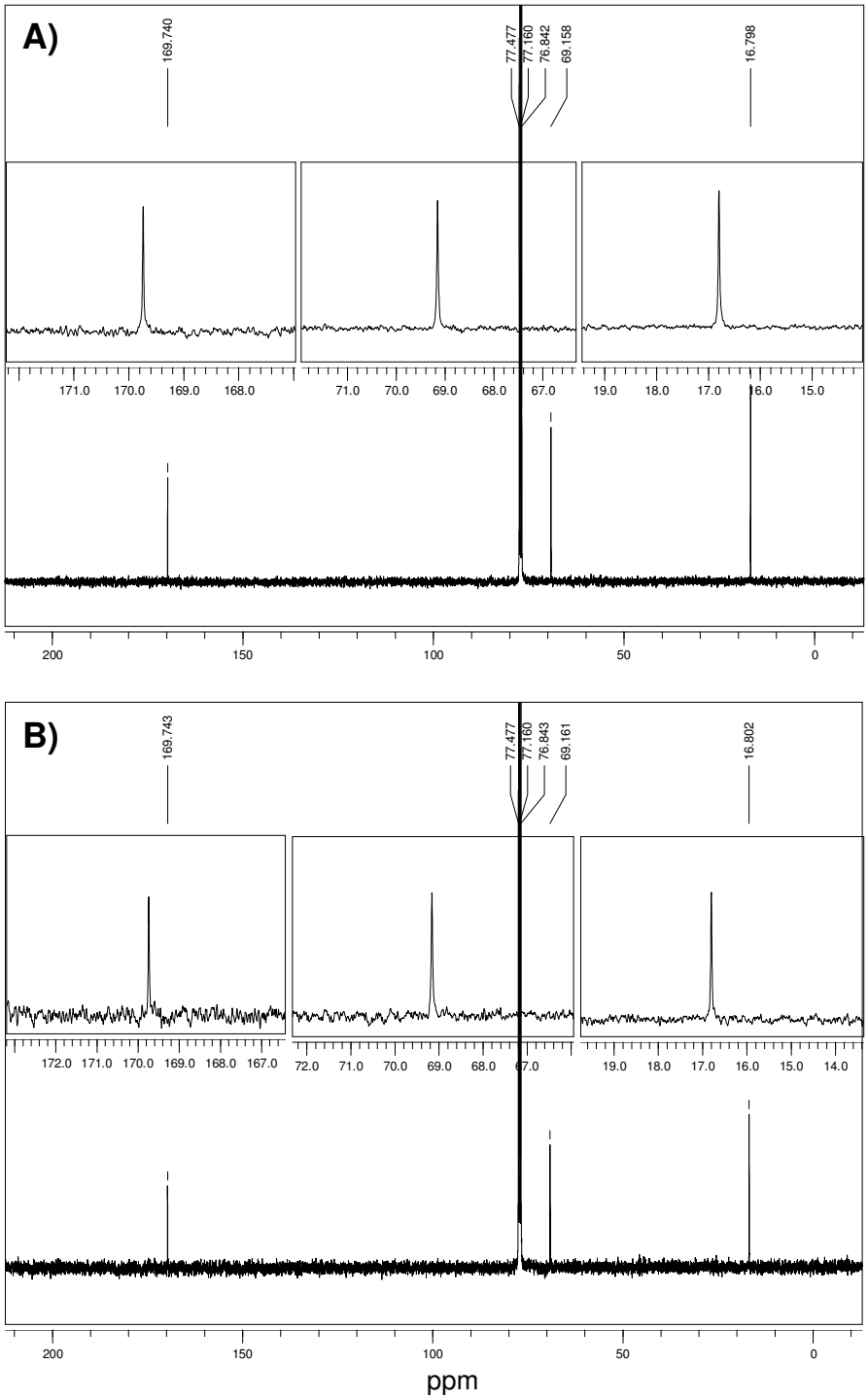

Figure A2.2. ^{13}C–NMR spectra of (A) $PLLA_{19k}$–OH and (B) $PLLA_{19k}$–Br. Insets show single peaks in expanded view.

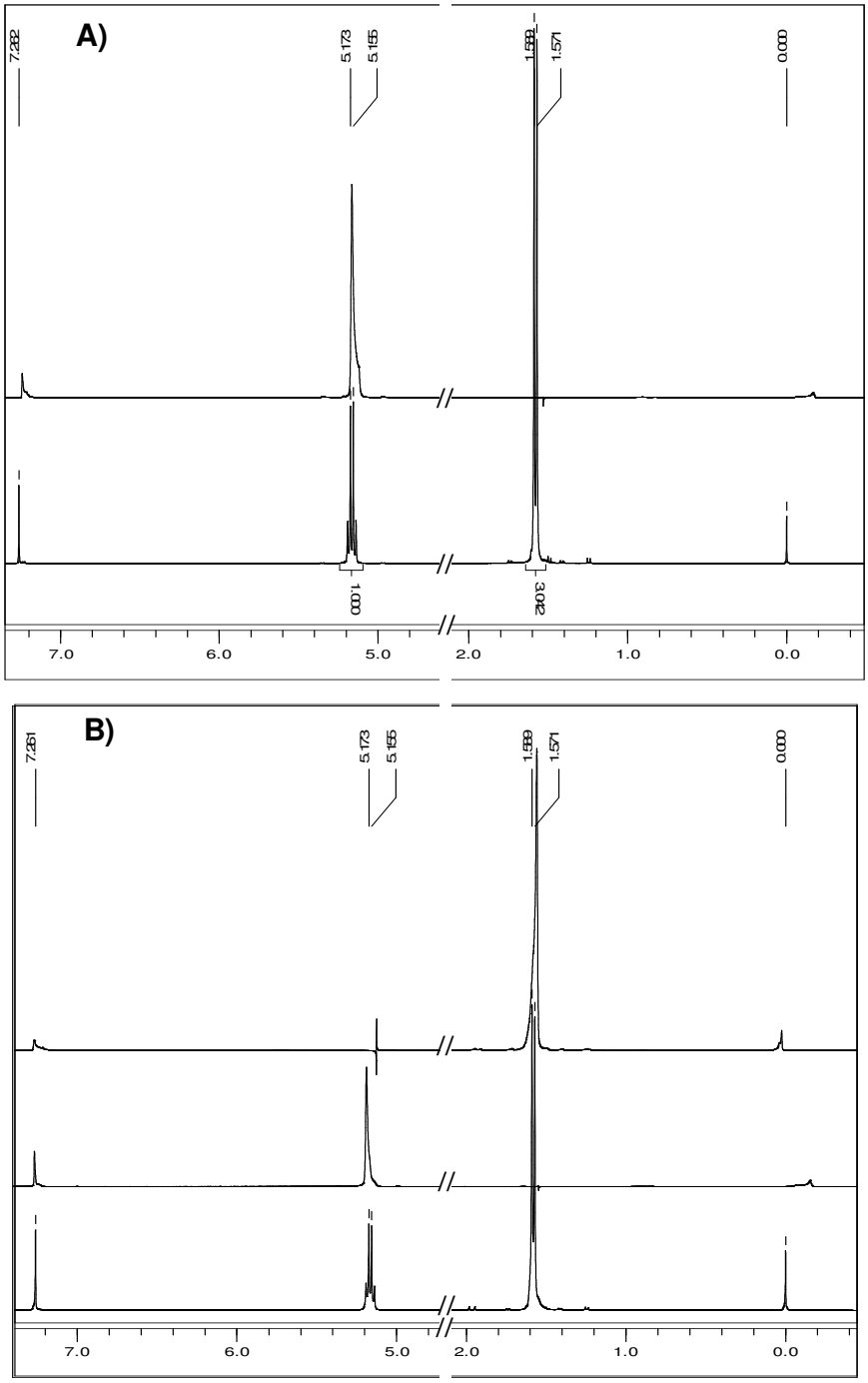

Figure A2.3. (A) Fragments of ^{1}H (lower) and ^{1}H–HD NMR (upper) spectra of $PLLA_{19k}$–OH [1.58 ppm (632 Hz) was used as a decoupling frequency]. (B) Fragments of ^{1}H (lower) and ^{1}H–HD (middle and upper) NMR spectra of $PLLA_{19k}$–Br [1.58 ppm (632 Hz), middle, and 5.16 (2064 Hz), upper, were used as decoupling frequencies].

LINEAR AMPHIPHILIC DIBLOCK COPOLYMERS OF LACTIDE AND 2–DIMETHYLAMINOETHYL METHACRYLATE USING BIFUNCTIONAL INITIATOR AND ONE–POT APPROACHES

3

3.1 Introduction

At present, a three–step combination of ring–opening polymerization (ROP) of cyclic esters and, typically, atom–transfer radical polymerization (ATRP) is recognized as an efficient tool for the preparation of polyester–containing block copolymers in a controlled fashion.[1] It usually starts with ROP, followed by an intermediate terminal group modification step to enable polymerization of the second block. An alternative approach is to use a single bifunctional initiator capable of initiating the polymerization of both monomers and that is stable in both polymerization conditions. This allows omitting the terminal group modification step, since the bifunctional initiator simultaneously initiates polymerization of the first block and functionalizes it to make it a suitable macroinitiator. Generally, the

macroinitiator is isolated before proceeding with the polymerization of the next block. When not isolated, it is termed a one–pot sequential polymerization.

The concept of using a single initiator to perform two (or more) mechanistically different polymerizations was first introduced by Puts and Sogah[2] to combine controlled free–radical, cationic and anionic polymerizations of styrene, oxazoline and lactides/lactones, respectively. Shortly afterwards, a bifunctional initiator was used to combine ROP of ω–caprolactone (CL) and nitroxide–mediated polymerization (NMP) of polystyrene (PS) or ATRP of methyl methacrylate (MMA).[3] Since then, the use of a bifunctional initiator for the synthesis of diblock copolymers in the two–step process was also reported in combinations such as ATRP–NMP (PMMA–b–PS),[4] cationic–ATRP (polyTHF–b–PS),[5] and cationic–anionic (polyoxetane–b–PCL).[6] For the combination of ROP and ATRP, 2'–hydroxyethyl and 2'–hydroxybutyl 2–bromoisobutyrate (HEBIB[7,8] and HBBIB,[9] respectively), which provide the –OH functionality for ROP and the –Br functionality for ATRP, are good candidates for dual initiation and can be synthesized easily in one step from affordable chemicals. HEBIB was used, in particular, for synthesizing PLLA–b–PDMAEMA by sequential ROP using $Sn(Oct)_2$ followed by ATRP.[10]

Since the reactive sites survive each of the polymerization processes involved, the number of synthetic steps in block copolymer synthesis can be further reduced by conducting both polymerizations simultaneously in a one–pot synthesis. For this, both polymerizations should have optimal polymerization temperatures that are sufficiently similar to ensure good control over the polymerization process. This is the case, for

example, for the ROP of ω–caprolactone (CL), catalyzed by $Sn(Oct)_2$, and conducted at 125 °C simultaneously with NMP of styrene,[11] using a custom–made bifunctional initiator possessing a secondary benzyl group linked to an alkoxyamine (termed "nitroxide") and a primary alcohol for efficient initiation of NMP and ROP, respectively. Simultaneous ATRP of methacrylates and ROP of CL, using HBBIB with $AlEt_3$[9] or CBr_3CH_2OH with $Al(OiPr)_3$,[11] can also be conducted at a temperature (70 °C) that is optimal for both polymerizations..

In contrast, simultaneous ATRP of acrylate and ROP of CL using HEBIB with $Sn(Oct)_2$, conducted at 120 °C (optimal for ROP as opposed to 70 °C for ATRP), did not proceed smoothly.[8] Moreover, since the rates of the two polymerizations are different, the final block copolymer can be modulated only by the initial feed. In the same study, one–pot sequential ATRP followed by ROP using HEBIB with $Sn(Oct)_2$ also failed due to interactions between accumulated Cu(II) resulting from the ATRP and the Sn(II) added for ROP. To the best of our knowledge, there are no reports of successful one–pot simultaneous polymerizations having quite different optimal temperatures.

In this chapter, we report on our attempts to synthesize diblock copolymers of poly(L–lactide) (PLLA) and poly(2–dimethylaminoethyl methacrylate) (PDMAEMA) by sequential polymerization, starting either with PDMAEMA or with PLLA, as well as one–pot simultaneous polymerization, combining ATRP and ROP using the dual initiator, HEBIB, with $Sn(Oct)_2$ as catalyzer for ROP. Previously (*Chapter 2*), we had prepared a series of PLLA–b–PDMAEMA copolymers using a three–step technique starting from PLLA, which includes an intermediate terminal group modification step to obtain the

PLLA macroinitiator suitable for ATRP. It was found that the maximum molecular weight possible for the PLLA block is limited to ca. 20,000 g/mol due to solubility issues, particularly because there are only a limited number of solvents for PLLA. Sequential polymerization initiated by a bifunctional initiator with the PLLA block synthesized first will be subject to the same limitations. In principle, this limitation can be palliated by polymerizing the PDMAEMA block first, since the latter may help maintain chain solubility up to higher PLLA molecular weight. One–pot simultaneous polymerization of the two blocks will also be tested, given that the optimal temperatures of the two polymerizations are only moderately far apart (70 vs. 120 °C). We will show that the latter two approaches lead to racemization of the block copolymer (though less in the one–pot polymerizations at lower temperatures) due to the presence of the PDMAEMA block or DMAEMA monomer. Moreover, all three approaches lead to a large quantity of homopolymer P(L)LA [homo–P(L)LA] contaminant, as found by a technique where the PDMAEMA block is quaternized allowing separation of the block copolymer as a precipitate and leaving homo–P(L)LA in the supernatant. Possible reasons for these complications will be discussed.

3.2 Experimental

3.2.1 Materials

All materials were obtained from Aldrich unless otherwise specified. Toluene and THF (EMD) were refluxed over CaH_2 and Na/K/benzophenone, respectively. LLA was recrystallized twice from either anhydrous toluene or anhydrous ethyl acetate (distilled over phosphorous pentoxide), and stored under dry nitrogen until use. Copper (I) bromide was refluxed in glacial acetic acid. A stock solution of $Sn(Oct)_2$ was distilled under vacuum and dissolved in dry toluene, and then kept in a closed container under dry nitrogen, with the necessary amount for polymerization withdrawn through a septum by a syringe under positive N_2 pressure. DMAEMA,[12] copper (I) chloride, copper (II) chloride, 1,1,4,7,10,10–hexamethyltriethylenetetramine (HMTETA), 2–bromoisobutyryl bromide (BIB), anhydrous ethylene glycol, triethylamine (TEA), and methyl iodide were used as received. The preparation of HEBIB is described elsewhere.[7] Synthetic experimental setup is described in *Chapter 2*.

3.2.2 Techniques of analysis

Details on the NMR, TGA, SEC–LS (including details on the dn/dc determination for homopolymers and block copolymers) and DSC instrumentation are given in *Chapter 2*. ^{1}H–NMR spectra were recorded using $CDCl_3$ or a 2:1 mixture of $CDCl_3$ and DMSO–d_6 with 0.03% of tetramethylsilane (TMS) as the internal standard. DSC scan details are given in Appendix to *Chapter 3*. Size exclusion chromatography (SEC) was carried out in DMF containing 0.025M LiBr at 55 °C using a Waters 600 liquid chromatograph equipped with

an A410 refractive index detector and Waters styragel HR columns (HR1, 100–5000; HR3, 500–30000; HR4, 5000–500000; HR5, 2000–40000000 g/mol). The flow rate was 1 $mL \cdot min^{-1}$. Poly(methyl methacrylate) (PMMA) standards ranging from 2500 to 900000 g/mol were used for calibration.

3.2.3 Synthesis of diblock copolymers

3.2.3.1 Sequential polymerization of DMAEMA followed by LLA (Route 1)

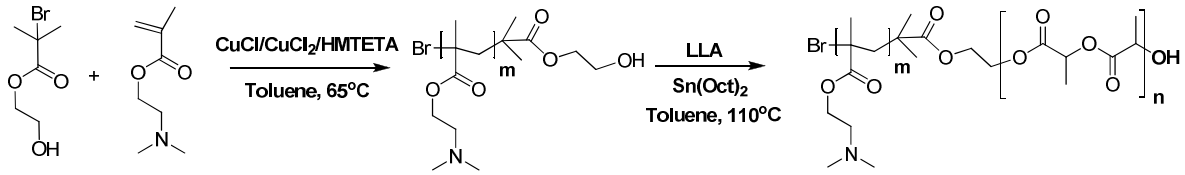

Scheme 3.1. Synthesis of PDMAEMA–b–PLA block copolymers: ATRP followed by ROP (**Route 1**)

The first step was ATRP of DMAEMA initiated by the bifunctional initiator (HEBIB) to obtain the PDMAEMA–OH macroinitiator. A freshly prepared toluene solution of HEBIB (0.25 M in dry deoxygenated toluene), CuCl, $CuCl_2$ and HMTETA in the HEBIB:CuCl:$CuCl_2$:HMTETA ratio of 1:1:0.1:2 was stirred at 40 °C until a clear solution was obtained. DMAEMA was then added dropwise and the mixture was left to stir at 65 °C for 24 h under nitrogen. The reaction was quenched by addition of 20 mL of THF and the resulting solution was passed through a short column (4×1.5 cm of 70–230 mesh silica gel) to remove the copper residue, then the column was flushed with 20 mL of additional THF.

The resulting light yellow solution was evaporated under reduced pressure until dry, redissolved in ca. 10 mL of $CHCl_3$, and precipitated dropwise into hexane. Sticky flakes were isolated by filtration, washed with abundant hexane and dried in vacuo at 40 °C for 72 h. ^{1}H–NMR (400 MHz, $CDCl_3$): δ_H, *ppm* 0.75–1.17 (3H, m, CCH_3), 1.67–2.10 (2H, m, CH_2C), 2.15–2.35 (6H, m, $N(CH_3)_2$), 2.45–2.65 (2H, m, NCH_2), 3.95–4.20 (2H, m, CH_2O).

The second step was ROP of LLA initiated by PDMAEMA–OH and catalyzed by $Sn(Oct)_2$. The desired quantities of PDMAEMA–OH and LLA were dissolved in 4 mL of dry toluene at 110 °C. Then a freshly prepared solution of $Sn(Oct)_2$ (0.00125M in dry toluene) was added to a $Sn(Oct)_2$:PDMAEMA–OH ratio of 1:200. The reaction mixture was left stirring at 115 °C for up to 72 h under nitrogen. The reaction was quenched by addition of 10 mL of dry toluene and the solution was precipitated into hexane. The sticky precipitate was collected by filtration and dried at 40 °C for 72 h. ^{1}H–NMR (400 MHz, $CDCl_3$): δ_H, *ppm* 0.75–1.15 (m, CCH_3, PDMAEMA), 1.44–1.64 (m, CH_3, PLA), 1.72–2.10 (m, CH_2C, PDMAEMA), 2.22–2.44 (m, $N(CH_3)_2$, PDMAEMA), 2.52–2.73 (m, NCH_2, PDMAEMA), 3.95–4.20 (m, CH_2O, PDMAEMA), 5.08–5.28 (m, CH, PLA).

3.2.3.2 Sequential polymerization of LLA followed by DMAEMA (Route 2)

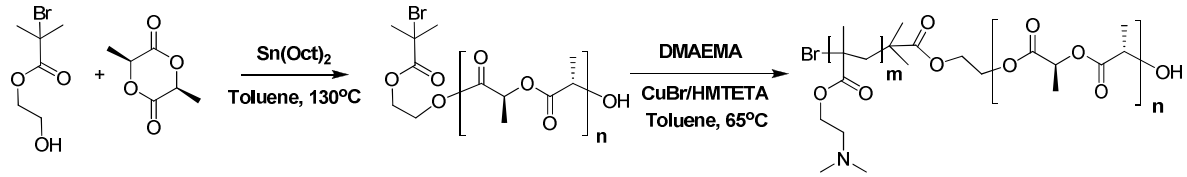

Scheme 3.2. Synthesis of PLLA–b–PDMAEMA block copolymers: ROP followed by ATRP (**Route 2**)

The first step was ROP of LLA initiated by the bifunctional initiator (HEBIB) and catalyzed by $Sn(Oct)_2$ to obtain PLLA–Br macroinitiator. LLA was melted at 100 °C, then freshly prepared solutions of tin octoate (0.00125 M) and HEBIB (0.25 M), at a $Sn(Oct)_2$:HEBIB ratio of 1:200, were added via a syringe through a septum under a nitrogen stream. The resulting solution was stirred at 130 °C for 46–52 h under nitrogen. After cooling to room temperature, 40 mL of methanol were added and a very fine white precipitate was isolated by centrifugation at 7000 rpm for 40 min. The crude product was dissolved in 20 mL of dry toluene and precipitated into 300 mL of methanol containing 1 mL of conc. HCl, again resulting in a fine precipitate that was isolated by centrifugation as above and dried under vacuum at 40 °C for 72 h. ^{1}H–NMR (400 MHz, $CDCl_3$): δ_H, *ppm* 1.58 (d, J = 7.0 Hz, CH_3), 1.92 (s, $BrC(CH_3)_2$, HEBIB), 5.16 (q, J = 7.0 Hz, CH).

The second step was ATRP of DMAEMA initiated by PLLA–Br. A solution of PLLA–Br, CuCl, $CuCl_2$, and HMTETA in the ratio PLLA–Br:CuCl:$CuCl_2$:HMTETA of 1:1:0.1:2 was prepared using 4 mL of anhydrous and deoxygenated toluene at 50 °C. Then

DMAEMA was added dropwise and the obtained solution was stirred at 65 °C for 18–30 h under nitrogen. The reaction was quenched by the addition of 20 mL of THF and the resulting solution was passed through a short column (8×3 cm of 70–230 mesh silica gel) to remove copper residue, followed by flushing of the column with 40 mL of additional THF. The obtained light yellow solution was evaporated under reduced pressure until dry, redissolved in ca. 10 mL of $CHCl_3$, and precipitated dropwise into hexane. The sticky flakes were isolated by filtration, washed with abundant hexane, and dried in vacuo at 40 °C for 72 h. ^{1}H–NMR (250 MHz, $CDCl_3$): δ_H, *ppm* 0.70–1.17 (m, CCH_3, PDMAEMA), 1.58 (d, J = 7.0 Hz, CH_3, PLLA), 1.69–2.10 (m, CH_2C, PDMAEMA), 2.10–2.45 (m, $N(CH_3)_2$, PDMAEMA), 2.45–2.75 (m, NCH_2, PDMAEMA), 3.90–4.20 (m, CH_2O, PDMAEMA), 5.16 (q, J = 7.0 Hz, CH, PLLA).

3.2.3.3 One–pot polymerization of LLA and DMAEMA (Route 3)

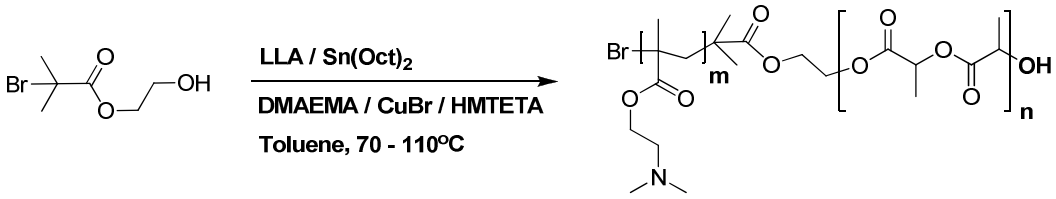

Scheme 3.3. Synthesis of PLA–b–PDMAEMA block copolymers: one–pot ROP and ATRP (**Route 3**)

Three reaction systems were prepared as follows. LLA (0.5–0.7 g), HEBIB, CuBr and HMTETA at a HEBIB:CuBr:HMTETA ratio of 1:1:4 were charged into the prepared flasks

and deoxygenated by several vacuum–nitrogen cycles. A freshly prepared $Sn(Oct)_2$ solution (0.44 M in toluene) was added to have a $Sn(Oct)_2$:HEBIB ratio of 1:5. Dry deoxygenated toluene (3 mL) was then added and the reaction mixtures were left to stir at 40 °C until clear green solutions were obtained. DMAEMA was then added dropwise and the three reaction mixtures were stirred at 70, 90 and 110 °C, respectively, for 69, 46 and 20 h, respectively, under nitrogen. When conversion (according to NMR of solution aliquots) of LLA was 90–95%, the reactions were quenched by cooling and addition of 10–15 mL of $CHCl_3$. The solutions were passed through Pasteur pipettes with 70–230 mesh silica gel to remove copper residue, and the light yellow solutions obtained were concentrated to ca. 10 mL under reduced pressure, then precipitated dropwise into hexane. The sticky precipitates were isolated by filtration, washed with abundant hexane and dried in vacuo at room temperature for 72 h.

3.2.4 Quaternization–precipitation technique

To determine if homo–P(L)LA contaminated the block copolymers synthesized, the latter were quaternized to provoke precipitation of the quaternized material, leaving any homo–P(L)LA in solution. To achieve this, 0.2–0.5 g of block copolymer were dissolved in 20 mL of dry DCM, then a 5–fold excess of CH_3I was quickly added under vigorous stirring. After 24–72 h, the precipitate obtained was filtered, washed thoroughly with DCM, dried in vacuum at room temperature and weighed. If the resulting reaction mixture was a gel, it was destroyed mechanically by addition of more DCM to obtain a precipitate, and then treated as described above. ^{1}H–NMR (400 MHz, DMSO:$CDCl_3$ 1:2): δ_H, *ppm* 0.74–1.34

(m, CCH_3, PDMAEMA), 1.45–1.63 (m, CH_3, PLA), 1.71–2.42 (m, CH_2C, PDMAEMA), 3.20–3.82 (m, $N^+(CH_3)_3$, PDMAEMA), 3.82–4.87 (m, NCH_2CH_2O, PDMAEMA), 5.05–5.25 (m, CH, PLA). Note that $CDCl_3$ (used here to make the PLA signals visible) is not a solvent for quaternized PDMAEMA and causes broadening and overlap of $^+N(CH_3)_3$ and $^+NCH_2CH_2O$ signals, making precise integration, and therefore the determination of the PLA:PDMAEMA ratio, impossible.

The filtered solution was also recuperated, evaporated until dry, and weighed. The residue (when present) was shown by NMR to contain only P(L)LA and no PDMAEMA, indicating that it is homo–P(L)LA. The weight of the original sample, the precipitate and the dried filtrate, along with the NMR–determined molecular weights of the original samples, allowed the recalculation of the true block copolymer molecular weights at the optimized degree of quaternization. The degree of quaternization was determined by the value that gave identical results for two different ways of recalculating the block molecular weights (see Supporting Information for details), and was always found to be $\geq$80%. The gravimetric data are given in *Tables A3.1* and *A3.2*.

3.2.5 P(D)LLA–b–PDMAEMA hydrolysis

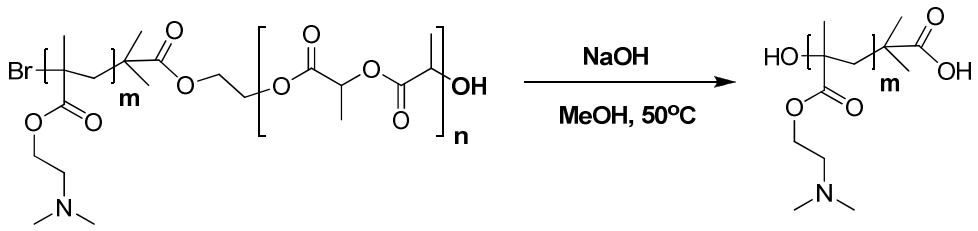

Scheme 3.4. Selective hydrolysis of PDMAEMA–b–PLA block copolymer.

An aliquot of block copolymer (0.10–0.15 g) was dissolved in 10 mL of methanol, containing 0.1 g of NaOH. After 4 h of stirring at 50 °C, the solution was heated to 60–70 °C to induce precipitation of PDMAEMA, which was then isolated by decantation. The sticky mass obtained was dried in vacuo at room temperature. NMR showed the complete absence of polylactide signals. ^{1}H–NMR (400 MHz, $CDCl_3$): δ_H, *ppm* 0.73–1.35 (m, $CH_2C\underline{CH_3}$), 1.70–2.42 (m, $\underline{CH_2}CCH_3$), 2.08–2.45 (m, $N(\underline{CH_3})_2$), 2.45–2.78 (m, $N\underline{CH_2}CH_2O$), 3.87–4.19 (m, $NCH_2\underline{CH_2}O$).

3.3 Results

3.3.1 Sequential polymerization of PDMAEMA–b–PLA (Route 1): racemization and free PLA

We found, using the three–step sequential polymerization approach starting from PLLA (*Chapter 2*), that trying to incorporate PLLA with a molecular weight of about 30,000 g/mol is unsuccessful due to the limited solubility of high molecular weight PLLA in

toluene or THF at the optimal temperature for ATRP (70 °C). The relatively good solubility of PLLA up to high molecular weight in only chlorinated solvents ($CHCl_3$, CH_2Cl_2) is also an issue, since ATRP does not proceed well in polar solvents due to their low boiling points and due to an increased possibility of terminal HBr elimination.[13,14] In contrast, PDMAEMA has good solubility in most common solvents, so that starting with PDMAEMA–OH macroinitiators may help in obtaining longer PLLA blocks if PDMAEMA can prevent precipitation of the block copolymer during growth of the PLLA block up to high molecular weights. In the following, we report on our exploration as to the feasibility of this polymerization sequence.

Three PDMAEMA–b–PLA block copolymers were synthesized, where the PDMAEMA blocks have fairly high molecular weights (>30k). The targeted molecular weights of the PLA block range from very short to similar molecular weight relative to the PDMAEMA block. The PDMAEMA–OH macroinitiators were prepared by ATRP in the bulk using HEBIB and a Cu^{I}/Cu^{II} catalyst combination (*Scheme 3.1*). The latter decreases the polymerization rate and lowers the PDI in bulk polymerizations by decreasing the number of chain terminations at the early stage of ATRP.[15] The M_ns determined by NMR and by SEC in DMF–LiBr using PMMA standards (*Table 3.1*) are in good agreement if a correction factor of 2.4 is applied to the latter, and the fairly low PDI (*Table 3.1*) indicates good ATRP control. Following the second step, SEC analysis, showing a decrease in retention time of each block copolymers compared with that of the corresponding PDMAEMA macroinitiator (see elugrams in *Figure 3.1 a,b,c*), indicates that polymerization of LLA took place; this, despite the possibility that PDMAEMA can

deactivate the $Sn(Oct)_2$ catalyst used and thereby prevent ROP, as mentioned in Ref. 7 in connection with the lack of success in adding a CL block [using $Sn(Oct)_2$] to a PDMAEMA block. The agreement between the total M_ns determined by NMR and SEC in DMF–LiBr (*Table 3.1*), after applying a correction factor of 2.4, is also good, although the PDI of the block copolymer, **R1–3.2**, appears to have increased significantly compared to the macroinitiator, **R1–3.1**. Thus, on first sight, the polymerization appears to have been successful.

Table 3.1. Molecular weight data for the PDMAEMA macroinitiators (R1–x.1), block copolymers (R1–x.2), and isolated PLA homopolymer (homo–PLA, R1–x.3), obtained in **Route 1**

Code	Sample	[M]/ [I] [a]	Conv. (%)	M_n (g/mol, NMR) original [b] recalcd (% quat) [c]	M_n (g/mol)/ PDI SEC [d] SEC–LS [e]
R1–1.1	$PDMAEMA_{45k}$	300	95	44900 [b]	17900 / 1.22 [d] 48600 / 1.10 [e]
R1–1.2	$PDMAEMA_{45k}$–PLA_{5k} [homo–PLA: 0% [f]]	50	63	44900–4500 [b,c]	20300 / 1.25 [d] 53000 / 1.10 [e]
R1–2.1	$PDMAEMA_{39k}$	250	100	39000 [b]	18100 / 1.30 [d] 55700 / 1.25 [e]
R1–2.2 **R1–2.3**	$PDMAEMA_{39k}$–PLA_{6k} [homo–PLA: 64% [f]]	125	76	39000–16800 [b] 39000–6000 (80) [c]	23100 / 1.38 [d] 57100 / 1.26 [e] [35900 / 1.08 [e]]
R1–3.1	$PDMAEMA_{31k}$	200	100	31400 [b]	12800 / 1.19 [d] 40700 / 1.20 [e]
R1–3.2 **R1–3.3**	$PDMAEMA_{31k}$–PLA_{6k} [homo–PLA: 79% [f]]	200	96	31400–31100 [b] 31400–6400 (83) [c]	23000 / 1.38 [d] 44100 / 1.22 [e] [11900 / 1.20 [e]]

[a] [I] = [HEBIB] for PDMAEMA; [I] = [PDMAEMA–OH] for PDMAEMA–b–PLA. [b] Data on original samples: for PDMAEMA, calculated from the intensity ratio of the $CH_2\mathit{CH_2}OH$ signal of HEBIB (ca. 3.8 ppm) relative to the $NCH_2\mathit{CH_2}O$ signal of PDMAEMA (ca. 4.1 ppm); for PDMAEMA–b–PLA, calculated from the intensity ratio of the $NCH_2\mathit{CH_2}O$ signal of PDMAEMA (ca. 4.1 ppm) relative to the $\mathit{CH}CH_3$ signal of PLA (ca. 5.2 ppm), using the NMR M_n of PDMAEMA as a reference. [c] Data in b recalculated to eliminate the contribution of homo–PLA; % quat refers to the degree of quaternization calculated for the PDMAEMA block (see Appendix to *Chapter 3* for details). [d] SEC data on original samples in DMF–LiBr, using PMMA standards; no correction factor applied. [e] SEC–LS data in THF/TEA: for block copolymers, on the original samples; for PDMAEMA, after PLA degradation of the corresponding copolymer. [f] Homopolymer PLA isolated by quaternization/precipitation, in wt % of total PLA content in original sample (see Appendix to *Chapter 3* for details).

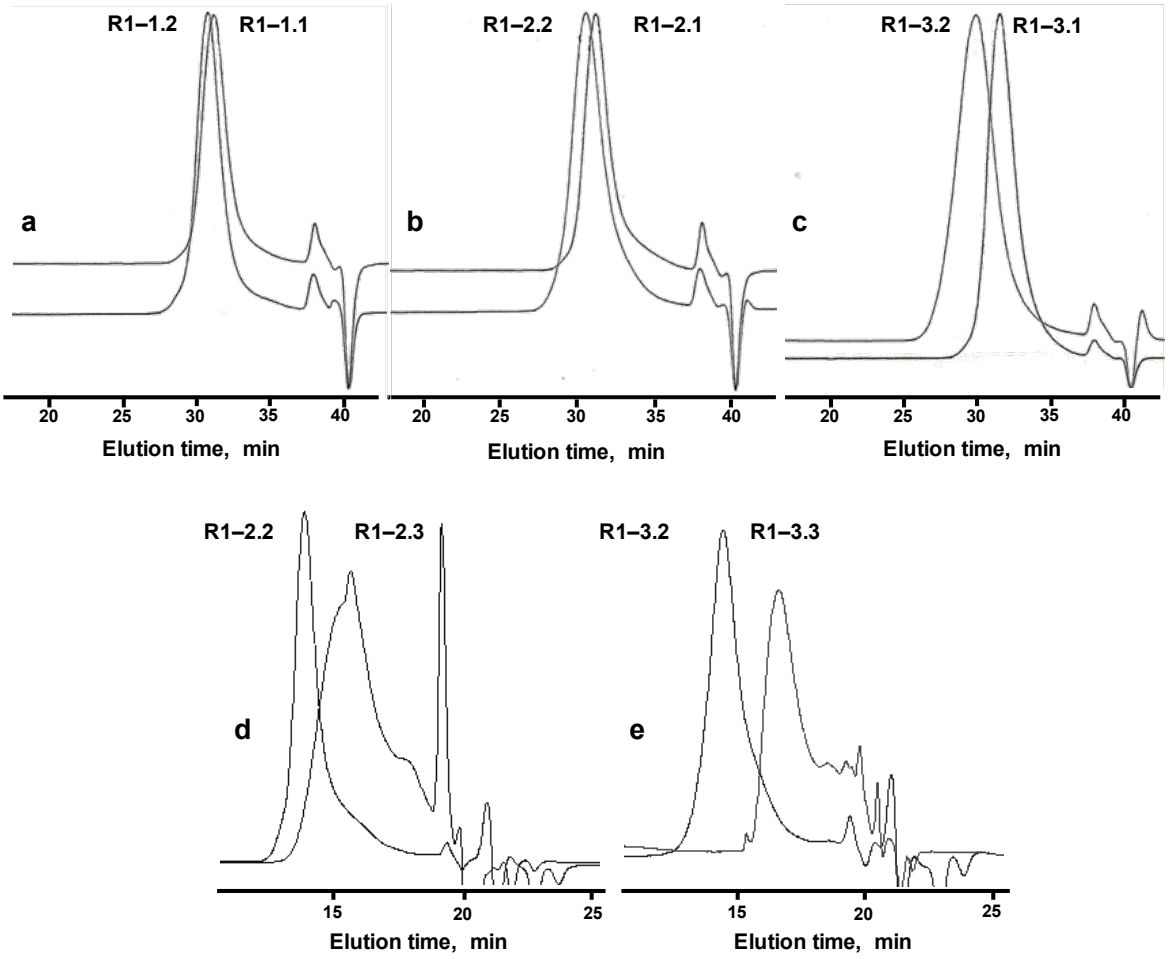

Figure 3.1. (a, b, c) SEC elugrams of PDMAEMA macroinitiators and original PDMAEMA–b–PLA copolymers in DMF–LiBr; (d, e) SEC–LS elugrams of original PDMAEMA–b–PLA copolymers and homo–PLA (isolated by quaternization/precipitation) in THF–TEA, obtained in **Route 1**

On closer analysis, however, two problems became apparent. The most obvious is that the NMR spectra of the block copolymers revealed that the polylactide is racemic, as shown by broad multiplets instead of a well–defined doublet and quartet (*b* and *g* in *Figure 3.2,* ***Route 1***) at 1.58 and 5.15 ppm, respectively. This was confirmed by DSC, which showed no evidence of crystallization or melting. The second problem was hinted at when a

reanalysis of the M_ns by SEC–LS to obtain absolute M_n values gave a significantly lower value than expected for **R1–3.2** (*Table 3.1*).

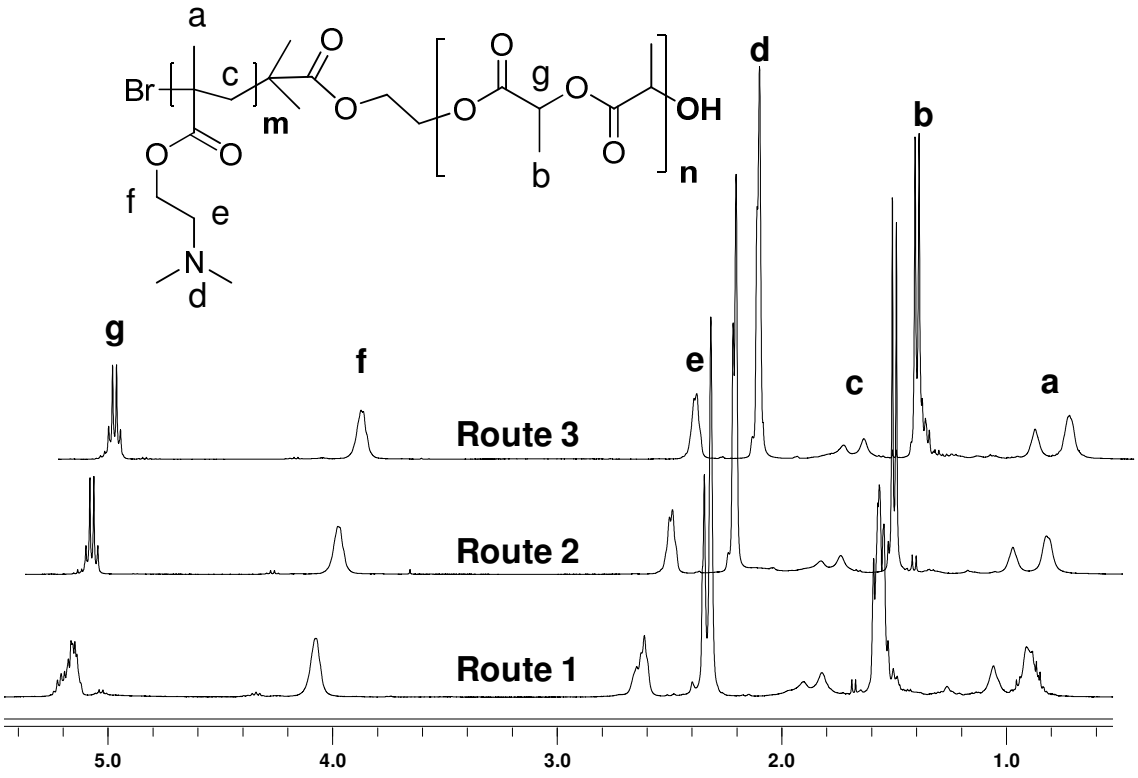

Figure 3.2. Representative ^{1}H–NMR spectra of block copolymers synthesized: R1–3.2 (**Route 1**), R2–1.2 (**Route 2**), R3–2.1 (**Route 3**). The upper spectra are progressively shifted to the right for clarity

Using a quaternization/precipitation procedure where the PDMAEMA in the block copolymer is highly quaternized (as verified by NMR), which provokes precipitation of the block copolymer and thereby allows its removal by filtration, it was found that block copolymers, **R1–2.2** and **R1–3.2**, contain a large proportion of PLA homopolymer, determined gravimetrically to be 64 and 79 wt %, respectively, of the total amount of PLA

in the mixture. The presence of this homopolymer is not at all evident in the SEC elugrams of the block copolymers using DMF–LiBr as eluent (*Figure 3.1a,b,c*) and only slightly apparent as weak "bumps" when using THF–TEA as eluent (*Figure 3.1d,e*, where elugrams of the isolated homo–PLA are also shown). The lack of visibility of homo–PLA in the elugrams can be attributed to its much lower refractive index increment compared to that of PDMAEMA (0.048 vs. 0.084 in THF–TEA, and 0.030 vs. 0.062 in DMF–LiBr), since the elugrams in *Figure 3.1d,e* show that the peak separation between homo–PLA and the block copolymer is sufficient to be observable otherwise. Knowing the weights of the isolated homo–PLA and precipitated block copolymer, the NMR M_ns of the block copolymers could be recalculated (*Table 3.1*). It is notable that the M_ns of the isolated homo–PLAs are significantly higher than the corrected M_ns of the PLA block (*Table 3.1*).

In contrast to **R1–2.2** and **R1–3.2**, no homo–PLA was found by the quaternization/precipitation method in the block copolymer with the short PLA block (**R1–1.2**). Possibly, given the low targeted molecular weight of the PLA block, the experimental conditions might not have favoured homo–PLA formation. It might also be speculated that only very short oligomer chains of a few repeat units or even just lactic acid dimers (LA–LA, opened lactide) were produced, and that this was eliminated during purification by precipitation if soluble in the precipitating non–solvent, hexane. As support for the latter, it is worth mentioning here that NMR showed that the reaction mixture resulting from **Route 3** contained LA–LA before but not after precipitation of the mixture in hexane (see *Figure A3.9*), indicative of its solubility in hexane. This loss might also explain the low conversion observed for R1–2.2. In this connection, it may be remarked that, since the conversion for

R1–2.2 is also lower than expected, it may likewise have produced LA–LA or short oligomer that was eliminated by precipitation in hexane.

It is of interest to mention that the M_n of PDMAEMA was also analyzed by SEC–LS (*Table 3.1*). Since all of the original macroinitiator had been consumed in the block copolymer synthesis, this was accomplished by first fully degrading the PLA block. For **R1–1.1** degraded from **R1–1.2**, the M_n determined by SEC–LS is in good agreement with the NMR value. However, for the block copolymers with the longer PLA blocks (**R1–2.1** degraded from **R1–2.2** and **R1–3.1** degraded from **R1–3.2**), the SEC–LS values are significantly higher than the NMR values. This might be explained by the degradation leaving a carboxylic acid end group (*Scheme 3.4*), and possibly also other carboxylic acid groups within the chain if some ester hydrolysis occurred (at the most in trace amounts, since there was no evidence of this by NMR). These groups can self–associate in solution[16,17] and/or complex with the amino moieties by proton transfer, leading to labile crosslinks in solution that can increase the apparent M_ns and PDIs. For **R1–1.1**, in contrast, the hydrolysis conditions are milder (less NaOH and shorter reaction time), which may minimize or preclude any main chain COOH formation, thus resulting in little aggregation in solution.

3.3.2 Sequential polymerization of PLLA–b–PDMAEMA (Route 2): free PLLA

Sequential polymerization via α–bromo–PLLA as macroinitiator is likely to avoid the problem of racemization (as indicated by the three–step polymerization discussed in

Chapter 2), and thus this approach was explored next. It also avoids possible complexation of DMAEMA units with $Sn(Oct)_2$ that can potentially create complications, as mentioned in Ref. 7. Two polymerization experiments to obtain PLLA–b–PDMAEMA were carried out, where, to preclude any solubility issues in the second step, the targeted molecular weight of the PLLA block was kept low (≤5k, *Table 3.2*). The NMR spectra of the two PLLA macroinitiators isolated after the first step contained a well–defined quartet at 5.16 and a doublet at 1.58 ppm, confirming that they are isotactic. Their M_ns and PDIs determined by SEC–LS are in fair agreement with those indicated by NMR (*Table 3.2*). The melting temperature of 152 °C determined by DSC for **R2–2.1** is in agreement with those observed in *Chapter 2* and Ref 18 for PLLA of very similar molecular weight. The lower melting point of 146 °C determined for **R2–1.1** is in accordance with the well–known dependence of T_m on molecular weight. The melting enthalpies obtained for both PLLA macroinitiators are ca. 65 J/g, indicating 71% crystallinity, also in agreement with *Chapter 2* (see *Table A3.3* for complete DSC data).

The second step, ATRP of DMAEMA, was carried out in concentrated solution because the PLLA macroinitiator is not soluble in the DMAEMA monomer. PDMAEMA molecular weights of 8,000 and 10,000, respectively, were targeted. The reaction was allowed to proceed to almost complete conversion (≥95%). NMR confirmed that the PLLA block remained isotactic after the reaction, as expected (*Figure 3.2*, **Route 2**). However, application of the quaternization/precipitation procedure again showed the presence of homo–PLLA, at about 65% of the total PLLA content in both block copolymers synthesized (*Table A3.1*). NMR of the isolated homo–PLLA showed that it was not

functionalized by Br [i.e. there is no $BrC(CH_3)_2$ signal at 1.92 ppm], thus making it impossible to add the PDMAEMA block. [It is worth noting that NMR spectra show that the reaction mixture before polymer purification (by passing through a silica column) have higher PLLA content than after purification (*Figure A3.3*), indicating that some homo–PLLA remained in the column (ca. 8% relative to the total PLLA from *Figure A3.3*). This might explain the discrepancy between the block ratio targeted by the monomer feed and that determined by NMR (*Table 3.2*).]

The presence of homo–PLLA means that the PDMAEMA block in the block copolymer is much longer than initially determined, as shown by the original and recalculated NMR data in *Table 3.2*. The recalculated molecular weights are in much better agreement with those determined by SEC–LS (using THF–TEA) than the original NMR–based values (*Table 3.2*). This time, the presence of the homopolymer is evident as a small peak in the SEC–LS elugrams (*Figure A3.2*). It may be added that the use of DMF–LiBr as an eluent is not suitable in this case, because PLLA tends to crystallize out of this solution over time. This was observed by the appearance of cloudiness and eventually a precipitate (for a maximum concentration used of 12 mg/mL), shown also by exaggeratedly high M_n values [unless the solution is relatively dilute (which also reduces the signal intensity) and freshly prepared just prior to the SEC analysis].

Table 3.2. Molecular weight data for the PLLA macroinitiators (R2–x.1), block copolymers (R2–x.2), and isolated PLLA homopolymer (homo–PLLA, R2–x.3), obtained in **Route 2**

Code	Sample	[M]/[I] [a]	Conv. %	M_n (g/mol, NMR) original [b] recalcd (% quat.) [c]	M_n (g/mol) / PDI; SEC [d] SEC–LS [e]
R2–1.1	$PLLA_{4k}$	50	68	5800 [b]	4600 / 1.12 [d] 4300 / 1.27 [e]
R2–1.2 **R2–1.3**	$PLLA_{4k}$–$PDMAEMA_{14k}$ [homo–$PLLA_{4k}$: 64% [f]]	50	95	4300–6400 [b] 4300–17900 (85) [c]	23000 / 1.28 [e] [4300 / 1.27 [e]]
R2–2.1	$PLLA_{5k}$	60	74	8100 [b]	5500 / 1.12 [d] 5300 / 1.25 [e]
R2–2.2 **R2–2.3**	$PLLA_{5k}$–$PDMAEMA_{37k}$ [homo–$PLLA_{6k}$: 65% [f]]	64	97	5300–19800 [b] 5300–45800 (87) [c]	43200 / 1.57 [e] [6300 / 1.27 [e]]

[a] [I] = [HEBIB] for PLA, [I] = [PLLA–Br] for PLLA–b–PDMAEMA [b] Data on original samples. For PLLA, calculated from the intensity ratio of $BrC(CH_3)_2$ signal of HEBIB (ca. 1.9 ppm) relative to $CHCH_3$ signal of PLLA (ca. 5.2 ppm); for PLLA–b–PDMAEMA, calculated from the intensity ratio of NCH_2CH_2O signal of PDMAEMA (ca. 4.1 ppm) relative to $CHCH_3$ signal of PLLA (ca. 5.2 ppm), using the SEC–LS M_n of PLLA as a reference. [c] Data in b recalculated to eliminate the contribution of homo–PLLA; % quat refers to the degree of quaternization calculated for the PDMAEMA block (see Appendix to *Chapter 3* for details). [d] SEC in THF, using PS standards. $M_{n(PLLA)} = 0.4055M_{n(PS)}^{1.048}$ [**19**]. [e] SEC–LS in THF–TEA, for block copolymers, on the original samples. [f] Homopolymer PLA isolated by quaternization/precipitation, in wt % of total PLA content in original sample (see Appendix to *Chapter 3* for details).

In DSC analysis of the two block copolymers (containing homo–PLLA), the glass transitions, melting points and degrees of crystallinity are consistent with our previous analysis of PLLA–PDMAEMA block copolymers, considering the low PLLA molecular weight of 5000 (*Table A3.3*). As before (*Chapter 2*), no cold crystallization peaks were

found during the cooling scans, indicating dramatic retardation of the crystallization rate by the presence of the PDMAEMA. In fact, it was shown that PLLA of molecular weight of ca. 5000 and less are miscible in PDMAEMA, shown also here by the appearance of a single T_g. However, weak and broad cold crystallization peaks (more intense in the first heating scan) were noticeable on both heating scans, unsurprisingly more intense for **R2–1.2**, which has a shorter PDMAEMA block. The melting endotherms of **R2–1.2** and **R2–2.2** exhibit complex behaviour, somewhat similar to that of $PLLA_{5k}$–$PDMAEMA_{10k}$ in *Chapter 2*; in particular, premelting and melting peak doubling related to parallel processes of melting and recrystallization. Notably, both cold crystallization exotherms and melting endotherms are shifted to higher temperatures compared to the correspondent PLLA macroinitiators. As the block copolymer samples are actually blends of PLLA and PLLA–b–PDMAEMA, similar shift was observed in the blend of **R2–1.3** with PDMAEMA (*Table A3.3*).

3.3.3 One–pot simultaneous polymerization of PDMAEMA–b–PLA (Route 3)

Simultaneous polymerization of LLA by $Sn(Oct)_2$ and DMAEMA by HMTETA/Cu(I) may be a challenge due to the different temperature regimes in which the two types of reactions are optimal: ROP using tin octoate works best at 110–130 °C, whereas the optimal temperature for ATRP is 60–70 °C. To test the feasibility of this one–pot polymerization, experiments were conducted at both of these temperatures (i.e., 110 and 70 °C) as well as at an intermediate temperature (90 °C).

All three polymerizations led to a mixture of block copolymer and PLA homopolymer, as determined by the quaternization/precipitation procedure. The molecular weight of the isolated homo–PLA was determined by SEC–LS. For calculation purposes, the same M_n was assumed for the PLA block in each case, allowing estimation, based on the NMR data, of the M_n of the PDMAEMA block and of the proportion of homo–PLA, determined to be greater than 50% of the total PLA content (*Table 3.3*). [SEC–LS analysis of the PDMAEMA block after hydrolysis of the PLA gave significantly higher M_ns (33,000–55,000), perhaps caused by the carboxylic acid groups at the end and possibly within the chains, resulting from the hydrolysis, and that may self–associate and/or complex with the amino moieties, as mentioned above.] Only the block copolymer synthesized at 90 °C was analyzed by SEC–LS, which indicates a molecular weight very similar to the recalculated NMR–based value. The polydispersity of the isolated homo–PLAs are significantly higher than those obtained from **Route 1**, and that of the single block copolymer analyzed is much higher (*Table 3.3*). The high polydispersity suggests that significant transesterification occurred during the reaction, which may have been provoked by the presence of a CuBr/HMTETA complex (see Appendix to *Chapter 3*).

Table 3.3. Molecular weight data for the block copolymers (R3–x.1) and isolated homo–PLA (R3–x.2), obtained in **Route 3**

Polym. temp., °C	Code	Sample	$[M_1]/[M_2]/[I]$ [a]	Conv. M_1 / M_2 %	M_n (g/mol, NMR) original [b] recalcd (% quat) [c]	M_n (g/mol) / PDI SEC–LS [d]
70	**R3–1.1**	PLA_{4k}–$PDMAEMA_{24k}$	62 / 105 / 1	90 / 81	4200–10300 [b] 4200–24400 (92) [c]	n/d
	R3–1.2	[homo–PLA_{4k}: 58% [e]]				[4200 / 1.33]
90	**R3–2.1**	PLA_{10k}–$PDMAEMA_{25k}$	70 / 125 / 1	99 / 70	9800–11900 [b] 9800–25400 (89) [c]	33100 / 2.45
	R3–2.2	[homo–PLA_{10k}: 53% [e]]				[9800 / 1.57]
110	**R3–3.1**	PLA_{8k}–$PDMAEMA_{25k}$	61 / 105 / 1	95 / 60	7800–9400 [b] 7800–25400 (85) [c]	n/d
	R3–3.2	[homo–PLA_{8k}: 63% [e]]				[7800 / 1.28]

[a] $[M_1]$ = [LLA], $[M_2]$ = [DMAEMA], [I] = [HEBIB]. [b] Data on original samples. Calculated from the intensity ratio of $NCH_2\mathit{CH_2}O$ signal of PDMAEMA (ca. 4.1 ppm) and $\mathit{CH}CH_3$ signal of PLA (ca. 5.2 ppm), assuming a molecular weight for the PLA block that is the same as homo–PLA. [c] Data in b recalculated to eliminate the contribution of homo–PLA; % quat refers to the degree of quaternization calculated for the PDMAEMA block (see Appendix to *Chapter 3* for details). [d] SEC–LS in THF–TEA. [e] Homopolymer PLA isolated by quaternization/precipitation, in wt % of total PLA content in original sample (see Appendix to *Chapter 3* for details).

The molecular weight determinations indicate that the PLA M_n is lowest (4k) for the 70 °C polymerization, and similar (8–10k) for the 90 and 110 °C polymerizations (relative to the optimal temperature being 110–130 °C), whereas the PDMAEMA block has similar M_n for all three temperatures. This suggests that LLA polymerization proceeds as well at 90 as at 110 °C and that DMAEMA polymerization equally well at all three temperatures.

NMR analysis (*Figure 3.3*, see Appendix to *Chapter 3* for full spectra) indicates some PLA racemization in the block copolymers and isolated homopolymers, although less than in the **R1** series. Those obtained from polymerization at 70 and 90 °C appear more highly isotactic than that obtained at 110 °C. No evidence of crystallization was observed by DSC in the products obtained at 70 and 110 °C, whereas that obtained at 90 °C showed a weak melting point at 126 °C on the first heating scan only (*Table A3.4*), which is significantly lower than that expected for completely isotactic PLLA (ex. 151–155 °C for $PLLA_{5k}$) (*Chapter 2*). Previously, it had been shown, by copolymerization of LLA with various amounts of meso–lactide, that incorporation of more than 15% meso–lactide produces PLA that is unable to crystallize,[20] and the T_m of PLA with 15% meso–lactide is 128 °C.[21] Based on this information, it can be concluded that the PLA in the copolymer and homopolymer obtained at 90 °C are ca. 85% isotactic, whereas that obtained at 70 °C is a little less than 85% isotactic and that obtained at 110 °C significantly less (judging from the NMR spectra combined with the apparent inability to crystallize according to DSC).

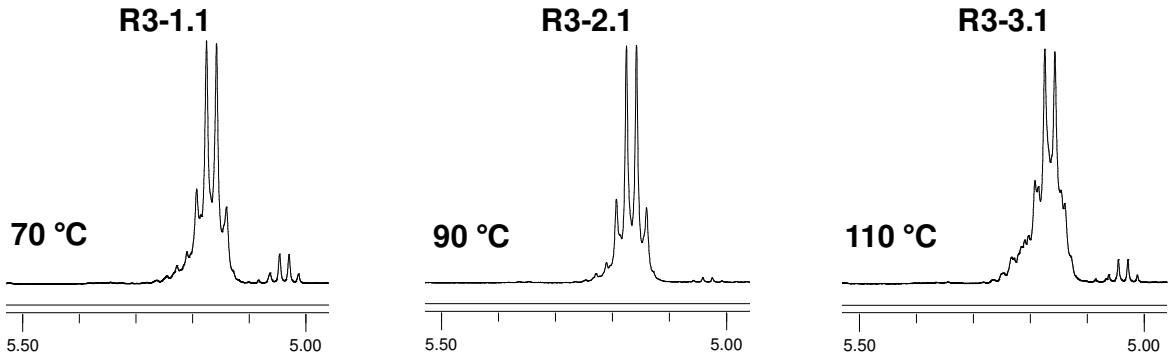

Figure 3.3. PLA methine regions of ^{1}H–NMR spectra of block copolymers, prepared via **Route 3**. The NMR spectra of the isolated homo–PLA in each sample are essentially identical

Analysis of the T_g regions of the block copolymers (*Table A3.4*) indicates that **R3–1.1** forms a miscible melt, as evidenced by a single T_g (22 °C) that is intermediate to that of the corresponding homo–P(L)LA (31 °C) and PDMAEMA (17 °C). The two other block copolymer show two distinct T_gs, but their values are a little higher and lower than those of PDMAEMA and PL(L)A of similar molecular weight (*Chapter 2*), respectively, thus indicating partial miscibility, probably of low molecular weight fractions. However, the T_gs are probably also decreased by the presence of residual lactide monomer (not soluble in the precipitating solvent, hexane) as observed by NMR (see *Figures A3.6–A3.8*).

3.4 Discussion

3.4.1 Racemization of LLA

Thermal racemization of lactides is well known, and proceeds through keto–enol tautomerism[22] that generally takes place at temperatures greater than ca. 200 °C. However, in the presence of nitrogen nucleophiles, LLA racemization takes place at lower temperatures (≤100 °C), as discussed in Ref. 23 in relation to organocatalytic polymerization of LLA by imidazole at 100 °C and hypothesized to occur by the mechanism shown in *Scheme 3.5*. The present results therefore suggest that PDMAEMA, a weak base, can similarly provoke the reversible formation of a delocalized carbanion at the ROP temperature, resulting in racemization of the LLA at the polymerization temperature. This cannot be traced easily since the NMR spectra of LLA and racemic lactide are similar, both showing a well–defined quadruplet at ca. 5 ppm (see *Figure 3.3*).

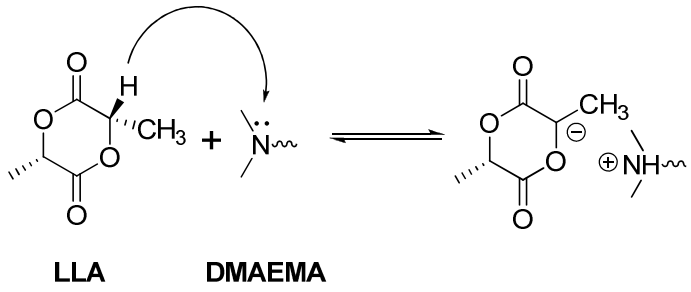

Scheme 3.5. Reversible deprotonation of a nitrogen nucleophile (e.g. DMAEMA), leading to racemization of LLA

This implies that it is not feasible to polymerize a PLLA block on a PDMAEMA block (nor any other nitrogen nucleophile–containing block); instead, the PLLA block must

always be prepared first. The PLLA block is not subject to the parasitic action of (P)DMAEMA because it is more stable to racemization than LLA,[22] and possibly also because the temperature of ATRP is lower (70 °C) than for $Sn(Oct)_2$ ROP. It may be added, in this connection, that literature evidence indicates that LLA racemization can be avoided by short polymerization times or low polymerization temperatures (e.g. 135 °C for 20 min or 35 °C for 4 days, the latter promoted by 4–dimethylamino pyridine),[24] neither of which is possible for PLA addition to PDMAEMA using ROP with $Sn(Oct)_2$.

3.4.2 Possible sources of homopolymer P(L)LA

Significant P(L)LA homopolymer contaminant was observed in all three routes described above. In **Route 2**, part of the PLLA macroinitiator was not functionalized for PDMAEMA chain extension, implying that LLA polymerization was initiated by something else in addition to HEBIB. In **Routes 1** and **3**, the desired PDMAEMA–OH initiation of LLA polymerization was also accompanied by a competitive initiator. These complications are discussed in what follows.

Several sources of the homopolymer contamination of the block copolymers synthesized above can be considered. First, in ROP of LLA by $Sn(Oct)_2$, alcohol compounds are generally used because $Sn(Oct)_2$ itself has poor catalytic activity and needs to be "activated".[25] The role of the activator (also called co–initiator) is also to serve as a chain control agent to help manage molecular weight and molecular weight distribution.

However, a mechanistic study on the $Sn(Oct)_2$–catalyzed polymerization of LLA by Kricheldorf et al.[26] showed that the polymerization of lactide can take place even in the

absence of the alcohol compound. In this case, the role of activator is played by traces of water that forms a strong complex with $Sn(Oct)_2$, and cannot be completely removed by distillation in vacuum, as was shown by the appearance of octanoic acid within minutes after distillation of tin octoate.[26] As a result, a catalytically active hydroxyltin derivative forms and initiates lactide polymerization, as shown in *Scheme 3.6*.

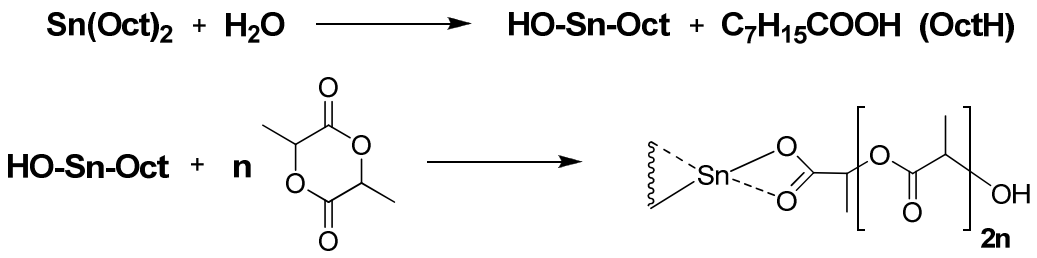

Scheme 3.6. Activation of tin octoate by water and ROP by hydroxyltin octoate

Furthermore, LLA can contain small amounts of LA–LA (lactoyl lactate, an opened form of lactide resulting from hydrolysis, as shown in *Scheme 3.7*) via two possible mechanisms, as rationalized by Schwah et al.[27] First, a very small amount of LA–LA that is difficult to detect by NMR because its signal overlaps with the "echo" signal of LLA (resulting from carbon–proton coupling) might remain in the purified lactide despite several recrystallizations. Second, traces of octanoic acid and water that contaminate tin octoate can hydrolyze lactide. This reaction can be considered to be self–catalyzed, because the newly formed LA–LA is more acidic than octanoic acid, and thus accelerates the hydrolytic opening of the lactide ring during polymerization (*Scheme 3.7*).

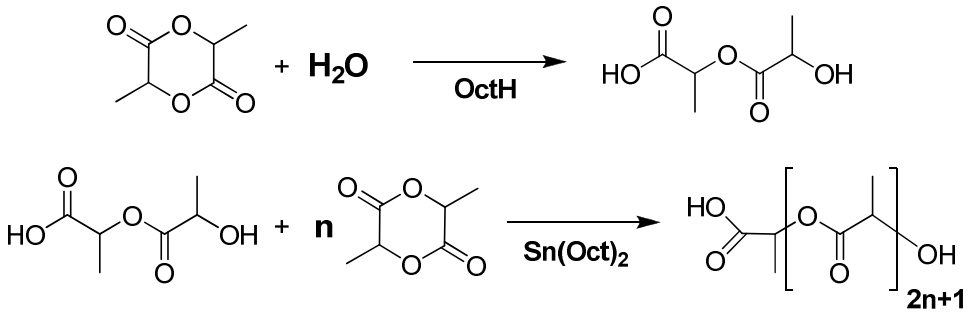

Scheme 3.7. Lactoyl–lactate (LA–LA) formation and its involvement as an initiator in ROP

In fact, NMR analysis of the reaction mixtures during polymerization via **Routes 1** and **3** revealed the presence of significant amounts of an additional product, assigned to LA–LA based on reports by Espartero *et al.*[28] and Schwach *et al.*[27] In contrast, this is not generally detectable during ROP by $Sn(Oct)_2$ alone (*Figure 3.4*). Therefore, the formation of such quantities of LA–LA is presumably related to the presence of (P)DMAEMA whose amino moiety provokes nucleophilic ring opening of LLA, as depicted in *Scheme 3.8*. This is supported by the decrease in the relative content of LA–LA with increasing PLA content during polymerization, indicative of its incorporation into the growing polymer chain (compare the NMR spectra of the reaction mixtures obtained after 20 h and 69 h, shown in *Figure 3.4*).

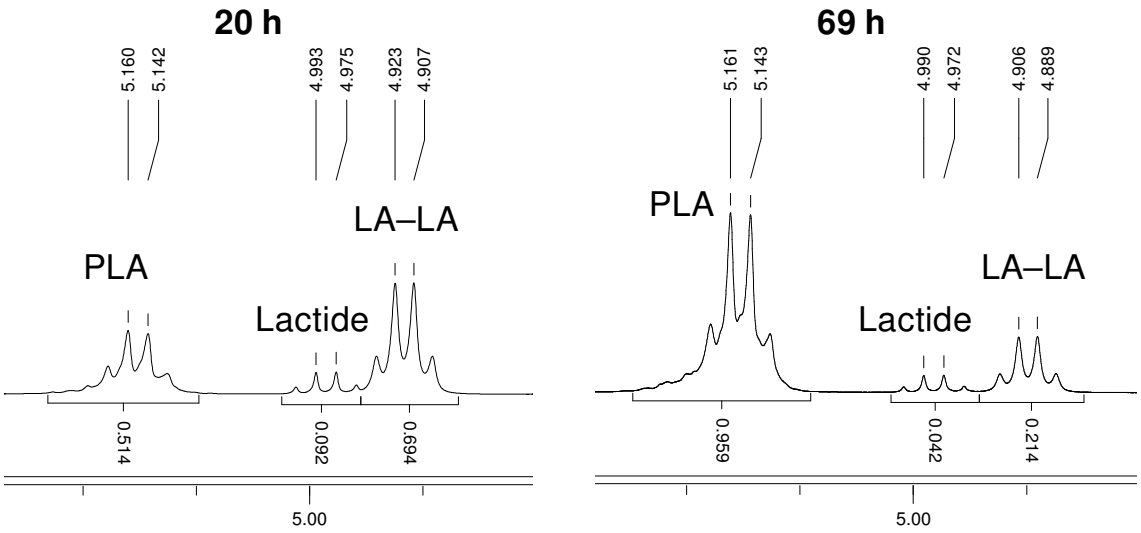

Figure 3.4. Fragments of ^{1}H–NMR spectra of the reaction mixture, **R3–1.1**, after different polymerization times

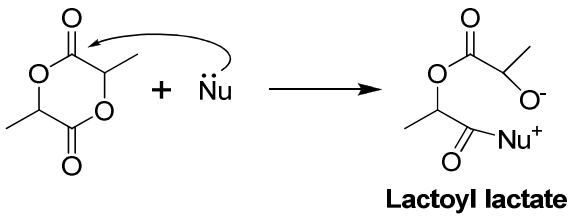

Scheme 3.8. Schematic representation of nucleophilic ring–opening of lactide by a nucleophile, such as (P)DMAEMA

Initiation of LLA polymerization by H_2O and by LA–LA will both produce polylactide chains with OH and a carboxylic acid end group, which are difficult to detect by NMR. Thus, in **Route 2**, the non–functionalized PLLA, which was not initiated by HEBIB, may have been initiated by hydroxyltin octoate (resulting from traces of water, *Scheme 3.6*) and/or LA–LA, neither of which contains an initiating site for ATRP.

Unlike in **Route 2**, where the first step of the block copolymer synthesis produces a mixture of functionalized and unfunctionalized polylactide homopolymers and only one of them can subsequently form a block copolymer, polymerization by **Route 1** (first step) and **Route 3** involves the formation of the PDMAEMA–OH macroinitiator. In this case, LLA polymerization can similarly be initiated not only by the macroinitiator to give the desired block copolymer, but also by hydroxyltin octoate and/or by LA–LA to form homo–PLA. Certainly, their NMR spectra of the homo–PLA contain no characteristic signal at 1.92 ppm from the HEBIB initiator.

If H_2O and LA–LA (also caused by traces of H_2O) account for the presence of homo–PLA, as discussed above, then it seems necessary to completely eliminate H_2O, such as by conducting ROP under high vacuum. However, reports on the successful polymerization of LLA by $Sn(Oct)_2$ under high vacuum and without the use of any alcohol initiator[25,29] indicate that the undesired initiation of LLA by tin octoate (i.e. *in situ* formed hydroxyltin octoate, as described above) rather than HEBIB is unavoidable.

Water and LA–LA initiation leading to unfunctionalized PLLA polymerization would also be expected to occur in the three–step synthesis we described earlier (*Chapter 2*); however, here the OH functionality will still be modified to Br in the second step, so that block copolymer can still form. It will, on the other hand, affect the NMR–based molecular weight determination (based on the isopropyl group from the 4–isopropylbenzyl alcohol initiator), making it appear higher than it really is. However, the very good agreement between the NMR and SEC–LS determined molecular weights in (*Chapter 2*) indicates that little if any of this undesired initiation occurred. Since this ROP

polymerization is conducted under the same conditions as for **Route 2**, except for the choice of initiator, this raises the question as to whether the bifunctional initiator itself might be the source of the problem.

Since the coordination–insertion mechanism of LLA polymerization by $Sn(Oct)_2$ involves its interaction with the ester moiety of LLA, it seems feasible that an undesired attack of $Sn(Oct)_2$ on the ester group of the HEBIB moiety might take place, which would lead to homo–P(L)LA formation, as shown in *Scheme 3.9*. The probability of such an interaction may be expected to increase as the concentration of the monomer decreases, i.e. homo–P(L)LA formation is most likely to occur in the later stage of polymerization. Whatever block is polymerized first, an attack on the HEBIB carbonyl would lead to non–functional homo–P(L)LA as well as triblock copolymer formation. The latter cannot be distinguished from diblock by NMR and SEC, and may be the reason for higher polydispersity. Generally, the presence of any of the side products depicted in *Scheme 3.9* cannot be traced by NMR because, having the same shift, their signals intensity will contribute to the intensity of the signals of the targeted products. Moreover, the formation of product (4) in **Route 2** (*Scheme 3.9*) is produce by the coupling of two growing chains that will result in a higher molecular weight homo–PLLA contamination. Depending on the targeted molecular weight of the block copolymer, high molecular weight homo–PLLA might not be visible in the SEC elugram.

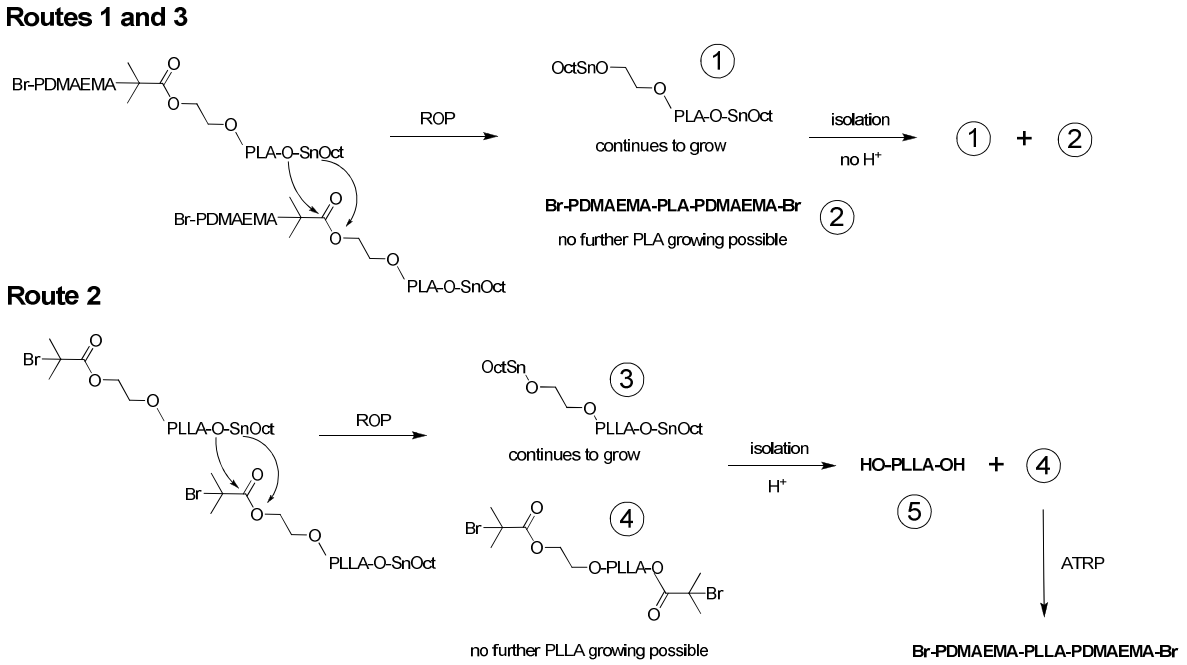

Scheme 3.9. A plausible path of homo–P(L)LA formation resulting from the attack of the HEBIB moiety

When polymerizing the PDMAEMA block before the PLA block, there is an additional disadvantage. Due to the isolation procedure used in **Routes 1** and **3**, where HCl cannot be used to eliminate tin octoate because it will protonate the PDMAEMA (unlike the ROP step in **Route 2**), tin octoate remains bonded to homo–PLA and the PLA block. This will affect the material properties, as each thermal and/or solvent treatment will engage transesterification reactions mediated by $Sn(Oct)_2$.

Finally, the possibility of unfunctionalized PDMAEMA in the final block copolymer was also considered. Unfortunately, attempts to separate PDMAEMA homopolymer from the mixture (and thus confirm or not its presence) were unsuccessful. In the quaternization/precipitation procedure, it would also be quaternized and therefore

would precipitate together with the quaternized block copolymer. An approach based on solubility differences between PDMAEMA and PLA in alcohols (methanol, ethanol) did not work because atactic PLA, unlike PLLA, is also soluble in the alcohols, and no precipitation of block copolymer occurred. Besides, the PDMAEMA block is long enough to ensure block copolymer solubility even in water.[10]

3.5 Conclusions

The results of this work show that, although the bifunctional initiator approach for preparing block copolymers is, in principle, advantageous for the synthesis of heterofunctional macroinitiators and seems beneficial for allowing either block to be prepared first, in reality it is more difficult if not impossible in some cases to avoid homopolymer impurity and a dependence on the sequence of block addition. In the particular case of LLA and DMAEMA monomers, if PDMAEMA is the first block prepared (to possibly allow the incorporation of long PLLA blocks), then not only is a large proportion of polylactide homopolymer found, but both the homopolymer and the polylactide block are racemic. If PLLA is the first block synthesized, racemization is avoided, but homo–PLLA is still produced, at least when using $Sn(Oct)_2$, due to the above–mentioned HO–Sn–Oct impurities. The formation of racemic PLA is rationalized by the racemization of LLA monomer through the influence of the amino moieties in PDMAEMA that reversibly deprotonate LLA at the polymerization temperature. Possible sources of the homopolymer impurity are competitive initiation of LLA by hydroxyltin octoate and/or lactoyl lactate (both resulting from the presence of trace amounts of H_2O). Another possible

route to homo–P(L)LA is the involvement of the ester group of the bifunctional initiator (HEBIB) in ROP, which can lead not only to homo–P(L)LA, but also to (undetectable) triblock copolymer formation. It was also found that homo–P(L)LA is not always obvious by conventional SEC (or SEC–LS) analysis, especially in the presence of relatively long PDMAEMA blocks, but can be unambiguously quantified by a quaternization/precipitation procedure. Simultaneous one–pot synthesis suffers from the same problems as the route via the PDMAEMA macroinitiator. Nevertheless, if those problems could be avoided, it seems that one–pot polymerization at the compromise ROP–ATRP temperature of 90 °C can be tolerated, providing relatively isotactic (ca. 85%) PLLA.

References to Chapter 3

1. Dove, A. P. *Chem. Commun.* **2008**, 6446–6470.
2. Puts, R. D.; Sogah, D. Y. *Macromolecules* **1997,** 30, 7050–7055.
3. Hawker, C. J.; Hedrick, J. L.; Malmström, E. E.; Trollsas, M., Mecerreyes, D.; Moineau, G.; Dubois, P.; Jérôme, R. *Macromolecules* **1998,** 31, 213–219.
4. Tunca, U.; Karliga, B.; Ertekin, S.; Ugur, A. L.; Sirkecioglu, O.; Hizal, G. *Polymer* **2001,** 42, 8489–8493.
5. Bernaerts, K. V.; Schacht, E. H.; Goethals, E. J.; Du Prez, F. E. *J. Polym. Sci. Part A: Polym. Chem.* **2003,** 41, 3206–3217.
6. Takeuchi, D.; Aida, T. *Macromolecules* **2000,** 33, 4607–4609.
7. Jakubowski, W.; Lutz, J.–F.; Slomkowski, S.; Matyjaszewski, K. *J. Polym. Sci. Part A: Polym. Chem.;* **2005**, 43, 1498–1510.
8. Wilbon, P.A.; Zheng, Y.; Yao, K.; Tang, C. *Macromolecules* **2010**, 43, 8747–8754.
9. Nasser–Eddine, M.; Delaite, C.; Hurtrez, G.; Dumas, P. *Eur. Polym. J.* **2005**, 41, 313–318.
10. Mao, J.; Ji, X.; Bo, S. *Macromol. Chem. Phys.* **2011**, 212, 744–752.
11. Mecerreyes, D.; Moineau, G.; Dubois, P.; Jérôme, R.; Hedrick, J. L.; Hawker, C. J.; Malmström, E. E.; Trollsas, M. *Angew. Chem. Int. Ed.* **1998**, 37, 1274–1276.
12. The inhibitor was not observed to affect the ATRP process significantly.
13. Matyjaszewski, K.; Davis, K.; Patten, T. E.; Wei, M. *Tetrahedron* **1997,** 53, 15321–15329.
14. Matyjaszewski, K.; Xia, J. *Chem. Rev*. **2001,** 101, 2921–2990.
15. Huang, J.; Murata, H.; Koepsel, R.; Russell, A.; Matyjaszewski, K. *Biomacromolecules* **2007,** 8, 1396–1399.
16. Blagodatskikh, I. V.; Sutkevich, M. V.; Sitnikova, N. L.; Churochkina, N. A.; Pryakhina, T. A.; Philippova, O. E.; Khokhlov, A. R. *J. Chromatography A* **2002,** 976, 155–164.
17. Fetters, L. J.; Graessley, W. W.; Hadjichristidis, N., Kiss, A. D.; Pearson, D. S.; Younghouse, L. B. *Macromolecules* **1988,** 21, 1644–1653.

18. Celli, A.; Scandola, M. *Polymer* **1992,** 33, 2699–2703.

19. Van Dijk, J. A. P. P.; Smit, J. A. M. *J. Polym. Sci. Polym. Chem. Ed*. **1983,** 21, 197–208.

20. Huang, J.; Lisowski, M. S.; Runt, J.; Hall, E. S.; Kean, R. T.; Buehler, N.; Lin, J. S. *Macromolecules* **1998,** 31, 2593–2599.

21. Drumright, R. E.; Gruber, P. R.; Henton, D. E. *Adv. Mater.* **2000**, 12, 1841–1846.

22. Tsukegi, T.; Motoyama, T.; Shirai, Y.; Nishida, H.; Endo, T. *Polym. Degrad. Stab*. **2007,** 92, 552–559.

23. Kricheldorf, H. R.; Lomadze, N.; Schwarz, G. *Macromolecules* **2008,** 41, 7812–7816.

24. Nederberg, F.; Connor, E. F.; Möller, M.; Glauser, T.; Hedrick, J. L. *Angew. Chem. Int. Ed*. **2001,** 40, 2712–2715.

25. Leenslag, J. W.; Pennings, A. J. *Makromol. Chem.* **1987**, 188, 1809–1814.

26. Kricheldorf, H. R.; Kreiser–Saunders, I.; Boettcher, C. *Polymer* **1995**, 36, 1253–1259.

27. Schwach, G.; Coudane, J.; Engel, R.; Vert, M. *J. Polym. Sci. Part A: Polym. Chem*. **1997**, 35, 3431–3440.

28. Espartero, J. L.; Rashkov, I.; Li, S. M.; Manolova, N.; Vert, M. *Macromolecules* **1996,** 29, 3535–3539.

29. Nijenhuis, A. J.; Grijpma, D. W.; Pennings, A. J. *Macromolecules* **1992,** 25, 6419–6429.

Appendix to Chapter 3

A3.1. SEC–LS elugrams of block copolymers, prepared via Routes 1 and 2

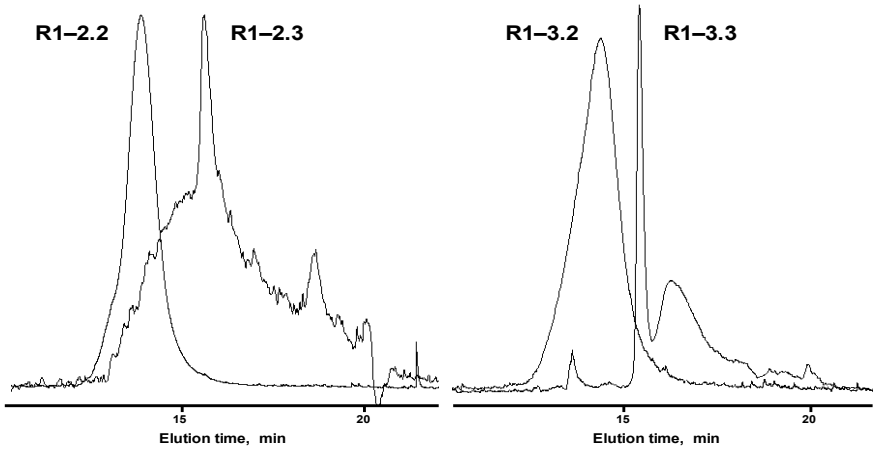

Figure A3.1. SEC–LS (in THF–TEA) elugrams (signals from LS detector) of PDMAEMA–b–PLA copolymers and homo–PLA, isolated by the quaternization/precipitation procedure in THF–TEA, prepared via **Route 1**

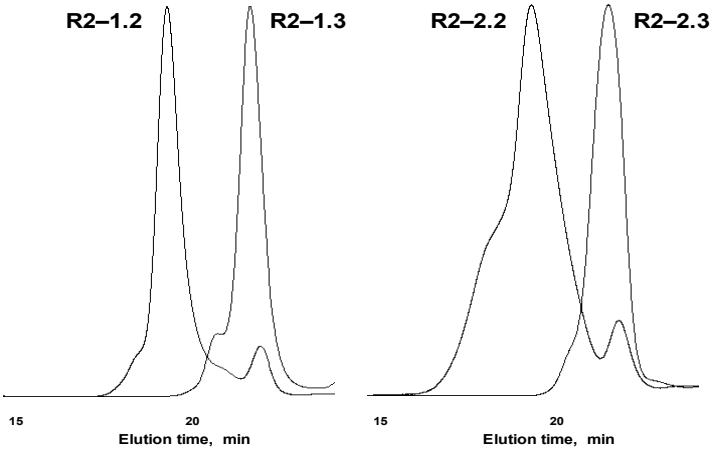

Figure A3.2. SEC–LS (in THF–TEA) elugrams (signals from RI detector) of PLLA–b–PDMAEMA copolymers and homo–PLLA, isolated by the quaternization/precipitation procedure, prepared via **Route 2**

A3.2. Gravimetrical determination of the composition of P(L)LA–b–PDMAEMA prepared via Routes 1–3.

Equations used for calculations:

$m_{quaternized} = m_{initial} - m_{homoPLA} - x + Qx$ (1)

x is the weight of the PDMAEMA block ($m_{PDMAEMA}$)

Q is the relative increase of molecular weight of DMAEMA unit for a given degree of quaternization:

$Q = [157 \cdot (1 - q) + 299 \cdot q] / 157$ (2)

q is the degree of PDMAEMA quaternization

By varying *q* and solving equations (2) and (1), different values for *block ratio* and *% of PLA incorporation* were obtained, and used for molecular weights determination by two methods, as follows.

Method 1. Knowing *block ratio* and using the reference molecular weight of PDMAEMA, PLLA and PLA block for **Routes 1, 2** and **3**, respectively, molecular weight of the second block is calculated.

Method 2. Knowing *% of P(L)LA incorporation*, the contribution of homo–PLA is eliminated and "true" molecular weight of the PLA block was calculated for **Route 1**, and "true" molecular weight of the PDMAEMA block was calculated for **Routes 2** and **3**.

Table A3.1. Composition of block copolymers obtained via **Routes 1** and **2**

Parameters / **Expt**	**Route 1, R1–2.2**	**Route 1, R1–3.2**	**Route 2, R2–1.2**	**Route 2, R2–2.2**
Initial aliquot, g	1.24	0.205	1.283	0.505
Quaternized, g	1.63	0.201	1.542	0.718
homo–PLA, g	0.24	0.081	0.331	0.083
% quaternization [a]	80	83	85	87
Block ratio, w/w PLA/PDMAEMA	1:6.48	1:4.89	1:4.16	1:8.67
PLA, % incorp. [b]	36	21	36	34

[a] optimized to give identical results by *Methods 1* and *2*

[b] % incorp. = $m_{(PLA\ block)}/m_{(homo\ PLA)}+m_{(PLA\ block)}$

Table A3.2. Composition of block copolymers obtained via **Route 3**

Parameters / **Expt**	**One–pot 70 °C, R3–1.1**	**One–pot 90 °C, R3–2.1**	**One–pot 110 °C, R3–3.1**
Initial aliquot, g	0.215	0.250	0.256
Quaternized, g	0.306	0.300	0.291
homo–PLA, g	0.036	0.060	0.073
% quaternization [a]	92	89	85
Block ratio, w/w PLA:PDMAEMA	1:5.83	1:2.59	1:3.25
PLA, % incorp. [b]	42	47	37

[a] optimized to give identical results by *Methods 1* and *2*

[b] % incorp. = $m_{(PLA\ block)}/m_{(homo\ PLA)}+m_{(PLA\ block)}$

A3.3. NMR characterization of homopolymers and block copolymers obtained in Routes 1–3.

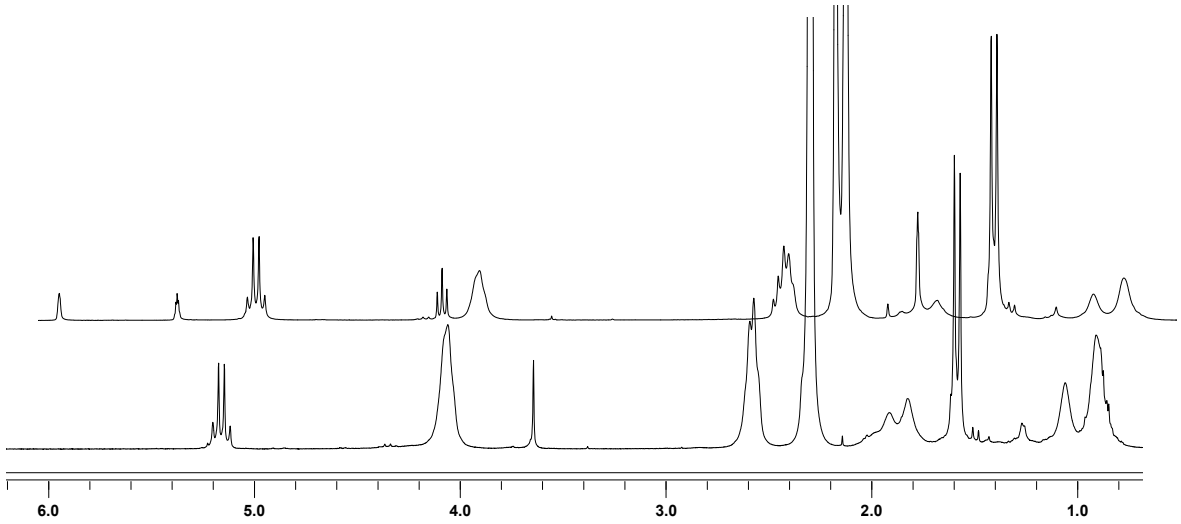

Figure A3.3. ^{1}H–NMR spectra of **R2–2.2** before (upper spectrum) and after (lower spectrum) the isolation procedure. The spectra are normalized to the PLLA signal. The upper spectrum is shifted to the right for clarity

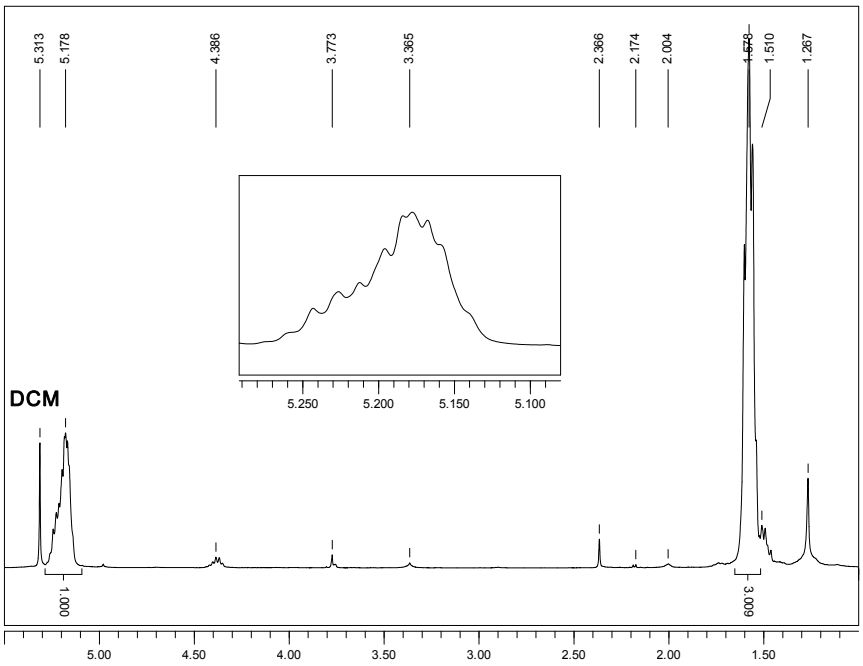

Figure A3.4. ^{1}H–NMR spectrum of PLA homopolymer **R1–3.3**, formed as undesired product in **Route 1**

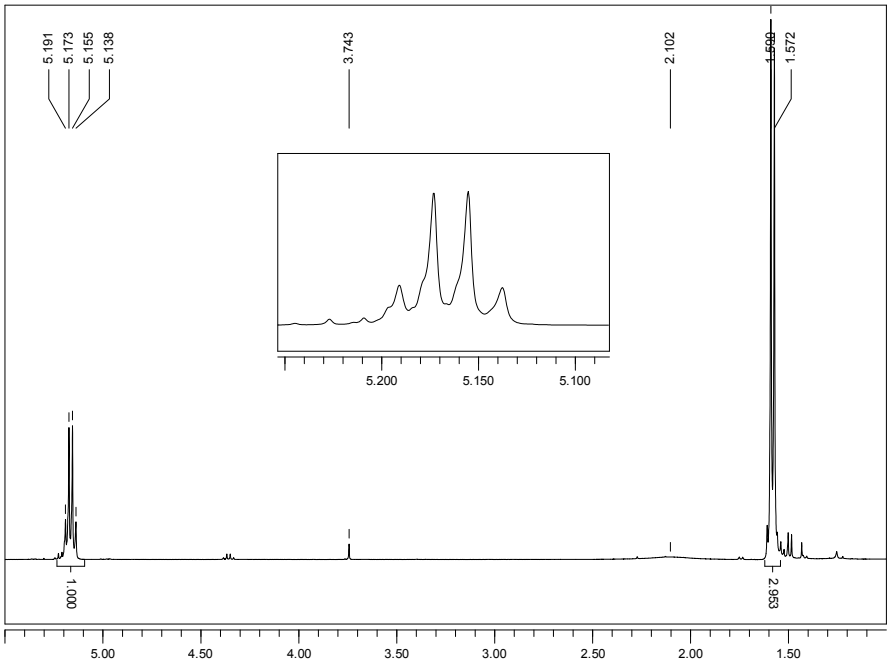

Figure A3.5. ^{1}H–NMR spectrum of PLA homopolymer **R2–1.3**, formed as undesired product in **Route 2**

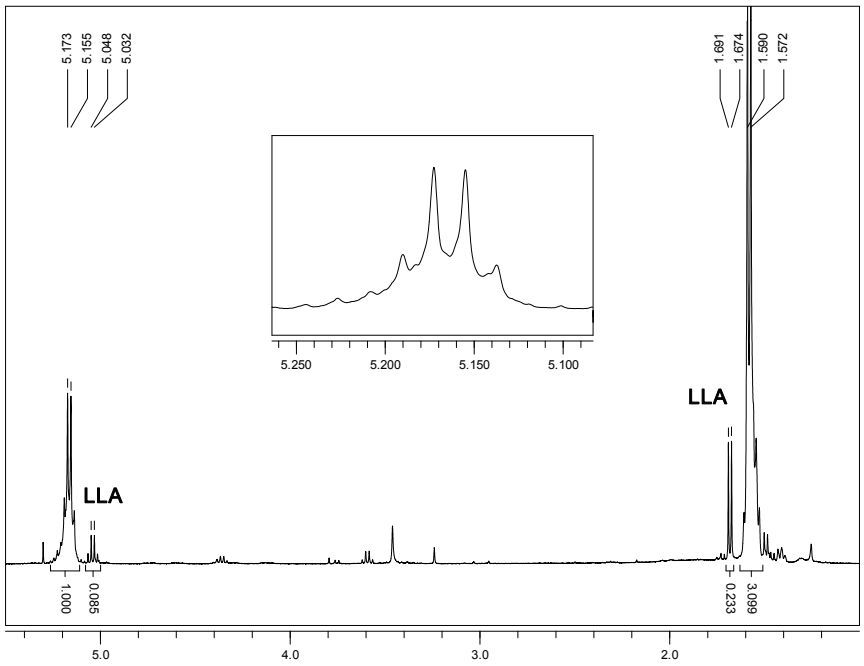

Figure A3.6. ^{1}H–NMR spectrum of PLA homopolymer **R3–1.2**, formed as undesired product in **Route 3**, **70 °C**

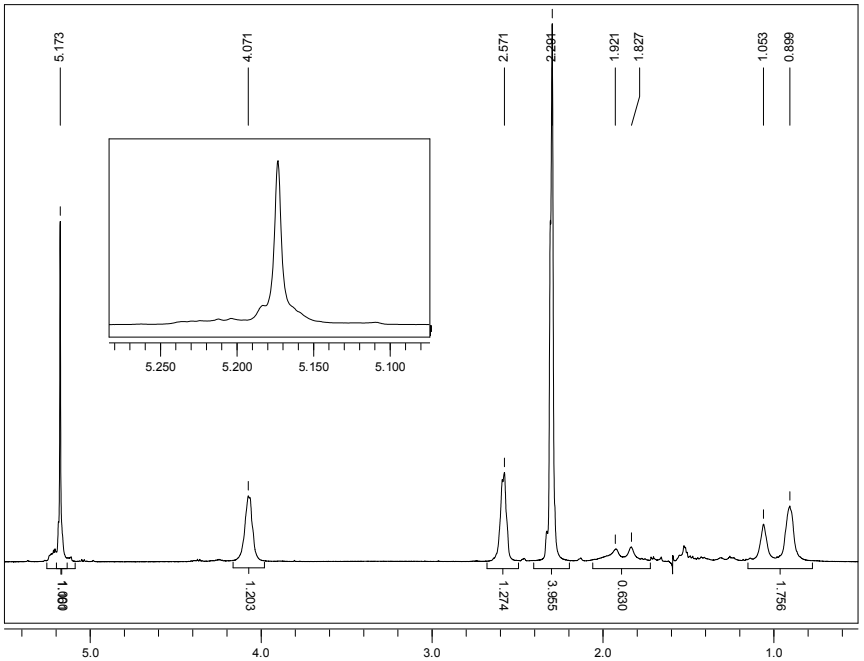

Figure A3.7a. ^{1}H–^{1}H–decoupled NMR spectrum of block copolymer **R3–2.1**, formed in **Route 3**, **90 °C**. Decoupling frequency was 1.58 ppm (632 Hz)

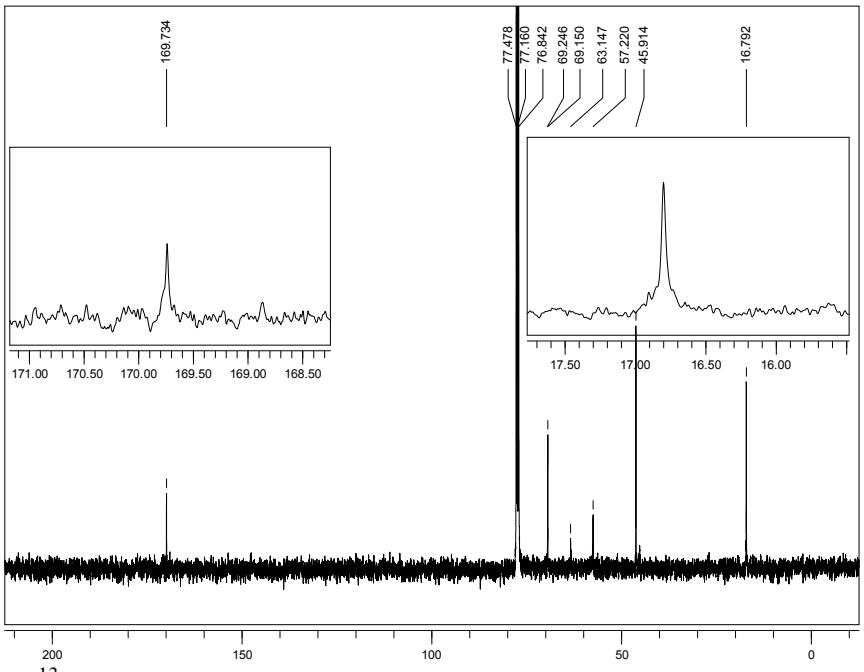

Figure A3.7b. ^{13}C–NMR spectrum of block copolymer **R3–2.1**, formed in **Route 3**, **90 °C**

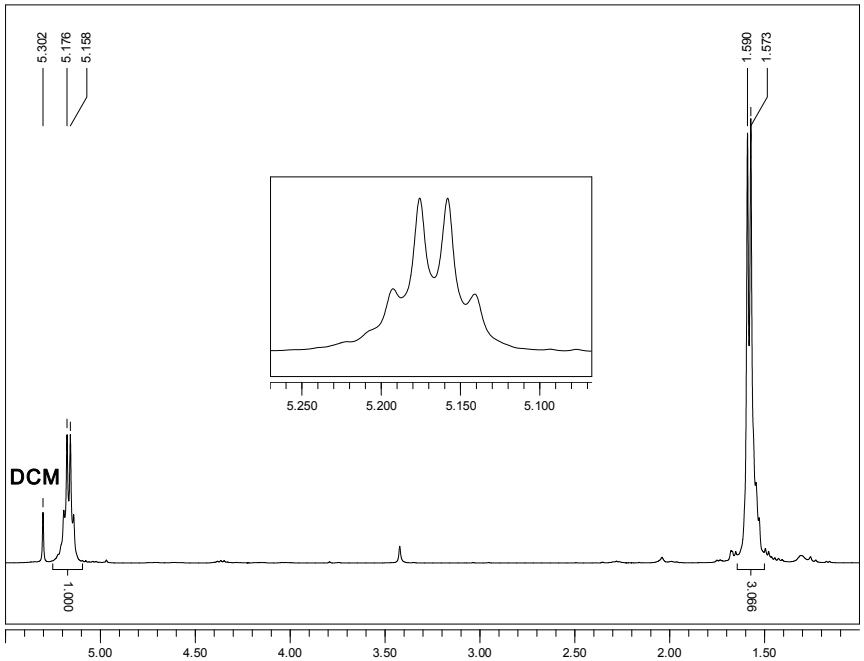

Figure A3.7c. ^{1}H–NMR spectrum of PLA homopolymer **R3–2.2**, formed as undesired product in **Route 3**, **90 °C**

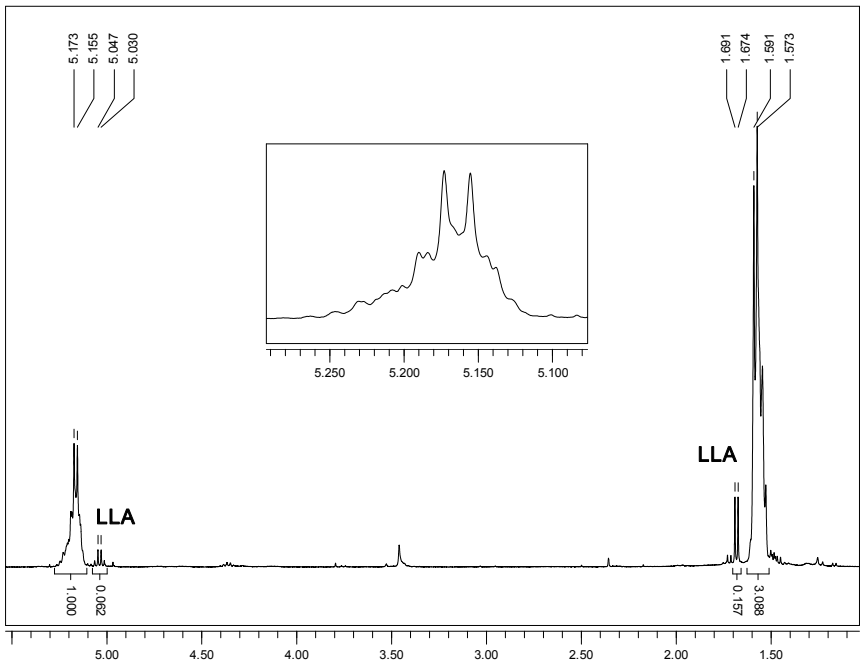

Figure A3.8. ^{1}H–NMR spectrum of PLA homopolymer, formed as undesired product in **Route 3**, **110 °C**

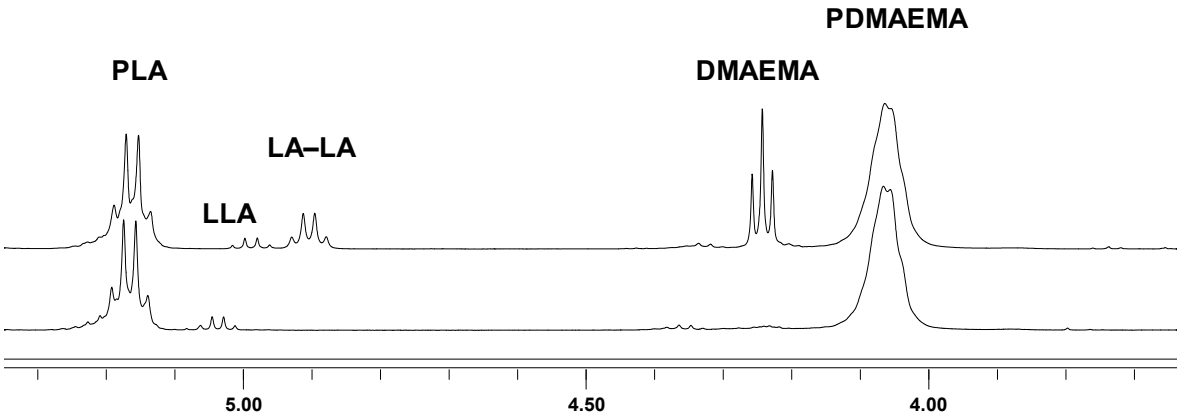

Figure A3.9. ^{1}H–NMR spectra of **R3–1.2** before (upper spectrum) and after (lower spectrum) the isolation procedure. The spectra are normalized to the PLA signal.

A3.4. DSC studies of homopolymers and block copolymers obtained via Routes 2 and 3

Table A3.3. DSC characterization of the polymers obtained by **Route 2** *

Sample	W_{PLLA}, %		T_g, °C (ΔC_p, J/g·K) [a]	T_c, °C	ΔH_c, J/g	T_g, °C (ΔC_p, J/g·K) [b]	T_m, °C	ΔH_m, J/g (% cryst)
R2–1.1 4300	100	1 heat. 1 cool. 2 heat. 2 cool.		 81 84 80	 16 24 15	42 (0.12) 44 (0.27)	146 145	64 (70) 63 (69)
R2–1.2 4300–6400 [c]	40 [c]	1 heat. 1 cool. 2 heat. 2 cool.	 20 (0.15)	99 94	3 6		154 141	17 (47) 6 (17)
R2–1.3 4300	100	1 heat. 1 cool. 2 heat. 2 cool.		73 83 93 84	16 6 38 3	49 (0.53) 44 (0.56)	145 144	62 (68) 56 (62)
R2–1.3 blend PDM_{16k}	50	1 heat. 1 cool. 2 heat. 2 cool.	 23 (0.42)	82; 118 106	9; 2 16	39 (0.28)	147 141	29 (64) 16 (35)
R2–2.1 5300	100	1 heat. 1 cool. 2 heat. 2 cool.		 90 90	 47 47	71 (0.14) [d] 40 (0.15)	152 151	68 (75) 67 (74)
R2–2.2 5300–19800 [c]	21 [c]	1 heat. 1 cool. 2 heat. 2 cool.	 20 (0.16)	138 125	3 0.3		157 154	3 (16) 1 (5)

* Two heating/cooling cycles at 10 °C/min between the temperature limits of 10 and 200 °C, which may cause slight degradation.

[a] PDMAEMA–rich phase

[b] PLLA–rich phase

[c] As determined on original samples; i.e. homo–PLLA contaminant included

[d] Initially crystalline as–prepared sample

Table A3.4. DSC characterization of the polymers obtained via **Route 3** *

Sample	W_{PLLA}, % [a]		T_g, °C (ΔC_p, J/g·K) [a]	T_c, °C	ΔH_c, J/g	T_g, °C (ΔC_p, J/g·K) [b]	T_m, °C	ΔH_m, J/g (% cryst)
R3–1.1 4200–10300 [c]	29 [c]	1 heat. 2 heat. 3 heat.	– 22 (0.34) 22 (0.35)					
R3–1.2 4200	100	1 heat. 2 heat. 3 heat.				30 (0.50) 31 (0.43) 33 (0.45)		
R3–2.1 9800–11900 [c]	45 [c]	1 heat. 2 heat. 3 heat.	 19 (0.19) 21 (0.16)	85	2	 46 (0.19) 47 (0.21)	126	5 (12)
R3–2.2 9800	100	1 heat. 2 heat. 3 heat.		106	3	 37 (0.45) 39 (0.52)	126	3 (3)
R3–3.1 7800–9400 [c]	45 [c]	1 heat. 2 heat. 3 heat.	20 (0.16) 20 (0.17) 23 (0.19)			40 (– [d]) 36 (0.15) 36 (0.11)		
R3–3.2 7800	100	1 heat. 2 heat. 3 heat.				35 (0.51) 36 (0.41) 37 (0.47)		

* Three heating/cooling cycles between the temperature limits of –20 and 180 °C: (1st cycle) initial heat of as–prepared samples at 10 °C/min, cool at 10 °C/min; (2nd cycle) heat at 10 °C/min, cool at 200 °C/min; (3rd cycle) heat at 20 °C/min, cool at 10 °C/min

[a] PDMAEMA–rich phase

[b] PLLA–rich phase

[c] from NMR of original sample (containing homo–PLA and LLA)

[d] hindered by an exothermal peak

A3.5. One–pot polymerization of LLA and DMAEMA using CuBr/HMTETA complex (Route 4)

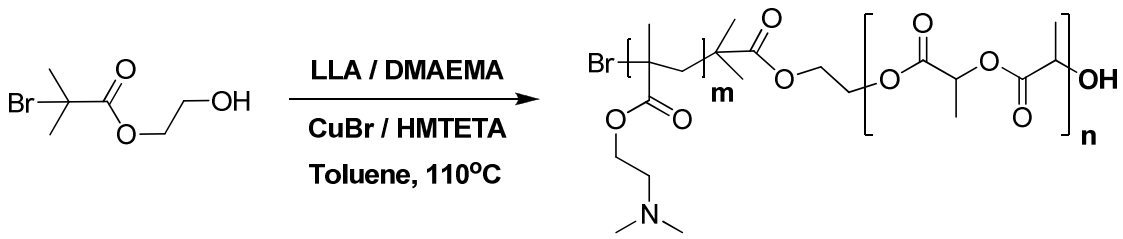

Scheme A3.1. Synthesis of PLA–b–PDMAEMA block copolymers: one–pot ROP and ATRP (**Route 4**)

The preparation and isolation procedures are similar to that described in 2.3.3, except that no tin octoate was added, the ratio of HEBIB:CuBr:HMTETA was 1:2:8, and the reaction mixture was stirred at 110 °C for 26 h.

The observation that PLA–b–PDMAEMA/PLA blends are formed in the one–pot combination of ROP by $Sn(Oct)_2$ and ATRP by CuBr, and the possibility of LA–LA (observed by NMR) as an active polymerizable intermediate, suggest conducting an experiment where tin octoate is eliminated and both polymerizations are conducted simultaneously using only a Cu(I) complex. We speculate that *in situ* formed copper lactoyl lactate ($CuLA_2$) is able to catalyze ROP of LLA, as was shown for iron lactide, although accompanied by LLA racemization [*].

*. Kricheldorf, H. R.; Damrau, D. O. *Macromol. Chem. Phys.* **1997**, 198, 1767–1774.

First, we found that heating of the anisole solution of LLA and CuBr/HMTETA complex in the presence of HEBIB for 22 h at 50 °C leads only to lactoyl lactic acid (LA–LA), along with a small amount of residual LLA and PLA (*Figure A3.10*, lower spectrum). However, when the polymerization was conducted at 130 °C, more than 90% of the LLA was consumed in less than 3 h and the formation of the polymer is observed (*Figure A3.10*, upper spectrum). This indicates that LLA polymerization proceeds through initial formation of LA–LA, followed by its incorporation into the polymer (taking place at 130 °C, but not at 50 °C).

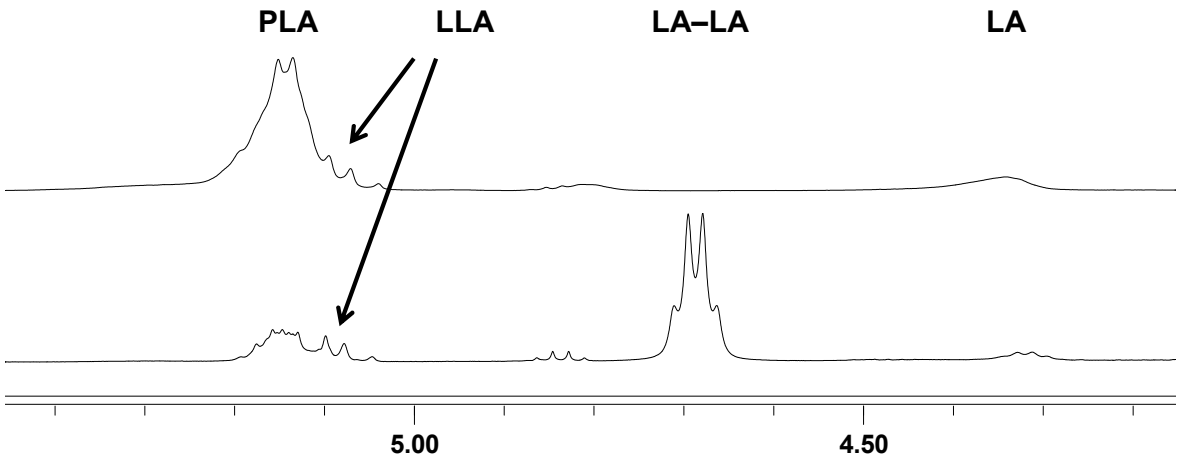

Figure A3.10. ^{1}H–NMR spectra of the products of LLA polymerization, using CuBr/HMTETA as a catalyst, performed at 50 °C for 22 h (lower spectrum) and at 130 °C for 3 h (upper spectrum).

Then, the polymerization of LLA and DMAEMA was conducted simultaneously at 110 °C using CuBr/HMTETA as a mutual catalytic system. The quaternization/precipitation method proved that both block copolymer and homo–PLA (gravimetrically determined as 51% of the total PLA content) were formed. The molecular

weight of the homo–PLA, determined by SEC–LS using THF-TEA, was very close to the one determined by the initial monomer feed (*Table S6*).

Table A3.5. Composition of block copolymer obtained via **Route 4**

Parameters	**R4–1.1**
Initial aliquot, g	0.250
Quaternized, g	0.360
homo–PLA, g	0.039
% quaternization [a]	95
Block ratio, w/w, PLA:PDMAEMA	1:4.72
PLA, % incorp. [b]	49

[a] optimized to give identical results by *Methods 1* and *2*, as described above
[b] % incorp. = $m_{(PLA\ block)}/m_{(homo\ PLA)}+m_{(PLA\ block)}$

Table A3.6. Molecular weight data for the block copolymers (R4–x.1) and isolated homo–PLA (R4–x.2), obtained in **Route 4**

Code	Sample	$[M_1]$ / $[M_2]$ / [I]	Conv. M_1 / M_2 %	M_n (g/mol, NMR) original [b] recalcd (% quat) [c]	M_n (g/mol) / PDI SEC–LS [d]
R4–1.1	PLA_{10k}–$PDMAEMA_{28k}$	73 / 125 / 1	90 / 80	10400–23800 [b] 10400–49000 [c]	n/d
R4–1.2	homo–PLA_{10k}: 51% [e]				10400 / 1.51

[a] $[M_1]$ = [LLA], $[M_2]$ = [DMAEMA], [I] = [HEBIB]. [b] Data on original samples. Calculated from the intensity ratio of $NCH_2\mathit{CH_2}O$ signal of PDMAEMA (ca. 4.1 ppm) and $\mathit{CH}CH_3$ signal of PLA (ca. 5.2 ppm), assuming a molecular weight for the PLA block that is the same as homo–PLA. [c] Data in b recalculated to eliminate the contribution of homo–PLA; % quat refers to the degree of quaternization calculated for the PDMAEMA block (see above for details). [d] SEC–LS in THF–TEA. [e] Homopolymer PLA isolated by quaternization/precipitation, in wt % of total PLA content in original sample (see above for details).

CRYSTALLIZATION, MORPHOLOGY AND KINETICS IN LINEAR DIBLOCK COPOLYMERS OF L–LACTIDE AND 2–DIMETHYLAMINOETHYL METHACRYLATE, AND EFFECT OF PARTIAL QUATERNIZATION

4

4.1. Introduction

In block copolymers, where phase separation is limited to the molecular level, the melt morphology is driven by the strength of the segregation between the two blocks. Depending on the block ratio, different nanoscale domains (e.g. spheres, cylinders, lamellae etc.) can be formed.[1] When one of the blocks is semi–crystalline, crystallization is a second driving force in structure development, resulting in the formation of semi–crystalline and amorphous regions.[2] If the amorphous block is glassy at the crystallization temperature, then the melt structure is preserved and crystallization occurs in the microdomains prescribed by the microphase separation.[3,4] But if the noncrystallizing block is soft during crystallization, then phase separation and crystallization compete. In weakly segregated

systems, crystallization completely changes the morphology formed by self–assembly in the melt.[5] However, if the segregation strength between the crystallizable block and the amorphous matrix is sufficiently strong, then the crystallization can be confined to the microdomains established in the melt.[6] Since the segregation strength can also be tuned by varying the total molecular weight while maintaining block ratio, both phenomena (destruction and preservation of the melt morphology) can be observed in one block copolymer system.[7,8]

Strongly segregated block copolymers of poly(L–lactide) (PLLA) with a second block that is rubbery at the PLLA crystallization temperature, like polyethylene (PE), crystallize within the microstructure formed in the melt. As a result, no spherulites are observed during isothermal crystallization.[9] If the PE block is able to crystallize, PLLA can crystallize either before or simultaneously with the PE block, both within their respective microdomains.[10,11] In the case of atactic polystyrene (PS) as a second block, PLLA can be crystallized either below or above the glass transition of the PS block, i.e. in a hard or a soft confinement environment.[12,13] When the PS block is glassy, PLLA crystallizes in its predefined microdomains. However, despite the strong segregation between PLLA and PS in the melt, spherulites are obtained at temperatures higher than the T_g of the PS block.[14]

Numerous reports on crystallization studies of PLLA block copolymers of different architectures with poly(ε–caprolactone) (PCL) and poly(ethylene oxide) (PEO) were recently summarized in a review by Castillo and Müller.[15] Weakly segregated PLLA–PCL block copolymers form either a phase–separated melt at high molecular weight ($M_{n(total)}$ = 77,000 g/mol, w_{PCL} = 0.32) or a miscible melt at low molecular weight ($M_{n(total)}$ = 19,000

g/mol, w_{PCL} = 0.37).[16] The presence of the PCL melt during crystallization of the PLLA block decreases its crystallization rate (compared to the PLLA homopolymer) in both the phase–separated and homogeneous melts. In contrast, all of the PLLA–PEO block copolymers were reported miscible in the melt at any molecular weight and composition studied. The effect of the PEO block was reported to accelerate[17] and to retard[18] the crystallization of PLLA, although similar molecular weights and block ratios were reported in both studies.

The state of phase separation in the melt for diblock copolymers composed of a semi–crystalline PLLA block and an amorphous poly(2–dimethylaminoethyl methacrylate) (PDMAEMA) block was described in Chapter 2. The system is completely miscible when the molecular weight of either block is ca. 5000 g/mol or less. In this case, phase separation is driven by the crystallization of the PLLA. Recently, the miscibility of low molecular weight PLLA and PDMAEMA (ca. 5000 g/mol) was also confirmed by small–angle X–ray scattering (SAXS) studies.[19]

At higher molecular weights of each block (>10,000 g/mol), a phase–separated melt is formed and the crystallization of the PLLA block is expected to occur in a soft confinement environment, given that the PDMAEMA block is above its T_g at the PLLA crystallization temperature. The strength of segregation between the two blocks can be increased by quaternizing PDMAEMA (even of low molecular weight), as it will increase its T_g and allow obtaining a templated crystallization environment for the PLLA block at low PDMAEMA content, and confined crystallization environment at high PDMAEMA content.

In our research, we are interested in studying the crystallization behaviour of the PLLA block of different molecular weight (5000–20,000 g/mol) in the presence of the soft (at crystallization temperature of PLLA) amorphous PDMAEMA block of different molecular weight (5000–35,000 g/mol). The preparation and thermal characterization of nine block copolymers was described in *Chapter 2*. SAXS analysis of a presumably lamellae–forming phase-separated block copolymer will be used to study the melt morphology. Selected block copolymers will be partially quaternized (quaternization degrees of ca. 35, 55 and 80 %), and the isothermal crystallization experiments in bulk, using differential scanning calorimetry, and in thick films, using polarized optical microscopy, will be conducted on the parent and partially quaternized samples at 100, 120 and 150 °C, i.e., in all three crystallization regimes described for PLLA (Regime III, below 120 °C, Regime II, 120–145 °C and Regime I, above 145 °C).[20]

4.2. Experimental

4.2.1 Techniques

Details on the NMR, TGA and DSC instrumentation are given in *Chapter 2*. The following scan sequence, between the temperature limits of –20 and 185 °C, was applied to isothermal crystallization DSC analysis of PLLA homopolymers and block copolymers: initial heat of as–prepared samples at 10 °C/min to 185 °C, isothermal for 1 min, followed by isothermal experiment (cool at 50 °C/min to 100, 120, 150 °C, isothermal for 1 h [2 h at 150 °C], then cool at 50 °C/min to –20 °C), each followed by heat at 10 °C/min to 185 °C.

Polarized optical microscopy (POM) data were acquired using a Zeiss Axioskop 40 microscope coupled with a Linkam Scientific Instrument THMS600 hot stage and a TMS94 temperature controller.

Powder wide–angle X–ray diffraction (WAXD) analysis on samples packed in 1.0 mm diameter glass capillaries (Charles Supper) was performed on a Bruker D8 Discover system equipped with a 2D Bruker AXS wire–grid detector, using Cu Kα radiation. The sample temperature was controlled by an Instec HCS410 heating stage and STC200 temperature controller. Small–angle X–ray scattering (SAXS) patterns[21] were collected with an Anton–Paar compact Kratky camera fitted with a custom hot stage, a PANalytical PW3830 X–ray generator with a long–fine focus Cu tube producing CuKα radiation (λ=0.15418 nm) and an MBraun OED–50M position sensitive detector. Data were corrected for detector sensitivity and positional linearity, empty beam scattering, sample thickness and transmittance, placed on an absolute intensity scale via a polyethylene standard, and desmeared for slit length.[22] Absolute SAXS intensities (I/IeV) are plotted against the magnitude of the scattering vector $q = (4\pi/\lambda)\sin\theta$, where θ is half the scattering angle; calibration was via silver behenate.[23] Intensities were multiplied by q^2 to approximately correct for the form factor of lamellae.[24]

4.2.2 Materials

All chemicals were supplied by Aldrich and used as received, unless otherwise specified. The preparation and characterization of all of the homopolymers (PLLA–Br) and block copolymers for the present study were described earlier (*Chapter 2*).

4.2.3 PLLA–b–PDMAEMA partial quaternization

Block copolymers, 19k–5k, 19k–17k and 5k–4k [three aliquots (75–150 mg) of each], were dissolved in 20 mL of dry DCM, and then a 0.35, 0.55 or 0.80 equivalent of methyl iodide was quickly added in one portion under vigorous stirring. The solution obtained was stirred in a closed system under N_2 pressure at room temperature. The reaction solution remained clear for lower degrees of quaternization, with slight opalescence in the case of 80% quaternization in all three samples. Increased viscosity and the appearance of yellow coloration indicated successful quaternization of the PDMAEMA block. After 48 h, the solvent was evaporated under vacuum until dryness and the yellow solid obtained was further dried *in vacuo* for at least 72 h prior to use. ^{1}H–NMR (400 MHz): δ_H, *ppm* 0.74–1.20 (m, CH_3, PDMAEMA), 1.49–1.65 (d, J = 7.2 Hz, CH_3, PLLA), 1.68–2.05 (m, CH_2, PDMAEMA), 2.20–2.45 (m, $N(CH_3)_2$, PDMAEMA), 2.50–2.70 (m, NCH_2, PDMAEMA), 3.44–3.86 (m, $^+N(CH_3)_3$, PDMAEMA), 3.96–4.20 (m, OCH_2, PDMAEMA), 5.09–5.22 (m, CH, LLA unit).

4.2.4 Preparation of the films

Drop–cast films for POM experiments were prepared by deposition of block copolymer solutions in $CHCl_3$ on the round glass slides (d = 15 mm, thickness is 0.15 mm), cleaned with a freshly prepared Piranha solution (1 mL 98% H_2SO_4 + 1 mL 30% H_2O_2). The amount of solution (50 μL) and its concentration (10 mg/mL) were calculated to aim for a thickness of 2–3 μm (given that the density of PLLA is about 1.27 mg/cm^3 [25] and PDMAEMA is 1.32 mg/cm^3 [26]). To create a solvent–saturated atmosphere around the

sample and to allow uniform film formation, glass slides were placed in a covered Petri dish containing 2 mL of $CHCl_3$ and left at room temperature until complete solvent evaporation.

4.2.5 Crystallization of the films

The films were heated on a POM hot stage to a temperature 10–15 °C higher than the melting temperature of the PLLA block (i.e. 165, 175 and 185 °C for 5k, 13k and 19k series, respectively), where they were held for 7 min to erase thermal history. Then the sample was cooled at 40 °C/min to the desired crystallization temperature (100, 120 or 150 °C). For crystallization at 150 °C, the samples were first cooled to 100–110 °C to induce crystallization, and then reheated back to 150 °C. Images of the growing spherulites were taken at fixed time intervals varying from 1 s (for pure PLLA) to 300 s for block copolymers with the longest PDMAEMA block. The linear spherulite growth rate *G* was averaged through the entire time range of the experiment.

4.3. Results and Discussion

The focus of our studies here is on the crystallization kinetics and crystalline morphologies in PLLA–PDMAEMA diblock copolymers, and their variation with block lengths (relative and absolute) as well as with degree of quaternization of the PDMAEMA block. The background thermal and crystallization properties of the nonquaternized diblock copolymer series is described in *Chapter 2*. Since these properties have not been previously described for the quaternized copolymers, these are presented first in what follows. Then the kinetic

studies and morphologies of the nonquaternized, followed by those for the quaternized copolymers are presented.

4.3.1 Thermal characterization of selected partially quaternized block copolymers

For the partial quaternization experiments, the choice of block copolymers was determined by the following considerations. When quaternized, qPDMAEMA becomes insoluble in DCM and $CHCl_3$, most preferable solvents for PLLA and nonquaternized PDMAEMA copolymers, which compromises its characterization by NMR and the preparation of homogeneous films; this problem is minimized with a short qPDMAEMA block compared to PLLA. On the other hand, a long PLLA block ensures a high melting point so that PLLA crystallization can be carried out either in hard or in soft confinement environment, given that the T_g of fully quaternized PDMAEMA is ca. 140 °C (see below). This leads to 19k–5k as the first choice. Next, it is of interest to determine how the length of the qPDMAEMA block affects crystallization kinetics and morphology, making sample 19k–17k the second choice. Finally, for further comparison, the effect of qPDMAEMA on a low molecular weight PLLA was investigated on sample 5k–4k.

The degree of quaternization was estimated from NMR spectra in $CDCl_3$ by comparison of the intensity of the signal at 1.57 ppm (CH_3 of PLLA) with that at 4.06 ppm (CH_2O of nonquaternized PDMAEMA), which gradually decreases to zero with degree of quaternization (*Figure 4.1*) due to the formation of qPDMAEMA core micelles in chloroform solution. It should be mentioned that the degree of quaternization of 55 and

80% for 19k–17k was estimated presuming the completeness of the reaction after 48 h, as no PDMAEMA signal at 4.06 ppm was observed in NMR spectra.

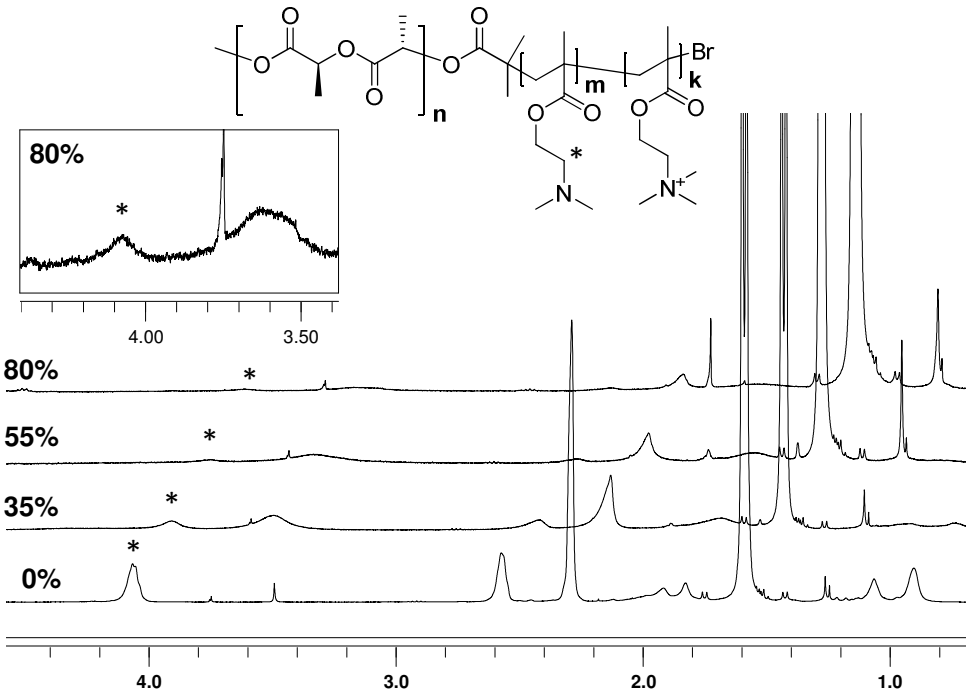

Figure 4.1. NMR spectra of partially quaternized 19k–5k PLLA–b–PDMAEMA in $CDCl_3$ (progressively shifted horizontally and zoomed vertically for clarity). Inset shows zoomed region of interest of 80% quaternized sample

The thermal properties of partially quaternized 19k–5k [q19k–5k(%)], 19k–17k [q19k–17k(%)] and 5k–4k [q5k–4k(%)] block copolymers are summarized in *Table 4.1*. Complete quaternization of a PDMAEMA homopolymer (16,000) increases its T_g from 17 to ca. 140 °C (*Figure 4.2*). This implies that, during isothermal crystallization experiments at temperatures < 140 °C, the crystallization of the PLLA block should proceed in a templated environment, although the broadness of the apparent T_g (>20 °C) must be

considered. Unfortunately, in the quaternized block copolymers, the very small ΔC_p change of the glass transition of qPDMAEMA, along with the overlapping of the cold–crystallization region of PLLA with the expected glass transition region of the qPDMAEMA block, made it impossible to observe any clear T_g in the heating scans of either crystallized or quenched samples for all three series studied. As expected, no crystallization was detected by DSC in any sample during cooling scans from the melt at 10 °C/min, as for the nonquaternized samples described in *Chapter 2*.

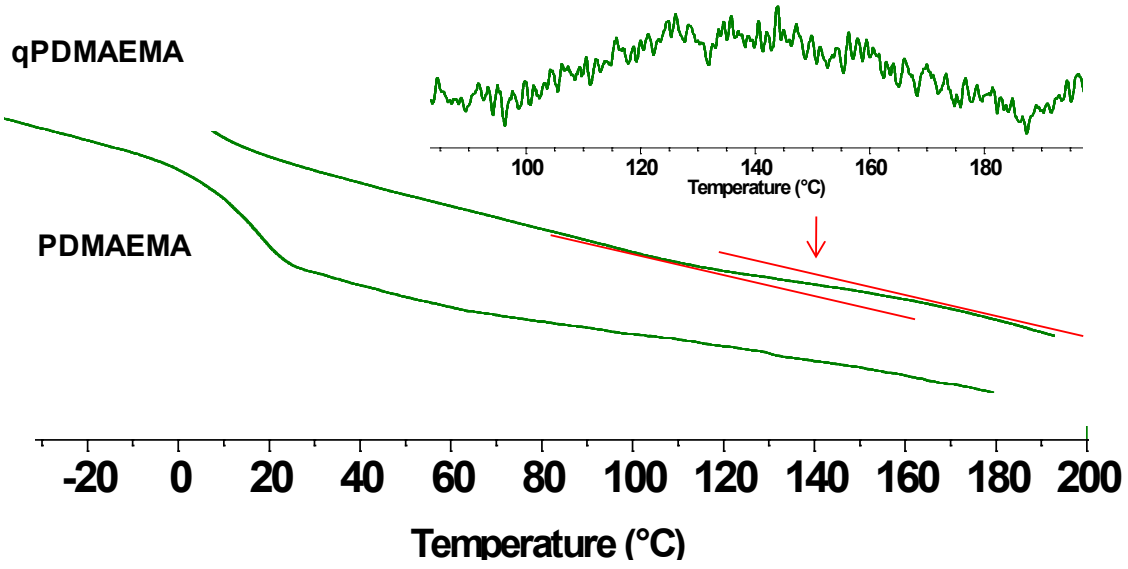

Figure 4.2. DSC thermograms of PDMAEMA and qPDMAEMA (16,000). Inset shows a 1st derivative curve, indicating the T_g region of qPDMAEMA

Table 4.1. DSC characterization of partially quaternized block copolymers

Sample (% quat.) [a]		W_{PLLA} % [b]	T_g (ΔC_p), °C ($J \cdot g^{-1} \cdot K^{-1}$)	T_c, °C	T_m, °C	ΔH_m^{total}, J/g (% cryst) [c]
19k–5k (0%)	(cr)	78	45 (0.22) [d]		167	43 [d] (61)
	(am)		52 (0.50)	116		
19k–6.6k (35 ± 4%)	(cr)	74	65 (0.16) [e]		166	31 [e] (48)
	(am)		60 (0.39)	121		
19k–7.7k (55 ± 6%)	(cr)	71	65 (0.17) [e]		166	30 [e] (49)
	(am)		60 (0.37)	112		
19k–8.6k (80 ± 6%)	(cr)	69	63 (0.15) [e]		164	26 [e] (45)
	(am)		60 (0.35)	110		
19k–17k (0%)	(cr)	54			167	26 [d] (53)
	(am)		56 (0.23)	134		
19k–23k (38 ± 3%)	(cr)	45	56 (0.14) [f]		164	21 [f] (53)
	(am)		55 (0.25)	132		
19k–25k (55%)	(cr)	43	56 (0.11) [f]		163	13 [f] (35)
	(am)		55 (0.19)	143		
19k–29k (80%)	(cr)	40	57 (0.16) [g]		165	4 [g] (12)
	(am)		55 (0.19)	145		
5k–4k (0%)	(cr)	56			144	30 [d] (59)
	(am)		35 (0.48)	122		
5k–5.1k (30 ± 2%)	(cr)	49	48 (0.12) [h]		138	18 [h] (40)
	(am)		50 (0.29)	127		
5k–6.1k (58 ± 5%)	(cr)	45	51 (0.19) [h]		139	1 [h] (3)
	(am)		51 (0.21)	140		
5k–6.7k (75 ± 9%)	(cr)	43	52 (0.21) [h]		156	1 [h] (3)
	(am)		52 (0.21)	143		

(Ended on the next page)

(Ending of **Table 4.1**)

[a] molecular weight of PDMAEMA block is recalculated assuming the % of quaternization. Am and cr denote amorphous (quenched from the melt at 185 °C) and semi–crystalline (isothermally crystallized) samples. Experimental uncertainty of % quat. was estimated from NMR. [b] assuming % of quaternization. [c] The ΔH_m^{total} values are relative to the total copolymer weight. % of crystallinity is relative to PLLA fraction, eliminating the volatiles determined by TGA. [d] crystallized for 1 h at 100 °C. [e] crystallized for 1 h at 110 °C. [f] crystallized for 2 h at 110 °C. [g] crystallized for 1 h at 120 °C. [h] crystallized for 2 h at 100 °C.

As described in *Chapter 2*, 19k–5k and 5k–4k form a miscible melt, whereas 19k–17k forms a phase–separated system, as indicated by one intermediate T_g and two distinct T_g values, respectively (*Figure 4.3*). From this, one might expect q19k–5k and q5k–4k to be miscible too, at least for lower quaternization levels. Unfortunately, as mentioned above, no T_g for the qPDMAEMA block could be observed in the thermograms of any sample. However, a closer look at the T_g regions in the heating thermograms of quenched samples shows that the T_g values of the PLLA block in the q19k–17k are very close to that of the parent 19k–17k (as well as PLLA macroinitiator), indicating no miscibility between the blocks. In contrast, persistently higher T_g values of PLLA in q19k–5k and q5k–4k compared to 19k–5k and 5k–4k, respectively, indicate some degree of miscibility between PLLA and the low molecular weight qPDMAEMA block (*Table 4.1*, *Figure 4.3*).

The constancy of the values with degree of quaternization may actually indicate partial miscibility that decreases with degree of quaternization (i.e. increase in degree of quaternization should increase T_g, but decrease in miscibility opposes so that the two

effects seem to balance out), although there is also a question of humidity – more serious the higher the quaternization level.

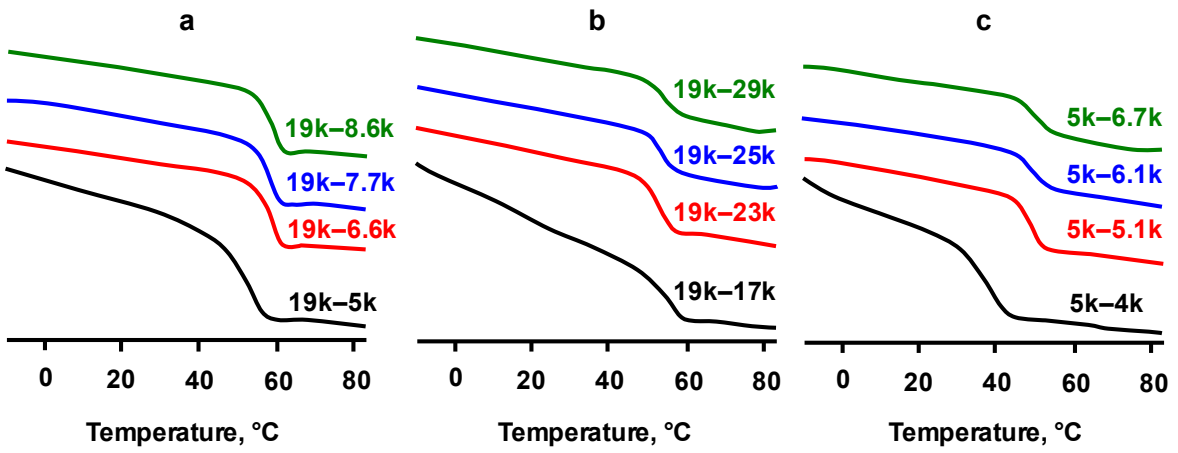

Figure 4.3. Glass transition regions of DSC thermograms of partially quaternized samples quenched from the melt (am); a) 20 °C/min, b) and c) 10 °C/min heating scans

Heating scans at 20 °C/min of the 19k–5k and q19k–5k samples exhibited relatively sharp cold crystallization peaks, with a tendency to shift to lower temperatures as the degree of quaternization increases (*Figure A4.1*). In contrast, during heating scans of 19k–17k and q19k–17k (10 °C/min), a cold crystallization exotherm becomes weaker and broader, and shifts towards lower temperatures as the degree of quaternization increases. The melting endotherm dramatically decreases as the degree of quaternization increases, indicating that crystallization of PLLA is significantly hindered by the hard qPDMAEMA block (*Figure A4.2*). Interestingly, all three q5k–4k samples showed the absence of cold crystallization and a melting endotherm in 10 °C/min heating scans (*Figure A4.3*).

The degree of crystallinity in partially quaternized samples that were annealed at 100–120 °C for 1–2 h is decreased compared to the parent block copolymers. Specifically, the degree of crystallinity in q19k–5k is 45–48%, which is smaller than that in 19k–5k (*Table 4.1*), irrespective of the degree of quaternization, indicating that hard qPDMAEMA domains effectively hinder crystallization of the PLLA block. A shoulder located ca. 20 °C lower than the main melting peak (termed pre–melting) is also indicative of poorly ordered crystalline regions. However, the melting temperature is reduced by only a few degrees compared to 19k–5k. A more pronounced dependence of the degree of crystallinity on the degree of quaternization is observed in the q19k–17k series. Thus, the degree of crystallinity of q19k–17k(38) is similar to the parent 19k–17k (53%), whereas in q19k–17k(55) the degree of crystallinity drops to 35% and in q19k–17k(80) to 12%. Again, the melting temperatures are reduced by only a few degrees, compared to 19k–17k. Finally, quaternization of the PDMAEMA block of 5k–4k results in the inability to crystallize for q5k–4k(58) and q5k–4k(75), and in a 30% decrease in the degree of crystallinity in q5k–4k(30) compared with the parent 5k–4k. Thus, the entire q5k–4k series and q19k–17k(80) were excluded from further crystallization studies.

4.3.2 WAXD and SAXS measurements on PLLA–PDMAEMA block copolymers

The diffraction patterns of the block copolymers of $PLLA_{19k}$ series, obtained after 1 h of isothermal cold–crystallization at 110 °C (i.e. the freshly prepared samples were not melted, as no difference in the diffraction angles was observed between melt–crystallized

and cold–crystallized PLLA samples),[17] exhibit five main well–resolved diffraction peaks at 7.6, 12.3, 14.7, 16.5 and 22.1° (*2θ)* (*Figure 4.4a*). A broad signal at ca. 8° (*2θ)*, corresponding to a *d*-spacing of 11.6 Å, is associated with the presence of the phase–separated PDMAEMA domains, as this signal becomes more apparent as the contents of PDMAEMA increase. Another broad signal at ca. 17° (*2θ)*, also becoming more apparent at higher PDMAEMA contents, corresponds to amorphous PLLA domains, as was observed in a completely melted PLLA–b–PEO sample.[27] Crystalline modification of the PLLA block was assigned to the α form, where a left–handed 10_3 helix is packed into an orthorhombic unit cell, based on comparison with the diffraction patterns obtained in Refs 17 and 28.

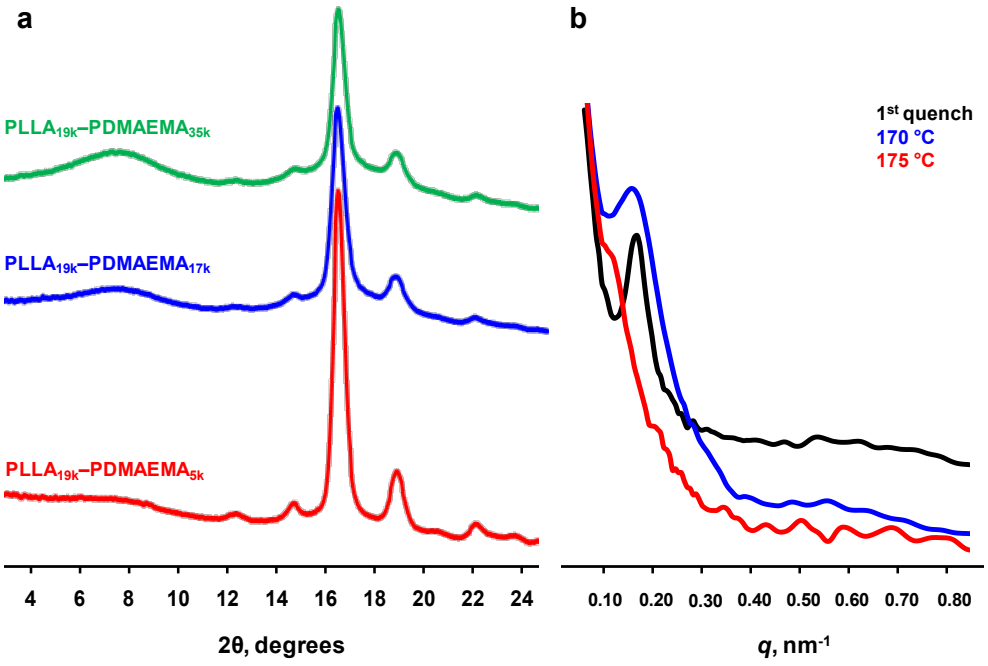

Figure 4.4. a) WAXD patterns of the polymers of $PLLA_{19k}$ series, isothermally cold–crystallized at 110 °C. b) Evolution of 19k–17k SAXS patterns after successive melting

By conducting a SAXS experiment one can gain information about the state of phase separation in the PLLA–PDMAEMA couple. Preliminary SAXS studies were made on sample 19k–17k, which probably possesses lamellar morphology in the bulk, judging from its composition.[1] The sample quenched from the melt at 175 °C displays a relatively narrow microdomain peak at $q = 0.169$ nm^{-1}, corresponding to a Bragg spacing $d = 37$ nm. This periodicity is indicative of microphase separation, although the broad peak at around 0.6 nm^{-1} (corresponding to residual crystalline PLLA) obscures any higher–order peaks from the microdomain structure, making confirmation of its probable lamellar morphology impossible (*Figure 4.4b*, 1st quench curve). An attempt to measure the melt morphology *in situ* was then made at 170 °C, accumulating the data for 1 h at this temperature. As evidenced from the reduction in the SAXS intensity for $q > 0.3$ nm^{-1}, the PLLA crystals were completely melted and the microdomain peak is still present at about the same q, although significantly broadened (*Figure 4.4b*, 170 °C). Further heating at 175 °C for 10 min caused the peak to drop in intensity, becoming a shoulder at 0.13 nm^{-1} (*Figure 4.4b*, 175 °C). Slow cooling of the sample to room temperature or requenching from the melt at 180 °C (to reproduce the initial thermal history) did not restore the peak to its original position.

This permanent change in microdomain spacing, coupled with visual yellowing of the sample, indicated degradation. Since the sample was still able to crystallize, PLLA chain scission was suspected. This was confirmed by NMR by comparing the spectra of the freshly synthesized 19k–17k and the sample after SAXS experiment (*Figure 4.5*). The signals at 4.34 ppm and 5.02 ppm, assigned to terminal lactide units from hydroxyl and carboxyl ends of PLLA homopolymers, respectively[29] (normally not present in the block copolymer due to the synthetic conditions), is indicative of random PLLA chain scission resulting from undesired transesterification reactions, and leading to PLLA homopolymer formation. Since other studies in the literature of PLLA–containing block copolymers, notably PS–PLLA and PMMA–PLLA, do not appear to present this problem, it might be related to the presence of PDMAEMA. Indeed, a probable transesterification agent is the amino group of DMAEMA that was shown to be able to polymerize LLA at 100 °C (see Appendix to *Chapter 3*) by nucleophilic ring–opening polymerization, similar to described in Ref. 30 for 4–dimethylamino pyridine and in Ref. 31 for imidazole. Due to this degradation problem, and since it is necessary to be able to obtain the microdomain spacing in the absence of crystallinity, further SAXS experiments were abandoned.

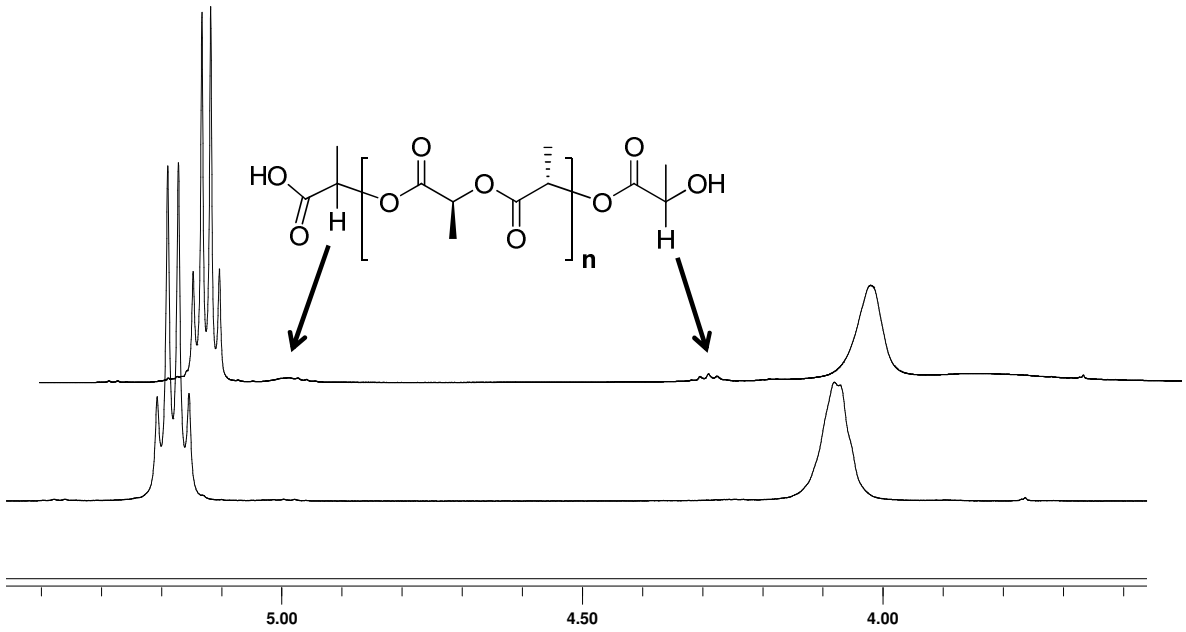

Figure 4.5. Spectrum of freshly synthesized 19k–17k (lower) and of 19k–17k sample after SAXS experiment (upper), indicating PLLA homopolymer appearance. The upper spectrum is shifted for clarity

4.3.3 Isothermal crystallization kinetics of homopolymers and native block copolymers

Isothermal crystallization data were obtained by DSC, as described in Ref. 32. The Avrami equation (1)[33] was applied to these DSC data, obtained from the curves of the PLLA homopolymers and block copolymers:

$$1 - V_c = \exp(-Kt^n). \quad (1)$$

Here, *K* is the crystallization constant and *n* is the Avrami coefficient (also called mechanism constant); *t* is the time to reach the volume crystallinity V_c, which is defined as:

$$V_c = W_c/[W_c + \rho_c/\rho_a(1-W_c)] \quad (2)$$

where ρ_c and ρ_a are 1.40 and 1.25 g/cm^3, respectively,[34] and the crystalline mass fraction $W_c = \Delta H_{c(t)}/\Delta H_{c(total)}$,[32] where $\Delta H_{c(t)}$ is the enthalpy at time *t*, and $\Delta H_{c(total)}$ is the maximum enthalpy value reached at the end of isothermal crystallization. When the Avrami equation is converted into a double logarithmic form,

$$\log[-\ln(1-V_c)] = n \log t + \log K, \quad (3)$$

a linear Avrami plot can be built in coordinates $\log[-\ln(1-V_c)]$ vs. log t, and the overall crystalline growth rate constant *K* and Avrami coefficient *n* can be determined. The main assumption that simplifies the Avrami model is the absence of secondary crystallization, which is the thickening of crystalline lamellar aggregates after they impinge on each other in the late stages of crystallization. The Avrami coefficient *n* is composed of two terms, $n_n + n_d$.[32] The term n_n represents the type of nucleation, instantaneous or sporadic, and can only possess the values of 0 and 1, respectively. The term n_d represents the growth dimension, one–, two– and three–dimensional, thus having the values 1, 2 and 3, respectively. For example, $n = 4$ for sporadically nucleated three–dimensional crystallization.

Another important parameter, the half–crystallization time, $t_{1/2}$, allows direct comparison of the overall crystallization rates of given crystallizations. It can be determined from DSC isothermal crystallization curves as the time when half of the V_c is reached, and can also be predicted from the Avrami equation ($V_c = 0.5$). The results of the analysis of isothermal crystallization data using the Avrami equation are summarized in *Table 4.3*.

Table 4.3. Parameter *n* and crystallization rate constant *K* of homopolymers and diblock copolymers during isothermal crystallization

Sample	T, °C	$t_{1/2}$, min [a]	n [b]	logK [b]	$K\times10^2$, min^{-n} [b]	$K\times10^2$, min^{-2} [c]
PLLA–5k	120	2.8	2.2	–1.2	6.30	8.8
5k–2k	100	3.9	2.4	–1.6	2.50	4.6
5k–4k	100	6.2	2.2	–1.9	1.30	1.8
5k–10k	100	23.8	1.8	–2.7	0.20	0.12
PLLA–13k	100	1.7	2.4	–0.7	20.00	24
	120	3.3	2.3	–1.4	4.00	6.4
13k–5k	100	4.3	3.3	–2.3	0.50	3.8
	120	24.2	3.0	–4.3	0.01	0.12
13k–12k	100	11.8	2.5	–2.9	0.13	0.5
	120	17.6	2.6	–3.5	0.03	0.22
13k–23k	100	15.9	2.2	–2.8	0.16	0.27
	120	43.5	2.1	–3.7	0.02	0.037
PLLA–19k	120	2.3	2.3	–1.0	0.10	13
19k–5k	100	3.1	2.7	–1.5	3.20	7.2
	120	9.0	2.2	–2.3	0.50	0.86
19k–17k	100	6.4	2.3	–2.0	1.00	1.7
	120	17.9	2.0	–2.7	0.20	0.22
19k–35k	100	28.5	1.9	–2.9	0.13	0.085

[a] experimental values. [b] values obtained from linear part of Avrami plot (Eq. 3). [c] values obtained from Eq. 3 at $t_{1/2}$ and n = 2

Usually, Avrami plots exhibit linear behaviour with slight deviation at the early stages of crystallization, related to the stabilization of the equipment and the relatively small heat quantity evolved and, at the end of crystallization, when secondary

crystallization sets in. Only the linear part of the Avrami plots should be used to estimate the crystallization parameters, and the usual range of relative crystallinity used is 3–50%.[32]

The symmetrical shape of the exothermic crystallization peaks in DSC thermograms indicates that no secondary crystallization was present, which, most probably, took place during subsequent heating, as in all the cases the overall measured enthalpy of melting was greater than the overall enthalpy of preceding crystallization.

Typical experimental values of the Avrami coefficient, *n,* for PLLA homopolymers of low molecular weight (4000–24,000 g/mol, PDI 1.10–1.26) reported for 120 °C vary from 2.05 to 2.85.[9,17,19,35] For high molecular weight PLLA (120,000–640,000 g/mol, PDI 1.8–2.0), the Avrami coefficient, reported for the temperature range of 90–140 °C, varies from 2.3 to 3.4.[36–39] The overall crystallization constants for PLLA homopolymers at 120 °C reported in the literature cited above vary from 0.19 to $8 \cdot 10^{-3}$ min^{-n} for low molecular weight PLLA and from 0.02 to 10^{-3} min^{-n} for high molecular weight PLLA with a tendency to decrease with increase in temperature. Generally, the Avrami coefficient tends to increase with molecular weight and the crystallization constant decreases dramatically with molecular weight. The half crystallization time ($t_{1/2}$) decreases with temperature, and its value for 120 °C lies in the range of 2–15 min for low molecular weight PLLA (see above).

In our series, the crystallization constant varies slightly with molecular weight (at 120 °C), but, unfortunately, due to instrumental limitations (inability to reach the necessary cooling rate during quenching, thus the crystallization starts before the instrument stabilizes), we were unable to obtain isothermal crystallization data at 100 °C for all three

PLLA macroinitiators. However, $PLLA_{13k}$ shows only a slight increase of K with decrease in temperature from 120 to 100 °C.

Comparison of the kinetics data for the diblock copolymers with those for the PLLA homopolymers reveals that the crystallization constant decreases with the addition of the PDMAEMA block, although its value does not change much with the size of the PDMAEMA block (*Table 4.3*). A similar trend was observed with PLLA–PCL[35] and PLLA–PEO block copolymers.[17] Surprisingly, the crystallization constant for the $PLLA_{13k}$ block is lower than those for the $PLLA_{5k}$ and $PLLA_{19k}$ blocks. Moreover, isothermal spherulite growth rate studies (see next section) show the same trend, indicating that such a drop in the value of the crystallization constant is most probably related to the samples themselves rather than to experimental uncertainty. From the characterization data given in Chapter 2, one may speculate that the reason for this is relatively high polydispersity of $PLLA_{13k}$ compared with the other two macroinitiators (a similar effect of increased polydispersity on the crystallization kinetics was shown for PEO–PDMS block copolymers.[40]

The significant increase in the half–crystallization time with the length of the PDMAEMA block indicates a retardation effect of the PDMAEMA block on the overall crystallization rate of PLLA. Moreover, the decrease of the Avrami coefficient as the length of the PDMAEMA block increases indicates that it also affects the dimensionality of the growing crystalline aggregates, as will be shown by polarized optical microscopy images in the next section. A similar decrease in the Avrami coefficient was observed in the series of

weakly segregated PLLA–PCL block copolymers,[35] indicating that PCL (and, in our case, PDMAEMA) may create a soft confinement environment for PLLA crystallization.

4.3.4 Isothermal crystallite growth rate and morphology of homopolymers and block copolymers

As observed by polarized optical microscopy, crystallization of the PLLA homopolymer films resulted in the formation of typical spherulitic morphology with the characteristic well–defined maltese–cross extinction pattern, as depicted in *Figure 4.6*. Two main tendencies can be traced within the present series. Generally, the radius of the spherulites decreases with crystallization temperature as the degree of supercooling increases and thus nucleation density increases, leading to earlier impingement of spherulites. On the other hand, at the same crystallization temperature (say 100 °C), the size of the spherulites becomes smaller as the molecular weight of PLLA increases because the melting temperatures become higher (*Chapter 2*) and, therefore, the degree of supercooling increases for the higher molecular weight PLLA (13,000 and 19,000 g/mol), thus leading to smaller spherulites.

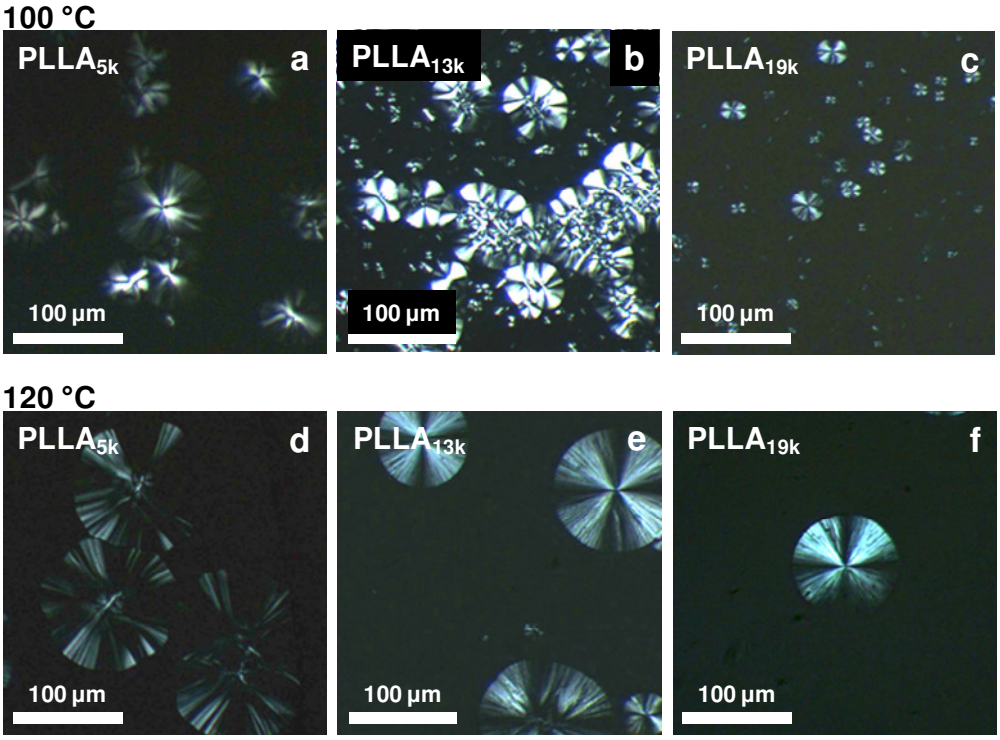

Figure 4.6. The morphology of the spherulites obtained in the films of the PLLA homopolymers: a–c) after 1 min, d), e) and f) after 1, 3 and 4 min, respectively

The growth rate of the spherulites was determined from the linear increase in spherulite radii with time during isothermal crystallization, determined from micrographs taken at suitable periods of time, and are given in *Table 4.4*. The spherulite growth rate *G* of the PLLA homopolymers is well documented in the literature. Generally, it decreases with increase in molecular weight, and for a particular molecular weight, its value changes in respect to the expected bell–shape curve with the maximum at 110–120 °C. For PLLA molecular weight of 5000, 10,000 and 20,000 g/mol, the reported values of *G* at 120 °C are 42, 38 and 12 µm/min, respectively.[41,42] For higher molecular weight PLLA (50,000–200,000 g/mol) the *G* value is in the range of 7–3 µm/min, respectively.[41,43]

Generally, the presence of the second block retards the crystallization rate of the semi–crystalline block in block copolymers.[44] In the series of PLLA block copolymers with PEO[42] and PCL[45] (weakly interacting with PLLA), spherulite growth rate decreases with the increase in the content of the second block, and the maximum of the bell–shape curve shifts to lower temperature due to the block miscibility and thus increased effective crystallization window.

In our case, isothermal spherulite growth rate was found to decrease as the PLLA molecular weight increases (at 100 and 120 °C), which is in accordance with the known dependence of the growth rate on the degree of supercooling (compare $PLLA_{5k}$ T_m with the other two in *Table 4.4*). The block copolymer films exhibit a richer morphology compared to that of the PLLA homopolymers. As shown in *Chapter 2*, the PDMAEMA block retards crystallization, decreasing the crystallization rate, indicated by the absence of the cold crystallization in the DSC cooling scans. Although the Avrami fits did not indicate a substantial decrease in the value of the crystallization rate constant of PLLA with the addition of PDMAEMA (*Table 4.3*), the crystallite (spherulite or axialite) growth rate gradually decreases with increase in PDMAEMA content, with the most pronounced effect of the PDMAEMA block on the crystallite growth rate of the PLLA block (compared to PLLA homopolymer) observed in the $PLLA_{5k}$ series (*Table 4.4*).

Table 4.4. Isothermal spherulite (or axialite) growth rate of the homopolymers and block copolymers

Sample	PLLA T_m, °C	% PLLA	Cryst. Temp., °C	G, μm/min [a]
$PLLA_{5k}$	154	100	100 120	57 62
5k–2k	148	71	100 120	2.5 5.3
5k–4k	149	56	100 120	1.9 2.7
5k–10k	146	33	100 120	0.13 0.18
$PLLA_{13k}$	168	100	100 120	11 16
13k–5k	168	72	100 120	1.6 4.0
13k–12k	167	52	100 120	1.2 2.9
13k–23k	165	36	100 120	0.08 0.42
$PLLA_{19k}$	172	100	100 120 150	9 13 6
19k–5k	169	79	100 120 150	2.3 4.5 2.1
19k–17k	169	53	100 120 150	1.6 3.3 1.4
19k–35k	169	35	100 120	0.05 0.25

[a] experimental uncertainty is estimated at ±10%

The Avrami calculations indicate that samples 5k–2k, 13k–5k and 19k–5k (PLLA: PDMAEMA block molar ratio ca. 4:1), given the relatively high degree of supercooling (at 100 °C), crystallize in instantaneously nucleated spherulites (*Figure 4.7*, upper set). When the crystallization temperature is raised to 120 °C, the morphology of the crystalline aggregates in the 5k–2k films becomes less ordered (axialitic growth[45]). Interestingly, 13k–5k and 19k–5k exhibit a well-defined banded spherulitic morphology (*Figure 4.7*, lower set). Similar behaviour of the PLLA block was observed in a $PLLA_{15k}$–PEO_{5k} block copolymer: at 100 °C, only regular spherulites formed, whereas at 120 °C, the formation of banded spherulites was observed.[17]

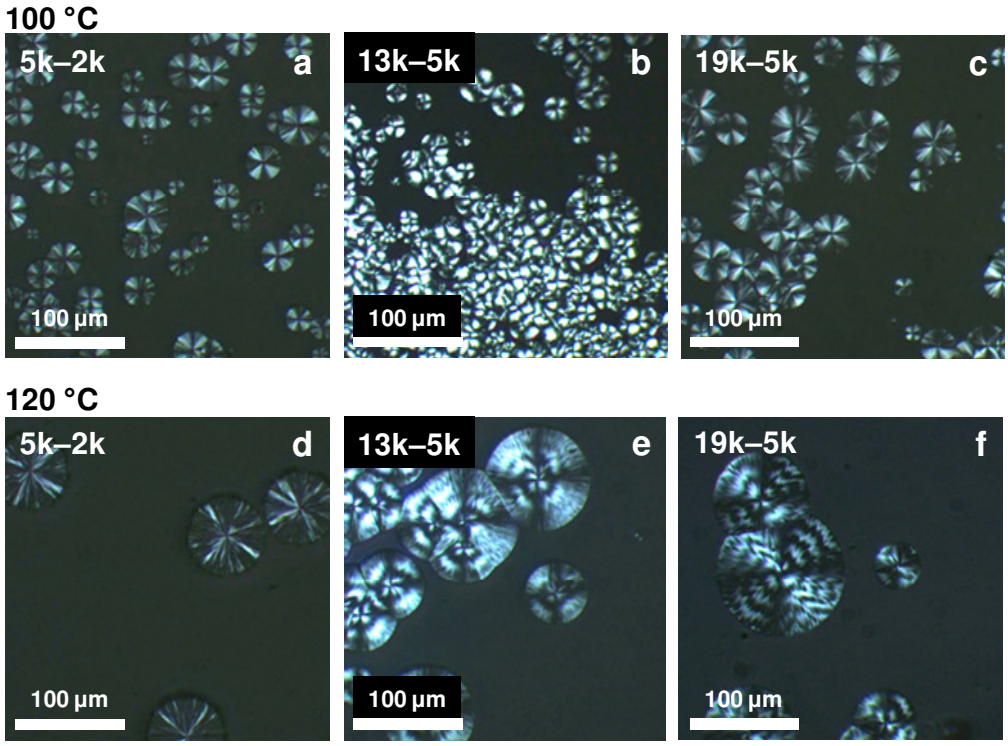

Figure 4.7. The morphology of the spherulites obtained in the films of the block copolymers indicated. Crystallization times for a–f are 8, 8, 9, 6, 11, 12 min, respectively

For PLLA:PDMAEMA block molar ratios of ca. 2:1, miscible 5k–4k crystallizes in axialitic morphology at both temperatures (*Figure 4.8*). Similarly, Castillo *et al*. showed the formation of axialites in miscible $PLLA_{2.2k}$–PCL_{22k}, but, if the block ratio was close to 1, normal spherulites were formed.[45]

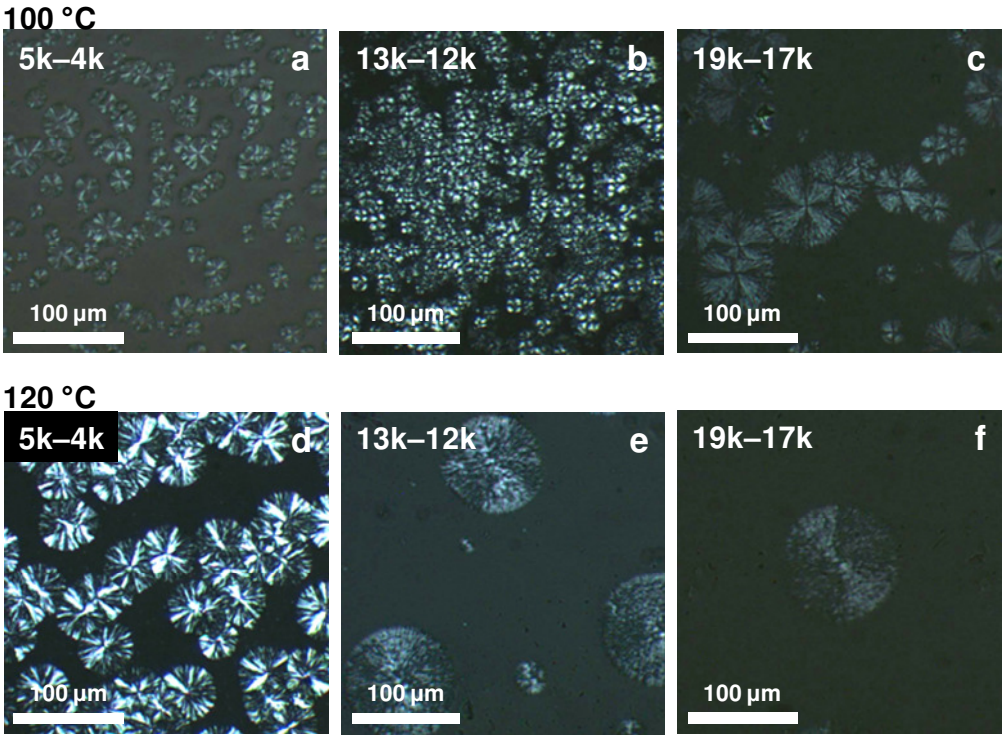

Figure 4.8. The morphology of the spherulites obtained in the films of the block copolymers indicated. Crystallization times for a–f are 8, 17, 25, 10, 17, 15 min, respectively

Immiscible samples, 13k–12k and 19k–17k (*Chapter 2*), crystallize in spherulite–like superstructural morphology at 100 and 120 °C (*Figure 4.8*). The morphology of the obtained crystalline aggregates indicates that, even though crystallization drives the morphological transformation, as the crystalline lamellae grow, noncrystallizable

PDMAEMA remains between the crystalline stems, and thus normal spherulites do not form. Related morphology was reported for the poly(p–dioxanone) (PPDX) block in a phase–separated PPDX–PCL block copolymer crystallized at a temperature where PCL is in the melt [**46**,**47**].

As the size of the PDMAEMA block increases, crystalline lamellar aggregates formed by the PLLA block in copolymers with PLLA:PDMAEMA block molar ratio of about 1:1 become increasingly separated by amorphous regions, composed of amorphous PDMAEMA and the amorphous part of PLLA (*Figure 4.9*).

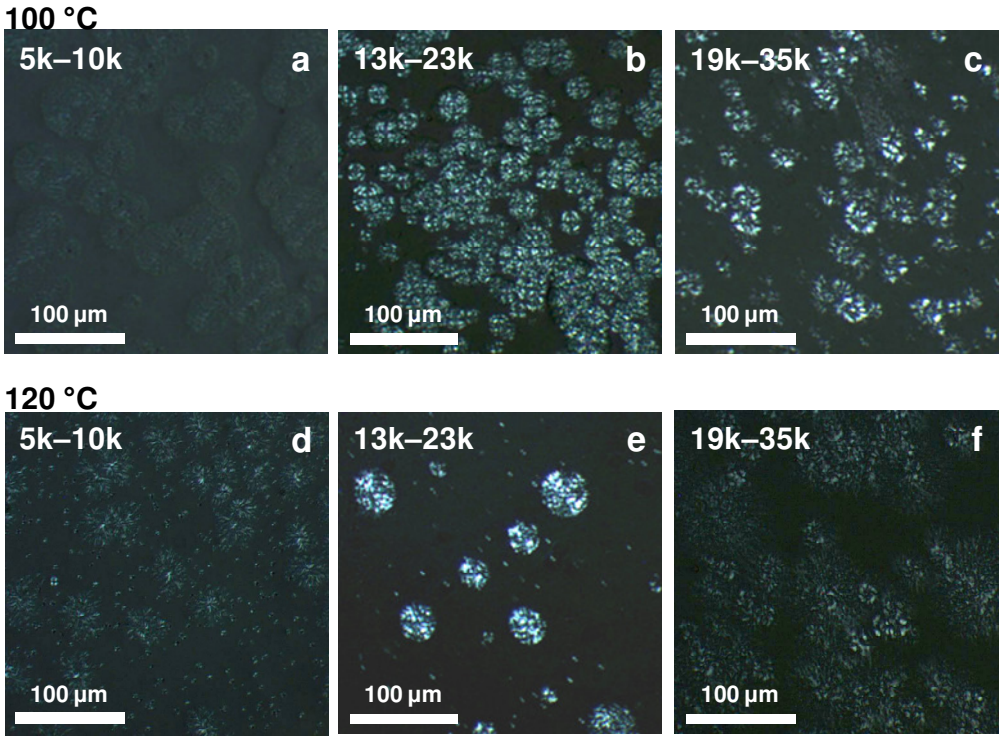

Figure 4.9. The morphology of the spherulites obtained in the films of the block copolymers indicated. Crystallization times for a–f are 3, 3, 6, 2, 1, 3 h, respectively

As mentioned above, soft confinement in lamellar (or cylindrical) morphology might cause a PLLA crystalline lamellae (or cylinder) to grow linearly in two dimensions rather than in three dimensions, finally forming circular crystalline lamellar aggregates. Interestingly, sample 13k–23k exhibits banded spherulite–like morphology (with the noticeable maltese cross texture) at both temperatures, unlike the other two block copolymers.

Correlation analysis of isothermal crystallization in the bulk and in thick films reveals an excellent fit of the Avrami equation to the experimental data, i.e. between the crystallization constant and the spherulite (axialite) growth rate. This is shown by the linear correlation between the growth rate and the crystallization constant for the 13k and 19k series at two crystallization temperatures in *Figure 4.10*. A similar linear correlation at 100 °C for the 5k series, as well as the generalized linear trend showing a decrease in both the crystallization constant and the growth rate as a function of the PDMAEMA block size, are presented in *Figure 4.11*.

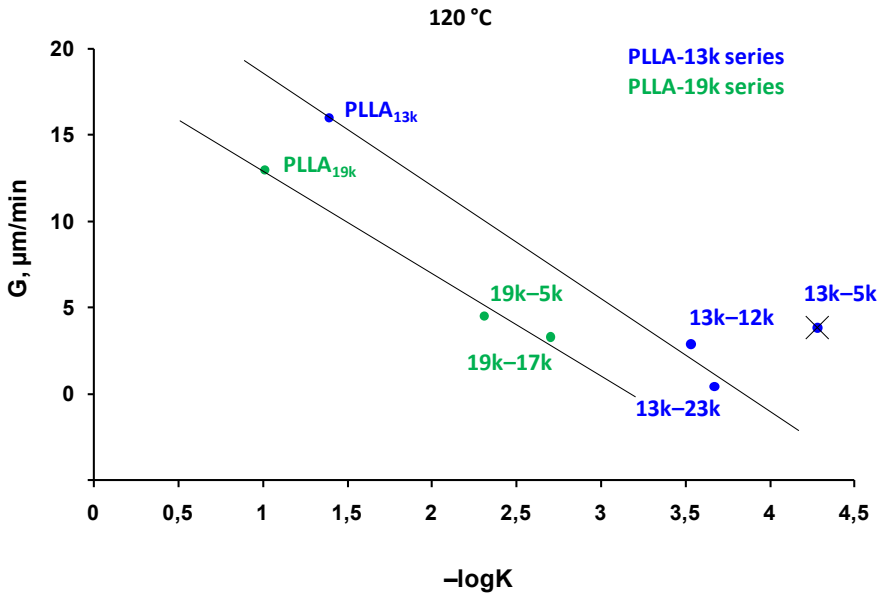

Figure 4.10. Correlation at 120 °C between the crystallization constant and the spherulitic (axialitic) growth rate values in block copolymer series indicated (note that the point corresponding to 13k–5k is not included in the trendline)

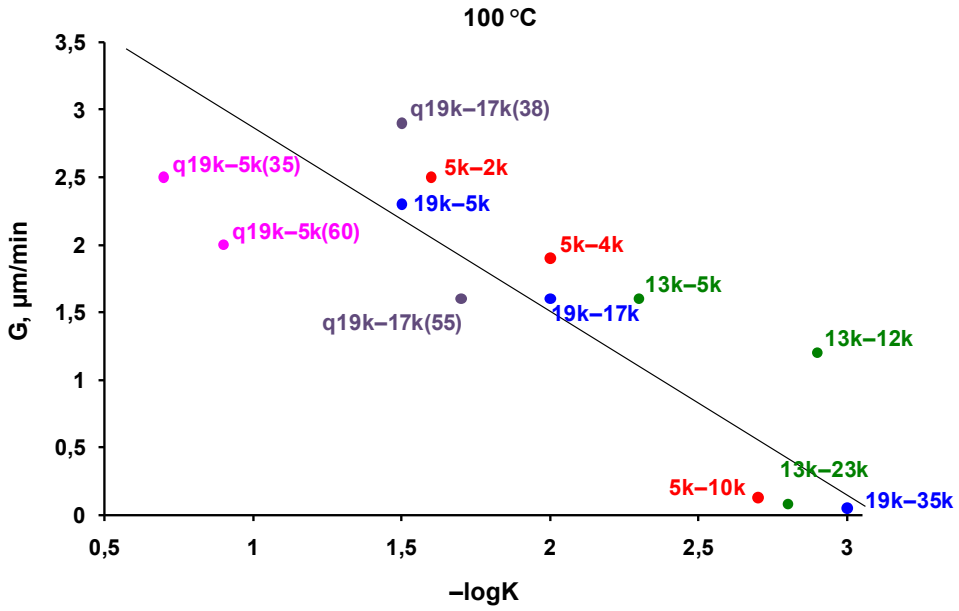

Figure 4.11. Correlation at 100 °C between the crystallization constant and the spherulitic (axialitic) growth rate values and the general dependence of these values on the PDMAEMA block size (and quaternization degree) in all three block copolymer series

4.3.5 Isothermal crystallization kinetics and morphology of partially quaternized block copolymers

When quaternized by methyl iodide, qPDMAEMA becomes a rigid block, and for the reasons mentioned in *Section 4.3.1*, only partially quaternized samples q19k–5k, q19k–17k and q5k–4k were further investigated. Compounds q19k–5k and q5k–4k are apparently partially miscible, so one cannot say about crystallization environment, though can expect templated crystallization at higher degree of quaternization. Lamellae–forming 19k–17k, when quaternized, is expected to have an apparent T_g of ca. 140 °C for qPDMAEMA, thus most definitely creating confinement crystallization environment for the PLLA block, remaining glassy in the main region of the present crystallization studies. At the temperatures above 140 °C, qPDMAEMA block will soften and the strength of segregation will further determine if the crystallization proceeds in soft confinement (strong segregation), or overwhelm microphase separation (weak segregation).[48]

The results of the analysis of isothermal crystallization DSC data at 100 and 120 °C using the Avrami equation are summarized in *Table 4.5*. It should be pointed out that, at the time of isothermal crystallization at high temperature (150 °C), only ca. 25% of the final crystallinity was reached, and the rest was reached during cold–crystallization during the subsequent heating scan. Thus, no exothermic response was recognized by the DSC instrument during the time of crystallization, limited to 2 h to avoid thermal degradation of the sample.

Table 4.5. Parameter *n* and crystallization rate constant *K* of partially quaternized block copolymers during isothermal crystallization

Sample (% quat.)	T, °C	$t_{1/2}$, min [a]	n [b]	logK [b]	$K\times10^2$, min^{-n} [b]	$K\times10^2$, min^{-2} [c]
19k–5k	100	3.1	2.7	–1.5	3.20	7.20
(0)	120	9.0	2.2	–2.3	0.50	0.86
19k–6.6k	100	2.1	2.2	–0.9	13.00	16.00
(35)	120	5.5	2.2	–1.8	1.60	2.30
19k–7.7k	100	1.7	2.2	–0.7	20.00	24.00
(60)	120	3.8	2.0	–1.3	5.00	4.80
19k–8.6k	100	2.6	2.4	–1.2	6.30	1.00
(80)	120	5.0	2.1	–1.7	2.00	2.80
19k–17k	100	6.4	2.3	–2.0	1.00	1.70
(0)	120	17.9	2.0	–2.7	0.20	0.22
19k–23k	100	4.3	2.4	–1.7	2.00	3.70
(38)	120	12.5	2.6	–3.1	0.08	0.44
19k–25k	100	6.8	1.6	–1.5	3.20	1.50
(55)	120	19.7	2.7	–3.7	0.02	0.18

[a] experimental values. [b] values obtained from linear part of Avrami plot (Eq. 3). [c] values obtained from Eq. 3 at $t_{1/2}$ and n = 2

All of the Avrami plots exhibit linear behaviour in a wide range of relative crystallinities (related to the maximum crystallinity reached during isothermal crystallization), indicating that a single mechanism governs the crystallization process at each given temperature.[39] The absence of secondary crystallization is indicated by the symmetric shape of the exothermic crystallization peaks in the DSC thermograms. The crystallization constants of the PLLA block in the partially quaternized samples remain almost the same or decrease slightly with temperature, in accordance with the well

documented crystallization constant change with temperature.[17,19] Interestingly, their values are slightly higher than those of the parent block copolymers at 100 °C.

Comparison of the half–crystallization times in the partially quaternized samples and those in the parent block copolymers indicates that the crystallization of the PLLA block slightly accelerates when the PDMAEMA block is partially quaternized in q19k–5k samples (*Table 4.5*). Since the qPDMAEMA block (due to its size) does not create any confinement to the PLLA crystallization, this might be related to the nucleation effect of the relatively small hard qPDMAEMA domains on the $PLLA_{19k}$ block, as was observed for crystallization of PLLA in a blend containing up to 20 wt% poly(vinyl alcohol), is the latter being hard at the crystallization temperature of PLLA.[49] However, stronger segregation in q19k–17k, along with presumably lamellar morphology, makes the PLLA block in these samples crystallize in a harder confinement environment as the degree of quaternization increases, and this is known to decrease the crystallization rate.[50,51]

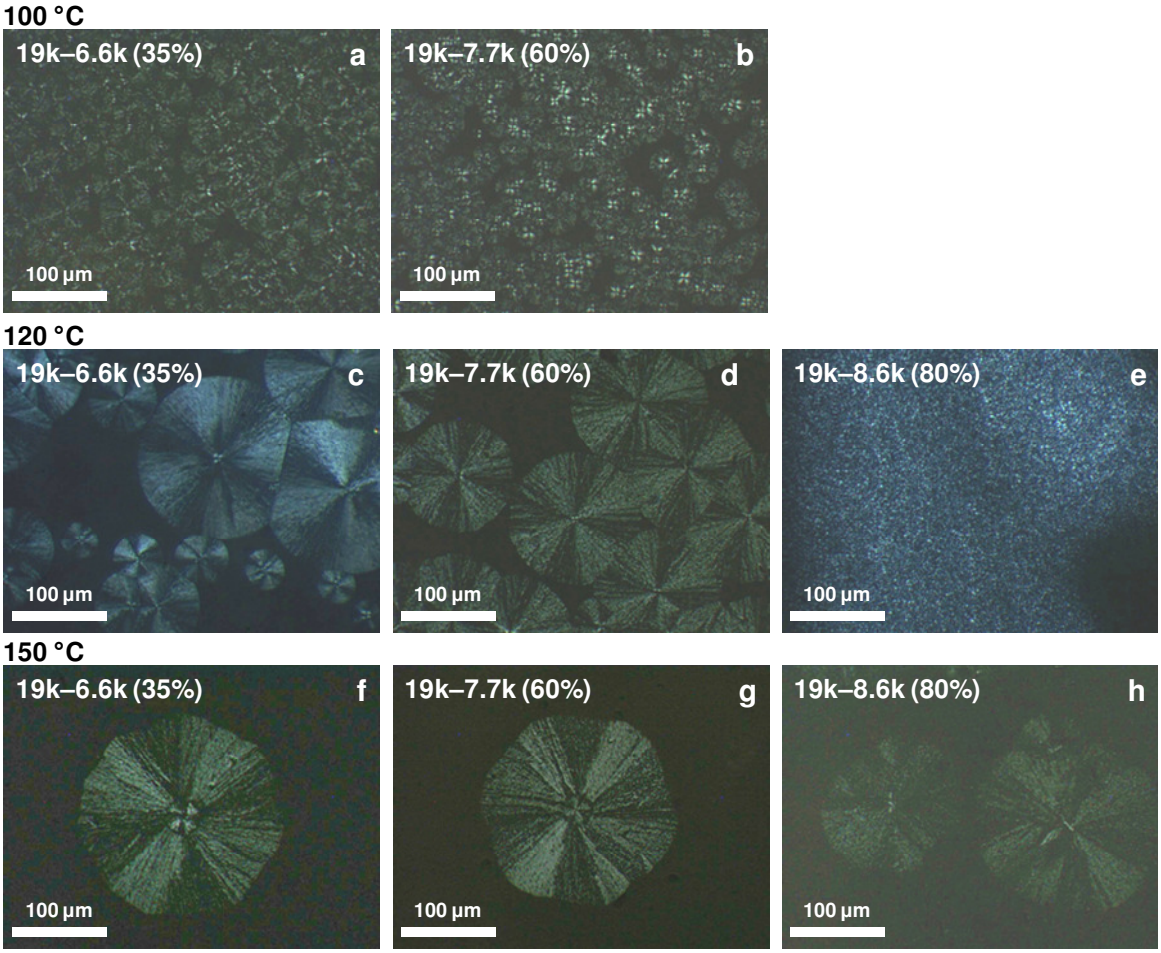

Figure 4.12. The morphology of the spherulites obtained in the films of quaternized block copolymers indicated. Crystallization times for a–h are 15, 7, 18, 15, 1, 62, 68, 41 min, respectively

The values of Avrami coefficient for the q19k–5k samples are ca. 2.2 (±0.2), indicative of two–dimensional instantaneously nucleated crystallization. Samples q19k–5k(35) and q19k–5k(60) crystallize in spherulite–like morphology at all three experimental temperatures. However, q19k–5k(80) forms no superstructures at 100 and 120 °C, but crystallization of this sample at 150 °C ($T_{c(PLLA)} > T_{g(qPDMAEMA)}$) leads to the formation of spherulite–like crystalline superstructures (*Figure 4.12*). This is, most probably, due to the

restricted crystallization of the PLLA block templated by strongly segregated hard qPDMAEMA domains at 120 °C, but at 150 °C they soften, eliminating constraints for the growing crystalline lamellae. As for the q19–17k samples, spherulitic–like morphology with a noticeable maltese cross was observed at 100 and 120 °C (*Figure 4.13*). Such a discrepancy between the observed morphology and the Avrami theory is known and reported for many polymers,[52] and it is advisable that predictions by Avrami theory are independently confirmed by POM.[9,50]

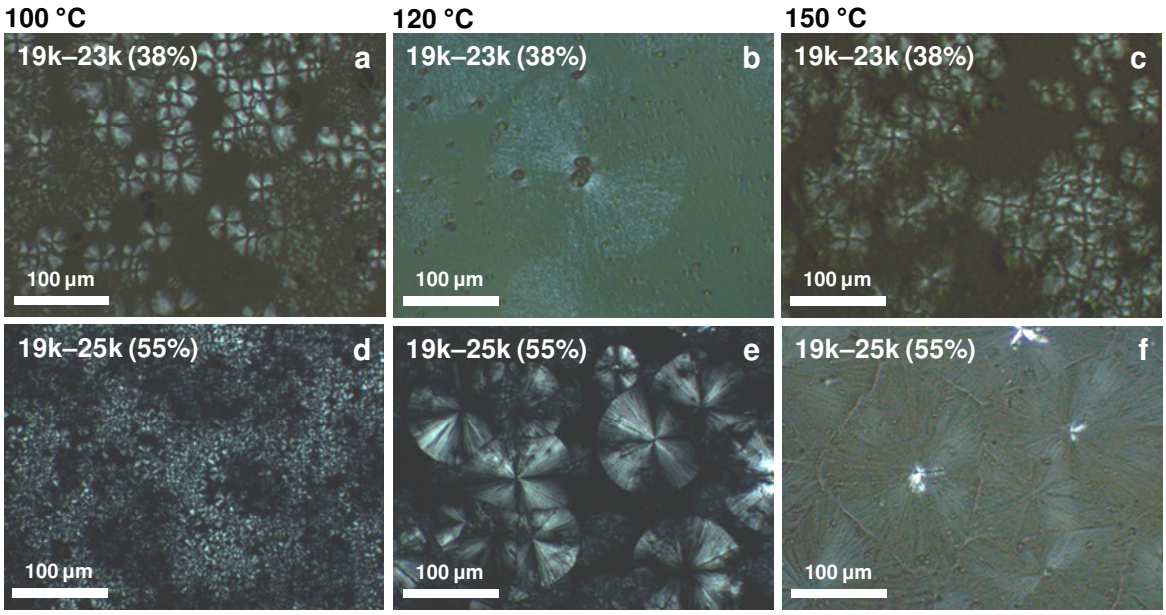

Figure 4.13. The morphology of the spherulites obtained in the films of quaternized block copolymers indicated. Crystallization times for a–f are 9, 40, 15, 3, 16, 35 min, respectively

The isothermal spherulitic (or axialitic) growth rates determined by polarizing optical microscopy for the partially quaternized samples are summarized in *Table 4.6*. In comparison with the spherulite growth rate determined for sample 19k–5k, quaternization

and the degree of quaternization of the PDMAEMA block do not significantly influence the growth rate of the PLLA block, and, except for the sample with the highest degree of quaternization (due to lack of data for comparison), the q19–5k samples exhibit the expected bell–shape dependence of the spherulite (axialite) growth rate on temperature. As mentioned above, a hard qPDMAEMA block may facilitate nucleation of PLLA, which would compensate a stronger retardation effect of the qPDMAEMA block on crystallization, thus no change is observed in spherulite growth rate for q19k–5k compared with 19k–5k. The same explanation can apply to q19k–17k: at lower temperature, rigid qPDMAEMA confines crystallization and simultaneously facilitates nucleation; at higher temperature, qPDMAEMA softens, thus decreasing its nucleation effect and simultaneously eliminating confinement. This possibility is supported by the observed increase of the Avrami coefficient with temperature, indicating a gradual change to sporadic nucleation. A similar effect of temperature on the values of the Avrami coefficient was described for the crystallization of a PLLA–PS block copolymer at temperatures close to the T_g of the PS block.[12]

Table 4.6. Isothermal spherulite (or axialite) growth rate of the partially quaternized block copolymers

Sample (% quat.)	PLLA T_m, °C	% PLLA	Cryst. temp., °C	G, μm/min [a]
19k–5k (0)	169	79	100 120 150	2.3 4.5 2.1
19k–6.6k (35)	166	74	100 120 150	2.0 4.7 1.7
19k–7.7k (60)	166	71	100 120 150	2.5 4.7 1.8
19k–8.6k (80)	164	69	100 120 150	n/d [b] – [c] 3.0 [d]
19k–17k (0)	169	53	100 120 150	1.6 3.3 1.4
19k–23k (38)	164	45	100 120 150	2.9 2.8 2.1
19k–25k (55)	163	43	100 120 150	3.9 [d] 2.8 3.7 [d]

[a] experimental uncertainty is estimated at ±10%. [b] experiment at this temperature was not done, because no spherulites were expected. [c] no spherulites were observed. [d] experimental uncertainty is estimated at ±20%.

An additional observation was made using a sensitive tint plate (λ–filter) in POM, notably that all of the spherulites, spherulite–like aggregates and axialites in all nonquaternized and quaternized block copolymers (as well as in PLLA homopolymers) show negative birefringence at 100 and 120 °C, as observed by the characteristic coloration

of the maltese cross when a λ–filter is used: a yellow coloration appears in quadrants 1 and 3, whereas quadrants 2 and 4 are blue (clockwise order). This means that the crystalline lamellae in the crystalline superstructure tend to be oriented radially,[53,54] and the formation of negative spherulites is commonly related to the presence of predominantly polarizable groups in PLLA backbone.[55] Negative spherulites were also reported for other PLLA block copolymers like PLLA–b–PCL (T_c up to 140 °C),[35,45] PLLA–b–PS (T_c up to 130 °C)[14] and PLLA–b–PEO (T_c up to 140 °C).[42]

In contrast, we observed the formation of spherulite–like aggregates with positive birefringence at 150 °C in quaternized samples (*Figure 4.14*), meaning that most of the crystalline lamellae flip their orientation in the crystalline superstructure, becoming oriented tangentially. Based on other reports on positive spherulites observed in semi–crystalline systems, several possible explanations can be considered for this phenomenon. First, the change in the lamellae orientation might be related to the change in the crystallization regime that was proposed as a factor leading to the change in sign of spherulites in poly(4–hydroxybutyric acid–co–glycolic acid)[56] and PEO.[57] For PLLA, a transition from regime III to regime II and from regime II to regime I occurs at ca. 120 and ca. 145 °C, respectively.[20,58] Moreover, the transition from regime II to regime I (147 °C) induces a change in morphology of the crystalline aggregates, whereas the transition between regimes II and III does not lead to a noticeable morphology change.[20] Second, the change in the sign of the crystalline superstructures was not observed in nonquaternized block copolymers at 150 °C, so one may consider the presence of quaternized amino moieties as a factor influencing the orientation of lamellae in the crystalline superstructure.

Despite the number of other reports describing the formation of positive spherulites in semi–crystalline systems in different conditions,[59–61] no mechanism that can explain lamellae flip in spherulites has been proposed yet. We presume that the presence of the charged qPDMAEMA moieties and regime I thermal conditions cooperatively influence the preferable crystalline lamellae orientation of PLLA.

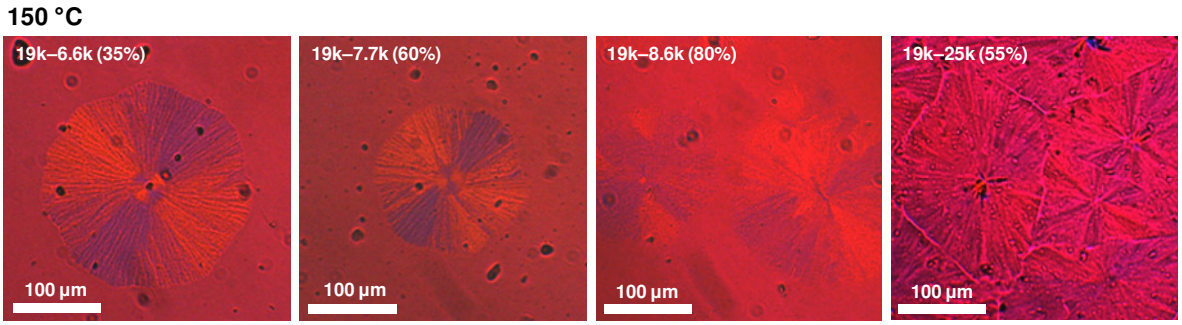

Figure 4.14. Positive spherulites, observed at 150 °C, in quaternized block copolymers. The central part with negative birefringence was formed during seeding at lower temperature

4.4. Conclusions

A detailed investigation of isothermal crystallization kinetics and morphology in the series of PLLA–PDMAEMA linear block copolymers with a wide range of molecular weights and block ratios was carried out by DSC in bulk and by POM in thick films. The introduction of the PDMAEMA block leads to a decrease in the overall crystallization rate constant, obtained by application of the Avrami equation to isothermal DSC data. The relatively low Avrami coefficients for the block copolymers, along with the decrease in their values as the weight fraction of PDMAEMA increases, indicates a tendency of the PLLA block to form two–dimensional rather than three–dimensional crystalline lamellar

aggregates in the bulk. Crystallization in thick films of parent block copolymers revealed that the most pronounced retardation effect of the PDMAEMA block on the spherulite growth rate (compared to PLLA homopolymer) is observed in the $PLLA_{5k}$ series, most probably related to block miscibility. A correlation analysis of the spherulitic (axialitic) growth rate dependence on the crystallization constant revealed a linear relationship, indicating an excellent fit of the Avrami theory to the experimental data. Also, a general linear decrease of both the crystallization constant and the growth rate as the size of the PDMAEMA block increases is established. SAXS data are consistent with a lamellar morphology for the sample with similar weight fractions of the blocks; however, significant thermal degradation, arising from PDMAEMA–induced chain scission of PLLA, as confirmed by NMR, prevented more detailed studies. Partial quaternization of the PDMAEMA block in miscible 19k–5k and 5k–4k does not lead to significant phase separation, and these quaternized block copolymers remained partially miscible. Interestingly, quaternization hardly affects the overall crystallization rate constant and the spherulite growth rate of q19k–5k and q19k–17k compared with parent block copolymers; however, it drastically affects the crystallization behaviour of q5k–4k samples, of which only q5k–4k(30) was able to crystallize. As the degree of quaternization increases, rigid qPDMAEMA domains in q19k–5k hinders the formation of spherulite–like crystalline aggregates at lower temperatures (≤120 °C), but they form readily at 150 °C, which is above the qPDMAEMA T_g. In contrast, q19k–17k [except for q19k–17k(80)] forms spherulites (axialites) at all three temperatures tested, as the longer nonquaternized PDMAEMA block can maintain the PLLA chain mobility necessary for the spherulites

(axialites) to form. Moreover, the change in the sign, from negative to positive, of the crystallites formed by q19k–5k and q19k–17k samples at 150 °C, which was observed neither at lower temperatures nor in native block copolymers at 150 °C, indicates that the change in the crystalline lamellae aggregate orientation might be the result of a cooperative effect of the higher temperature (change in crystallization regime for PLLA) and the presence of ionic qPDMAEMA moieties.

References to Chapter 4

1. Khandpur, A.; Förster, S.; Bates, F.; Hamley, I.; Ryan, A.; Bras, W.; Almdal, K.; Mortensen, K. *Macromolecules* **1995,** 28, 8796–8806.

2. Hamley, I. W. *Adv. Polym. Sci.* **1999**, 148, 113–137.

3. Zhu, L.; Cheng, S. Z. D.; Calhoun, B. H.; Ge, Q.; Quirk, R. P.; Thomas, E. L.; Hsiao, B. S.; Yeh, F.–J.; Lotz, B. *J. Am. Chem. Soc.* **2000**, 122, 5957–5967.

4. Quiram, D. J.; Register, R. A.; Marchand, G. R.; Adamson, D. H. *Macromolecules* **1998**, 31, 4891–4898.

5. Ryan, A. J.; Hamley, I. W.; Bras, W.; Bates, F. S. *Macromolecules* **1995**, 28, 3860–3868.

6. Loo, Y.–L.; Register, R. A.; Ryan, A. J. *Phys. Rev. Lett.* **2000**, *84*, 4120–4123.

7. Quiram, D. J.; Register, R. A.; Marchand, G. R. *Macromolecules* **1997**, 30, 4551–4558.

8. Loo, Y.–L.; Register, R. A.; Ryan, A. J. *Macromolecules* **2002,** 35, 2365–2374.

9. Müller, A. J.; Castillo, R. V.; Hillmyer, M. *Macromol. Symp*. **2006**, 242, 174–181.

10. Castillo, R. V.; Müller, A. J.; Lin, M.–C.; Chen, H.–L.; Jeng, U–S.; Hillmyer, M. A. *Macromolecules* **2008**, 41, 6154–6164.

11. Lin, M.–C.; Wang, Y.–C.; Chen, J.–H.; Chen, H.–L.; Müller, A. J.; Su, C.–J.; Jeng, U–S. *Macromolecules* **2011**, 44, 6875–6884.

12. Ho, R.–M.; Lin, F.–H.; Tsai, C.–C.; Lin, C.–C.; Ko, B.–T.; Hsiao, B. S.; Sics, I. *Macromolecules* **2004**, 37, 5985–5994.

13. Fu, J.; Luan, B.; Pan, C.; Li, B.; Han, Y. *Macromolecules* **2005**, 38, 5118–5127.

14. Chao, C.–C.; Chen, C.–K.; Chiang, Y.–W.; Ho, R.–M. *Macromolecules* **2008**, 41, 3949–3956.

15. Castillo, R. V.; Müller, A. J. *Prog. Polym. Sci*. **2009**, 34, 516–560.

16. Kim, J. K.; Park, D.–J.; Lee, M.–S.; Ihn, K. J. *Polymer* **2001**, 42, 7429–7441.

17. Yang, J.; Zhao, T.; Liu, L.; Zhou, Y.; Li, G.; Zhou, E.; Chen, X. *Polymer J*. **2006**, 38, 1251–1257.

18. Kim, K.–S.; Chung, S.; Chin, I.–J.; Kim, M.–N.; Yoon, J.–S.; *J. Appl. Polym. Sci.* **1999**, 72, 341–348.

19. Michell, R. M.; Müller, A. J.; Spasova, M.; Dubois, P.; Burattini, S.; Greenland, B. W.; Hamley, I. W.; Hermida–Merino, D.; Cheval, N.; Fahmi, A. J. Polym. Sci. B: Polym. Phys. **2011**, 49, 1397–1409.

20. Abe, H.; Kikkawa, Y.; Inoue, Y.; Doi, Y. *Biomacromolecules* **2001,** 2, 1007–1014.

21. Performed by Bryan Beckingham and Prof. Richard Register, Department of Chemical and Biological Engineering, Princeton University, Princeton NJ, USA.

22. Register, R. A.; Bell, T. R. *J. Polym. Sci. B: Polym. Phys*. **1992**, 30, 569–575.

23. Huang, T. C.; Toraya, H.; Blanton, T. N.; Wu, Y. *J. Appl. Crystallogr*. **1993**, 26, 180–184.

24. Russell, T. P., in *Handbook on Synchrotron Radiation*, Brown, G. S.; Moncton, D. E. (Eds.); North–Holland, New York, **1991**, 379–469.

25. Lao, L.; Tan, H.; Wang, Y.; Gao, C.; *Colloid Surface B: Biointerfaces* **2008,** 66, 218–225.

26. Slim, C.; Tran, Y.; Chehimi, M. M.; Garraud, N.; Roger, J.–P.; Combellas, C.; Kanoufi, F. *Chem. Mater.* **2008,** *20,* 6677–6685.

27. Yang, J.; Zhao, T.; Cui, J.; Liu, L.; Zhou, Y.; Li, G.; Zhou, E.; Chen, X. *J. Polym. Sci. Part B: Polym. Phys*. **2006**, 44, 3215–3226.

28. Pan, P.; Zhu, B.; Kai, W.; Dong, T.; Inoue, Y. *J. Appl. Polym. Sci*. **2008**, 107, 54–62

29. Espartero, J. L.; Rashkov, I.; Li, S. M.; Manolova, N.; Vert, M. *Macromolecules* **1996,** 29, 3535–3539.

30. Nederberg, F.; Connor, E. F.; Möller, M.; Glauser, T.; Hedrick, J. L. *Angew. Chem. Int. Ed*. **2001**, 40, 2712–2715.

31. Kricheldorf, H. R.; Lomadze, N.; Schwarz, G. *Macromolecules* **2008**, 41, 7812–7816.

32. Lorenzo, A. T.; Arnal, M. L.; Albuerne, J.; Müller, A. J. *Polym. Test* **2007**, 9, 222–231.

33. Gedde, U. W. Polymer Chemistry, *Chapman & Hall*, London, **1985**.

34. Henton, D. E.; Gruber, P.; Lunt, J.; Randall, J. *Polylactic acid technology*, in: Mohanty, A. K. ; Misra, M.; Drzal, L. T. (Eds.), *Natural Fibers, Biopolymers, and Biocomposites*, CRC Press, **2005**, Ch. 16, 527–577.

35. Hamley, I. W.; Parras, P.; Castelletto, V.; Castillo, R. V.; Müller, A. J.; Pollet, E.; Dubois, P.; Martin, C. M. *Macromol. Chem. Phys*. **2006**, 207, 941–953.

36. Tsuji, H.; Takai, H; Saha, S. K. *Polymer* **2006**, 47, 3826–3837.

37. Zhou, W. Y.; Duan, B.; Wang, M.; Cheung, L. W. *Isothermal and Non–isothermal Crystallization Kinetics of Poly(L-Lactide)/Carbonated Hydroxyapatite Nanocomposite Microspheres* in Advances in Diverse Industrial Applications of Nanocomposites (Ed. Reddy, B. S. R.), *InTech*, Rijeka, **2011**.

38. Kolstad, J. J. *J. Appl. Polym. Sci*. **1996**, 62, 1079–1091.

39. Iannace, S.; Nicolasi, L. *J. Appl. Polym. Sci*. **1997**, 64, 911–919.

40. Galin, M.; Mathis, A. *Macromolecules* **1981**, 14, 677–683.

41. Tsuji, H.; Miyase, T.; Tezuka, Y.; Saha, S. K. *Biomacromolecules* **2005**, 6, 244–254.

42. Wu, T.; He, Y.; Fan, Z.; Wei, J.; Li, S. *Polym. Eng. Sci*. **2008**, 48, 425–433.

43. Miyata, T.; Masuko, T. *Polymer* **1998**, 39, 5515–5521.

44. Reiter, G.; Strobl, G. R. *Progress in Understanding of Polymer Crystallization*, Springer, Berlin Heidelberg, **2007**.

45. Castillo, R. V.; Müller, A. J.; Raquez, J.–M.; Dubois, P. *Macromolecules* **2010**, 43, 4149–4160.

46. Albuerne, J.; Marquez, L.; Müller, A. J.; Raquez, J. M.; Degee, Ph.; Dubois, Ph.; Castelletto, V.; Hamley, I.W. *Macromolecules*, **2003**, 36, 1633–1644.

47. Müller, A. J.; Albuerne, J.; Esteves, L. M.; Marquez, L.; Raquez, J. M.; Degee, Ph.; Dubois, Ph.; Collins, S.; Hamley, I.W. *Macromol. Symp*. **2004**, 215, 369–382.

48. Hamley, I. W. Developments in Block Copolymer Science and Technology. John Wiley & Sons, Ltd, Chichester, **2004**.

49. Yeh, J.–T.; Yang, M.–C.; Wu, C.–J.; Wu, X.; Wu, C.–S. *Polym.–Plast. Tech. Eng*. **2008**, 47, 1289–1296.

50. Hamley, I. W.; Fairclough, J. P. A.; Bates, F. S.; Ryan, A. J. *Polymer* **1998**, 39, 1429–1437.

51. Shiomi, T.; Tsukuda, H.; Takeshita, H.; Takenaka, K.; Tezuka, Y. *Polymer* **2001**, 42, 4997–5004.

52. Brandrup, J.; Immergut, E. H.; Grulke, E. A. (Eds), *Polymer Handbook*, 4th ed., *John Wiley and Sons*, New York **1999**.

53. Hamley, I. W.; Castelletto, V.; Castillo, R. V.; Müller, A. J.; Martin, C. M.; Pollet, E.; Dubois, Ph. *Macromolecules* **2005**, 38, 463–472.

54. Stoiber, E.; Morse, S. A. *Crystal Identification with the Polarizing Microscope*, Chapman and Hall, New York, **1994**.

55. Wang, X.; Prud'homme, R. E. *Macromol. Chem. Phys*. **2011**, 212, 691–698.

56. Martinez–Palau, M.; Franco, L.; Puiggali, J.; Ungar, G. *J. Polym. Sci.: Part B: Polym. Phys*. **2007**, 45, 2640–2653.

57. Shi, W.; Yang, J.; Zhang, Y.; Luo, J.; Liang, Y.; Han, C. C. *Macromolecules* **2012**, dx.doi.org/10.1021/ma202046c.

58. Mazzullo, S.; Paganetto, G.; Celli, A. *Progr. Colloid Polym. Sci*. **1992**, 87, 32–34.

59. Wang, C.; Chen, C.–C.; Cheng, Y.–W.; Liao, Y.–P.; Wang, M.–L. *Polymer* **2002**, 43, 5271–5279.

60. Murayama, E. *Polym. Prepr. Japan* **2002**, 51, 460–462.

61. Ishikawa, S.; Kurita, T.; Suzuki, E. *J. Polym. Sci. Part A: General Papers* **1964**, 2**,** 2349–2355.

Appendix to Chapter 4

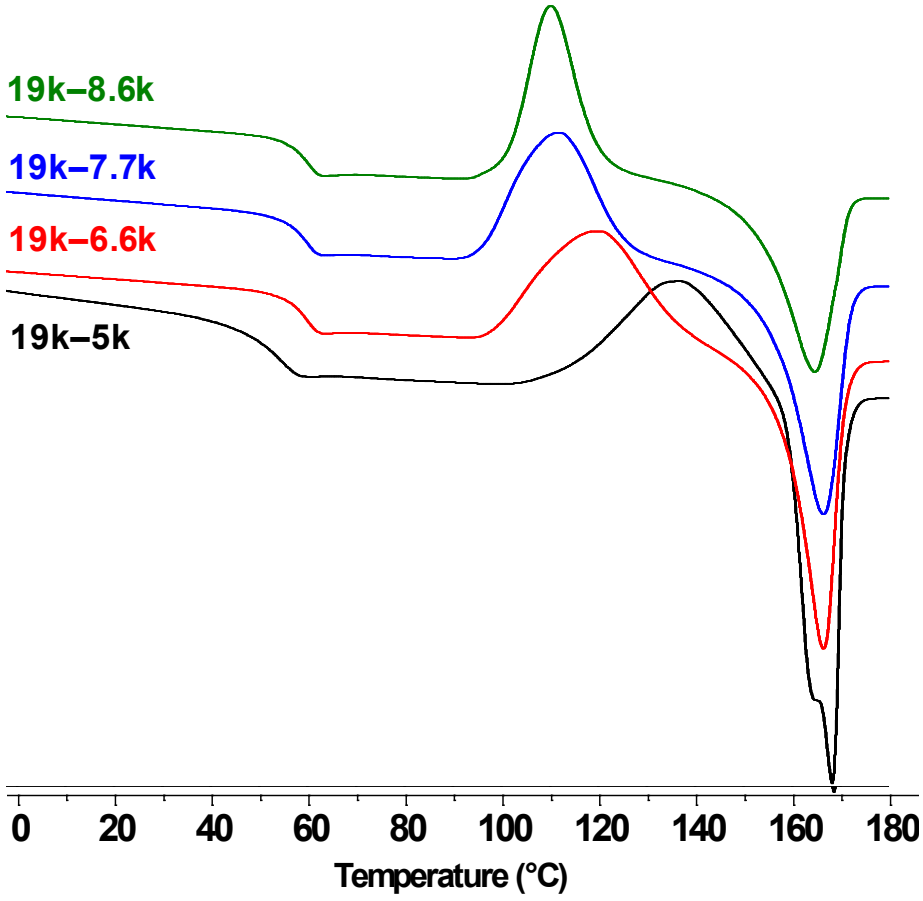

Figure A4.1. Heating scans of the quenched q19k–5k samples at 20 °C/min

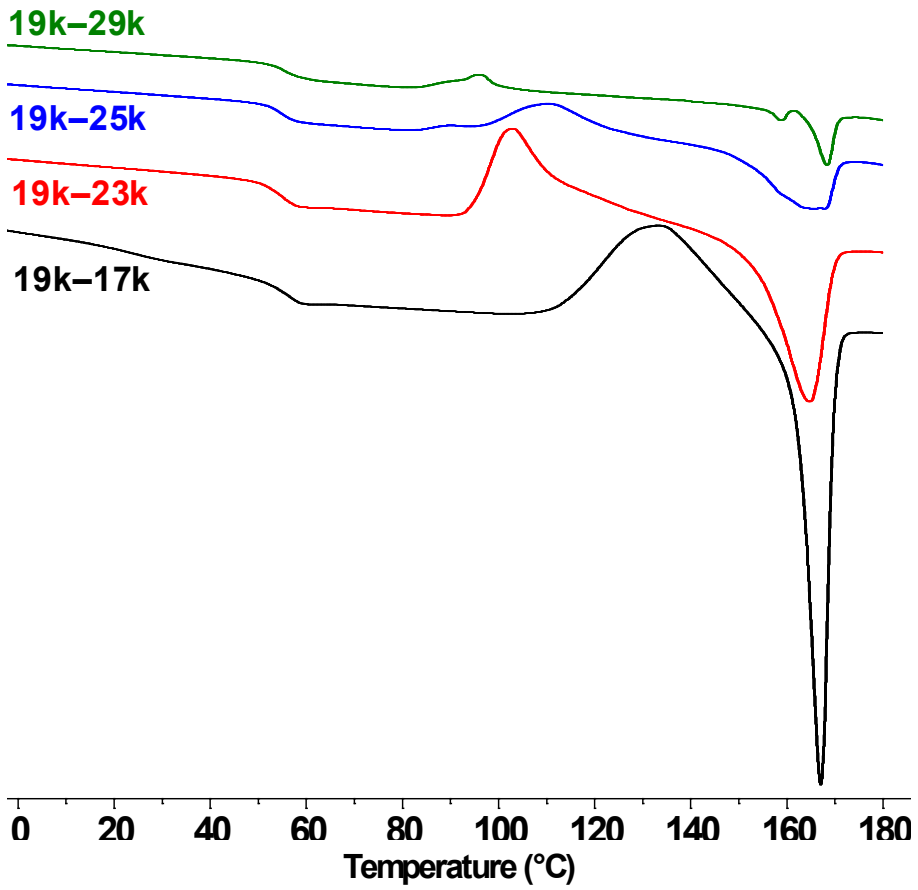

Figure A4.2. Heating scans of the quenched q19k–17k samples at 10 °C/min

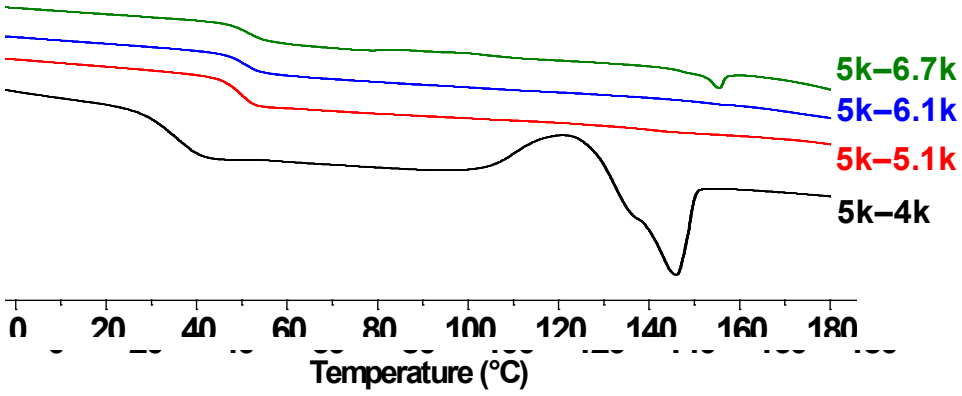

Figure A4.3. Heating scans of the quenched q5k–4k samples at 10 °C/min

19k–35k, 120 °C

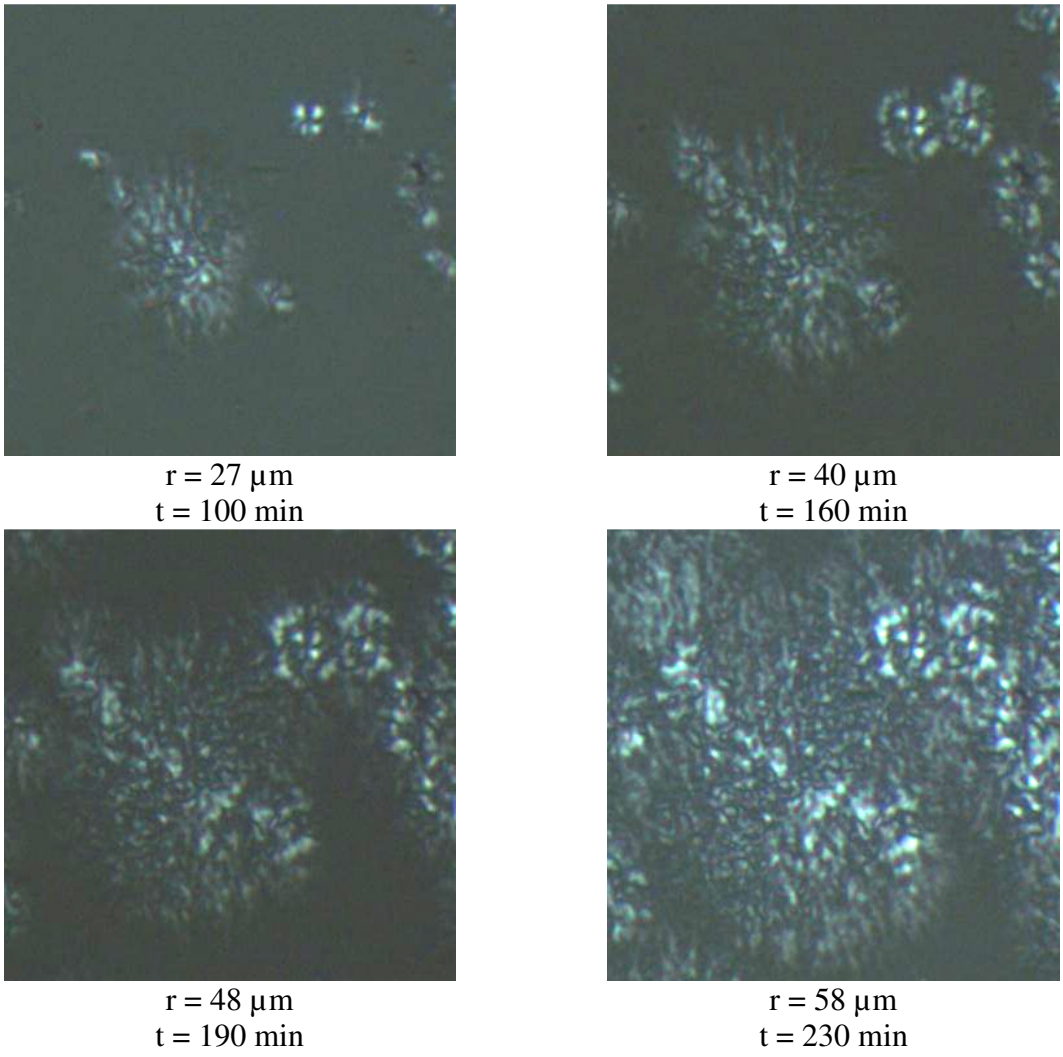

Figure A4.4. Time evolution of crystallite growth in sample 19k–35k at 120 °C

5k–10k, 120 °C

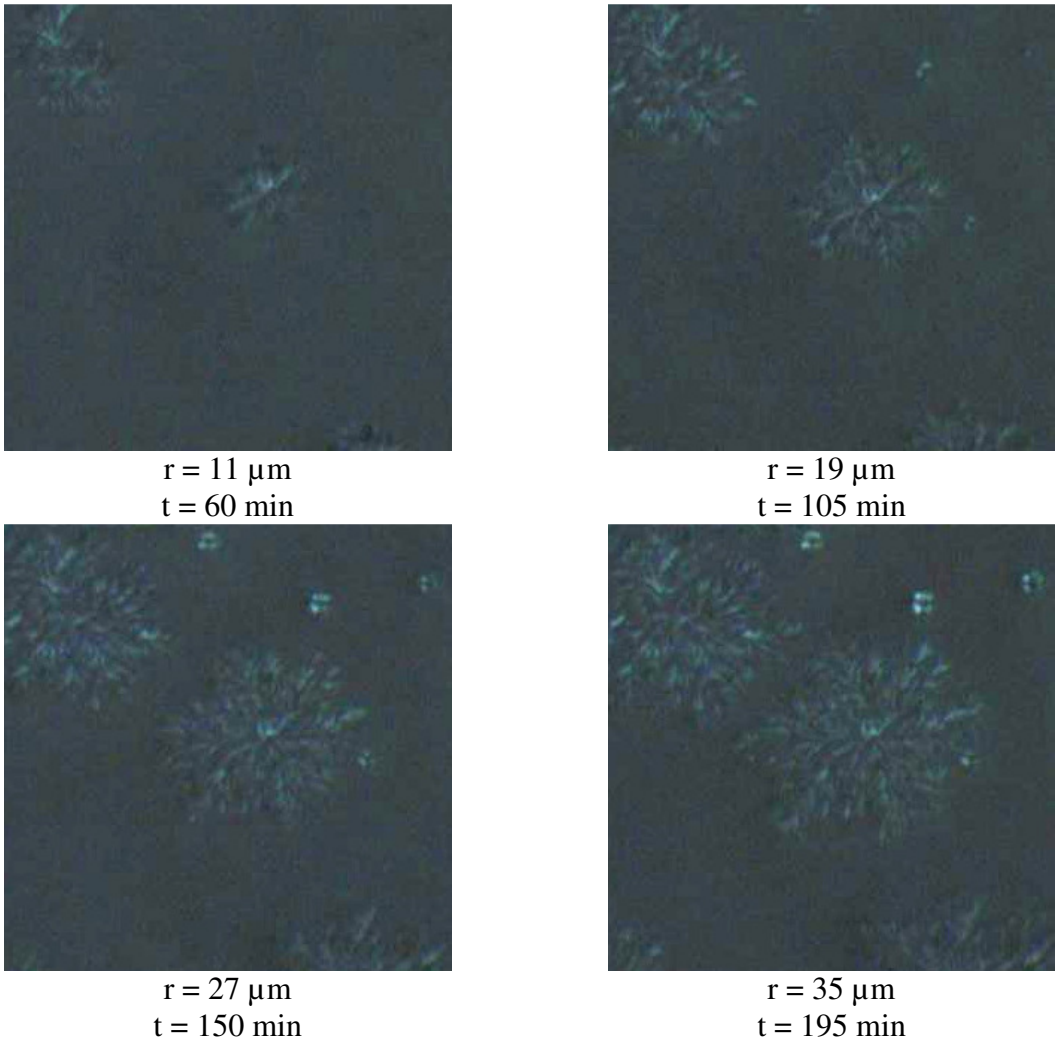

Figure A4.5. Time evolution of crystallite growth in sample 5k–10k at 120 °C

SYNTHESIS AND CRYSTALLIZATION STUDIES OF LINEAR ABA–TYPE TRIBLOCK COPOLYMERS OF 2–DIMETHYLAMINOETHYL METHACRYLATE WITH POLY(L–LACTIDE) AS A CENTRAL BLOCK

5

5.1 Introduction

Amphiphilic triblock (multiblock) copolymers with different hydrophilic/hydrophobic balance afford versatile materials with unique self–assembling properties. Multiblock copolymers can often aggregate in a complex fashion, leading to formation of non–spherical and rodlike aggregates,[1] as well as regular bicontinuous phases (lamellar, cylinders), thus attracting attention in environmental[2] and biomedical applications.[3] Particular interest is paid to poly(lactic acid), a hydrophobic and semi–crystalline (in its optically active form) polymer, and to hydrophilic poly(2–dimethylaminoethyl methacrylate) (PDMAEMA) due to its pH and temperature responsiveness and availability of amine functionality for further modification. Reports on the combination of these

polymers into multiblock copolymer systems appeared only during the last decade and include graft diblock,[4] star diblock,[5] and star triblock[6] copolymers. These P(L)LA–PDMAEMA block copolymers were prepared by a combination of ROP of lactide and atom–transfer radical polymerization (ATRP) of DMAEMA via a three–step (mechanism transformation) technique. The advantage of this technique was used for the preparation of ABA–type triblock copolymers containing either PDMAEMA as the outer blocks and PCL central core[7,8] or PLLA as the central core and poly(methyl methacrylate) (PMMA) as outer blocks.[9] The more complex architecture of triblock copolymers compared to that of diblock copolymers may improve drug–loading/release efficiency,[8] and provide additional control over the crystallinity,[9,10] which is a key parameter in controlling biodegradability.[11]

In this chapter we describe the synthesis, characterization and crystallization behaviour of novel ABA–type triblock copolymers of PLLA and PDMAEMA, with PLLA as the central block. We used a synthetic procedure similar to that described in *Chapter 2* involving the ROP of LLA initiated by a double–headed alcohol initiator, followed by conversion of the PLLA end groups to obtain a double–headed PLLA macroinitiator, suitable for addition of the PDMAEMA blocks using ATRP. The molecular weights of the PDMAEMA blocks were targeted to be half of and equal to the PLLA block. We investigated the thermal properties of the obtained triblock copolymers to observe transition temperatures and the effect of the PDMAEMA blocks on PLLA crystallization compared to the PLLA block behaviour in diblock copolymers. Application of the Avrami equation to thermal DSC data obtained during DSC isothermal crystallization allowed the calculation of the overall crystallization rate constant and the Avrami coefficient values. The

spherulitic (axialitic) morphology in thick films along with the crystallite growth rate were determined by isothermal crystallization studies using polarized optical microscopy.

5.2 Experimental Section

5.2.1 Techniques

Details on the NMR, TGA, SEC–LS and DSC instrumentation are given in *Chapter 2*, details on the POM instrumentation are given in *Chapter 4*. The following scan sequence, between the temperature limits of –20 and 180 °C, was applied to DSC analysis of the macroinitiator PLLA: (a) initial heat of as–prepared sample at 10 °C/min, (b) first cool at 10 °C/min, (c) second heat at 10 °C/min, (d) second cool at 200 °C/min to 110 °C, anneal for 30 min, cool at 200 °C/min, (e) third heat at 10 °C/min, (f) third cool at 200 °C/min, (g) fourth heat at 20 °C/min. Then the PLLA sample was scanned using the following sequence within the same temperature range: (a) heat at 10 °C/min, (b) cool at 200 °C/min to 100, 110, 120, 130 °C, anneal for 30 min, then cool at 200 °C/min to –20 °C, followed by heat at 10 °C/min to 180 °C. An expanded sequence was applied to the triblock copolymers: (a) initial heat of as–prepared sample at 10 °C/min, (b) first cool at 10 °C/min, (c) second heat at 5 °C/min, (d) second cool at 200 °C/min, (e) third heat at 20 °C/min, (f) third cool at 200 °C/min to 110 °C, anneal for 120 min, cool at 200 °C/min, (g) fourth heat at 10 °C/min, (h) fourth cool at 10 °C/min, (i) fifth heat at 10 °C/min, (j) fifth cool at 200 °C/min to 110 °C, anneal for 120 min, cool at 200 °C/min, (k) sixth heat at 10 °C/min, (l) sixth cool at 10 °C/min, (m) seventh heat at 10 °C/min.

5.2.2 Materials

All chemicals were supplied by Aldrich and used as received, unless otherwise specified. Synthetic experimental setup is described in *Chapter 2*.

5.2.3 Synthesis of double–headed bromine–terminated poly(L–lactic acid) (Br–PLLA–Br)

A Br–PLLA–Br macroinitiator was synthesized by ROP, as shown in *Scheme 5.1*, to obtain first HO–PLLA–OH, followed by terminal group modification with BIB, using the same procedure described previously (*Chapter 2*). ^{1}H–NMR (400 MHz, $CDCl_3$): δ_H, *ppm* 1.58 (d, J = 7.2 Hz, CH_3, PLLA), 1.95 (s, CH_3, BIB endgroup), 1.98 (s, CH_3, BIB endgroup), 5.16 (q, J = 7.2 Hz, CH, PLLA), 7.32 (s, 4H–Ar, BDM).

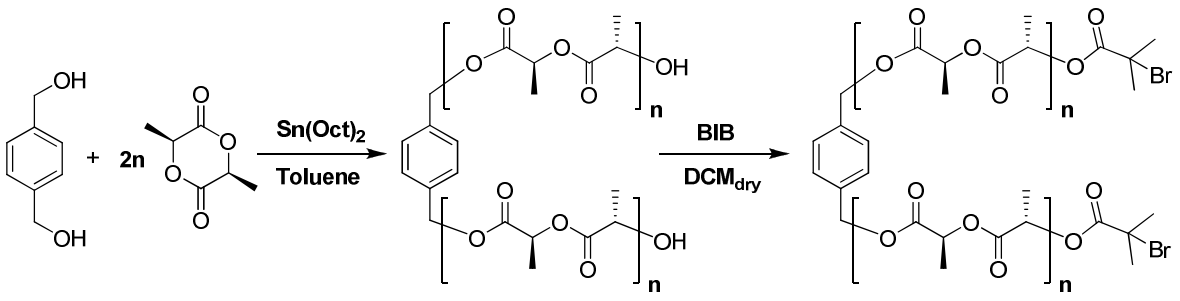

Scheme 5.1. Synthesis of double–headed Br–PLLA–Br macroinitiator by ROP followed by terminal group modification

5.2.4 Synthesis of PDMAEMA–b–PLLA–b–PDMAEMA (*Scheme 5.2*)

Macroinitiated atom–transfer radical polymerization (ATRP) of DMAEMA was conducted as described previously (*Chapter 2*). ^{1}H–NMR (400 MHz, $CDCl_3$): δ_H, *ppm* 0.78–1.14 (m, CH_3, PDMAEMA), 1.58 (d, J = 7.2 Hz, CH_3, PLLA), 1.72–2.11 (m, CH_2, PDMAEMA), 2.19–2.36 (m, $N(CH_3)_2$, PDMAEMA), 2.47–2.66 (m, NCH_2, PDMAEMA), 3.96–4.17 (m, OCH_2, PDMAEMA), 5.16 (q, J = 7.2 Hz, CH, PLLA), 7.32 (s, 4H–Ar, BDM).

The nomenclature of the triblock copolymers (tBC) is given in terms of number–average molecular weights, as in $PDMAEMA_{yk}$–$PLLA_{xk}$–$PDMAEMA_{yk}$, where x and y refer to the molecular weight rounded off to the nearest thousand (k). They will also be referred to as yk–xk–yk. Br/HO–PLLA–OH/Br, due to the similarity of all the properties, will be referred as $PLLA_{13k}$ or PLLA.

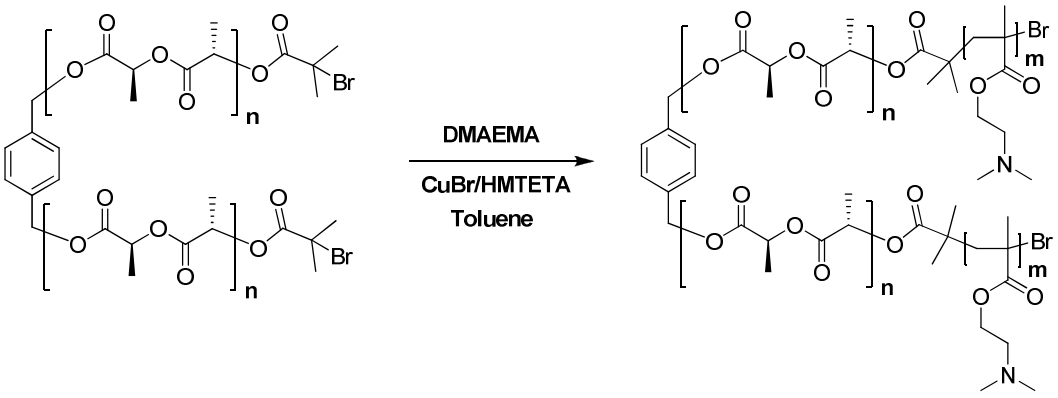

Scheme 5.2. Synthesis of PDMAEMA–*b*–PLLA–*b*–PDMAEMA block copolymers following standard ATRP procedure

5.2.5 Preparation and isothermal crystallization of the films

Drop–cast films were prepared and isothermal crystallization experiments using POM with the hot stage were carried out as described in *Chapter 4*.

5.3 Results and Discussion

5.3.1 Synthesis and molecular weight characterization of homopolymers and triblock copolymers

In our previous work (*Chapter 2*), we have shown that PLLA and PDMAEMA are miscible in the melt if either block has a molecular weight ca. 5000 g/mol or less and that they are at least partly immiscible if the shortest block is more than ca. 10,000 g/mol. In the present work, we prepare two triblock copolymers with the same central block size, aiming for a molecular weight of ca. 10,000 for the common PLLA block and molecular weight of 5000 g/mol and 10,000 g/mol for the PDMAEMA blocks, respectively, in two block copolymers. The latter were chosen so that at least one block copolymer shows some immiscibility. At the same time, the molecular weights were kept fairly low for ease of verification of triblock copolymer architecture (see below) and to be able to proceed with ATRP in solution without unduly high viscosity. 1,4–Benzenedimethanol (BDM) was chosen as the double–headed ROP initiator due to the proven efficiency of benzyl alcohol derivatives in ROP[12] and to optimize molecular weight determination by ^{1}H–NMR. For the latter, this initiator provides a well–defined and isolated 4–proton signal at 7.32 ppm [C_6H_4; BDM in *Figure 5.1*] that is sufficiently separated from the solvent ($CDCl_3$) signal. End–capping with BIB introduces another well–defined and isolated 6–proton signal at 1.96 ppm

[C(C***H*****3**)$_2$Br; *c* in *Figure 5.1*]. Comparison of the integrals of the signals at 7.32 ppm from the BDM moiety and at 1.96 ppm from the BIB moiety allows judging the completeness of the terminal group modification.

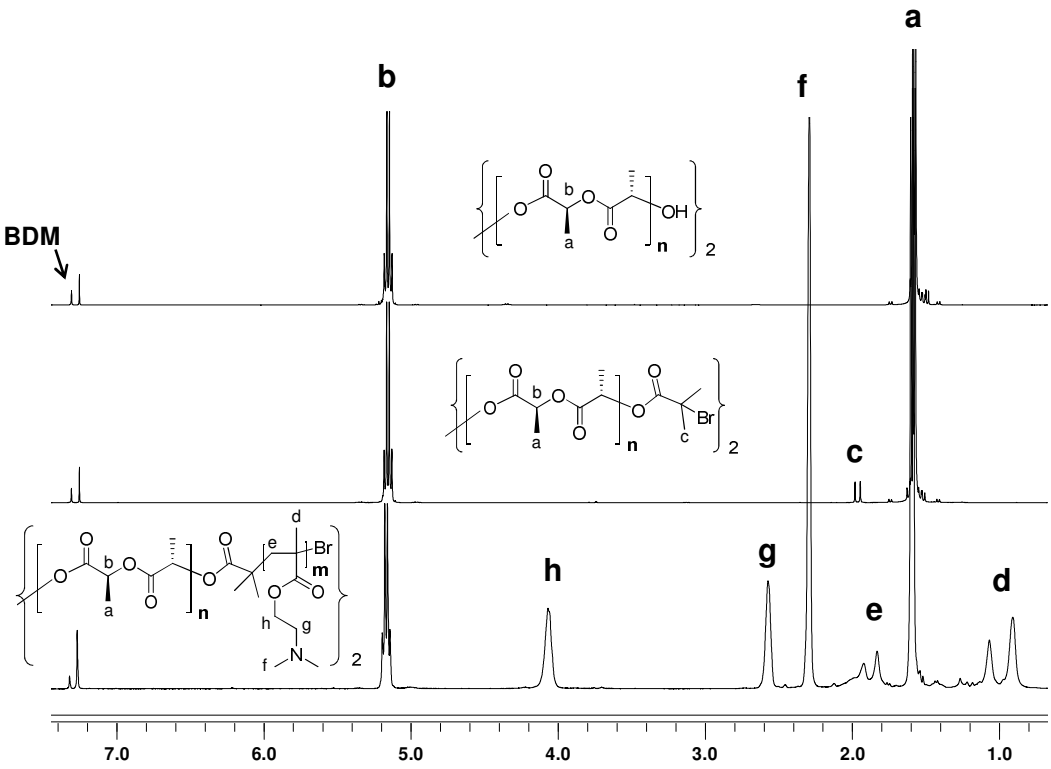

Figure 5.1. ^{1}H–NMR spectra of HO–PLLA$_{13k}$–OH (upper), Br–PLLA$_{13k}$–Br (middle) and PDMAEMA$_{7k}$–PLLA$_{13k}$–PDMAEMA$_{7k}$ (lower).

The molecular weights of PLLA determined by NMR– and SEC–LS are given in *Table 5.1*. The M_n of HO–PLLA–OH is in excellent agreement with the corresponding Br–PLLA–Br. Their values are a little higher than the theoretical M_ns determined from the monomer/initiator feed ratio. The relatively narrow PDIs of 1.15 are indicative of good control over the polymerization and good initiating efficiency of BDM.

Table 5.1. Molecular weight characteristics of the PLLA homopolymers/macroinitiators and PDMAEMA–PLLA–PDMAEMA triblock copolymers synthesized

Sample	M_n, g/mol	M_n (NMR) g/mol	M_n (SEC–LS [d]) g/mol	PDI (SEC–LS [d])
HO–$PLLA_{13k}$–OH [a]	9700 [b]	12100	14000	1.15
Br–$PLLA_{13k}$–Br [a]	10100 [b]	12900	14500	1.14
7k–13k–7k (tBC1)	26600 [c]	26500	28900	1.19
13k–13k–13k (tBC2)	39900 [c]	39800	41400	1.24

[a] The subscript indicates the average molecular weight of the four M_n values from the NMR and SEC–LS measurements considering both the OH and Br forms. [b] Theoretical assuming 95% conversion, $M_n = [([LLA]_0/[I]_0) \times 144 \times 0.95] + M_{BDM}$ (+ M_{BIB}). [c] Determined by NMR by comparison of the integrals for the PLLA *b* and PDMAEMA *h* signals (see *Figure 5.1*), using the average PLLA M_n (*a*) as a reference. [d] Dn/dc's are 0.048, 0.068 and 0.073 mL/g for $PLLA_{13k}$, 7k–13k–7k and 13k–13k–13k, respectively (*Chapter 2*).

Reaction feeds for each triblock copolymer were calculated to target two compositions, namely 1:1 and 2:1 DMAEMA:LLA weight ratio. The block molar ratios obtained were determined from ^{1}H NMR spectra (*Figure 5.1*) by comparison of the integrals of the PLLA methine signals at 5.16 ppm [C*H*CH_3, *b* in *Figure 5.1*] with the integrals of the PDMAEMA signal at 4.06 ppm [O$C\mathit{H}_2CH_2$, *h* in *Figure 5.1*]. The molecular weights of the PDMAEMA blocks based on the block molar ratios and on the average of the four NMR and SEC–LS molecular weight values for PLLA correspond well to that expected from the reaction feed. The SEC elugrams of the block copolymers are monomodal and shifted towards shorter retention time compared to the PLLA macroinitiator. Furthermore, there is no shoulder on the longer elution time side, thus

showing no evidence of unreacted macroinitiator (*Figure 5.2*). The molecular weights obtained by SEC–LS correspond well to those determined by NMR (*Table 5.1*). Again, the low PDI, ca. 1.2, is indicative of well–controlled polymerization. To determine if there is any PLLA homopolymer impurity in the block copolymers, the quaternization/precipitation procedure previously described (*Chapters 2* and *3*) was used, which separates quaternized block copolymer from any PLLA. This was tested on sample 13k–13k–13k only, and no trace of PLLA homopolymer was found, thus confirming complete macroinitiation.

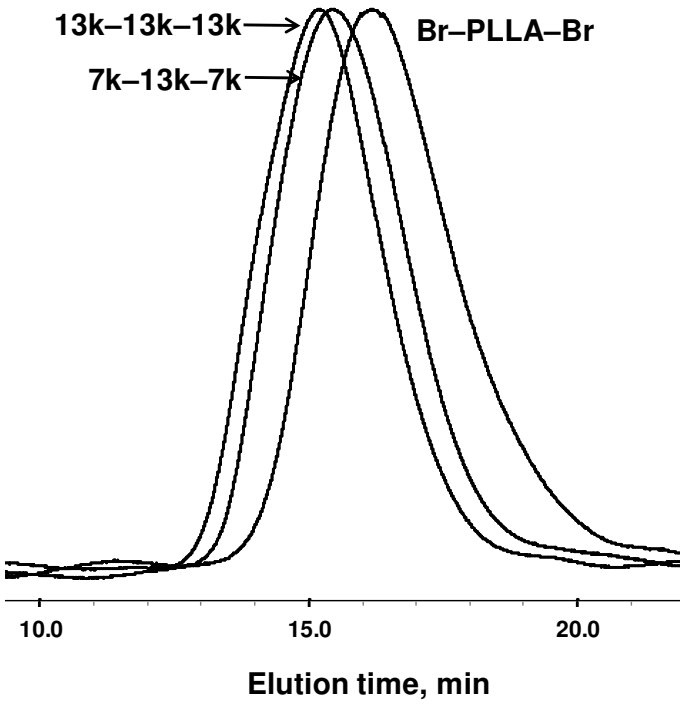

Figure 5.2. SEC–LS elugrams (RI curves) of PLLA macroinitiator and triblock copolymers

TGA thermograms of the triblock copolymers compared with the two homopolymers are shown in *Figure 5.3*. As we previously showed (*Chapter 2*), TGA can be used to roughly estimate the relative block composition, since two blocks degrade in

distinct temperature regions. As can be seen in *Figure 5.3*, degradation of the PLLA proceeds in a single step in the 300–370 °C region, whereas PDMAEMA degrades in two steps, the first in the 250–325 °C region, and the second in the 375–425 °C region. Thus, by determining the wt % sample remaining in the block copolymers at 375 °C (where the PLLA block is completely degraded) relative to the wt % sample remaining in the PDMAEMA homopolymer at 375 °C, it is possible to estimate block copolymer composition. The resulting estimations are presented in *Table 5.2* and correspond well to the ^{1}H–NMR data.

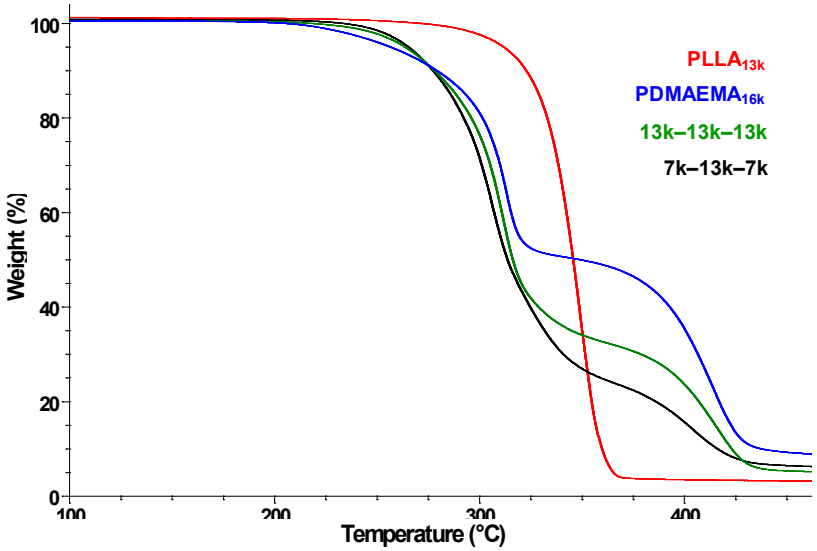

Figure 5.3. TGA thermograms of the triblock copolymers and corresponding homopolymers

Table 5.2. Composition of PLLA–*b*–PDMAEMA determined by TGA compared with NMR

Sample	wt % PDMAEMA, NMR [a]	wt % residue at 375 °C, TGA	wt % PDMAEMA, TGA [b]
$PDMAEMA_{16k}$		46	100
7k–13k–7k	50	22	48
13k–13k–13k	66	30	65

[a] Calculated from the NMR–determined block ratios.

[b] wt % $_{PDMAEMA}$ = wt % $_{residue\ (yk–xk–yk)}$×100% / wt % $_{residue\ (homo–PDMAEMA)}$.

5.3.2 DSC characterization of PLLA and triblock copolymers

DSC data for the PLLA macroinitiator is given in *Table 5.3*. The highest melting temperature of 164 °C (1st heating scan only) was observed for the quenched and cold–crystallized sample of the PLLA macroinitiator, which is a little lower than 168 °C found for the monofunctionalized $PLLA_{13k}$ from our previous study (*Chapter 2*). The appearance of two melting peaks in a heating scan following quenching (*Figure 5.4a*) could be ascribed to melting–recrystallization and/or to two different crystalline forms, α (highly ordered and more stable) and α' (relatively disordered and less stable).[13–15] Its heat of fusion after annealing for 30 min at 110 °C (*Table 5.3*) indicates a degree of crystallinity of 62% when referenced to 91 J/g for 100% crystalline PLLA,[16] very similar to monofunctionalized $PLLA_{13k}$. The T_g of quenched sample is 57 °C (*Figure 5.4a*) with a ΔCp of 0.57 $J{\cdot}g^{-1}{\cdot}K^{-1}$, as was determined for monofunctionalized $PLLA_{13k}$ (0.58) and close to the value of 0.61 $J{\cdot}g^{-1}{\cdot}K^{-1}$ reported in Ref. 16 for a completely amorphous sample.

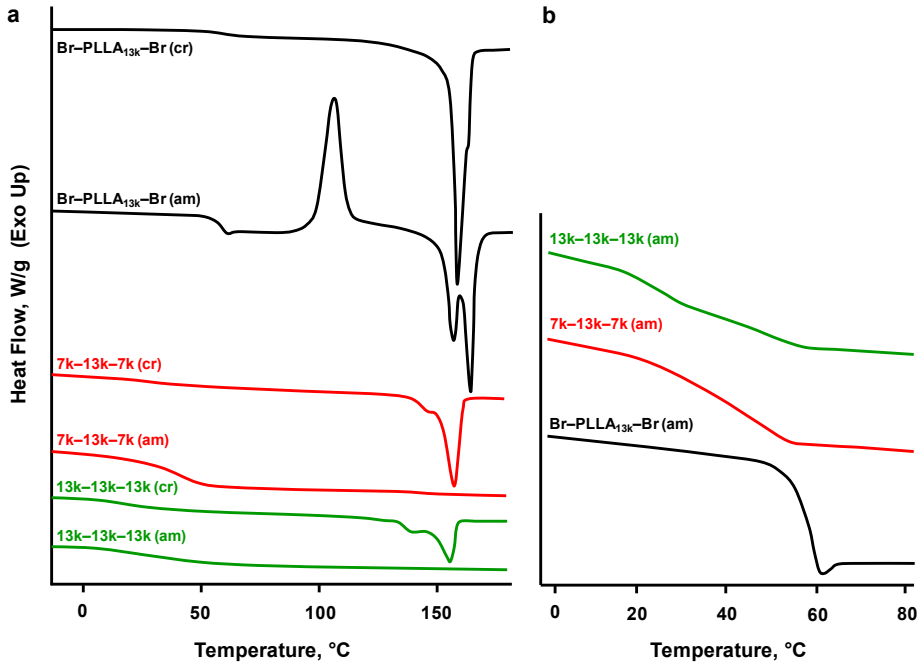

Figure 5.4. DSC thermograms of PLLA (a) and triblock copolymers (b), scanned at 20 °C/min (amorphous samples, quenched from the melt, "am") and 10 °C/min (crystalline samples, annealed at 110 °C for 30 and 120 min for PLLA and tBCs, respectively, "cr")

DSC thermograms of triblock copolymers are illustrated in *Figure 5.4b* and the results of the DSC analysis are summarized in *Table 5.3*. As found previously for the diblock copolymers (*Chapter 2*), no crystallization was detected by DSC in any of the triblock copolymer samples during cooling (scanned from the melt at 10 °C/min) indicating that the PDMAEMA blocks significantly slow down the crystallization rate of the PLLA block. Relatively sharp cold crystallization peaks show up at ca. 115 °C only on the first heating scan of as–prepared samples (i.e. not previously melted), and the absolute value of the enthalpy of cold crystallization is very close to the enthalpy of melting, meaning that the initial samples were almost completely amorphous. In subsequent heating scans of non–crystallized samples, relatively weak cold crystallization occurs at ca. 135 °C for 7k–13k–

7k, and very weak (at the limit of detection) cold crystallization for 13k–13k–13k. Moreover, in contrast to diblock copolymers, 13k–5k (where the PDMAEMA block is of similar size to each block in tBC1) and 13k–12k (with similar total PDMAEMA content as in tBC1), where the melting peak was present when the quenched samples were heated at a rate of 20 °C/min, tBC1 (as well as tBC2) does not crystallize at this scan rate. This more pronounced retardation of the crystallization rate by the PDMAEMA blocks can be explained by the PLLA being connected at both ends to PDMAEMA in the triblock as opposed to diblock copolymers.

Table 5.3. DSC characterization of the PLLA homopolymer and PLLA–*b*–PDMAEMA copolymers synthesized

Sample [a]	W_{PLLA} [b] %	T_g (ΔCp) [c,d] °C ($J \cdot g^{-1} \cdot K^{-1}$)	T_g (ΔCp) [c,e] °C ($J \cdot g^{-1} \cdot K^{-1}$)	T_m °C	ΔH_m^{total} J/g (% cryst) [f]
Br–$PLLA_{13k}$–Br	100		57 (0.57)	160	56 (62)
tBC1 (cr)	50	25 (0.24)		158	26 (57)
tBC1 (am)	50	25–30 (shoulder)	45 (0.51)		
tBC2 (cr)	34	22 (0.22)		156	17 (55)
tBC2 (am)	34	25 (0.25)	48 (0.11)		

[a] The notations "cr" and "am" refer to crystallized samples (annealed at 110 °C for 30 and 120 min for PLLA and tBCs, respectively) and amorphous samples (quenched from the melt). [b] $W_{PLLA} = [M_{n(PLLA)} \times 100\%] / [M_{n(PLLA)} + M_{n(PDMAEMA)}]$, using the M_n values given in *Table 2*. [c] The T_g's were determined from first derivative maxima in 20°C/min curves. [d] PDMAEMA or PDMAEMA–rich phase. [e] PLLA or PLLA–rich phase. [f] Obtained from 10 °C/min heating curves of previously annealed samples. The ΔH_m^{total} values are relative to the total copolymer weight. The % cryst (= % crystallinity) is relative to the PLLA weight fraction: $[(\Delta H_m / W_{PLLA})/\Delta H_{m(ideal\ PLLA\ cryst)}] \times 100\%$, where $\Delta H_{m(ideal\ PLLA\ cryst)} = 91$ J/g.[16]

The degree of crystallinity in the triblock copolymers (samples annealed for 2 h at 110 °C, *Table 5.3*), relative to that in PLLA, decreases only a little, and is similar for both triblock copolymers (ca. 56% compared to ca. 62% for PLLA). It was observed that even in well–crystallized samples (after annealing), although the melting peaks are sharp and intense, the main peak is accompanied by a shoulder located a few degrees lower ("pre–melting"), indicative of the melting of poorly ordered regions. Compared to the PLLA macroinitiator, the peak values of the melting temperature are reduced by 5–8 °C, which may be related, as will be shown below, to partial miscibility of the blocks.

As mentioned above, our previous work based on T_g analysis showed that low molecular weight (ca. 5000 g/mol) PLLA and PDMAEMA blocks are miscible in the melt, whereas for molecular weights of either block of ca. 12–13,000 g/mol or higher they are essentially immiscible. Thus, in the present case, analysis of the T_g regions of the block copolymers will not only provide information about block miscibility, but also confirm if the present polymers are triblock rather than diblock copolymers. For this purpose, we examined the T_g region in the 20 °C/min heating thermograms, obtained either after quenching of the melt (at 200 °C/min, amorphous samples) or after 2 h annealing at 110 °C (semi–crystalline samples). These T_g data are given in *Table 5.3*.

The triblock copolymer, tBC2, in its amorphous state shows two clear T_g's, at 25 and 48 °C. The first is almost 10 °C higher than the T_g of the PDMAEMA homopolymer [18 °C reported in Ref. **17** for $PDMAEMA_{100k}$, and 17 °C reported in *Chapter 2* for the $PDMAEMA_{16k}$]. The second one is about 10 °C lower than that of the PLLA parent homopolymer. This indicates partial miscibility of the blocks, which are thus phase–separated into a PDMAEMA–rich phase and a PLLA–rich phase. In the corresponding

semi–crystalline sample, the PDMAEMA–rich T_g lies at 22 °C, which is still a little higher than that of the PDMAEMA homopolymer. The T_g is decreased compared to the totally amorphous sample because the crystallized PLLA no longer participates in the T_g phenomenon, which effectively increases the PDMAEMA composition of the amorphous phase. Similar thermal behaviour was observed for the PDMAEMA–rich phase in sample 13k–12k, supportive of tBC2 containing similar PDMAEMA block lengths to the diblock (and not a single PDMAEMA block of ca. 25,000 g/mol). The lower T_g of the PLLA–rich phase compared to the 13k–12k indicates higher miscibility for the triblock than the diblock, although one might also consider that this results from slightly asymmetrical PDMAEMA chain lengths in the triblock copolymer, which can lead to a higher fraction of essentially miscible lower molecular weight blocks.[18]

In contrast to tBC2, the T_g region in tBC1 (7k–13k–7k) looks more like a single, albeit very broad T_g. Indeed, the first derivative curve of the DSC thermogram in this region shows a peak at 45 °C and a shoulder indicative of a second T_g at 25–30 °C. Clearly, tBC1, which has shorter PDMAEMA blocks, shows much greater block miscibility than tBC2, to the point of being almost completely miscible at the DSC detection level. Indeed, the T_g behaviour of tBC1 is much more similar to that of the 13k–5k diblock compared to 13k–12k diblock (*Chapter 2*), thereby providing further confirmation of the triblock architecture. The relatively high level of miscibility (ca. 50%) is also supported by the predicted T_g for a completely miscible PLLA–rich phase (43 °C compared to experimentally derived 45 °C), according to the Fox equation,

$$1/T_g = w_A/T_{gA} + w_B/T_{gB}$$

where w_A and w_B represent the weight fractions of A (PLLA) and B (considering one totally miscible PDMAEMA block) and T_{gA} and T_{gB} their glass transition temperatures (assuming a molecular weight–independent T_g of 17 °C for PDMAEMA and 57 °C for PLLA). In the crystallized sample, the fraction of amorphous PLLA is much smaller than in the amorphous sample, and can be estimated using the degree of crystallinity. The predicted T_g of a PDMAEMA–rich phase for crystallized sample (considering the entire PDMAEMA) is 28 °C, which is also in good agreement with the experimental 25 °C.

5.3.3 Isothermal crystallization kinetics

Numerous publications on the crystallization studies of PLLA, as homopolymer or as a block, report spherulitic morphology as being the most common for unconfined or soft–confinement conditions in weakly segregated systems, where phase separation is driven by the crystallization of PLLA. Crystalline phase growth kinetics were determined by application of the Avrami equation to the DSC data obtained during isothermal crystallization as described in detail in *Chapter 4*.

The value of K and $t_{1/2}$ for $PLLA_{13k}$ (*Table 5.4*) changes in accordance with the known "bell–shape" dependence of crystallization kinetics of semi–crystalline polymers on the temperature, reaching its maximum at ca. 110 °C (the temperature of cold crystallization of completely amorphous PLLA, *Figure 5.4*),[19,20] and compares well with the values of K for $PLLA_{13k}$–Br, given in *Chapter 4*. According to the number of different values of the Avrami coefficient reported for PLLA (see *Chapter 4*), the values of n

obtained for Br–PLLA$_{13k}$–Br (2.4±0.3) are fairly consistent with spherulitic instantaneously nucleated crystalline lamellae growth in bulk.

Table 5.4. Avrami parameters of PLLA$_{13k}$ macroinitiator

Sample	T_c, °C	$t_{1/2}$, min [a]	n [b]	logK [b]	$K\times10^2$, min^{-n} [b]	$K\times10^2$, min^{-2} [c]
Br–PLLA$_{13k}$–Br	100	1.0	2.7	–0.2	63.0	69.0
	110	0.8	2.5	0.1	130.0	110.0
	120	2.9	2.1	–1.2	6.3	8.2
	130	10.2	2.5	–2.7	0.2	0.7

[a] experimental values. [b] values obtained from linear part of Avrami plot (Eq. 3). [c] values obtained from Eq. 3 at $t_{1/2}$ and n = 2

Table 5.5. Crystallization kinetics parameters of the PLLA homopolymer and triblock copolymers at 110 °C

Sample	$t_{1/2}$, min [a]	n [b]	logK [b]	$K\times10^2$, min^{-n} [b]	$K\times10^2$, min^{-2} [c]
Br–PLLA$_{13k}$–Br	0.8	2.5	0.1	130.00	110.00
7k–13k–7k	11.3	2.2	–2.5	0.32	0.54
13k–13k–13k	20.3	1.9	–2.6	0.25	0.17

[a] experimental values. [b] values obtained from linear part of Avrami plot (Eq. 3). [c] values obtained from Eq. 3 at $t_{1/2}$ and n = 2

The Avrami equation was applied to the DSC data obtained during isothermal crystallization of the triblock copolymer samples at 110 °C, as at this temperature PLLA$_{13k}$ shows the highest value of the crystallization constant (*Tables 5.4* and *5.5*). The Avrami parameter, $n \approx 2$, that is determined for both triblock copolymers, suggests two–dimensional (axialitic) crystallization in bulk. The values of the crystallization constants *K* for the tBCs are significantly lower compared to that of PLLA; however, they do not

change with increase in length of the PDMAEMA block. Similar values were determined in 13k–12k and 13k–23k samples at 100 °C (*Chapter 4*). On the other hand, the overall crystallization rate, as indicated by the $t_{1/2}$, decreases dramatically with an increase in PDMAEMA content.

5.3.4 Isothermal crystallization morphology

Typically, PLLA homopolymers crystallize in spherulites showing a well–defined maltese–cross extinction pattern, with a maximum intensity of the transmitted light for area of the spherulite at an angle of 45° to the polarizer/analyzer pair. However, regular variations in the light intensity as a function of radial distance in the spherulite (termed "banding") may appear as a result of lamellae twisting in the radial direction of the crystal growth under certain conditions, differing from polymer to polymer, although cooperative packing of the twisting lamellae into the regular bands is still poorly understood.[21,22] Banded spherulites are not typical for PLLA homopolymers, but can be obtained by "crystallization after annealing" aiming to completely melt all the crystalline residues first by annealing the sample for several minutes at 240 °C, followed by 2 h annealing at 160 °C, and finally crystallization at 110–140 °C.[23] On the other hand, banded spherulites were observed in block copolymers of PLLA with poly(ε–caprolactone),[24] polystyrene,[25] and poly(ethylene oxide)[26] under certain conditions without any special pretreatment.

Optical micrographs obtained during isothermal thick films crystallization at various crystallization temperatures are presented in *Figure 5.5*. As described in the literature cited above, constrained geometry, relatively strong PLLA–PDMAEMA

interblock interaction and chirality of the PLLA block seem likely to favour the twisting of the growing crystalline lamellae, resulting in the formation of banded spherulites or spherulite–like aggregates.

Thus, sample tBC1 crystallizes in well–defined banded spherulitic morphology, with regular bands forming at 100–110 °C and becoming less ordered as the temperature increases to 120 °C. The periodic distance of the extinction rings increases with temperature, as is typically observed for banded spherulites in polymers.[27]

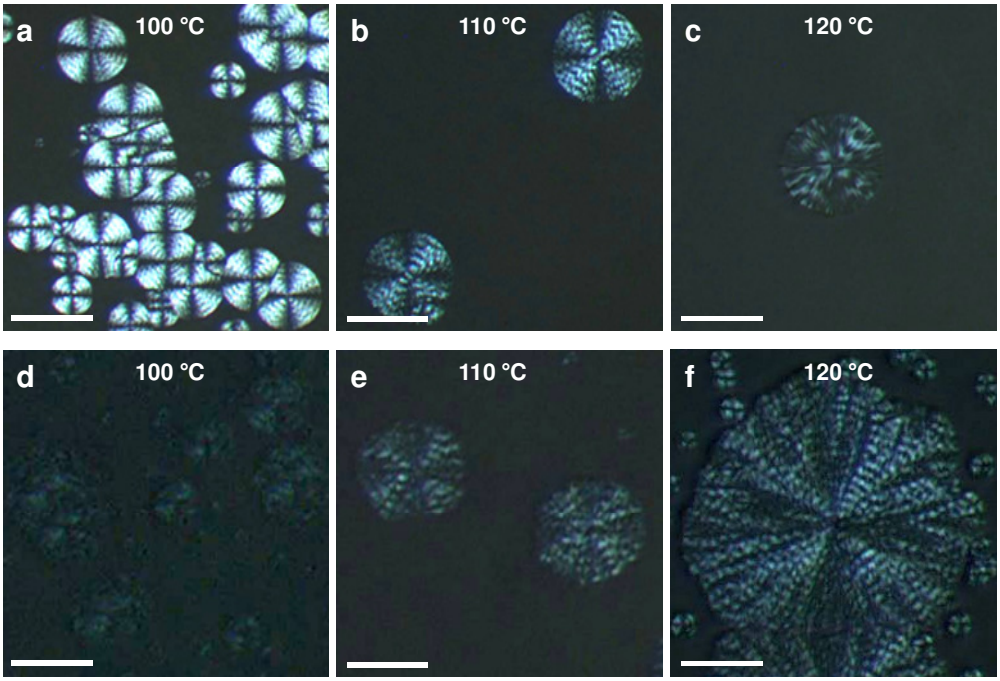

Figure 5.5. Polarized optical microscopy images of tBC1 (a–c) and tBC2 (d–f), obtained after isothermal crystallization for 60, 70, 50 min (a–c) and for 160, 380, 490 min (d–f), respectively. Scale bar is 50 µm for images a–c and 30 µm for images d–f

However, the change in spacing between extinction rings was not observed for sample tBC2, where the average value of the periodic distance remains the same in the

studied temperature interval (100–120 °C). A possible explanation for this phenomenon was found by comparison of the reports on the banded spherulites formed by the PLLA block in PLLA–b–PEO, PLLA–b–PCL and PLLA–b–PS. A band spacing increase with crystallization temperature was observed for PLLA spherulites in PLLA–b–PEO[26] and PLLA–b–PCL.[24] In contrast, band spacing in spherulites obtained in PLLA–b–PS change little with crystallization temperature. Interestingly, the first two systems are miscible in the melt, and the third one is immiscible. In our case, the band spacing in the spherulites formed by the PLLA block in miscible tBC1 increases with temperature, and remains almost the same in immiscible tBC2. Consequently, it appears that the strength of segregation affects the twisting power of the growing lamellae due to the confinement effect.

As plotted in *Figure 5.6*, the maximum spherulite (axialite) growth rate in both 7k–13k–7k and 13k–13k–13k was observed at 120 °C. The crystallite growth rates in tBC1 and tBC2 (0.62 and 0.10 μm/min at 120 °C, respectively) are significantly lower than those in the diblock copolymers of the same composition (2.90 and 0.42 for 13k–12k and 13k–23k at 120 °C, respectively, *Chapter 4*), showing more pronounced retardation effect of two outer PDMAEMA blocks on the crystallization of the inner PLLA block.

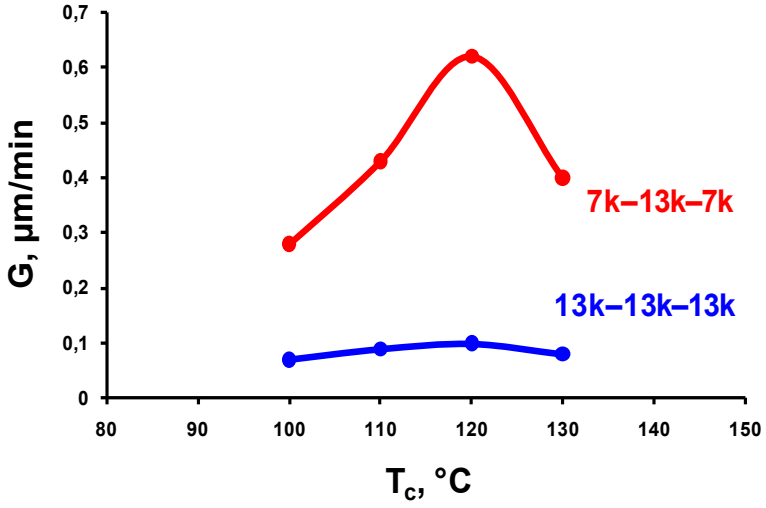

Figure 5.6. Spherulites growth rate in the triblock copolymers thick films as a function of crystallization temperature

Such influence of block copolymer architecture on the crystallization of the middle block was observed previously in related "soft amorphous–crystalline–soft amorphous" di– and triblock copolymers of PDMS (1000–5000) and PEO (6000 and 10,000), where a strong decrease in crystallinity and in melting temperature of di– and, especially, triblock copolymers compared to the PEO homopolymer was observed.[28] Furthermore, triblock copolymers of PEO (50,000) and PMMA (10,000), where PMMA is a "hard amorphous" block and PEO is tethered to two PMMA blocks, are unable to crystallize, in contrast to diblock copolymer.[10] Similar suppression of crystallization of the $PLLA_{22k}$ block was observed in $PMMA_{5k}$–$PLLA_{22k}$–$PMMA_{5k}$ triblock copolymers,[9] indicating that not only the relative contents of the amorphous block, whether soft or hard at the crystallization temperature, but, to a greater extent, the block copolymer architecture affects or hinders the crystallization process.

5.4. Conclusions

Using a convenient three–step technique of sequential block copolymerization of LLA and DMAEMA, starting from the PLLA block initiated by commercial 1,4–benzenedimethanol, a novel triblock copolymer system with PLLA as a central block and two PDMAEMA outer blocks of approximately one–fourth and one–half of the length of PLLA was successfully prepared and characterized. The composition of the block copolymers was determined by NMR and TGA, and molecular weight characterization was performed by NMR and SEC–LS. Transition temperatures and degrees of crystallinity obtained by DSC indicated that 7k–13k–7k forms an essentially miscible melt (indicated by a single T_g that matches that calculated using Fox equation for the miscible systems), and that 13k–13k–13k, which shows two distinct T_gs but with values that are higher than for PDMAEMA and lower than for PLLA, respectively, is partially miscible. Kinetic studies revealed that the PLLA block in the triblock copolymer crystallizes in two–dimensional crystalline lamellar superstructures in the bulk, as indicated by the Avrami coefficient. The value of the PLLA crystallization constant significantly decreases with introduction of the two PDMAEMA blocks compared to that of the PLLA macroinitiator, and does not change with the length of the latter. However, the overall crystallization rate, indicated by the half–crystallization time, $t_{1/2}$, drops significantly with increase in the PDMAEMA length. The regular banding of the spherulite or spherulite–like crystalline morphology of the triblock copolymer films is characterized by relatively low extinction ring spacing, indicating high twisting power of the growing lamellae. Moreover, in tBC2 the band spacing does not change with

temperature, indicating stronger interaction between the immiscible blocks leading to PLLA crystallization in soft confinement environment.

References to Chapter 5

1. Narrainen, A. P.; Pascual, S.; Haddleton, D. M. *J. of Polym. Sci.: Part A: Polym. Chem*. **2002**, 40, 439–450.

2. Williams, P. A. Handbook of Industrial Water Soluble Polymers, *Blackwell Publishing*, Oxford, **2007**.

3. Oh, J. K. *Soft Matter*, **2011**, 7, 5096–5108.

4. Firmenich, S.; Berthier, D.; Ouali, L. Patent No. WO 2005/108471 A1.

5. Yuan, W.; Yuan, J.; Zheng, S.; Hong, X. *Polymer* **2007**, *48*, 2585–2594.

6. Li, J.; Ren, J.; Cao, Y.; Yuan, W. *Polymer* **2010**, 51, 1301–1310

7. Motala–Timol, S.; Jhurry, D. *Eur. Polym. J*. **2007**, 43, 3042–3049.

8. San Miguel, V.; Limer, A. J.; Haddleton, D. M.; Catalina, F.; Peinado, C. *Eur. Polym. J*. **2008**, 44, 3853–3863.

9. Shen, J.; Jiang, W.; Liu, Y.; Wei, R.; Liu, X.; Zhong, Y.; Xu, J.; Li, L.; Xue, G. *J. Appl. Polym. Sci.* **2012**, DOI 10.1002/app.35503.

10. Kretzschmarl, H.; Donth, E.–J.; Tanneberger, H.; Garg, D.; Höring, S. *Thermochimica Acta* **1985**, 93, 151–154.

11. Albertsson, A.–C. (Ed.) Degradable Aliphatic Polyesters, *Adv. Polym. Sci*. **2002**, 157, 1–161.

12. Dechy–Cabaret, O.; Martin–Vaca, B.; Bourissou, D. *Chem. Rev.* **2004**, *104*, 6147–6176.

13. Zhang, J.; Tashiro, K.; Domb, A. J.; Tsuji, H. *Macromol. Symp*. **2006**, *242*, 274–278.

14. Kawai, T.; Rahman, N.; Matsuba, G.; Nishida, K.; Kanaya, T.; Nakano, M.; Okamoto, H.; Kawada, J.; Usuki, A.; Honma, N.; Nakajima, K.; Matsuda, M. *Macromolecules* **2007**, *40,* 9463–9469.

15. Shieh, Y.–T.; Liu, G.–L. *J. Polym. Sci: Part B: Polym. Phys.* **2007**, *45*, 466–474.

16. (a) Pyda, M.; Bopp, R. C.; Wunderlich, B. *J. Chem. Thermodynamics* **2004**, *36*, 731–742. (b) Pyda, M.; Wunderlich, B. *Macromolecules* **2005**, *38,* 10472–10479.

17. Arce, A.; Fornasiero, F.; Rodrıguez, O.; Radke, C. J.; Prausnitz, J. M. *Phys. Chem. Chem. Phys.* **2004**, *6*, 103–108.

18. Müller, A. J.; Balsamo, V.; Arnal, M. L. *Adv. Polym.Sci.* **2005**, 190, 1–63.

19. Abe, H.; Kikkawa, Y.; Inoue, Y.; Doi, Y. *Biomacromolecules* **2001,** 2, 1007–1014

20. Auras, R.; Lim, L.–T.; Selke, S. E. M.; Tsuji, H. Poly(lactic acid). Synthesis, Structures, Properties, Processing and Applications, *John Wiley and Sons*, Hoboken, **2010**

21. Gedde, U. W. Polymer Chemistry, *Chapman & Hall*, London, **1985**.

22. Lotz, B.; Cheng, S. Z. D. *Polymer* **2005**, 46, 577–610.

23. Xu, J.; Guo, B.–H.; Zhou, J.–J.; Li, L.; Wu, J.; Kowalczuk, M. *Polymer* **2005**, 46, 9176–9185.

24. Wang, J.–L.; Dong, C.–M. *Macromol. Chem. Phys*. **2006**, 207, 554–562.

25. Chao, C.–C.; Chen, C.–K.; Chiang, Y.–W.; Ho, R.–M. *Macromolecules* **2008**, 41, 3949–3956.

26. Yang, J.; Zhao, T.; Liu, L.; Zhou, Y.; Li, G.; Zhou, E.; Chen, X. *Polymer J*. **2006**, 38, 1251–1257.

27. Keith, H. D.; Padden Jr., F. J. *Macromolecules* **1996**, 29, 7776–7786.

28. Galin, M.; Mathis, A. *Macromolecules* **1981**, 14, 677–683.

GENERAL CONCLUSIONS AND FUTURE WORK

6

6.1 Conclusions

The main idea of the present work was to create a novel block copolymer composed of a hydrophobic thermoresponsive crystallizable block and a functional hydrophilic block that can also be complexed with other appropriately functionalized molecules, in view of obtaining a versatile stimuli–responsive polymeric material. In parallel, to have a material that can also be suitable for biomedical purposes, the choice was made in favour of biocompatible and/or biodegradable blocks. In this context, the blocks chosen were PLLA, a well–known semi–crystalline polymer, obtained from renewable resources like corn, and therefore biocompatible and biodegradable, and PDMAEMA, known for its ability to bind DNA, its biocompatibility and non–toxicity (in non–charged form), and possessing an easily modified amine moiety. At the start of the project, there were no previous reports of PLLA–PDMAEMA block copolymers in the literature. Some publications on the subject

appeared in the course of our own research, and are complementary to our work, as indicated in the introduction to Chapter 2

We synthesized a series of block copolymers using a convenient three–step technique starting with ROP of PLLA followed by intermediate terminal group modification to provide an initiating site for ATRP of PDMAEMA as the third step, as described in detail in *Chapter 2*. The molecular weights of the PLLA block vary from 5000 to 20,000 and those of the PDMAEMA block were targeted to be half of, equal to or double that of PLLA. The successful preparation of the block copolymers was indicated by NMR and SEC–LS, providing evidence of the block incorporation and successful chain extension, respectively. A novel initiator for LLA polymerization (iPBA) was used to facilitate molecular weight determination by NMR. The term, "controlled preparation", also means that no homopolymer impurities should be present in the block copolymer. For the particular system of PLLA–PDMAEMA, we developed a simple quaternization/ precipitation technique, based on the quaternization of PDMAEMA by methyl iodide, which makes it insoluble in the reaction media and induces precipitation of the entire block copolymer. If any homo–PLLA is present, it will remain soluble and easily detectable by analysis of the filtrate. Application of this technique to selected block copolymers showed no traces of homo–PLLA.

Thermal studies of the block copolymers obtained allowed determination of the transition temperatures for both blocks and of the degree of crystallinity of the PLLA block. It was observed that a block molecular weight of ca. 5000 g/mol is in the region of sharp dependence of the glass transition and melting temperature on molecular weight. Also, at this molecular weight for either block, the blocks are miscible in the melt, as indicated by

analysis of the T_gs: the experimental T_gs were close to the ones calculated using the Fox equation for miscible phases.

It may be added that, even though ROP and ATRP were shown to work well for the preparation of PLLA– and PDMAEMA–based block copolymers, our very first attempt to prepare PLLA–b–PDMAEMA via the three–step technique starting from PLLA was not successful. In this case, the synthetic goal was to prepare a PLLA block of high molecular weight, 30,000 g/mol being achieved. Unfortunately, the relatively low solubility of this molecular weight PLLA in toluene and THF made continuation with the final step, i.e. ATRP of PDMAEMA, impossible. Therefore, as a possible solution while still maintaining high PLLA molecular weight, the polymerization sequence was reversed to start with the PDMAEMA block, which is well soluble in most common solvents, and should help maintain the solubility of the growing block copolymer during LLA polymerization. To do this, a bifunctional initiator (HEBIB), capable of initiating both ROP and ATRP, was used, as discussed in detail in *Chapter 3*. Unfortunately, although chain extension with polylactide took place (high molecular weight was, in fact, not targeted in these initial attempts), it was found that the PDMAEMA amine moieties caused racemization of LLA leading to the formation of atactic polylactide. This result means that it is not possible to prepare PDMAEMA–PLLA block copolymers starting with the PDMAEMA block.

Thus, to prevent racemization, the sequence was reversed to start with the PLLA block using the same bifunctional initiator, limiting its molecular weight to ca. 5000 to avoid potential solubility issues. The PLLA in the resulting block copolymers remained isotactic as expected, but other complications became apparent from two observations. First, the PDMAEMA block was unexpectedly long, indicating either low initiating

efficiency of the PLLA macroinitiator or its incomplete functionalization. Second, some PLLA loss during the isolation procedure indicated the presence of homo–PLLA. Application of the quaternization/precipitation technique to the HEBIB–initiated block copolymers prepared via both PLLA–first and PDMAEMA–first approaches revealed the presence of a large fraction of homo–P(L)LA, shown by NMR to be non–functionalized. This explains the formation of the longer than expected PDMAEMA blocks in the PLLA–first approach, since part of PLLA was not able to initiate ATRP. Further analysis of this phenomenon led us to consider the possibility that LLA polymerization was initiated by hydroxyltin octoate, which reappears in tin octoate even after its vacuum distillation, and/or by lactoyl lactate (open lactide), either present in a very small amount in recrystallized LLA or formed *in situ* by hydrolytic ring–opening catalyzed by octanoic acid. Both mechanisms can lead to the formation of a non–functional polylactide that remains in the final block copolymer after purification. Moreover, it was found that homo–P(L)LA is not always easily detectable by SEC analysis, and in this case its presence can be revealed by the quaternization/precipitation procedure only.

Nevertheless, to take further advantage of bifunctional initiator approach, we conducted one–pot simultaneous polymerization of LLA and DMAEMA at three different temperatures, 70 (optimal for ATRP), 90 and 110 [optimal for ROP by $Sn(Oct)_2$] °C. It turned out that ATRP of PDMAEMA proceeds well at all three temperatures, but the optimal temperature for ROP of LLA is achieved at 90 °C, where 85% isotactic P(L)LA was obtained. Thus, this appears to be a compromise between racemization and the rate of P(L)LA chain extension, Again, the presence of a large fraction of P(L)LA homopolymer was detected in all cases.

Given that there is no evidence of the homo–P(L)LA problem in the three–step synthesis (*Chapter 2*), as would be expected if caused by hydroxyltin octoate or lactoyl lactate, the possible implication of the bifunctional initiator (HEBIB) itself was considered. Significantly, it contains an ester moiety that might be involved in a transesterification reaction during LLA polymerization. With this in mind, we proposed a plausible mechanism based on transesterification that can lead to the formation of non–functional homo–P(L)LA; it also leads to possible undesired formation of triblock copolymer (with PLLA as a central block). The presence of the latter cannot be easily shown by NMR, SEC or the quaternization/precipitation technique. We conclude that the preparation of PLLA–b–PDMAEMA using HEBIB (or other bifunctional initiators of the same type; i.e. with ester groups) and tin octoate as a catalyst for LLA polymerization will inevitably lead to the formation of polylactide homopolymer impurity. To avoid this, a different bifunctional initiator that cannot participate in transesterification reactions must be developed, and/or a different catalyst must be used.

As a continuation of the characterization studies of the PLLA–PDMAEMA block copolymers in *Chapter 2*, *Chapter 4* is dedicated to detailed studies of the crystallization behaviour of the PLLA block in bulk and in thick films. Isothermal crystallization data obtained by DSC was analyzed using the Avrami equation to calculate the overall crystallization rate constant and the Avrami coefficient (nucleation parameter). It was observed that the presence of the PDMAEMA block does not affect the value of the crystallization rate constant very much, but the overall crystallization rate decreases substantially as the length of the PDMAEMA block increases, as shown by the half–crystallization times measured. It must be pointed out that the value of the nucleation

constant decreases from ca. 3 for PLLA and the block copolymers with the shortest PDMAEMA block (miscible phase) to ca. 2 for longer PDMAEMA blocks (where the block copolymer morphology is likely lamellar or hexagonal), indicating a tendency of the growing crystalline lamellae to form two–dimensional rather than three–dimensional superstructures in bulk. As indicated by SAXS analysis of one of the block copolymers (19k–17k), the two blocks are moderately segregated in the melt and crystallization of PLLA changes the melt morphology. The observation of PLLA crystallization in thick films using POM allowed the determination of the spherulitic (or axialitic) growth rate. The spherulitic growth rate of block copolymers decreases substantially compared with the PLLA homopolymer. The morphology of the crystallized films changes from spherulitic to axialitic as the size of the PDMAEMA block increases, and, as the segregation strength increases, noncrystallized PLLA and PDMAEMA remain in between crystalline stems, preventing the formation of normal spherulites.

Since the PDMAEMA block possesses an amine functionality, it can be quaternized, and the glass transition of the resulting qPDMAEMA will lie above the "normal" PLLA crystallization region (100–130 °C). This will increase the segregation between two blocks and allow investigation of PLLA crystallization restricted by hard qPDMAEMA domains. Thus, selected block copolymers were quaternized to various degrees of quaternization (35–80%), as confirmed by NMR. Analysis of the DSC isothermal crystallization data by the Avrami theory revealed that the values of the crystallization constants do not change much compared to non–quaternized block copolymers. The value of the nucleation parameter generally decreases as the degree of quaternization increases, indicating PLLA crystallization in two–dimensional crystalline

lamellar aggregates. Observation of PLLA crystallization in thick films shows spherulite–like (axialitic) morphology for lower degrees of quaternization at all of the experimental temperatures (100–150 °C). The samples with a high degree of quaternization do not crystallize in spherulitic–like morphology at lower temperatures (100–120 °C). However, spherulite–like superstructures were obtained at 150 °C, as this crystallization temperature is higher than the T_g of qPDMAEMA (ca. 140 °C). Interestingly, in contrast to selected nonquaternized samples, crystallized at 150 °C and forming superstructural crystalline aggregates with negative birefringence, crystallization of the quaternized block copolymers at 150 °C results in the formation of crystallites with positive birefringence, presumably driven by the combined effect of the higher temperature (change in crystallization regime) and the charged qPDMAEMA moieties, leading to a change in the orientation of most of the crystalline lamellae from radial to tangential, although the true reason of the lamellae flip is still unclear.

Additional interesting morphologies and more complex phase behaviour can be observed in triblock copolymers. With this in mind, novel ABA–type triblock copolymers of PDMAEMA, with the PLLA as a central block (to avoid polymerization of LLA in the presence of PDMAEMA, which provokes racemization as indicated above), were prepared and characterized, as summarized in *Chapter 5*. The molecular weight of PLLA was chosen to be above the region of sharp dependence of T_g and T_m on molecular weight (13,000), and the molecular weight of each PDMAEMA block was targeted to be half of or equal to the molecular weight of the PLLA block. NMR and SEC–LS analyses provided evidence of block incorporation and successful chain extension, respectively. Furthermore, thermal studies not only allowed the determination of the transition temperatures and degree of

crystallinity of the PLLA block, but also provided indirect evidence of triblock rather than diblock architecture of the prepared copolymers. Notably, diblock copolymer 13k–12k (*Chapter 2*), which has the same PDMAEMA content and PLLA block length as 7k–13k–7k, displays two distinct T_gs in DSC heating thermograms. In contrast, triblock copolymer 7k–13k–7k displays only one T_g, which is intermediate to the T_gs of PLLA and PDMAEMA. This is consistent with the presence of two PDMAEMA blocks of lower molecular weight and therefore miscible with PLLA (one T_g) rather than one block of higher molecular weight, which is not miscible with PLLA (two T_gs). Analysis of the DSC isothermal crystallization data by Avrami theory indicated that the crystallization rate constant does not drop significantly with the introduction of the PDMAEMA blocks. However, the spherulite growth rate, determined from POM images, decreases more significantly for triblock copolymers compared to diblock copolymers of similar PLLA molecular weight and similar PDMAEMA content. This is also indicative of the more complex architecture of these copolymers. Banded crystallites were observed in all of the samples. This is generally attributed to crystalline lamellae twisting, most probably originating from unbalanced surface stress on the lamellae fold plane.

6.2 Ideas for future work

Aside from the great potential of PLLA–PDMAEMA block copolymers for biomedical applications, where they can be used for targeted drug delivery of either hydrophobic or hydrophilic drugs due to the amphiphilic nature of this copolymer, or serve as a dual drug/DNA containing vector for targeted drug delivery, there are many interesting unexplored areas that are worthy of further attention. Below are just a few examples.

Improved synthesis of PLA–b–PDMAEMA

The unsuccessful polymerizations described in *Chapter 3* could lead to success if the problem of simultaneous LLA homopolymerization can be avoided. If indeed related to transesterification reactions involving the bifunctional initiator, as well as via undesired initiation by the catalyst, alternative catalyst/initiator system can be used. Aluminium isopropoxide, although was not reported to give high molecular weights PLLA[1] and cannot be used for preparation of copolymers for biomedical purposes,[2] has several advantages over tin octoate. First, when redistilled, it does not form any complex with water, thus during ROP initiation by the product of catalyst hydrolysis is eliminated. Second, the optimal temperature for ROP by $Al(OiPr)_3$ is 70 °C, same as for ATRP, and it would also be feasible to perform successful one–pot polymerization of PLA–PDMAEMA, or even

---

1. Guptaa, V. B.; Anithaa, S.; Hegdea, M. L.; Zeccab, L.; Garrutoc, R. M.; Ravidd, R.; Shankare, S. K.; Steinf, R.; Shanmugavelu, P.; Jagannatha Rao, K. S. *Cell. Mol. Life Sci.* **2005**, 62, 143–158.

2. Dubois, P.; Jacobs, C.; Jerômé, R.; Teyssié, P. *Macromolecules* **1991**, 24, 2266–2270.

PLLA–PDMAEMA of relatively high stereoregularity, as racemization of LLA by DMAEMA at 70 °C is believed to proceed to lower extent as at 90 °C (*Chapter 3*). To conduct ROP and ATRP, a model bifunctional initiator CBr_3CH_2OH can be suggested. It contains no ester groups that could be involved in transesterification reaction at early stage of ROP, and was efficient in simultaneous ROP of CL and ATRP of MMA.[3]

Electrospun fibers

It has already been demonstrated that PLLA–PDMAEMA diblock copolymers can form stereocomplex fibers by electrospinning from a solution of stereomixtures of PD(L)LA/ PL(D)LA–b–PDMAEMA or PLLA–b–PDMAEMA/PDLA–b–PDMAEMA.[4] Generally, the successful formation of fibers by electrospinning requires relatively high molecular weight polymers (≥50,000 g/mol), so that entanglement occurs in the spinning solution. However, ongoing research in our group has recently shown that block copolymers of low molecular weight PLLA (5000 g/mol) with a short PDMAEMA block (2000 g/mol) can also form fibers. Preliminary data also indicates that, depending on the solvent used, the fibers can contain partially crystallized or completely amorphous PLLA, meaning that the state of PLLA can be controlled. Thus, it is worthwhile to investigate the properties of electrospun fibers based on PLLA–PDMAEMA block copolymers as a function of block

---

3. Mecerreyes, D.; Moineau, G.; Dubois, P.; Jérôme, R.; Hedrick, J. L.; Hawker, C. J.; Malmström, E. E.; Trollsas, M. *Angew. Chem. Int. Ed.* **1998**, 37, 1274–1276.

4. Spasova, M.; Manolova, N.; Paneva, D.; Mincheva, R.; Dubois, P.; Rashkov, I.; Maximova, V.; Danchev, D. *Biomacromolecules* **2010**, 11, 151–159.

molecular weight in greater detail. If desired, the PLLA content in the fibers can be increased by preparing blends with high molecular weight PLLA homopolymer. Homopolymers and block copolymers that do not form fibers by themselves but can interact with the PDMAEMA block [ex. poly(acrylic acid) or poly(methacrylic acid)–based copolymers] are expected to give fibers with interesting properties (ex. adhesive, antistatic). It is also of interest to explore fiber formation as a function of quaternization degree of PDMAEMA; as such fibers will maintain biocompatibility and, in parallel, possess bacteriostatic properties. Overall, fibers obtained from modified and/or non–modified block copolymers have good potential in the biomedical field for tissue engineering, cell culture growth and drug delivery.

Complexation of PDMAEMA block

To expand the potential of the PDMAEMA block, it can be complexed with surfactants or mesogenic molecules to make it liquid crystalline. Solubility issues that will certainly arise on quaternization and/or complex preparation can be overcome by partial quaternization, to maintain the solubility in good solvents for PLLA. Azo–containing mesogenic molecules will also add light–responsiveness to the obtained material, thus enabling elongation or shrinking of fibers or films, in response to the wavelength of irradiating light. Studies of PLLA–PDMAEMA diblock and, eventually, triblock copolymers complexed with surfactants/mesogens in bulk may also reveal interesting morphologies of the novel hybrid crystalline/liquid–crystalline material, with potential applications in non–linear optics or as an optical data storage material.

Thin and ultra–thin film patterning

Given the rich morphology of the PLLA–PDMAEMA block copolymers' thick films, it is of interest to investigate in detail the influence of PDMAEMA block on the formation of individual crystalline lamellae and to observe the formation of lamellae aggregates and/or single crystals *in situ* by AFM. Using dip–coating and spin–coating techniques, crystallization behaviour of PLLA can be investigated in thin and ultra–thin films. Preliminary experiments have shown that the PLLA block crystallizes during the preparation of dip–coated films, prepared from diblock and triblock copolymers, forming separate crystalline lamellae aggregates (AFM). Spin–coated films contain amorphous PLLA meaning that its crystallization would take place within the context of the pattern formed by the block copolymer self–assembly, and can be investigated *in situ* by AFM.

PLLA–b–PDMAEMA–b–PLLA

Triblock copolymers of PLLA with PDMAEMA as a central block are inaccessible by either the three–step procedure or the bifunctional initiator approaches due to the racemization of the LLA by the amino moieties of PDMAEMA. However, this triblock copolymer can be obtained via simple and convenient azide–coupling ("click"–reaction) between appropriately functionalized homopolymers (bifunctional azide–PDMAEMA and monofunctional acetylenyl–PLLA) or a diblock copolymer and a homopolymer (PLLA–b–PDMAEMA–azide and acetylenyl–PLLA). Although the "click" approach towards multiblock copolymers has already been shown successful, there is still a possibility for incomplete coupling; thus the final triblock copolymer will inevitably be contaminated by

diblock copolymer and homopolymer. Nevertheless, the advantage of the proposed approach is that it will allow preparing triblock copolymers with different lengths of the outer blocks, which is not possible through a direct three–step synthesis. Moreover, in the case of PDMAEMA–b–PLLA–b–PDMAEMA preparation by the "click" reaction, using a diblock copolymer and a homopolymer, quaternized and non–quaternized PDMAEMA blocks can be combined in one copolymer which is not possible by simply quaternizing the final triblock copolymer. Introducing different blocks will enable additional control over the phase separation (when only one of the blocks is miscible with the central one) that will affect self–assembly and might lead to the formation of interesting morphologies. Such hybrid, partially miscible triblock copolymers might be useful as compatibilisers for incompatible blends or as an effective surfactant with a potential use as a flocculating agent and in other environmental applications.